Light Rays Illuminating the Universe

Thesis by

Yakov Landau

In Partial Fulfillment of the Requirements for the
degree of
Doctorate of Philosophy

CALIFORNIA INSTITUTE OF TECHNOLOGY
Pasadena, California

2026
Defended May 26 2026

Yakov Landau
ORCID: 0000-0002-3744-1294

ACKNOWLEDGEMENTS

It takes a village to raise a child, the old saying goes, and looking back I realize that I have been exceptionally fortunate to have been cared for by so many villages. Writing this section has been the warm blanket and hot cocoa in the storm that is wrapping up a PhD thesis. If I got nothing from my PhD other than that, *dayenu*.

The first people I have to thank are my parents. You have supported me and stood by my side through all of my crazy shenanigans. The endless love you have for me, and the self-confidence you instilled in me, has been the fuel that has taken me around the world, and can keep doing so ten times over. I wish everyone in the world a set of parents like mine. You also gave me the most amazing siblings anyone could ask for: Draizy, Chuma, Mechy, Chesky, Devorah Leah, and Aron Tzvi, the absolute best gang of weirdos to grow up with.

My advisor, David Simmons-Duffin, you are not just a great physicist, but also a good and kind one. I have learned from you how to explore, how and when to pivot, when to publish, and how to look for the simplest example that captures all the complexity. More importantly, though, I felt supported by you in my research. You were a breath of fresh air in an environment that can be stifling without it. I would not have had the confidence to explore the physics that I cared about without feeling your support. I can't thank you enough.

The fourth floor has always been loaded with amazing people, but there are some I need to call out by name.

Cyuan-Han, my first collaborator, you taught me a lot about CFT, helped me through my first project, and I will never cease to be amazed by your intuition for beating Mathematica into doing what you need it to do.

Sam, my great Latino[1] friend, I was lucky to have you as an officemate and as a neighbor. From comparing recipes to comparing languages, from going clubbing to going for pizza, from sharing gossip to sharing struggles, it was amazing to spend the last n years with you. From when we first met online on Zoom in QFT class, to getting pizza last week, there is never a dull moment with you. You are always so warm and loving, I feel like I could talk to you about anything. I am sorry that I am an uncultured boor who fell asleep at the classical concert you took me to.

[1] I am pretty sure this is the proper term for someone who speaks Latin.

My academic sibling Yixin, we spent so much time together, and I can't believe this is winding down. You stood by my side through some of the roughest times, and you consistently destroyed me at Catan. I loved the "Saturday Night Live" game nights you organized, and I hope that one day I might find a game that I can beat you at. I admire your ability to jump into problem-solving mode at the drop of a hat, and your ability to get into such a wide range of problems. You are one of the most sincere people I know, but still have some of the funniest takes on life and notice things no one else does 😁.

Nathan, you are a really great friend, and a kind and caring human being. You also have great taste in books and the same terrible sense of humor I do.

Shounak, you were an amazing collaborator, and also a great friend. From the pre-plague days in India where we bonded over our love for heavy metal, to California and Rhode Island where we shed light on the expanding universe, to camping in Vermont, we have had an amazing time. Hopefully I'll see you on the East Coast next year. You and Maddie were such great hosts in Rhode Island, and I wish you two only the best.

My main crew, the "Yosemite" crew: Andre, Sahangi, and Shruti, (and eventually Scott). You guys made grad school so much fun. We partied, road-tripped, drank and painted, watched all the Jesus movies, ate all the pancakes, finally had eggnog, did catwalks for the aunties[2], and raised Pepper to be the best cat ever. I could do anything with you guys; grad school would not have been the same without you.

My "Trivial Exercise" team: Aron, Leonardo, Sridip, Sam, and Davide. We only won a handful of times, but we discovered so many dark matter signals that we probably deserve a Nobel Prize. It was a blast getting routinely destroyed on account of our ignorance of 1950s Hollywood, but on nights that we were on fire, we were on fire.

The "Shabbosdige Yidden": Kal, Idy, Devorah, Jed, Bracha, Mordy, Chana, Rena, Bayla, and Shmuli. You gave me a sense of warmth and comfort that no one else can. I hope we make our T-shirts one day. Daniel and Andy, you are great terrible friends. Thanks to you I am poorer, and my liver is more strained. In five years' time I will be discussing you at an AA meeting. I just know it.

Ben Strozewski, I had four housemates in my time at Caltech. Three were chosen by me; you were randomly assigned by Caltech. You are by far the best housemate

[2] except for Andre

I ever had. Not only are you so easy to get along with, you have such good taste in books, music, and whiskey. I miss you already.

Lolly, you are probably the only person who has seen my entire academic experience and really understood me and supported me through all of it. I can't start listing how many ways I owe you everything[3], but I do.

Lefty, you knew me at my craziest and are still friends with me, what is wrong with you? You are one of the few people I know that I can talk to about anything, and unfortunately for you, I do. Tziri, the same goes for you. The fact that the three of us survived is mind blowing. I hope that the two of you appreciate how much your wins inspire me.

At Brooklyn College I need to thank Ken Miyano for being so supportive when I first started. I also need to thank Kishore Marathe for showing me the beauty of mathematical physics, a subject which seduced me and derailed my life more than any of my exes.

At Stony Brook I need to thank first and foremost Martin Rocek. When I knocked on your office door as an undergrad, not in any of your classes, you sat with me for over two hours and just answered all my questions. It remains one of the highlights of my academic experience. You supported me through everything and gave me more level-headed advice than almost anyone else in academia ever did. You are such a kind and caring human being, and I wish everyone in academia had a Martin in their life.

Chris Herzog, you honestly taught the best course I ever took. I still think about the HW problems you assigned probably about once a month; they were so good. Thank you also for all the great advice when I was applying to grad school. Eden Figueroa and Tom Wienacht, you two embody the fun of physics for me, and both of you let me run loose in your respective labs on equipment I should not have been touching.

Zohar Komargodski, you gave me my first real research problem in theoretical physics. It was the first time I knew something about physics before any other human did. It was a powerful experience that I won't forget.

Shiraz Minwalla, you inadvertently dragged me off the mathematical physics path back to the physics path. I know lots of curious people, humble people, energetic

[3] and suspect you will ask me to do so

people, and brilliant people. You are the only one who maxes out on all of those; it was a real privilege to experience physics around you. I also need to thank Sandip Trivedi and the whole crew at TIFR. It was such an amazing experience to be in an environment that lived and breathed physics. I can't and won't forget that. I also need to thank Jen Green at Stony Brook for all the work she did to help me get the Fulbright scholarship to go to India.

I was a latecomer to physics, and I first learned how to think in yeshiva, many yeshivas to be honest. I need to thank the many Rebbiem who were the first people outside my family to take my thinking seriously and gave me some of the thinking tools I still use today. Iv'e had many Rebbeim, but I need to thank the following by name, Rabbi Landynski, Rabbi Nussbaum, Rabbi Ehrenfeld, Rabbi Lopian, Rabbi Rappaport, and Rabbi Steinwurtzel. I dont think any of you thought this is where I would end up using what you taught me, but here we are, and I really appreciate all the time and effort you put into me.

I also want to thank some of the people who got me to this point with some semblance of sanity, in particular Trish. You steadied me through some of the most chaotic periods of my life, and pushed me to "give school a try" when I was thinking about anything but going to school. From the same era, I need to thank Yankel, a great neighbor whose home was a second home, and who really listened to me in some of my rougher years. Thank you Michael for keeping me grounded and present over the last few years. Your mastery of soft direction is an art you must've picked up from the artists, you introduced me to myself in a way that no one else ever has. I am also very grateful for the little cyborg that kept me from being too grounded, your wild imagination and playfulness was soul food I didn't realize I was missing.

Finally I need to acknowledge the wavefunction of the universe. Everything I am, everything I have ever been given, has only ever been you. Every joy and every wound has been a revelation of your existence. You were me before I was, and after I pass from this world of action I will forever remain in you. In you I cannot die, I can only be hidden, present as ever in your unitary evolution. I cannot thank you from outside you, as even that thanks would be yours. You are all that ever was, that is, and ever will be. There is no space devoid of your existence, and no existence beyond yours. For the sake of unity, may this small existence within your unfolding reveal the oneness it never left: in love and in awe, to manifest the hidden unity within the many, the light beyond the horizon, the revealed and concealed in perfect oneness.

ABSTRACT

This thesis studies Lorentzian structures in quantum field theory through the use of null integrated operators, with application to bounding the flat space corrections to Einstein's gravity via the AdS/CFT correspondence, as well as to quantum field theory in de Sitter. The first part of this thesis leverages the commutativity of null-integrated operators on the same null plane to construct dispersive CFT sum rules for spinning operators. The contribution of heavy blocks to these sum rules is dominated by a saddle configuration that we call the "scattering crystal." Correlators in this configuration have a natural flat-space interpretation, which allows us to build a dictionary between dispersive CFT sum rules for stress-tensors and flat-space dispersion relations for gravitons. This dictionary is a crucial step for establishing the HPPS conjecture for stress tensor correlators. The second part of this thesis initiates the study of light-ray operators in four-dimensional de Sitter space focusing on null integrals of the stress tensor. In Minkowski space, the null integral of the stress tensor unifies several ostensibly different constructions, functioning simultaneously as the energy flux operator, the angular contribution to a conserved charge, the averaged null energy operator, and the light transform of the stress tensor. However, we show that the de Sitter analogs of these various interpretations do not necessarily coincide but rather lead to distinct, observer-dependent light-ray operators. We construct four such de Sitter analogs and analyze their matrix elements in a free, conformally coupled scalar theory, showing that they exhibit the expected symmetry and positivity properties

TABLE OF CONTENTS

Acknowledgements iii
Abstract vii
Table of Contents viii
List of Illustrations x
List of Tables xiv
Chapter I: Introduction 1
1.1 (Introduction)^2 1
1.2 Perturbing the Universe 2
1.3 Balls Through the Air 3
1.4 A report from the quantum universe 7
1.5 Effective field theory is effective 9
1.6 Quantum gravity and what I did about it 12
1.7 Detectors in de Sitter 14
Chapter II: Background 19
2.1 Layout 19
2.2 Euclidean and Lorentzian correlators 19
2.3 Minimal CFT toolkit 23
2.4 Analyticity and inversion in Lorentzian CFTs 26
2.5 Bootstrap 27
2.6 QFT in curved spacetimes 30
2.7 de Sitter QFT 32
Chapter III: Spinning Dispersive CFT Sum Rules and Bulk Scattering 36
3.1 Introduction 36
3.2 Review: superconvergence sum rules 39
3.3 Heavy action from a spacetime saddle-point analysis 47
3.4 Flat space interpretation 71
3.5 Discussion 97
3.A Conventions for two-point and three-point structures 100
3.B Heavy action formula from the large ν limit 103
3.C Details on matching partial waves 108
3.D Dual structures at large ν 114
3.E CFT four-point structures 119
Chapter IV: De Sitter Light Ray Operators 121
4.1 Introduction 121
4.2 de Sitter space: coordinate systems and tilings 123
4.3 Minkowski light-ray operators: a quick primer 138
4.4 De Sitter light-ray operators 142
4.5 Discussions and outlook 157
4.A Regularizing the stress tensor 159

Bibliography 164

LIST OF ILLUSTRATIONS

Number *Page*

1.1 Me and my friends at lunch (ref photo, not actual) From Randall Munroe, *xkcd* 2501, "Average Familiarity." Used under the Creative Commons Attribution-NonCommercial 2.5 License. 1

1.2 The perturbative expansion organizes the complicated trajectory in terms of a leading approximation plus successively smaller corrections. 7

1.3 At low energies, beta decay can be treated as a fact of life, like air resistance. At higher energies, we see that the interaction is really caused by an intermediate particle called the W^- boson. This is just like discovering that everything about air resistance is really caused by small things called molecules which make up the air 11

1.4 The star marks a fixed observer, the dashed circle represents that observer's horizon, and the spiral galaxies are points carried apart by the expansion. The arrows indicate increasing separations on the balloon surface; at late times, galaxies cross outside the observer's horizon. 15

3.1 Contour of the light transform on the Lorentzian cylinder, where the two dashed lines should be identified. The contour starts at point x and ends at x^+ on the next Poincaré patch. 41

3.2 Causality configuration of the functional. The left figure shows the configuration in the original definition (3.33). Points $1, 3$ both start from 0 and are integrated along two different null directions. The right figures shows the configuration after applying $\mathcal{T}_1^{-1}, \mathcal{T}_2^{-1}, \mathcal{T}_4$, which becomes $4 > 3 > 0 > 1 > 2$. 50

3.3 Our gauge fixing condition is $x_3 = -x_1 = y, x_4 = -x_2 = \frac{x}{-x^2}, x_5 = e$. The causality constraint is $4 > 5 > 3 > 0 > 1 > 2$. 53

3.4 The two delta functions $\delta(x_{10}^2)\delta(x_{30}^2)$ force x_0 to be on an S^{d-2} (the blue curves). The directions of the variables $\widetilde{t}_0, \widetilde{x}_0$ defined in (3.59) are also indicated. 55

3.5 The bulk-point limit localizes the spacetime integral to a saddle locus that we call the scattering-crystal. The entire saddle satisfies the causality constraint $4 > 5 > 3 > 0 > 1 > 6 > 2$. The two delta functions restrict x_0 to be on an S^{d-2} shown by the red circle in the figure. The saddle locus further restricts x_0 to an S^{d-3}, which is represented by the two red dots (0-sphere). Points 5 and 6 are localized at $\pm e$. Points $1, 2, 3, 4$ are restricted to be timelike vectors, although in practice they have purely imaginary spatial components (see (3.81)). 61

3.6 Our functional is a special $6j$ symbol (or a tetrahedron) where one of the three-point structures is a celestial structure. The cross in the left figure stands for the contraction of the $\langle \widetilde{O}^{\dagger} \widetilde{O} \rangle$ tensor. The flat space limit is the limit where the two red legs have large quantum numbers. (More precisely, the two legs have large scaling dimensions.) 62

3.7 The steepest descent flow of the saddle integral (3.267). The red point is the saddle point. We show the deformed contour passing through the saddle in green and orange. The green part starts at infinity, goes in the opposite direction of the flow, and gradually spirals in toward the saddle. Along the green contour, the integrand keeps increasing and reaches maximum at the saddle point. It passes through the saddle point along a direction that is rotated by $e^{-\frac{3\pi i}{4}}$ relative to the real axis. After passing through the saddle point, the contour (in orange) goes in the same direction as the flow and gradually spirals out to infinity. The integrand at infinity goes as $\alpha^{-i\nu}$, so by making the contour spiral many times clockwise at infinity, we ensure that the contribution $\alpha^{-i\nu} \propto e^{2\pi\nu \arg(\alpha)}$ can be made arbitrarily small. . . . 116

4.1 The usual Penrose diagram for global dS_4 space. Each horizontal slice represents a 3-sphere S^3. At $\zeta = 0$, the spatial slice is a 3-sphere S^3 of unit radius (in units of H^{-1}), which grows hyperbolically toward $\mathscr{I}^{\pm}$, where it becomes infinitely large. Each point on such a slice represents a two-sphere S^2 that expands toward the center of the diagram and shrinks to a point at the left and right edges. The observer is conventionally placed on the left, at the South Pole. 124

4.2 It will be more useful for our purposes to adopt the observer's point of view. We therefore place the observer at the center and work with the doubled Penrose diagram, where the left and right edges are identified. 125

4.3 The Penrose diagram of dS space covered by the expanding (EPP) and contracting (CPP) Poincaré patches, with the observers worldline at the center of the CPP. The boundary between the patches is the $\mathscr{H}^+$ of the observer at the center of the CPP and the $\mathscr{H}^-$ of the observer at the center of the EPP. 126

4.4 Static patch (gold) seen as the overlap between two Poincaré patches (red and blue). This is the causal patch of our observer at the center sitting at $r = 0$. 126

4.5 The embedding of dS_4 as a hyperboloid in $\mathbb{R}^{1,4}$. The observer sits at the South Pole (denoted by the red line on the left). Each horizontal cross-section represents a spatial S^3 slice of the global geometry. Two overlapping Poincaré patches define a static patch. The static patch always has the same size (of unit radius) but its portion of the overall global dS slice varies with ζ. At $\zeta = 0$ it coincides with the entire left half of the S^3. As the global S^3 slices grow away from $\zeta = 0$, the static patch remains a fixed-radius disk that occupies a decreasing fraction of the full sphere. 127

4.6 The observer at the center can travel along geodesics in any direction: timelike (shown in blue), spacelike (shown in red), or null in between. There also exist regions (shown in green) that cannot be reached from the origin by any geodesic. 128

4.7 Two neighboring Minkowski patches on the Lorentzian cylinder shown in two dimensions, where their embedding coordinates differ by $X^+ = \pm 1$. From the perspective of Patch I, the surface $X^+ = 0$ coincides with $\mathscr{I}^+_{\mathrm{M}}$ with the spatial infinity $X_{i^0} = (0, 1, 0)$ and timelike infinity $X_{i^+} = (0, -1, 0)$ as its end points. The full Lorentzian cylinder is tiled by an infinite number of such Minkowski patches. . . 133

4.8 A null line going from the origin of one CPP (in blue), to that of a neighboring EPP (in red) on the Lorentzian cylinder. The two points in question are related by the transformation $X \to \mathcal{T}X = -X$. 135

4.9 Two neighboring dS embeddings, and hence four associated Poincaré patches on the Lorentzian cylinder. Regions I and II are the CPP and EPP, respectively, of the dS patch labeled by $X^0 = +1$. Regions III and IV are the EPP and CPP, respectively, of the neighboring dS patch labeled by $X^0 = -1$. As in the Minkowski case, the full Lorentzian cylinder is tiled by an infinite sequence of dS embeddings, or equivalently by neighboring EPP/CPP pairs. 136

4.10 The energy flux operator $\mathcal{E}(\widehat{\mathbf{n}})$ in Minkowski space shown as a limiting procedure in two dimensions. A calorimeter (i.e. a stress-tensor insertion) placed at fixed radial distance r, integrated over all time, and then pushed out to $\mathscr{I}^+_{\text{M}}$ as defined by the integral (4.43). 138

4.11 The three singularities of the ${}_2F_1$ function occur at $h = +1$ (lightlike separation), $h = -1$ (antipodal separation), and $h = +\infty$. The solid line indicates spacelike separated points with $h < 1$, while the zigzag line indicates timelike separated points with $h > 1$. 144

4.12 In this diagram, the thick green segments represent not just lines, but integrals over the suppressed orthogonal S^2 as well. The Hamiltonian may be evaluated on any of these Cauchy slices, whether on the $t = 0$ slice at the center, on the horizon $\mathscr{H}^+$, or on any interpolating surface in between. The full-horizon energy flux operator $\mathcal{E}_F(\widehat{\mathbf{n}})$ is defined on the entire CPP horizon $\mathscr{H}^+$. 147

4.13 The observer sits at the center worldline, surrounded by their timelike Killing field. If they place a calorimeter at fixed radial distance and then move it out to the static patch horizon $\mathscr{H}^+_{\text{SP}}$, the resulting dS light-ray operator $\mathcal{E}_S(\widehat{\mathbf{n}})$ is integrated over $\mathscr{H}^+_{\text{SP}}$, which is half of the future CPP horizon $\mathscr{H}^+$. 148

4.14 Two bulk points X_1, X_2 in dS space with their lightcones intersecting a full-horizon light-ray operator $\mathcal{O}_F = \mathcal{E}_F, \mathcal{A}_F$ defined on the CPP horizon $\mathscr{H}^+$ (in blue). Since X_1 lies in the static patch, we can restrict the integral (4.87) to begin at its singularity, so that the entire contribution is constrained to lie along the static patch horizon $\mathscr{H}^+_{\text{SP}}$. . 153

LIST OF TABLES

Number *Page*

4.1 A summary of the four types of dS light-ray operators classified in this work. 157

Chapter 1

INTRODUCTION

1.1 (Introduction)^2

This introduction is primarily aimed at everyone in my life who has been wondering what the hell I've been doing with my life for the last few years. If that's not you, you can skip to the next section. Or hang around and read this, I think it's fun. I will try to explain the state of the field in a very narrow corner of physics and what I have done to contribute to it. This might be an insane idea since I haven't really tried explaining my work to anyone who doesn't do physics professionally, and of course there is a relevant XKCD comic that I might run into headfirst

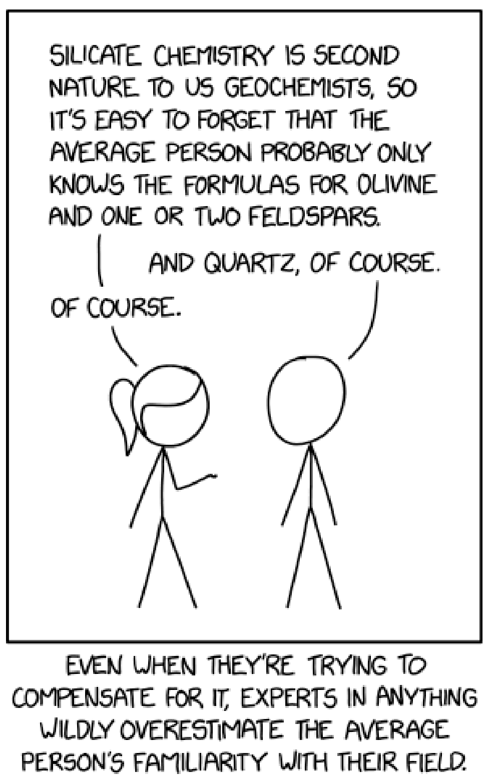

Figure 1.1: Me and my friends at lunch (ref photo, not actual) From Randall Munroe, *xkcd* 2501, "Average Familiarity." Used under the Creative Commons Attribution-NonCommercial 2.5 License.

There will be jargon, I will try to be light on it and explain the jargon whenever I can. Some of the most important aspects of my work sit behind a veil of math, and

I am sorry about that, there isn't much I can do here. I am not apologizing, it isn't my fault. Math is the only language we know that allows us to talk about corners of nature evolution didn't prepare us for, but I am sorry it's really pretty far back behind the veil and I wish you could see it. If there are parts that are confusing, treat it as you would an impressionist painting. Not every detail is important, but there should be enough here that you will hopefully get a picture of what's going on[1].

The most important thing I am going to try and get across is perturbation theory. This isn't my idea, it's a way of thinking that is hundreds of years old and quite possibly one of the greatest tools for thinking physicists ever invented. If you get nothing out of this other than understanding perturbation theory, you will have learned a lot. It is a way of approaching problems that I wish more people used, and can be used very widely, far beyond physics. Then I am going to tell you about effective field theory, it is a framework that is built on perturbation theory, and most of what we know about the universe at a fundamental level is in terms of effective field theory. It might be all we ever know. Finally I am going to tell you about my two projects.

1.2 Perturbing the Universe

Nature can't be understood in one go, or at least we haven't figured out how to do that yet. That is fine. If we waited until we understood everything before studying electricity, we would all be sitting in the dark.

Physics works because nature has regularities that can be understood in pieces. We isolate a pattern, find the regime where that pattern is cleanest, and study it there. Sometimes this means separating scales. Chemistry can be studied without constantly talking about subatomic particles, and planetary motion can be studied without constantly talking about atoms. Sometimes we study a toy model, a mathematical fiction which exhibits the same pattern we see in nature, now in a cleaner setting.

You don't want to include everything all at once. The art is to know how to isolate an effect, study that effect, and then figure out how to reincorporate it back into the real world model.

A real physical system is always being pushed, pulled, heated, cooled, shaken, and influenced by the rest of the universe. If I drop a cup, the earth pulls it downward, the air pushes against it, light from the room presses on it, the moon pulls on it,

[1] or, failing that, have enough that you can pass it on to your favorite AI who will explain it. Or call me, I like talking about this stuff

distant stars pull on it, the cup radiates heat, the atoms inside it vibrate, and so on. All of these effects are real. But they are not all equally important.

Good physics begins by finding a hierarchy. What is the largest effect? Are there necessary improvements? Are there effects we can ignore? This is the basic approach of perturbation theory. We solve a simple problem first, then add the complications in order of importance, and then stop once we hit good enough.

It allows you to study complicated things by find parameters that characterize the strengths of competing effects. If some of these parameters are larger than others, then we can simplify by focusing on those dominating effects at first while ignoring the weaker effects. After we have this first tentative, we can adjust it by incorporating the changes due to the weaker effects. We don't need to solve all of physics to understand some given problem.

1.3 Balls Through the Air

Imagine a ball flying through the air. Let's predict what happens next.

If you actually imagined it, you probably imagined some specific ball: a baseball, a cannonball, a ping-pong ball, or a beach ball. These are all governed by the same physics, but they will all behave differently, because different effects matter in different regimes.

Start with the cannonball. A cannonball is heavy, dense, and usually moving fast. If nothing acted on it after it left the cannon, it would travel in a straight line at constant speed. That is the zeroth-order story: the simplest story, the one we expand around.

Of course, that story is not quite right. The earth's gravity pulls the cannonball downward. The air pushes back against it. Sunlight pushes on it too, because light carries momentum. All of these effects are real. But they are not all equally important, and we will not make progress by considering all of them at once.

In schematic language, we might write

$$\begin{aligned}\text{behavior of the flying object} = {} & (\text{free motion}) \\ & + \epsilon_g(\text{gravitational effect}) \\ & + \epsilon_{\text{drag}}(\text{air-resistance effect}) \\ & + \epsilon_{\text{light}}(\text{sunlight-pressure effect}) + \cdots .\end{aligned} \tag{1.1}$$

This is not a literal equation. It is bookkeeping. The first term is the leading approximation. The numbers $\epsilon_g, \epsilon_{\text{drag}}, \epsilon_{\text{light}}, \ldots$ are the parameters that measure how strong each effect is, and how big the corresponding correction is.

These numbers are not just pulled out of a hat. They are made by comparing different kinds of information.

First, there are facts about the physics of the world: the strength of gravity on earth is encoded in a number g, the density of air ρ_{air}, the intensity of sunlight I, the speed of light c, and so on. These set the scales of the environment, or of the underlying laws.

Second, there are facts about the particular problem we are trying to solve: the size R of the ball, its density ρ_{ball}, its speed v, the height H it is fired from, and how accurately we care about the answer. These are the scales of the experiment in front of us.

There can also be dimensionless coefficients, like drag coefficients, that package messy details we do not want to solve from scratch every time. These coefficients remember things like shape, texture, spin, and the way air flows around the object. They are part of the real physics, but they are not usually the main hierarchy. The main hierarchy comes from combining the scales.

Perturbation theory begins when we combine all of this data into dimensionless ratios. A force is not automatically important just because it exists. What matters is whether it is large or small compared to the other scales in the problem. Gravity, drag, and sunlight pressure all exist at the same time, but their relative importance depends on the ball, the air, the speed, and the question we are asking.

For example, let's look at the importance of air resistance. All things being equal, this depends on the ratio of the density of the air to the density of the ball. So if you imagine hitting a baseball with a bat or a beachball with a bat we will get different effects. The ratio of the density of the air to the density of a baseball $\rho_{\text{air}}/\rho_{\text{baseball}}$ is very small, so at a first pass we can ignore air resistance. On the other hand, the ratio of the density of the air to the density of a beachball $\rho_{\text{air}}/\rho_{\text{beachball}}$ is pretty close to 1, so the effect of air resistance moves up in importance.

This idea will come back later in a more sophisticated form. In particle physics, we will compare the energy E of an experiment to a heavier scale M, and small ratios like E/M will tell us which effects are leading and which are suppressed. The cannonball is easier to imagine, but the logic is the same: find the scales, form dimensionless ratios, and then decide what matters.

For a cannonball, the leading story is mostly "it keeps moving forward." Gravity is the first important correction. To estimate its size, we combine a fact about the environment, g, with facts about this particular problem, the height off the ground it starts off at H and the launch speed v.

Suppose the cannonball is fired horizontally from a height H. Then gravity has a time

$$t_g \sim \sqrt{\frac{2H}{g}} \tag{1.2}$$

to act before the cannonball hits the ground. This sets an important scale of the problem. During that time, a cannonball with speed v travels a horizontal distance $L \sim vt_g$. This gives us a length scale for the problem. It is set by the time gravity has to act.

The gravitational correction is the change in velocity due to gravity, compared to the initial speed:

$$\epsilon_g \sim \frac{gt_g}{v} = \frac{\sqrt{2gH}}{v}. \tag{1.3}$$

This is a dimensionless number made from both the physics, g, and the particular setup, H and v.

For an ordinary cannonball fired fast from a height of a few meters, this is roughly

$$\epsilon_g \sim 0.1\ . \tag{1.4}$$

So gravity is important, but it is still only a correction to the leading fact that the cannonball was fired forward very quickly.

Air resistance is controlled by a different dimensionless ratio. Now we need facts about the air, facts about the ball, and a dimensionless coefficient C_D that packages details of the shape and flow:

$$\epsilon_{\text{drag}} \sim \left(\frac{3C_D}{8}\frac{\rho_{\text{air}}v^2}{\rho_{\text{ball}}Rg}\right)\epsilon_g. \tag{1.5}$$

The factor in parentheses compares the air resistance to the gravitational acceleration. It mixes environmental data, like ρ_{air} and g, with object data, like ρ_{ball}, R, and v. The coefficient $3C_D/8$ is the annoying real-world part: it remembers details like the shape of the object and the way air flows around it. It can be derived from first principles as well.

For a dense iron cannonball, this comes out to roughly

$$\epsilon_{\text{drag}} \sim 10^{-2}. \tag{1.6}$$

So air resistance is real, but it is smaller than gravity in this regime.

Sunlight pressure is controlled by the same kind of comparison:

$$\epsilon_{\text{light}} \sim \left(\frac{3}{4}\frac{I}{c\rho_{\text{ball}}Rg}\right)\epsilon_g. \tag{1.7}$$

Here I/c is the pressure scale coming from sunlight, while $\rho_{\text{ball}}Rg$ is the scale set by the weight of the ball per unit area. This captures the effect that sunlight will have on something like a cannonball, and it is absurdly small:

$$\epsilon_{\text{light}} \sim 10^{-11}. \tag{1.8}$$

Thus, in the cannonball regime, the expansion looks like

$$\begin{aligned}\text{behavior of a cannonball} \sim\ & \underbrace{1\,(\text{free motion})}_{\substack{\text{leading-order}\\ \text{effect}}} \\ & + \underbrace{10^{-1}\,(\text{gravitational effect})}_{\substack{\text{subleading}\\ \text{effect}}} \\ & + \underbrace{10^{-2}\,(\text{air-resistance effect})}_{\substack{\text{sub-subleading}\\ \text{effect}}} \\ & + \underbrace{10^{-11}\,(\text{sunlight-pressure effect})}_{\substack{\text{negligible}\\ \text{effect}}} + \cdots .\end{aligned} \tag{1.9}$$

But now imagine a ping-pong ball. It is light and hollow and air resistance is no longer a tiny correction. It can be one of the dominant effects. A beach ball is even worse, the wind can easily blow it off course. Very much unlike a cannonball. A baseball is somewhere in between. It is dense enough that gravity matters a lot, but air resistance, spin, and the seams on the ball can also matter. Of course the best pitchers dont necessarily know perturbation theory, they just have a very good effective[2] intuition for how baseballs work. But we can understand all these cases by doing the same analysis. We compute the dimensionless ratios. This then tells us the relevant “perturbative regime" we should be thinking about.

[2]This is called foreshadowing

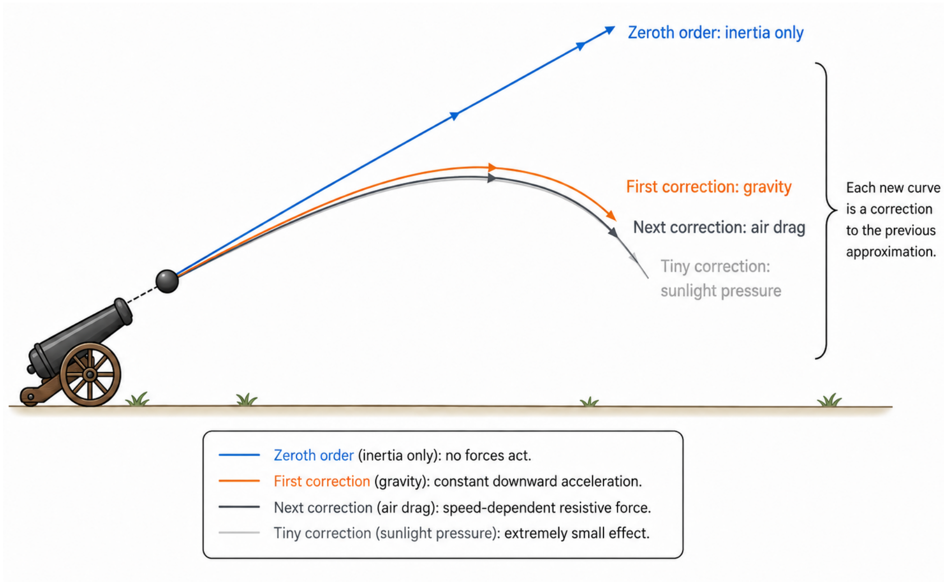

Figure 1.2: The perturbative expansion organizes the complicated trajectory in terms of a leading approximation plus successively smaller corrections.

If we think of really small things, like a grain of dust, pollen, or a tiny bacterium floating in air, we have in principle the same physics, but in reality a very different perturbative regime. At that scale we shouldn't even talk about "the air" it is really a bunch of molecules that are zipping around in every direction. Random kicks from air molecules can dominate. This is of course the same air that the cannonball dealt with, but at that scale we could treat it as a single background object "the air," at smaller scales we cant get away with that.

All of these are subject to the same physics but if we want to make headway in understanding these, we start by organizing these effects, which starts by identifying the relevant scales. There are scales that belong to the underlying physics, those that belong to the environment, and those that belong to the particular object and experiment. Once we combine them into dimensionless ratios, we can organize our hierarchy, realize what needs attention, what needs correction, and what we can ignore.

1.4 A report from the quantum universe

Ok, let's talk about the electron.

A quantum mechanical electron is not just a tiny ball with different forces acting on it. It is a different kind of object. Explaining what that means is famously subtle, and I am not going to do the whole thing here. That way lies philosophy, operator algebras, and people yelling at each other about the measurement problem.

Instead, I am going to do something more modest. We'll look at one perturbative regime of nature and I'll tell you what particles can do there. This is a report from the frontlines. I am not going to justify quantum mechanics from first principles.

The first thing to know is that quantum mechanics is probabilistic. If I fire a cannonball through the air, the natural questions are things like: where will the cannonball be in five seconds? Will it hit the wall? If it hits the wall, will the cannonball break, will the wall break, or will both break? Why does Yanky have a cannon? All reasonable questions.

Classically[3], these questions have definite answers, at least in principle. If we know where the cannonball is, how fast it is moving, and what forces act on it, then we can predict where it will go. Maybe the calculation is hard. Maybe the air resistance is annoying. Maybe the cannonball has legal implications. But the structure of the question is clear: there is a thing, it is doing something, and the laws of physics tell us what happens next.

At scales where quantum effects matter we have to change the kind of answer we are allowed to ask for. If an electron is sitting in an atom, we might want to know where it will be five seconds from now. But quantum mechanics does not generally give one definite answer. It gives probabilities. The electron might still be near the atom. It might be found somewhere else. In principle, it might even be found on the other side of the universe.

In fact quantum theories only answer one type of question, "If I tell you everything there is to know about a system now, can you tell me the probabilities of different measurement outcomes later." That is it, that's all that quantum theories ever do. Nature still follows precise patterns, but the patterns are in the probabilities.

The next thing to know is that particle number is not fixed. You can start with one particle and end with one particle, or two particles, or three particles, or a whole spray of particles. Not every process is allowed, and not every allowed process is likely, but the number of particles is no longer sacred. We can calculate the probability for each of these outcomes, usually using a toolbox called "Quantum Field Theory"

[3]Classical here and in most of this thesis means not quantum

1.5 Effective field theory is effective

A good example that combines both quantum weirdnesses is beta decay.

Atoms are not indivisible. They are made of protons, neutrons, and electrons. A neutron has an interesting feature: if it is sitting alone, outside a nucleus, it can decay. It can disappear and leave behind a proton, an electron, and an antineutrino:

$$n \to p + e^- + \overline{\nu}_e. \tag{1.10}$$

This is already very quantum. The neutron is not a tiny ball that slowly leaks something that becomes new particles. It is a quantum state, and one of the possible things it can do is turn into several other particles.

We can organize this in the same spirit as the balls flying through the air:

$$\begin{aligned} \text{behavior of the neutron} = {} & (\text{it remains a neutron}) \\ & + \epsilon_3 (\text{it decays into } p + e^- + \overline{\nu}_e) \\ & + \epsilon_5 (\text{it decays into five-particle final states}) \\ & + \cdots . \end{aligned} \tag{1.11}$$

The meaning is different now. For the cannonball, the expansion organized corrections to a trajectory. For the neutron, the expansion organizes probabilities. The leading behavior is that the neutron remains a neutron. The corrections are the probabilities for other outcomes.

Now we need to know whether the ϵ's are small. This is the same logic as before. For a ball flying through the air, we had to combine facts about the world, like g, ρ_{air}, and I, with facts about the particular ball, like its size, density, and speed. Here we do the same thing, but the scales are different.

The relevant low-energy theory of beta decay contains an interaction that schematically looks like

$$\mathcal{L}_{\text{int}} \sim G_F \, (\overline{p}\gamma^\mu n) \left(\overline{e}\gamma_\mu \nu_e\right) + \cdots . \tag{1.12}$$

Do not stare at this too hard. The symbols are not the point. The point is that the interaction contains one neutron, one proton, one electron, and one neutrino field. This term is the bookkeeping device that says: a neutron can interact in a way that produces a proton, an electron, and an antineutrino.

The coefficient G_F measures the strength of this interaction. More fundamentally, it is controlled by the weak scale:

$$G_F \sim \frac{g^2}{M_W^2}. \tag{1.13}$$

Here g is a dimensionless coupling (don't confuse this with the g of gravity), and M_W is the mass scale of a particle called the W-boson. This is the particle-physics version of what we saw before. Some data belong to the underlying physics, like g and M_W. Some data belong to the particular experiment, like the energy E available in the decay. The small parameter comes from combining them:

$$\frac{E}{M_W}. \tag{1.14}$$

At neutron-decay energies, E is tiny compared to M_W so we can just treat it as a background effect. That is why the low-energy interaction is weak. The neutron does not instantly explode into other particles. It mostly remains a neutron, and only occasionally decays. This is similar to what we were dealing with air resistance. We started by treating the air like it was one homogeneous thing. We know of course that the air is made of individual molecules. When you are dealing with things much bigger than air molecules or their average separation, you can ignore that. But if you want to talk about a piece of dust or pollen moving through the air, you can't really get away with that. At the scale of dust and pollen the air isn't a smooth continuum, it's made up of a bunch of molecules that hit the pollen individually, one by one, from different directions. As we got smaller, this interaction became the dominant one and we had to entirely switch up our perturbative regime.

More generally, effective field theory says the following. Pick the energy regime you care about. List every interaction allowed by the rules. Then organize those interactions by powers of small dimensionless ratios, usually ratios like

$$\frac{\text{energy of your experiment}}{\text{mass scale of heavier physics}}. \tag{1.15}$$

The details get technical fast, but the conceptual point is simple. Low-energy observers do not need to know every detail of high-energy physics. They need a list of allowed interactions and a list of coefficients.

Those coefficients are like the drag coefficient for the flying ball. They package information you are not resolving directly. If you know the deeper theory, you can calculate them. If you do not, you can measure them. Either way, once you have them, the effective theory tells you what happens in the regime where it applies.

The other nice thing about effective field theory is that it usually tells you where this effective theory is, well, effective. The beta-decay theory above works when $E \ll M_W$. If you crank the energy up toward M_W, the description starts falling

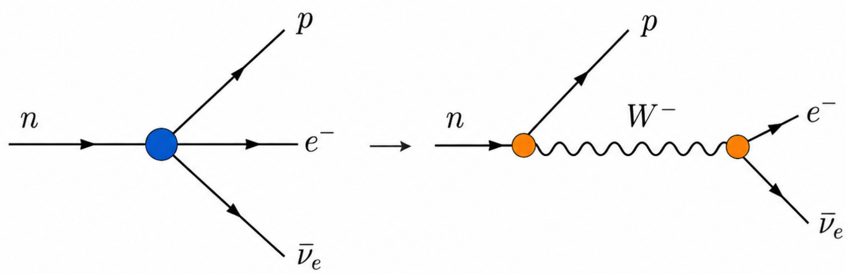

Figure 1.3: At low energies, beta decay can be treated as a fact of life, like air resistance. At higher energies, we see that the interaction is really caused by an intermediate particle called the W^- boson. This is just like discovering that everything about air resistance is really caused by small things called molecules which make up the air

apart, or rather, blowing up. The low-energy theory was not wrong. It was just not built for that regime. You need the more complete electroweak theory, where the W-boson is no longer hidden inside a coefficient.

This is one of the great organizational principles of modern physics. Newtonian mechanics is an effective theory. The Fermi theory of beta decay is an effective theory. The Standard Model itself can be treated as an effective theory. This is how we describe physics at a particular scale while being modest about our ignorance beyond it. Effective really is effective.

And within its regime, this framework is absurdly successful. In some special cases, especially in quantum electrodynamics, theory and experiment agree to twelve decimal places, that is an almost indecent number of decimal places. Twelve decimal places is not normal human knowledge. That is not "75 percent of patients improved," where everyone politely understands that the number means "roughly, please don't sue us." Twelve decimal places is predicting the distance from Pasadena to Brooklyn and being wrong by no more than a hundredth the width of a human hair.

So yes, quantum theory predicts probabilities rather than definite outcomes. But those probabilities are not vague. They are some of the sharpest predictions humans have ever made. The universe always has patterns, they may be subtle, but they are there and they are robust.

1.6 Quantum gravity and what I did about it

Here is the problem with gravity.

Gravity also has an effective field theory. The leading behavior is Einstein's theory of gravity. Then come corrections. We can write the action schematically as

$$S_{\text{eff}} = \int d^4x\,\sqrt{-g}\left[\frac{M_{\text{Pl}}^2}{2}(R - 2\Lambda) + \alpha_2 R^2 + \alpha_3 \frac{R^3}{M_{\text{Pl}}^2} + \cdots\right]. \tag{1.16}$$

The first term is Einstein gravity, including the cosmological constant Λ. The rest are possible corrections. The precise list is more complicated than this, because gravity is not interested in making my life easy, but this is the right schematic picture.

The coefficients $\alpha_2, \alpha_3, \ldots$ are the analogues of the coefficients in the beta-decay story. They tell us how the low-energy theory of gravity is corrected by whatever more fundamental theory exists at higher energies. If we knew the full theory of quantum gravity, we could calculate them. If we had absurdly powerful experiments, we could measure them.

We currently have neither.

The scale where we expect ordinary gravitational effective field theory to break down is roughly the Planck scale, M_{Pl}. Unfortunately, the Planck scale is outrageously high. The way we measure quantities in particle physics is by building colliders. Currently the biggest one is at CERN and it's roughly 30 km around. If we wanted to build a collider that could measure things at the Planck scale, the collider would have to be roughly the size of our solar system and draw power which is roughly what a star outputs in its lifetime. So unless anyone gets any really clever ideas, this is just inaccessible to our species for the foreseeable future.

So we pull ourselves by our bootstraps using something called the bootstrap.

The bootstrap is actually a whole bag of tricks which does not try to guess the microscopic theory directly. Instead, it exploits consistency conditions that any reasonable theory must obey. It must obey causality. It must obey unitarity, meaning probabilities add up correctly. It must respect the relevant symmetries. It must have the right analytic structure. We don't actually know that any of these are true at a fundamental level, but we are exploring their consequences. We are thinking along the lines of "if causality is a fundamental aspect of our universe, what does that tell us about the allowed low energy theories?"

To see what this has to do with gravity, we need gravitons. Classically, we talk about gravity as a force. Quantum mechanically (in a perturbative regime), gravitational interactions can be described using particles called gravitons. When two objects gravitationally interact, the quantum field theory picture says, roughly, that they exchange gravitons.

Now imagine a scattering experiment with gravitons. Two gravitons come in, two gravitons go out. The question is, given their initial energies, directions, and polarizations, what are the possible final outcomes, and with what probabilities?

The answer is encoded in a function called a scattering amplitude. This amplitude depends on the kinematic data of the gravitons and on the coefficients of the effective field theory $\alpha_2, \alpha_3, \ldots$. Perturbatively, the leading answer is Einstein gravity. Then the higher-derivative corrections modify the answer. In cartoon form:

$$\text{graviton scattering} = \text{Einstein gravity} + \alpha_2(\text{first correction}) + \alpha_3(\text{next correction}) + \cdots . \tag{1.17}$$

The bootstrap idea is that this amplitude cannot be any random function. It has to satisfy consistency conditions. Causality restricts it. Unitarity restricts it. Crossing symmetry restricts it. Analyticity restricts it. If we are clever enough, these abstract consistency rules become concrete bounds on the coefficients α_i.

This is not the same as finding the final theory of quantum gravity. It is more like drawing a map of where the final theory is allowed to live. We may not know the exact theory that governs our universe, but we can start crossing out enormous regions labeled "nonsense," "causality violation," and "absolutely not."

What Cyuan-Han, David, and I did was sharpen one part of this story. In flat space, people had developed bootstrap style arguments that constrain the coefficients of the effective field theory. But some of the arguments rely on assumptions about the mathematical behavior of scattering amplitudes. These assumptions are physically well motivated, but one would like to derive them from something more solid. We used a workaround that avoided all of these assumptions by using one very well established conjecture called the AdS/CFT conjecture.

We can imagine many types of universes that are physically sensible, but there are simple ones called de Sitter space, flat space, and anti de Sitter space. Flat space has zero cosmological constant. de Sitter space has positive cosmological constant. Anti de Sitter space has negative cosmological constant. Practically, this means that in addition to all the usual physical forces, the universe itself contributes a sort of force through the cosmological constant. In anti de Sitter this force is attractive, pulling all things closer together, in de Sitter the force is repulsive, pushing things farther apart, and in flat space the universe contributes nothing. Our universe, on very large scales, appears to be closer to de Sitter than either flat space or anti de Sitter.

The AdS/CFT correspondence says that quantum gravity in anti de Sitter space can be described by a conformal field theory, or CFT, living on its boundary. A CFT is a very special kind of quantum field theory with a large amount of symmetry. That symmetry puts it in a mathematical straightjacket. We know the mathematical form and we can rigorously prove things.

So while anti de Sitter space is not where we live, we can calculate things there. Then we can find perturbative regimes that match perturbative regimes of flat space. So there are things we can calculate in AdS that teach us about flat space.

The strategy was this. Instead of trying to directly control graviton scattering in flat space, we studied the corresponding problem in AdS using the CFT. The CFT gives us a more rigorous mathematical toolbox. Then we went to a perturbative regime in AdS that matches a perturbative regime in flat space. This then showed that the bootstrap bounds that were placed on the flat space gravity effective field theory were actually justified.

1.7 Detectors in de Sitter

This next project is not about quantum gravity in de Sitter, it is about quantum field theory in de Sitter. Quantum gravity in de Sitter is a disastrously complicated mess right now, with claims more insane than anything we've discussed so far. We are avoiding that. Sticking with just quantum field theory, basically particle physics.

We briefly mentioned de Sitter, but as it seems to be a good description of our universe let's flesh it out a bit. I am going to use two analogies here, so something to keep in mind is that analogies are like theories, they capture some feature of the real physics, but like theories, they break down if you push them too hard.

The first analogy is the expanding balloon. Our expanding universe is like an

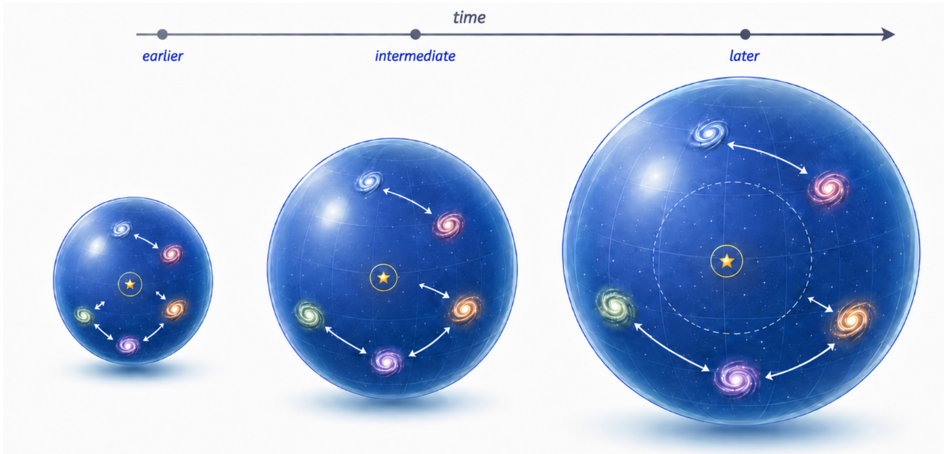

Figure 1.4: The star marks a fixed observer, the dashed circle represents that observer's horizon, and the spiral galaxies are points carried apart by the expansion. The arrows indicate increasing separations on the balloon surface; at late times, galaxies cross outside the observer's horizon.

expanding balloon. Imagine a balloon with a bunch of dots on it, as you blow up the balloon the dots move away from each other. If we imagine ourselves as one of these dots, then the nearest dots will move away slowly, and the further ones move away faster. This also means that as they move away, they are now further away, which means that they need to move even faster. So things in our universe that are relatively close to us are moving away slowly, but the further they get the faster they move, so when they get further they move away even faster. Eventually, things that are far enough from us (or things that are closer, if you wait long enough) are moving away from us faster than the speed of light.

Now I know, that you know, that we know, that nothing can move faster than the speed of light. But. This is the exception. The real rule is that nothing can move through space faster than the speed of light. Space itself can do whatever it likes. And if you are in space, you get to go along for the ride.

You can see this effect as a type of force, which means that it isn't always the dominant force. For example, consider our nearest neighbor big galaxy, the Andromeda galaxy. It does feel some force pulling it away from us, but even stronger than that is the gravitational attraction to our galaxy, so in a couple billion years we will collide. However, any galaxies beyond that will eventually rush away from us. If we wait long enough we will be in the new Andromeda-Milky way galaxy merger, but we won't see anything beyond it.

Anything outside it will be moving away from us faster than the speed of light.

Which means that nothing from beyond a certain region will ever be able to send us any signal, we will never be able to receive any information from it. In fact there are already portions of our universe today that are moving away from us faster than the speed of light and we will never be able to see them as they are today.

Every observer in such a universe has a dividing line beyond which things are traveling away from them faster than the speed of light, we call this their "cosmological horizon." One way to think of this is to imagine you're in a boat on a river. It all seems serene now, but up ahead there is a waterfall. There is an imaginary line in the water beyond which you won't be able to turn back, the water will be moving faster than your boat can go. This is a good analogy, and incidentally is also a good analogy for black hole horizons. However. Unlike the waterfall or the black hole, this isn't because of a fixed feature of the universe, it's about you. Well its about you and the universe. The waterfall and the black hole have a horizon that is universal, everyone agrees where it is, the cosmological horizon in de Sitter is personal. Everyone is their own dot on the balloon, everyone is the center of their own universe, everyone has their own cosmological horizon, and everyone has their own region of the universe that they have access to.

The distance to the horizon however is the same for everyone, we call it the de Sitter radius, or the Hubble scale, because Hubble was the first person to notice that our universe was expanding. This scale sets the perturbation regime. If you look at things much much smaller than the Hubble scale, then you can either entirely ignore the the universe's expansion, or at most treat it as a correction. If you are dealing with stuff that is around or larger than the Hubble scale then you really need to take this into account.

de Sitter has a lot of interesting features that are a consequence of this expansion, we lose a lot of features we are very used to from our small scale/flat space intuition. The most important is energy conservation. Energy is not conserved in de Sitter. Actually it's a bit more subtle, you can make choices on how to define energy, you can either define energy in such a way that it makes sense everywhere, but then it is not conserved, or you can choose something that is a good proxy for energy that is conserved, but it is only a good proxy for energy in some small region around you[4].

We also lose something that particle physics relies on heavily, something called asymptotic states. Particles interact, the closer they are the more they interact (usually). If we want to study particle interactions, we need to ask an appropriate

[4] this is called your "static patch"

quantum type question. We need a clean description of the start, and then we can ask for the precise probability for the different types of outcomes. In order to get a clean question for the beginning we want to say something like “suppose we started with two electrons, electron 1 with energy E_1 and electron 2 with energy E_2, we let them interact and we want to know what happens next". For that to make sense we need to start off with two electrons well isolated from each other, otherwise we will have to already know how they are interacting in the beginning too. So we imagine that we separate them on two opposite ends of our universe way far in the past, and then shoot them towards each other. When they start off on opposite sides of the universe, the interaction between them is negligible, so that gives us a good way to set up the problem.

We can’t do this in de Sitter. First of all if they start off too far away, they’ll never meet. But even worse, if they have been traveling for forever then we get bit by the lack of energy conservation. Because even if you did start off with an electron somewhere, you will almost definitely not end up with just one electron. That one electron will spontaneously turn into a shower of other particles, which will in turn into showers of other particles. There is nothing to stop this when energy isn’t conserved. So this whole picture just doesn’t work. Which is a problem because this is the basic setup for most solvable quantum field theory problems.

So what Shounak and I did was focus not on the particles, but on the particle detector. In flat space, or in the flat space limit of de Sitter, a.k.a. most of our experience, here is how we make measurements in particle experiments. We have particles going really fast and we make them collide at some point. Then we surround that point with lots of energy detectors. So if, in the collision, new particles were created, they shoot off and hit a detector. We then note that some particle went flying off in some direction with some energy, etc.

In the idealized mathematical version of detectors we imagine placing these detectors at the edge of the universe, as far away from the experiment as possible. You also let the detector run for forever so that it can capture all the energy from your collision. In practice the detector is tens of meters away and runs for fractions of a second. But this fact only gives small perturbative corrections.

The fact that it runs for forever is an enticing fact. If we really did this in de Sitter then we would have something that is sensitive to the de Sitter scale, simply because it runs for a long time. But we first had to ask, What is the de Sitter analog of the energy detector picture? We decided to at first, only look at the leading order behavior, so we ignored all interactions and just focused on the question “What is an energy detector in de Sitter"

There were two different choices we needed to make. First of all, what do we mean by energy? Secondly, where do we put this detector? The second question had a more obvious answer, it has to go at the horizon, because if it was placed any further then it is an experiment that we won’t ever be able to check because we lose the detector, it falls over the horizon. The energy question is a more subtle one, what we decided to do in the end was do both, study the conserved energy that only made sense locally, and study the sense of energy that made sense everywhere but wasn’t conserved.

This already led us to the notion that detectors in de Sitter had a richer structure than in flat space. Moreover, the flat space energy detector has a few different interpretations. Without getting too lost, I’ll just say the words. They can be seen as energy detectors, angular contributions to the Hamiltonian, the ANEC operator, and as the light transform of the stress tensor. In de Sitter these are mostly distinct operators, with the exception of ANEC and the light transform still being the same.

So by starting with the perturbative regime of regular flat space particle physics, and stretching it just to the limit where it is sensitive to de Sitter effects, we discovered that what in flat space was one object with multiple interpretations, in de Sitter led to distinct operators.

Chapter 2

BACKGROUND

2.1 Layout

The purpose of this introduction is to fill in some extra background material for Chapter 3 and give context for Chapter 4. While Chapter 3 gives a review of sum rules as they are used for the bootstrap, what is missing is the bootstrap itself, as well as the analytical properties of the conformal blocks which are leveraged to build and use these sum rules. The bulk of the background should serve as a good reference for these. Chapter 4 is more or less self contained and does not really need a lot of background to be understood. The last two sections therefore are more about setting the stage and giving the big picture overview of where that project lies, these two sections are not required reading to understand Chapter 4 and just serve as motivation.

A note about references used, I am not claiming that any of the references used here are necessarily the ones where an idea originated, these are often simply the references I encountered in the course of my research. Please take them in this light.

2.2 Euclidean and Lorentzian correlators

Quantum field theory as used to describe the fundamental physics of our universe is Lorentzian in nature; real time evolution, causal propagation, response functions, commutators, particle production, and scattering are all Lorentzian at their core. The basic local data of QFTs are correlation functions. When the order is fixed they are called Wightman functions[1], but they can also be advanced, retarded, or time ordered. Euclidean theories themselves also describe real world phenomena, such as in the context of thermal field theories. In flat space these two types of QFT are not entirely separate objects, as under the usual reconstruction/analyticity assumptions, all four types of Lorentzian correlators mentioned above can be recovered from Euclidean ones via appropriate analytic continuations, and in general these Euclidean versions are under better analytic control.

[1] These are not functions, nor were they first studied by Wightman

Schwinger and Wightman functions

Lorentzian correlators of local operators at points $x_i \in \mathbb{R}^{1,d-1}$ can be understood by starting with correlators having fixed ordering, known as Wightman correlators

$$W_{1\cdots n}(x_1, \ldots, x_n) = \langle \Omega | O_1(x_1) \cdots O_n(x_n) | \Omega \rangle. \tag{2.1}$$

The right hand side of this equation is the expectation value of the string of operators in the vacuum state $|\Omega\rangle$. In flat space these Wightman functions are usually best seen as tempered distributions, and are obtained as the boundary values of holomorphic functions in some domain in complexified Minkowski space (Streater and Wightman, 2016; Haag, 1992; Kravchuk, Qiao, and Rychkov, 2020).

For points in Euclidean space $X_i = (\tau_i, \vec{x}_i) \in \mathbb{R}^d$ their n point functions are known as Schwinger functions and can be similarly expressed as

$$S_{1\cdots n}(X_1, \ldots, X_n) = \langle O_1(X_1) \cdots O_n(X_n) \rangle_E, \qquad X_i \in \mathbb{R}^d. \tag{2.2}$$

If we want to understand these in terms of a vacuum expectation value, we need a vacuum state, and hence a Hamiltonian and a time direction. If we have these, and the Hamiltonian is bounded from below and unbounded from above, then the spectral factors converge in one Euclidean-time ordering and diverge in the reverse, so the operator ordering is forced on us by convergence. For $\tau_1 > \cdots > \tau_n$ we can now write

$$S_{1\cdots n} = \langle \Omega | O_1(\tau_1, \vec{x}_1) \cdots O_n(\tau_n, \vec{x}_n) | \Omega \rangle_E. \tag{2.3}$$

Although a time direction forces an operator ordering, this does not mean that upon analytic continuation to Lorentzian time there is only one allowable operator ordering for Lorentzian time. In Lorentzian time a correlator can have any operator ordering we wish, but the desired operator ordering in Lorentzian time will reveal which Euclidean correlator it is related to. That is to say, we can obtain the Lorentzian ordering in (2.1) by choosing the imaginary (Euclidean) time it is an analytic continuation of. A compact prescription is

$$t_i \to t_i - i\epsilon_i, \qquad \epsilon_1 > \epsilon_2 > \cdots > \epsilon_n. \tag{2.4}$$

The hierarchy of ϵ_i's specifies the order $O_1 \cdots O_n$. Exchanging two operators corresponds to approaching the real Lorentzian slice from a different imaginary-time ordering, and hence to a different distributional boundary value (Osterwalder and Schrader, 1973; Osterwalder and Schrader, 1975; Glimm and Jaffe, 1981; Kravchuk, Qiao, and Rychkov, 2020).

For example, we can write the translation invariant two point function as the limit of a holomorphic function as

$$W(x) = \lim_{\epsilon \to 0^+} W_{\text{hol}}(t - i\epsilon, \vec{x}), . \tag{2.5}$$

Note however that the light-cone or coincident-point limits are distributional, not pointwise limits of ordinary functions (Streater and Wightman, 2016; Kravchuk, Qiao, and Rychkov, 2020).

S-matrix, locality, unitarity, and crossing

In theories that admit asymptotic particle states we can construct an S-matrix which maps the incoming free particle states at $t \to -\infty$ to the outgoing ones at $t \to +\infty$ (Haag, 1992; Streater and Wightman, 2016)

$$S : \mathcal{H}_{in} \to \mathcal{H}_{out}, \qquad S^\dagger S = S S^\dagger = \mathbf{1}, \qquad S = \mathbf{1} + iT. \tag{2.6}$$

If we consider the case of $2 \to 2$ scattering of identical massive scalars we get

$$\langle p_3 p_4 | \, iT \, | p_1 p_2 \rangle = i(2\pi)^d \delta^{(d)}(p_1 + p_2 - p_3 - p_4) \, T(s,t), \tag{2.7}$$

where

$$s = -(p_1+p_2)^2, \qquad t = -(p_1-p_3)^2, \qquad u = -(p_1-p_4)^2, \qquad s+t+u = 4m^2, \tag{2.8}$$

are the usual Mandelstam variables. The LSZ reduction formula extracts scattering amplitudes from Fourier-transformed Lorentzian time-ordered correlators by amputating the external one-particle poles and taking all external momenta on shell. (Lehmann, Symanzik, and Zimmermann, 1955; Weinberg, 1995). We can realize causality in general in QFTs (Streater and Wightman, 2016; Haag, 1992; Kravchuk, Qiao, and Rychkov, 2020) by constraining

$$[O(x), O(y)] = 0 \quad ((x-y)^2 > 0). \tag{2.9}$$

Causality also gives constraints on the amplitudes by constraining their analytic properties. More generally, the singularities of $T(s,t)$ are constrained by the analytic structure of the S-matrix, including Landau/pinch singularities; the physical poles and unitarity cuts relevant for the discussion here occur when intermediate states can go on shell (Eden et al., 1966; Cutkosky, 1960; Correia, Sever, and Zhiboedov, 2022). Poles correspond to stable particles or bound states while cuts signify multiparticle production. Another important feature of quantum theories is the conservation of probability, which manifests itself as time evolution by a self adjoint Hamiltonian or the unitarity of the S-matrix

$$S^\dagger S = \mathbf{1} \qquad \Longleftrightarrow \qquad -i(T - T^\dagger) = T^\dagger T. \tag{2.10}$$

Looking at amplitudes, this manifests itself as cutting relations, amplitude discontinuities compute the sum over intermediate on shell states, for example the optical theorem gives us that in the forward limit ($t = 0$) (Eden et al., 1966; Cutkosky, 1960; Peskin and Schroeder, 1995)

$$\mathrm{Disc}_s T(s,0) \propto \sqrt{s(s-4m^2)}\, \sigma_{tot}(s) \tag{2.11}$$

A final important property of S-matrices is crossing. Crossing is the statement that a given scattering amplitude is related by analytic continuation to the amplitude where any of the momenta is swapped from incoming to outgoing, and that particle is replaced with its antiparticle. The s, t, u channels are therefore not independent functionals, but different boundary values of the same analytic function. For example, for $2 \to 2$ scattering of identical scalars this manifests as a permutation symmetry of all three Mandelstam variables, so

$$T(s,t) = T(t,s) = T(u,t), \qquad s + t + u = 4m^2. \tag{2.12}$$

Combined with unitarity and causality, crossing underlies dispersion relations, positivity bounds, and Froissart-Gribov bounds. All these statements are in the context of ordinary flat space scattering, they assume the existence of asymptotic particle states, infrared control, and a mass gap (or some appropriate substitute like soft dressing, or event shape type observables). These do not carry over for Lorentzian QFTs on arbitrary spacetimes, generic CFTs, or gravitational theories without qualification (Eden et al., 1966; Martin, 1965; Adams et al., 2006; Simon Caron-Huot and Van Duong, 2021; Correia, Sever, and Zhiboedov, 2020).

2.3 Minimal CFT toolkit

Conformal field theories are field theories which, in addition to the usual Poincaré symmetries, also have symmetry under rescaling (dilatation) and an inverted form of translations known as special conformal transformations (SCTs). These arise in many places in physics, such as the fixed points of RG flows, in the vicinity of second order phase transitions, and quantum gravity in universes with a negative cosmological constant (J. M. Maldacena, 1998; Witten, 1998; Aharony, Gubser, et al., 2000). A remarkable aspect of such theories is that the symmetry places such strong constraints that such theories can be entirely specified[2] by knowing the operator spectrum, and a set of numbers known as the OPE coefficients, this is known as the conformal data (Simmons-Duffin, 2017; Poland, Rychkov, and Vichi, 2019; Di Francesco, Mathieu, and Senechal, 1997). With this information the theory is entirely solved. As is the case in QFT, it will be useful to define our Lorentzian correlators as boundary limits of Euclidean correlators.

Primaries, descendants, and local data

CFTs in addition to their physical behaviour and mathematical solvability, give an organization scheme for operators, classifying their transformation properties as a representation of the conformal group in addition to their usual Poincaré[3] behavior. They have the usual Poincaré characteristics as being scalars, vectors, spinors, etc but also have their additional behavior under the unique conformal transformations, dilatations and SCTs. A primary operator is an operator whose transformation under dilatations, D, and SCTs, K_μ is given by

$$[D, \mathcal{O}(0)] = \Delta\, \mathcal{O}(0), \qquad [K_\mu, \mathcal{O}(0)] = 0, \tag{2.13}$$

up to convention dependent factors of i. The eigenvalue Δ is the conformal dimension of the operator. This along with its Poincaré behavior classifies its representation. Descendants are operators obtained from primaries by repeated application of the

[2] We are ignoring defects in this statement, as these will play no role in this thesis

[3] by which we mean translations and Lorentz transformations for the Lorentzian case, or translations and rotations for the Euclidean

translation generator P_μ, or equivalently by repeated differentiation of a primary operator. A conformal multiplet is a primary and its descendants, (modulo null states which are both primary and descendant). The two point function in any conformal theory is entirely fixed by symmetry up to an overall operator normalization. For two scalar primaries, appropriately normalized, we get

$$\langle O_i(x_1) O_j(x_2) \rangle = \frac{\delta_{ij}}{(x_{12}^2)^{\Delta_i}}, \qquad x_{ij} = x_i - x_j. \tag{2.14}$$

The functional form for three scalar primaries is similarly fixed to be

$$\langle O_1(x_1) O_2(x_2) O_3(x_3) \rangle = \frac{\lambda_{123}}{(x_{12}^2)^{\frac{\Delta_1+\Delta_2-\Delta_3}{2}} (x_{23}^2)^{\frac{\Delta_2+\Delta_3-\Delta_1}{2}} (x_{31}^2)^{\frac{\Delta_3+\Delta_1-\Delta_2}{2}}}. \tag{2.15}$$

where λ_{123} is the OPE coefficient, not fixed by conformal symmetry and is one of the crucial pieces of conformal data defining the theory. For non primary operators, they can be expanded into primary operators and the above applied. For non scalar operators, the two point function carries an additional unique tensor structure, for the three point function conformal symmetry allows a finite list of tensor structures which can enter, each carrying its own unknown coefficient (Di Francesco, Mathieu, and Senechal, 1997; Simmons-Duffin, 2017; Osborn and Petkou, 1994; Costa, Joao Penedones, et al., 2011).

OPE, conformal blocks, and crossing

While conformal symmetry can allow us to place 2 and 3 points in canonical fixed positions (called conformal frames) and thereby fix their functional form, the four point function has dependence on two independent numbers called conformal cross ratios

$$u = \frac{x_{12}^2 x_{34}^2}{x_{13}^2 x_{24}^2}, \qquad v = \frac{x_{14}^2 x_{23}^2}{x_{13}^2 x_{24}^2}, \qquad u = z\bar{z}, \qquad v = (1-z)(1-\bar{z}). \tag{2.16}$$

It will be useful to place these points in the conformal frame $\{x_1, x_2, x_3, x_4\} = \{0, (z, \bar{z}), e, \infty e\}$ where e is some unit vector. In Euclidean signature $z, \bar{z}$ are complex conjugates on the principal sheet of the four point function, while in Lorentzian signatures these are treated as independently continued numbers. The four point function will have singularities as $z, \bar{z}$ approach any of the other insertions and we can organize and expand the four point function around any of these. For example the s channel expansion is around the $z, \bar{z} \to 0$ singularity and so for identical scalar primaries we have

$$\langle \phi(x_1)\phi(x_2)\phi(x_3)\phi(x_4)\rangle = \frac{\mathcal{G}(z,\bar{z})}{(x_{12}^2 x_{34}^2)^{\Delta_\phi}}. \tag{2.17}$$

This is called the s-channel, in analogy to the s channel in ordinary QFT, since the four point function exhibits a structure similar to particle exchange due to the operator product expansion (OPE). The operator product expansion states that the product of two nearby local operators can be expanded in conformal multiplets,

$$\mathcal{O}_i(x)\mathcal{O}_j(0) \sim \sum_{\mathcal{O}} \lambda_{ij\mathcal{O}}\, C_{ij\mathcal{O}}(x,\partial)\, \mathcal{O}(0). \tag{2.18}$$

The sum is over primary operators, and $C_{ij\mathcal{O}}(x,\partial)$ is a differential operator which generates the descendants from the primary. The coefficient $\lambda_{ij\mathcal{O}}$ is called the OPE coefficient, it is the same as the three point function coefficient in (2.15), and for spinning operators also includes the same tensor structures as the relevant three point function. Iteratively using this allows one to reduce any n point function to an n-1 point function, and from there down to the known two and three point functions. It is in this sense that knowledge of the spectrum of operators and OPE coefficients completely solves the CFT. The OPE expansion is valid as an operator statement so long as there exists a radial quantization containing the two operators in question and no other operator (Pappadopulo et al., 2012; Hogervorst and Rychkov, 2013). In the three point function you can always do the OPE expansion, for higher point functions this will induce cuts.

We can use the OPE on pairs of operators in the four point function to reduce the correlation function to a sum of functions called conformal blocks. These functions encode the contribution of exchanged conformal multiplets, i.e. a primary of dimension and spin (Δ, J) and its descendants. If we do the s channel expansion, we do the OPE between operators at points 12, and 34, which then gives us the conformal block expansion

$$\mathcal{G}(z,\bar{z}) = \sum_{\mathcal{O}} \lambda^2_{\phi\phi\mathcal{O}}\, G_{\Delta,J}(z,\bar{z}). \tag{2.19}$$

The 12 OPE in a scalar four-point function is valid so long as operators 3 or 4 are not between 1 and 2. This condition is represented in the standard $z, \bar{z}$ convention by a crossed-channel cut usually drawn from 1 to ∞. Away from the cuts, we can do different OPE expansions and hence get different conformal block expansions. The equivalence of these expansions is crossing symmetry, a constraint which will be highly leveraged. Note, that we have an equivalence of the entire series, not block by block (Luscher and Mack, 1975; Pappadopulo et al., 2012; Dolan and Osborn, 2002; Simmons-Duffin, 2017; Poland, Rychkov, and Vichi, 2019).

2.4 Analyticity and inversion in Lorentzian CFTs

The conformal block plays an analogous but distinct role in CFTs to what the $2 \to 2$ scattering amplitude plays in ordinary QFTs. In flat space S-matrix theory discontinuities encode absorptive data, and unitarity relates poles and cuts to on shell intermediate states, and particle production. Generic CFTs have no S-matrix. The conformal block is not an on shell scattering amplitude in Mandelstam variables. However as we analytically continue the cross ratio space of (2.16) from Euclidean to Lorentzian signature the conformal block gets branch cuts giving rise to monodromies and discontinuities that play a similar role. A heuristic map is

$$\begin{aligned} T(s,t) &\leftrightarrow \mathcal{G}(z,\bar{z}), \\ \operatorname{Disc} T &\leftrightarrow \operatorname{dDisc} \mathcal{G}, \\ \text{Froissart–Gribov} &\leftrightarrow \text{Lorentzian inversion}. \end{aligned} \tag{2.20}$$

This is an analogy, not an equivalence. CFT unitarity is not flat space elastic unitarity, and the discontinuity is defined by analytic continuation of cross ratio space, not by on shell flat space unitarity (Simon Caron-Huot, 2017; Simmons-Duffin, Stanford, and Witten, 2018; Kologlu et al., 2020; Simon Caron-Huot, Mazac, et al., 2021a). Note in particular that it is the double discontinuity of the conformal block that plays an analogous role to the discontinuity of the scattering amplitude.

Commutators, the double discontinuity, and Lorentzian inversion

The cuts in the conformal block give rise to monodromies. As we analytically continue from Euclidean space, through complexified cross ratio space to Lorentzian space, we probe these monodromies. In the standard identical-scalar Lorentzian ordering/causal diamond used in the inversion formula, one has schematically (Simon Caron-Huot, 2017; Simmons-Duffin, Stanford, and Witten, 2018)

$$\langle[\phi(x_4),\phi(x_1)]\,[\phi(x_2),\phi(x_3)]\rangle_{\text{stripped}} \propto \mathcal{G}^{\circlearrowleft} + \mathcal{G}^{\circlearrowright} - 2\mathcal{G} \propto -\text{dDisc}\,\mathcal{G}. \tag{2.21}$$

The different operator orderings are boundary functionals of different Euclidean holomorphic functions, and hence realize different analytic continuations of the conformal block. When the continuation passes through a cut of the conformal block it is denoted by $\circlearrowleft$ or $\circlearrowright$ depending on the direction it passes through the cut. For nonidentical external operators this formula is modified by phases determined by the external dimensions. While this will play an analogous role to the discontinuity of the $2 \to 2$ scattering amplitude, this here is a double discontinuity, not a discontinuity.

The Lorentzian inversion formula leverages the analytic properties of the conformal blocks to extract a function $C(\Delta, J)$ whose residues at poles are $-\lambda^2_{\phi\phi\mathcal{O}}$.

$$c(\Delta, J) \;=\; \frac{\kappa_{\Delta+J}}{4}\int_0^1 dz\, d\bar{z}\; \mu(z,\bar{z})\, g_{J+d-1,\,\Delta-d+1}(z,\bar{z})\,\text{dDisc}[\mathcal{G}(z,\bar{z})] \;+\; \big(u\text{-channel}\big), \tag{2.22}$$

where μ and κ are known objects (Simon Caron-Huot, 2017; Simmons-Duffin, Stanford, and Witten, 2018).

2.5 Bootstrap

The bootstrap is a family of techniques that places constraints on allowed theories based on physical consistency conditions. In the conformal bootstrap the constraints are on the conformal data: the spectrum and the OPE coefficients. In the S-matrix bootstrap the constraints are on the Wilson coefficients of the low energy effective field theory (EFT).

The conformal bootstrap

The key ingredient in the conformal bootstrap is the crossing symmetry of the different expansions of the conformal block expansion discussed in section 2.3. We will mostly focus on the s and t channels. For identical scalars the stripped four point function $\mathcal{G}(z,\bar{z})$ produces the crossing equation

$$\big[(1-z)(1-\bar{z})\big]^{\Delta_\phi}\,\mathcal{G}(z,\bar{z}) = (z\bar{z})^{\Delta_\phi}\,\mathcal{G}(1-z,1-\bar{z}). \tag{2.23}$$

Incorporating (2.23) into the conformal block expansion gives us

$$\sum_{O \in \phi \times \phi} \lambda^2_{\phi\phi O} F_{\Delta,J}(z, \bar{z}) = 0, \tag{2.24}$$

where the sum is over all operators in the $\phi\phi$ OPE, and

$$F_{\Delta,J}(z,\bar{z}) = \left[(1-z)(1-\bar{z})\right]^{\Delta_\phi} G_{\Delta,J}(z,\bar{z}) - (z\bar{z})^{\Delta_\phi} G_{\Delta,J}(1-z, 1-\bar{z}). \tag{2.25}$$

Unitarity places constraints on the allowed dimensions and forces $\lambda^2 \geq 0$[4]. Acting on (2.24) by a linear functional ω gives us

$$\sum_{O \neq 1} \lambda^2_{\phi\phi O}\, \omega\left[F^{\Delta_\phi}_{\Delta,J}\right] \;=\; -\,\omega\left[F^{\Delta_\phi}_{0,0}\right]. \tag{2.26}$$

Where we have separated out the identity operator. If ω can be chosen so that $\omega[F^{\Delta_\phi}_{\Delta,J}] \geq 0$ for every (Δ, J) in some allowed region while $\omega[F^{\Delta_\phi}_{0,0}] \neq 0$, then any CFT in this spectrum is excluded. This is the heart of the numerical bootstrap, one tries to find such a functional, and use it to rule out conformal data, this recasts finite searches as semidefinite programs solved using SDPB. The 3d Ising CFT is the iconic application, but modern variants use mixed correlators, OPE coefficients, and spinning operators (Rattazzi et al., 2008; Simmons-Duffin, 2017; Simmons-Duffin, 2015; Poland, Rychkov, and Vichi, 2019; El-Showk and Paulos, 2013; El-Showk, Paulos, et al., 2014; Kos, Poland, and Simmons-Duffin, 2014; Kos, Poland, Simmons-Duffin, and Vichi, 2016).

There is a related cluster of techniques known as the analytical bootstrap which extracts information about the conformal data from analytic constraints on the four point function. These usually work leveraging a very small or very large parameter which makes extracting analytic information possible, parameters such as $\epsilon, 1/N, 1/J$. An example of the latter is seen in the fact that the s channel conformal blocks do not each exhibit the t channel lightcone singularity at $\bar{z} \to 1$. The s channel conformal expansion realizes this divergence at large J through an infinite tower of double twist operators $\tau_n \to 2\Delta_\phi + 2n + J$ and OPE coefficients asymptoting the generalized free field theory values (Fitzpatrick, Kaplan, et al., 2013; Komargodski and Zhiboedov, 2013; Simon Caron-Huot, 2017).

[4] Here this is the identical/real scalar setup; for mixed or spinning correlators the corresponding statement is matrix positivity.

The techniques in Chapter 3 are not quite in either camp, as they use analytic properties of conformal blocks to obtain sum rules which can then be used in the numerical bootstrap (Mazac, 2016; Mazac and Paulos, 2019; Carmi and Simon Caron-Huot, 2020; Mazáč, Rastelli, and X. Zhou, 2021; Joao Penedones, Silva, and Zhiboedov, 2020; Simon Caron-Huot, Mazac, et al., 2021b; Carmi, Joao Penedones, et al., 2021; Meltzer, 2021; Kologlu et al., 2020; Simon Caron-Huot, Mazac, et al., 2021a).

The S-matrix bootstrap

In gapped flat space QFTs, under the standard analyticity, crossing, unitarity, and Regge-boundedness assumptions used in dispersion theory, the $2 \to 2$ scattering amplitude $T(s,t)$ is taken to be analytic away from poles and cuts (Eden et al., 1966; Martin, 1965; Simon Caron-Huot and Van Duong, 2021; Correia, Sever, and Zhiboedov, 2020). This analyticity, along with partial wave unitarity and crossing as in (2.12), strongly constrains allowed dynamics. Supposing we have a theory where at fixed physical $t \leq 0$ the s channel cut begins at M^2, then we can relate the amplitude to an integral around the cut via a dispersion relation. For example,

$$T(s,t) \;=\; a(t) + s\,b(t) \;+\; \frac{s^2}{\pi}\int_{M^2}^{\infty} \frac{ds'}{(s')^2\,(s'-s)}\,\mathrm{Disc}_{s'}T(s',t) \;+\; \big(s \leftrightarrow u\big), \tag{2.27}$$

where M^2 is the s channel particle production threshold. The extra terms in (2.27) are related to the factor of $1/s^2$ in the integrand where it ensures that the arc at infinity can be neglected. These are called subtraction factors, and similar techniques will play a role in the analytic techniques in Chapter 3. The absorptive discontinuity is related by unitarity to partial wave amplitudes via $\mathrm{Disc}_s T_J(s) \geq |T_J(s)|^2 \geq 0$. If we expand both sides in the limits $(s, t \to 0)$ we can relate, order by order, low energy EFT coefficients on the left to positive contributions from the UV on the right. This bound can then, as with the conformal bootstrap, rule out EFT Wilson coefficients thus constraining the allowable consistent low energy EFTs.

In both the conformal and S-matrix bootstraps we are leveraging a sign definite UV absorptive contribution, integrated against a positive kernel, to give constraints on IR data (Adams et al., 2006; Bellazzini, Elias Miró, et al., 2021; Simon Caron-Huot and Van Duong, 2021; Arkani-Hamed, T.-C. Huang, and Y.-t. Huang, 2021; Tolley, Wang, and S.-Y. Zhou, 2021; Sinha and Zahed, 2021; Correia, Sever, and Zhiboedov, 2020).

2.6 QFT in curved spacetimes

At a local level, the difference between QFT in flat space vs curved space is analogous to the distinction between classical physics in co-inertial reference frames and general covariance. At first glance this seems to give us a lot of leverage, on a semi Riemannian manifold (M, g) we can write an action e.g. for a real scalar

$$S[\phi; g] = -\frac{1}{2}\int_M d^d x\sqrt{-g}\left(g^{ab}\nabla_a\phi\nabla_b\phi + m^2\phi^2 + \xi R\phi^2\right), \tag{2.28}$$

which generates equations of motion

$$P\phi = (\Box_g - m^2 - \xi R)\phi = 0. \tag{2.29}$$

This is structurally the same as flat space with just a metric introduced into the action and an appropriate metric informed $\Box_g$. We can compute correlation functions, if the spacetime is globally hyperbolic, there are unique advanced and retarded Green functions $E_{R/A}$ to go with it

$$PE_{R/A}f = f, \qquad \mathrm{supp}(E_R f) \subset J^+(\mathrm{supp} f), \qquad \mathrm{supp}(E_A f) \subset J^-(\mathrm{supp} f), \tag{2.30}$$

and a related causal propagator

$$E := E_R - E_A \tag{2.31}$$

We can quantize smeared fields

$$\phi(f) = \int_M d^d x\sqrt{-g}\,\phi(x)f(x), \qquad f \in C_0^\infty(M). \tag{2.32}$$

modulo

$$\phi(Pf) = 0, \qquad \phi(f)^* = \phi(\overline{f}), \qquad [\phi(f), \phi(h)] = iE(f, h)\mathbb{I}, \tag{2.33}$$

and define an algebra $\mathcal{A}(O)$ associated to any $O \subset M$ as the algebra generated by smearing test functions with support on O. With this construction, we get locality, covariance, causal propagation, and operator valued distributions (Wald, 1994; Hollands and Wald, 2015; Birrell and Davies, 1982; Parker and Toms, 2009).

We can define states as linear functionals which satisfy

$$\omega : \mathcal{A}(M, g) \to \mathbb{C}, \qquad \omega(A^*A) \geq 0, \qquad \omega(\mathbb{I}) = 1, \tag{2.34}$$

and n-point distributions

$$W_n(f_1, \ldots, f_n) = \omega\big(\phi(f_1) \cdots \phi(f_n)\big). \tag{2.35}$$

We even know what form these correlation functions need to take, the short distance limit of the two point function for example takes a Hadamard form

$$W_2(x, y) = \frac{1}{4\pi^2}\left[\frac{u(x, y)}{\sigma(x, y) + i0\,t(x, y)} + v(x, y)\log\left(\mu^2(\sigma(x, y) + i0\,t(x, y))\right)\right] + w_\omega(x, y), \tag{2.36}$$

where $\sigma(x, y)$ is the squared geodesic distance between x and y, and $w_\omega(x, y)$ is smooth. This constrains the singularities to be the physical null singularities familiar from Minkowski space. The singular part is universal and locally determined by the metric, and this allows us to do Wick contractions, define time ordered products, do point splitting regularization, and define finite stress tensors from composite operators. Renormalization ambiguities are local curvature terms and so perturbative renormalization still works (Wald, 1994; Radzikowski, 1996; Hollands and Wald, 2001; Hollands and Wald, 2002; Birrell and Davies, 1982).

What does not automatically carry over is anything related to global structure, there is no global asymptotics, and different observers may not have access to the same portion of the spacetime, in general there is no preferred vacuum, no preferred Fock like decomposition, the notion of global particle number need not exist, there is no Poincaré symmetry, nor Hamiltonian positivity, there may be no asymptotic particle states, and hence no S-matrix (Birrell and Davies, 1982; Wald, 1994; Parker and Toms, 2009; Hollands and Wald, 2015). In fact the notion of particle does not carry over since in flat space we define a particle as an irreducible representation of the Poincaré group, a manifestly flat space notion. Long range order and related notions such as instantons, and spontaneous symmetry breaking may not exist.

Analytic continuation to Euclidean signature does not work the same way either. Flat Minkowski space and Euclidean space are both the same manifold, but take a generic Lorentzian manifold, analytically continue its metric to Euclidean signature, and you have an entirely different manifold, moreover the continuation may not be unique.

So while quantum field theory in curved spacetimes makes sense, many of the techniques we are used to from Minkowski space do not simply carry over. As an incomplete list of techniques we lose in generic spacetimes, consider the following: the Källen-Lehmann spectral decomposition, Wigner classification, Mandelstam invariants, amplitudes, LSZ reduction, the canonical global flat-space momentum-space/S-matrix perturbation theory around a preferred vacuum, the optical theorem, cutting rules, cluster decomposition, Coleman-Mandula, the analytic continuation from Euclidean space, soft theorems and the IR triangle...

2.7 de Sitter QFT

de Sitter is of course a curved spacetime, it approximates the behavior of our universe during inflation, and may be the right description of the far future of our universe. Chapter 4 has a nice introduction to de Sitter which I will not reproduce here, rather, I will use this section to take a step back and just discuss the state of QFT in de Sitter since that isn't well known. If you need some refreshers on the basic geometry of de Sitter see Chapter 4, especially section 4.2. There are three main ways of studying QFT on a de Sitter background, the inflationary regime, global de Sitter, and the observer's point of view (S. Perlmutter et al., 1998; Riess et al., 1998; Achúcarro et al., 2022; Baumann et al., 2024).

The inflationary regime is the most well studied for two reasons, firstly it clearly describes the physics of an era in our universe, secondly it is amenable to slightly modified flat space techniques. This regime is tractable for two related reasons; the first is that the observables are not generic bulk fields in de Sitter, but spatial correlators of light degrees of freedom that survive the de Sitter redshift until reheating, the second is that in the far-future expanding Poincaré patch the scale factor diverges. In the expanding Poincaré patch, described by (4.3) and Figure 4.3, we are taking the $\eta \to 0^-$ limit which is a spacelike future boundary of de Sitter (Achúcarro et al., 2022; Baumann et al., 2024; Strominger, 2001). After stripping off this conformal factor, in the conformal frame described by (4.34) and (4.35), the late-time data live on Euclidean $\mathbb{R}^3$ and the de Sitter isometry group $SO(1,d)$ acts on it as its conformal group (Strominger, 2001; Baumann et al., 2024). This is why flat-space and conformal techniques become useful in the subhorizon and boundary-correlator regimes. One way to see this is to notice that bulk fields have fixed late time falloff

$$\phi(\eta, \vec{x}) \sim \eta^{\Delta_-} O_-(\vec{x}) + \eta^{\Delta_+} O_+(\vec{x}) \tag{2.37}$$

and so at late times behave like conformal primaries. Massive bulk fields only appear through their effects on late-time correlators, unless they remain light enough to be part of the late-time data. These tools do not automatically generalize to bulk de Sitter as their power comes from the late-time falloff and the approximate description in terms of flat conformal behaviour.

A second approach is to study de Sitter globally, a drawback of this approach is that this is a "god's eye view" of the spacetime in that there is no observer within de Sitter that can ever see this full spacetime, as illustrated by Figure 4.2 and Figure 4.4. Nonetheless what it has going for it is that it maximally leverages the symmetry of de Sitter. There is a clean analytic continuation to the sphere; in the Euclidean/Bunch-Davies construction this gives a preferred vacuum and strong analytic control on suitable invariant/Hadamard correlators in this vacuum (Bunch and Davies, 1978; Bros and Moschella, 1996; Bros, Epstein, and Moschella, 1998). The representation theory of fixed-background de Sitter QFT is well developed, and it is organized in a way that is very different from that in Minkowski space. For starters, it is dimension dependent. In Minkowski space we are used to the basic distinction between massive and massless representations, with labels such as (m^2, J). In de Sitter, representations are organized by labels such as (Δ, J) (Sun, 2024; Joao Penedones, Vaziri, and Sun, 2023); Δ is in some ways analogous to mass, but the structure is richer: there are massive representations below and above the de Sitter scale, massless representations, and genuinely new objects such as partially massless representations. The simplest Δ classes are the principal and complementary series, where Δ is complex or real depending on whether the relevant mass parameter is greater or smaller than the inverse length of de Sitter, and there are also exceptional series with Δ a real integer. For scalars, the relation between Δ and the mass parameter is particularly simple, and this is the one displayed later in Chapter 4 in (4.61). There are still open questions here, such as a clear understanding of how vector representations can appear in the tensor product of two scalar representations, and more generally what representations can lie in tensor products of spinor representations.

Nonetheless, we can use this to organize a Hilbert space of states, and can construct an analog of the Källen-Lehmann spectral decomposition with positive spectral densities (Joao Penedones, Vaziri, and Sun, 2023; Loparco et al., 2023). The IR was initially thought to be unmanageable and would lead to a breakdown of de Sitter quantities, but in recent years an EFT for the soft sector was studied, and in that regime some of the pressing issues have been brought under control (Akhmedov, Moschella, and Popov, 2019; Hu, 2018; Green, 2023; Cohen and Green, 2020). Another nice feature is that there exists a fully solved interacting QFT in global de Sitter although part of what makes it solvable is that the interactions reorganize the degrees of freedom to essentially be free particles again (Anninos, Anous, and Rios Fukelman, 2024; Aguilera-Damia et al., 2026). The status of long range order and SSB in de Sitter is similarly subtle. There were early arguments, analogous in spirit to the Coleman-Mermin-Wagner theorems in 2d Minkowski space, that IR effects obstruct persistent symmetry breaking in de Sitter (Ford and Vilenkin, 1986; Ratra, 1985). However, this should not be read as a universal no-go theorem: the conclusion depends on the symmetry, the observables, and the regime being studied. Recent exactly solvable examples show that discrete symmetries can remain spontaneously broken in de Sitter (Aguilera-Damia et al., 2026), while soft de Sitter EFT (Green, 2023; Cohen and Green, 2020) gives a more controlled way of organizing the IR effects that made the older arguments difficult to interpret.

A final approach is the one taken in this thesis, which we justify in greater detail in Chapter 4 and use in section 4.4: to organize QFT around an observer and what they can see and measure. This is the least studied approach, but also what I believe is the correct one. Taking our own universe for example, supposing we do have a positive cosmological constant, the only important questions we can ever test and confirm are those which take into account that we can only access part of the universe. We will never know if it is truly asymptotically de Sitter and so that cannot matter. All that matters is physics in the presence of a cosmological constant restricted to our observable section. A nice aspect of this approach is that it can be seen as the physics of an observer in the nicest spacetime where they do not have access to the asymptotics. The usual way to do this is to work strictly within the static patch, whose metric and causal diamond are reviewed in (4.4) and Figure 4.4. To make contact with the above, the static patch has a Euclidean thermal or periodic continuation, distinct from the global Euclidean-sphere continuation. Static-patch approaches include worldline/static-patch symmetry, static-patch scattering, horizon edge partition functions, and real-time thermal observables (Anninos, Hartnoll, and Hofman, 2012; Albrychiewicz and Neiman, 2021; Law, 2025; Grewal and Law, 2025). This generalizes more readily to a wider range of spacetimes, as discussed in section 4.5, and even has echoes in quantum gravity (Chandrasekaran et al., 2023;

Susskind, 2021).

Chapter 3

SPINNING DISPERSIVE CFT SUM RULES AND BULK SCATTERING

3.1 Introduction

Causality and unitarity imply constraints on the space of low-energy effective field theories (EFTs) (Aharonov, Komar, and Susskind, 1969; Pham and Truong, 1985). In a $2 \to 2$ scattering process, causality and unitarity manifest as analyticity, Regge boundedness, and crossing symmetry of the S-matrix. Using these properties, one can derive dispersion relations that express the Wilson coefficients of a low-energy EFT in terms of data in the ultraviolet (UV), which have positive spectral density thanks to unitarity (Adams et al., 2006; Camanho et al., 2016). By applying functionals (such as expanding around the forward limit) to dispersion relations, positivity of the UV spectral density can be used to obtain two-sided bounds on EFT Wilson coefficients, with the correct scaling in the EFT cutoff M expected by dimensional analysis. A systematic exploration of this approach was initiated recently in (Bellazzini, Elias Miró, et al., 2021; Simon Caron-Huot and Van Duong, 2021; Arkani-Hamed, T.-C. Huang, and Y.-t. Huang, 2021; Tolley, Wang, and S.-Y. Zhou, 2021; Sinha and Zahed, 2021).

Including gravitational interactions introduces another layer of complexity, since graviton exchange produces divergences in the forward limit. This issue was overcome in (Simon Caron-Huot, Mazac, et al., 2021c) by considering functionals that measure the scattering amplitude at small impact parameter. This method has paved the way for deriving bounds on higher-derivative corrections to General Relativity in flat space (Simon Caron-Huot, Li, et al., 2023a; Simon Caron-Huot, Li, et al., 2023b; Häring and Zhiboedov, 2022; Henriksson et al., 2022; McPeak, Venuti, and Vichi, 2023).

Similar questions can be explored in Anti-de Sitter (AdS) space as well. Furthermore, via the AdS/CFT correspondence, these questions can be phrased — and potentially answered — in CFT language. For example, HPPS conjectured in (Heemskerk et al., 2009) that a large-N CFT should have a local bulk EFT dual if its single trace spectrum has a large gap $\Delta_{\text{gap}} = MR_{\text{AdS}} \gg 1$ for $J > 2$, where R_{AdS} is the AdS radius and M is the cutoff scale of the bulk EFT. Significant progress towards establishing this conjecture using CFT techniques was made in e.g. (Camanho et al., 2016; Hartman, Jain, and Kundu, 2016; Afkhami-Jeddi et al., 2017; Meltzer and E. Perlmutter, 2018; Kulaxizi, Parnachev, and Zhiboedov, 2018; Simon Caron-Huot, 2017; Costa, Hansen, and João Penedones, 2017; Belin, Hofman, and Gregoire Mathys, 2019; Kologlu et al., 2020). Recently, part of the HPPS conjecture was established in (Simon Caron-Huot, Mazac, et al., 2021a) by building a dictionary between conformal bootstrap functionals and flat space dispersion relations. The authors of Simon Caron-Huot, Mazac, et al., 2021a considered a weakly-coupled EFT in AdS with a massless graviton and a scalar with mass $m_\phi = O(\frac{1}{R_{\text{AdS}}})$. Schematically, the low-energy effective action is

$$S = S_{\text{gravity}} + \int d^D x \sqrt{-g} \left(\frac{1}{2} \phi (\partial^2 - m_\phi^2) \phi + \sum_n g_n D^{2n} \phi^4 + \dots \right), \tag{3.1}$$

where S_{gravity} contains graviton interactions and will be given below. Using bootstrap methods, they derived bounds on the higher-derivative interactions g_n in (3.1) with the expected suppression in Δ_{gap}.

The main tool in this analysis is dispersive CFT sum rules (Mazac, 2016; Mazac and Paulos, 2019; Carmi and Simon Caron-Huot, 2020; Mazáč, Rastelli, and X. Zhou, 2021; Joao Penedones, Silva, and Zhiboedov, 2020; Simon Caron-Huot, Mazac, et al., 2021b; Carmi, Joao Penedones, et al., 2021; Meltzer, 2021; Knop and Mazac, 2022), which have double zeros at the locations of most double-twist operators. Such sum rules allow one to separate out light double-trace contributions in holographic CFTs, and express the light contribution ($\Delta < \Delta_{\text{gap}}$) described by (3.1) in terms of a sum of heavy conformal blocks with positive coefficients. Remarkably, in a certain “flat space limit" that we review in section 3.2, dispersive CFT sum rules reduce to the flat space sum rules previously studied in (Simon Caron-Huot, Mazac, et al., 2021c). As a result, flat space functionals can be uplifted to AdS and lead to bounds on the EFT couplings in (3.1).[1]

Given the bounds on graviton interactions in flat space obtained recently (Simon Caron-Huot, Li, et al., 2023a; Simon Caron-Huot, Li, et al., 2023b; Häring and Zhiboedov, 2022; Henriksson et al., 2022; McPeak, Venuti, and Vichi, 2023), we would like to derive similar bounds on graviton interactions in AdS, in particular establishing HPPS for purely gravitational theories. More precisely, let us consider

[1]The “uplifting" procedure only guarantees positivity of the functional in the “bulk point" regime discussed below. One must additionally check other regimes to derive a rigorous CFT bound.

an EFT with only a massless graviton with the effective action

$$S_{\text{gravity}} = \frac{1}{16\pi G} \int d^D x \sqrt{-g} \left(-2\Lambda + R + \alpha_2 R^2 + \alpha_3 R^3 + \dots \right), \tag{3.2}$$

where $\Lambda = -(D-1)(D-2)/(2R_{\text{AdS}}^2)$. We would like to obtain bounds like

$$|\alpha_2| \leq \frac{\#}{\Delta_{\text{gap}}^2}. \tag{3.3}$$

On the CFT side, this means we must construct dispersive sum rules for four-point functions of stress tensors whose flat space limit agrees with flat space sum rules for gravitons.

Conceptually, this task is similar to the one undertaken in (Simon Caron-Huot, Mazac, et al., 2021a). However, stress tensor four-point functions are technically more complicated due to the profusion of tensor structures, and we need to organize the calculation carefully. Our approach is to begin with "subtracted superconvergence" sum rules, which exploit the fact that the commutator of null-integrated operators on the same null plane should vanish (Kologlu et al., 2020). In particular, we focus on the action of such sum rules on a heavy conformal block (with $\Delta > \Delta_{\text{gap}}$). This action is a spacetime integral that, in the flat space limit, localizes to a certain saddle configuration that we call the "scattering crystal." Thus, the computation of the heavy action turns into evaluating conformally-invariant structures at this saddle, which is straightforward for spinning operators. Our calculation gives a "spacetime interpretation" of the results of (Simon Caron-Huot, Mazac, et al., 2021a) for scalar operators.

The result of our saddle analysis has a simple interpretation in flat space. The inserted conformal blocks become flat space partial waves, and the subtracted superconvergence sum rule becomes a sum rule for flat space "shock" amplitudes (Camanho et al., 2016; Kologlu et al., 2020). Thus, by comparing the action of CFT sum rules on heavy blocks to the action of flat-space sum rules on heavy states, we can deduce a concrete dictionary between dispersive CFT functionals and flat space sum rules.[2] Our sum rules for stress tensors become a subset of the known flat space sum rules for gravitons (Simon Caron-Huot, Li, et al., 2023b). The full set of flat space sum rules for gravitons includes additional sum rules that cannot be expressed in terms of "shock amplitudes" (because they have different choices

[2]Once we know the dictionary, it follows that the contributions of light states must match between AdS and flat space as well, though we leave exploration of light states to future work.

of external polarizations). We leave the problem of obtaining these additional sum rules using CFT techniques to future work. Our dictionary will be needed to convert the flat space functionals with positive action on partial waves into CFT functionals with positive action on heavy blocks.

This paper is organized as follows. In section 3.2, we briefly review superconvergence sum rules and the derivation of the scalar bounds in (Simon Caron-Huot, Mazac, et al., 2021a). In section 3.3, we derive a simple formula for the flat space limit of superconvergence sum rules for scalars using a spacetime saddle-point analysis. We then generalize the formula to spinning operators. In section 3.4, we explain how this formula can be matched to flat space sum rules, and obtain the dictionary between spinning CFT sum rules and flat space sum rules for photons and gravitons. We conclude in section 3.5. We summarize our conventions in appendix 3.A, and present an alternative derivation of the flat space limit formula in appendix 3.B. Technical details on matching the CFT sum rules to flat space are given in appendices 3.C, 3.D, and 3.E.

3.2 Review: superconvergence sum rules

Let us start by reviewing the idea of superconvergence in CFT, and explain how it can be related to flat space dispersive sum rules. Along the way we will introduce notation that we use throughout this work.

The light transform and superconvergence

Subtracted superconvergence sum rules come from studying the commutator of two null-integrated operators on the same null plane (Kologlu et al., 2020). For simplicity we first consider a four-point function of scalar operators. Let us choose lightcone coordinates $x = (u, v, \vec{y})$ with $x^2 = -uv + \vec{y}^2$. A subtracted superconvergence sum rule can be written explicitly as

$$\int_{-\infty}^{\infty} dv_1 \int_{-\infty}^{\infty} dv_3 f(v_1, v_3)\langle 0|\phi_4[\phi_3(0, v_3, \vec{y}_3), \phi_1(0, v_1, \vec{y}_1)]\phi_2|0\rangle = 0, \qquad (3.4)$$

where ϕ_1, ϕ_3 are placed on the same null plane $u = 0$. This integral vanishes for a simple reason: since $x_{13}^2 = \vec{y}_{13}^2 > 0$, the two operators ϕ_1, ϕ_3 are spacelike separated in the entire integration range, and therefore their commutator must vanish.

To obtain a sum rule, we would like to separate the two orderings $\phi_3\phi_1$ and $\phi_1\phi_3$ and perform the integral separately for each ordering. However, in order for this to be valid, we must check that each integral converges — in particular that there is no divergence from the endpoints of the integration contours. See (Kologlu et al.,

2020) for a detailed analysis of this convergence condition. In the end, convergence can be achieved by a suitable choice of the function $f(v_1, v_3)$, which we call a "subtraction" factor. Expressions for subtraction factors will be given in section 3.3.

Our goal in this section is to rewrite (3.4) as a conformally-invariant spacetime integral, using tools from (Kravchuk and Simmons-Duffin, 2018b). First, let us introduce index-free notation. For an ordinary integer-spin operator O, we contract the indices with a null polarization vector z:

$$O(x,z) = O^{\mu_1\cdots\mu_J} z_{\mu_1}\cdots z_{\mu_J}, \quad z^2 = 0. \tag{3.5}$$

More generally, for a representation ρ represented by a Young diagram with more than one row, we introduce polarizations $z, w, \widetilde{w}, \ldots$ for each row of the Young diagram. They should be null and mutually orthogonal. Due to antisymmetry between indices in different rows, we have gauge redundancies $w \sim w + \#z$, $\widetilde{w} \sim \widetilde{w} + \#w + \#z$, etc. The number of boxes in each row of the Young diagram encodes the homogeneity of the corresponding polarization vector. Generalizing to arbitrary homogeneity in the polarization vector z allows us to describe representations with continuous spin, which will be crucial in later calculations.[3]

Index-free notation can be viewed as the embedding space formalism (Dirac, 1936; Costa, Joao Penedones, et al., 2011) for the Lorentz group $\mathrm{SO}(d-1,1)$. In the embedding space of the d-dimensional conformal group $\mathrm{SO}(d,2)$, one promotes the position x and polarization z to $X, Z \in \mathbb{R}^{d,2}$ satisfying $X^2 = X\cdot Z = Z^2 = 0$ and $Z \sim Z + \#X$. Then, conformal transformations act linearly on X, Z, and conformally-invariant structures are simply built from dot products of X and Z. We can recover the Minkowski space operator by the dictionary

$$O(x,z) = O(X = (1, x^2, x^\mu), Z = (0, 2x\cdot z, z^\mu)), \tag{3.6}$$

where we again use lightcone coordinates $X = (X^+, X^-, X^\mu)$, and $X^2 = -X^+X^- + X^\mu X_\mu$. We will often go between embedding space and Minkowski space when writing expressions for conformally-invariant structures. In (3.208), we review the embedding space description of operators with more complicated representations.

The embedding space vector X lives on a projective null cone in $\mathbb{R}^{d,2}$, which is topologically $S^1 \times S^{d-1}$. Correlation functions of Lorentzian CFTs live on the universal cover $\widetilde{\mathcal{M}}_d = \mathbb{R}\times S^{d-1}$, also called the Lorentzian cylinder. More precisely,

[3] For the Lorentzian conformal group $\mathrm{SO}(d,2)$, their unitary principal representations have two continuous parameters, Δ and J (Kravchuk and Simmons-Duffin, 2018b).

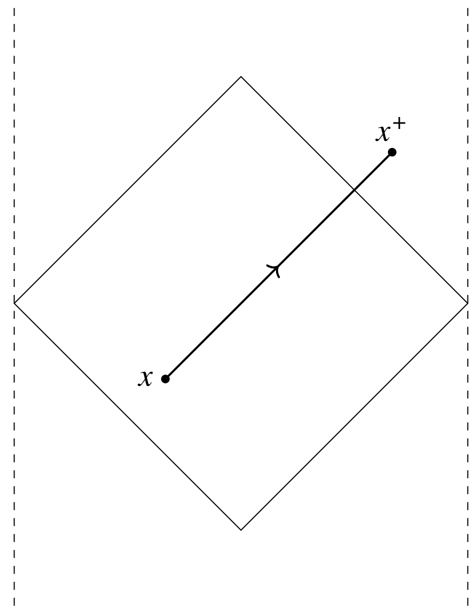

Figure 3.1: Contour of the light transform on the Lorentzian cylinder, where the two dashed lines should be identified. The contour starts at point x and ends at x^+ on the next Poincaré patch.

CFT correlation functions on $\mathbb{R}^{d-1,1}$ can be analytically continued to their Lorentzian cylinder counterparts (Luscher and Mack, 1975). The Lorentzian cylinder is tiled by Poincaré patches, where each patch represents a Minkowski space $\mathbb{R}^{d-1,1}$. The conformal group acting on $\widetilde{\mathcal{M}}_d$ is the universal covering group $\widetilde{\mathrm{SO}}(d,2)$. There exists a symmetry $\mathcal{T}$ such that for each point $p \in \widetilde{\mathcal{M}}_d$, all light-rays emanating from p will converge at $\mathcal{T}p$ in the next Poincaré patch. The action of $\mathcal{T}$ on an operator is most easily described in the embedding space, where we have

$$\mathcal{T}\mathcal{O}(X, Z_1, Z_2, \ldots)\mathcal{T}^{-1} = \mathcal{O}(-X, -Z_1, -Z_2, \ldots). \tag{3.7}$$

We will also use the notation $p^+ \equiv \mathcal{T}p$, $p^- \equiv \mathcal{T}^{-1}p$.

The null-integrated operators in (3.4) are an example of a conformally-invariant integral transform called the light transform (Kravchuk and Simmons-Duffin, 2018b). The light transform of a local operator $\mathcal{O}$ with quantum numbers (Δ, J) is defined as

$$\mathbf{L}[\mathcal{O}](x,z) = \int_{-\infty}^{\infty} d\alpha (-\alpha)^{-\Delta-J}\mathcal{O}\left(x - \frac{z}{\alpha}, z\right). \tag{3.8}$$

Under conformal transformations, $\mathbf{L}[\mathcal{O}](x,z)$ transforms like a primary operator at x. The light transform contour is shown in figure 3.1. It starts at the point x, goes along the direction of the polarization z, and eventually ends at the point $\mathcal{T}x = x^+$.

The previous description of the null-integrated operator in (3.4), where one puts the operator at $u = 0$ and integrates along v, can be obtained by putting x at past null infinity.

In the embedding space, the light transform (3.8) becomes

$$\mathbf{L}[\mathcal{O}](X,Z) = \int_{-\infty}^{\infty} d\alpha\, \mathcal{O}(Z - \alpha X, -X). \tag{3.9}$$

From this expression, it is not hard to see that the quantum numbers of $\mathbf{L}[\mathcal{O}]$ are $(1-J, 1-\Delta)$. The light transform of a local operator annihilates the vacuum (Kravchuk and Simmons-Duffin, 2018b):

$$\mathbf{L}[\mathcal{O}](x,z)|\Omega\rangle = 0. \tag{3.10}$$

With all this in place, we can now write the subtracted superconvergence sum rule as a conformally-invariant spacetime integral. We define a functional $\Psi_{k,v}$ by[4]

$$\Psi_{k,v}[\mathcal{G}] \equiv \int \frac{d^dx_2 d^dx_4 d^dx_0 D^{d-2}z_1 D^{d-2}z_3}{\mathrm{vol}(\widetilde{\mathrm{SO}}(d,2))} K_{k,v}(x_2,x_4,x_0,z_1,z_3) \\ \times \langle\Omega|\phi_4(x_4)[\mathbf{L}[\phi_3](x_0,z_3), \mathbf{L}[\phi_1](x_0,z_1)]\phi_2(x_2)|\Omega\rangle, \tag{3.11}$$

where $K_{k,v}$ is a kernel chosen such that the integral is conformally-invariant. Its explicit expression is given below in (3.33). The integral measure for the polarization $D^{d-2}z$ is defined as (Simmons-Duffin, 2014)

$$D^{d-2}z \equiv \frac{2d^dz\delta(z^2)\theta(z^0)}{\mathrm{vol}\,\mathbb{R}_+}, \tag{3.12}$$

where $\mathbb{R}_+$ acts by rescaling z. Then, the superconvergence condition (3.4) is equivalent to

$$\Psi_{k,v}[(\text{subtractions}) \times \mathcal{G}] = 0, \tag{3.13}$$

where $\mathcal{G}$ is a four-point function and (subtraction) corresponds to the factor $f(v_1, v_3)$ in (3.4) (we discuss them in more detail below).

Using (3.10), we can rewrite (3.11) as

$$\Psi_{k,v}[\mathcal{G}] = \int \frac{d^dx_2 d^dx_4 d^dx_0 D^{d-2}z_1 D^{d-2}z_3}{\mathrm{vol}(\widetilde{\mathrm{SO}}(d,2))} K_{k,v}(x_2,x_4,x_0,z_1,z_3) \\ \times \langle\Omega|[\phi_4(x_4), \mathbf{L}[\phi_3](x_0,z_3)][\mathbf{L}[\phi_1](x_0,z_1), \phi_2(x_2)]|\Omega\rangle - (1 \leftrightarrow 3). \tag{3.14}$$

[4] This functional is equivalent to the $\widetilde{C}_{k,v}$ functional defined in the appendix of (Simon Caron-Huot, Mazac, et al., 2021a).

When we replace the four-point function $\mathcal{G}$ with an s-channel conformal block $G^s_{\Delta,J}$, the double commutator $\langle\Omega|[\phi_4,\mathbf{L}[\phi_3]][\mathbf{L}[\phi_1],\phi_2]|\Omega\rangle$ will give a $\sin^2(\pi\frac{\Delta-J-2\Delta_\phi}{2})$ factor. For double-twist operators $\Delta - J = 2\Delta_\phi + 2n$, the $\sin^2$ factor then becomes a double zero. Therefore, $\Psi_{k,\nu}$ is a dispersive functional, meaning that it gives double zeros for all but finitely many double-twist operators.[5]

The flat space limit of superconvergence sum rules

Let us now review the argument in (Simon Caron-Huot, Mazac, et al., 2021a) that leads to bounds on the scalar AdS EFT (3.1). As explained in the introduction, the idea is that in a certain "flat space limit," dispersive CFT sum rules reduce to flat space sum rules.

Review: flat space sum rules

Let us first briefly review flat space sum rules for identical real scalars. Flat space sum rules for photons and gravitons will be reviewed in section 3.4.

Let $\mathcal{M}(s,u)$ be a $2\to 2$ scattering amplitude for identical scalars, which we assume satisfies analyticity, crossing symmetry, and Regge boundedness. This allows one to write down flat space dispersion relations for $\mathcal{M}(s,u)$ (see e.g., (Simon Caron-Huot and Van Duong, 2021; Simon Caron-Huot, Mazac, et al., 2021c) for more details),

$$-\oint_\infty \frac{ds}{2\pi i}\frac{1}{s}\frac{\mathcal{M}(s,u)}{(s(s+u))^{\frac{k}{2}}} = 0, \tag{3.15}$$

where s,u are the Mandelstam variables,

$$s = -(p_1+p_2)^2, \quad t = -(p_2+p_3)^2, \quad u = -(p_1+p_3)^2. \tag{3.16}$$

The contour in (3.15) can be deformed and separated into two parts: the low energy part, which can be computed using an EFT, and the high energy part, which can be decomposed into partial waves.

The partial wave decomposition of a scalar amplitude $\mathcal{M}(s,u)$ is given by

$$\mathcal{M}(s,u) = s^{\frac{4-D}{2}}\sum_J n_J^{(D)} a_J(s)\mathcal{P}_J\left(1+\frac{2u}{s}\right). \tag{3.17}$$

Here, $n_\rho^{(D)} = \frac{2^{d+1}(2\pi)^{d-1}\dim\rho}{\mathrm{vol}\, S^{d-1}}$, where in our case ρ is the spin-J traceless symmetric tensor representation of $\mathrm{SO}(d)$, and $d = D-1$. Meanwhile $\mathcal{P}_J$ is a Gegenbauer

[5] When there is a subtraction factor, the $\sin^2$ factor gets modified and can become nonzero at finitely many double twist locations (Simon Caron-Huot, Mazac, et al., 2021b).

polynomial,

$$\mathcal{P}_J(x) = {}_2F_1(-J, J+d-2, \tfrac{d-1}{2}, \tfrac{1-x}{2}). \tag{3.18}$$

After the partial wave decomposition, the high energy part of the the dispersion relation (3.15) becomes

$$\left\langle \frac{2m^2+u}{m^2+u} \frac{\mathcal{P}_J(1+\frac{2u}{m^2})}{(m^2(m^2+u))^{\frac{k}{2}}} \right\rangle, \tag{3.19}$$

where $\langle\cdots\rangle$ is a heavy average, defined as a sum with positive coefficients over heavy states with mass m and spin J,

$$\langle\cdots\rangle = \frac{1}{\pi}\sum_J n_J^{(D)} \int_{M^2}^{\infty} \frac{dm^2}{m^2} m^{4-D}\, \mathrm{Im}\, a_J(s)\,(\cdots)\,. \tag{3.20}$$

Unitarity implies that the spectral density $\mathrm{Im}\, a_J(s)$ should be positive (or more generally a positive semidefinite matrix). Therefore, by applying a functional that has positive action on all partial wave contributions (3.19), one can derive inequalities for Wilson coefficients of the low energy EFT. Without gravity, the functional can simply include taking the forward limit $u \to 0$. For amplitudes with graviton exchange, one can integrate (3.19) over u against some kernel (see (Simon Caron-Huot, Mazac, et al., 2021c; Simon Caron-Huot, Li, et al., 2023a; Simon Caron-Huot, Li, et al., 2023b)).

The flat space limit

Consider a large-N CFT whose single-trace spectrum consists of a scalar operator ϕ, the stress tensor $T^{\mu\nu}$, and operators with twists $\tau = \Delta - J$ greater than $\Delta_{\text{gap}} \gg 1$. By the HPPS conjecture, this theory is expected to be dual to an EFT in AdS with the effective action (3.1). The s-channel conformal block decomposition of $\langle\phi\phi\phi\phi\rangle$ is given by

$$\langle\phi\phi\phi\phi\rangle = G_1^s + f_T^2 G^s_{T^{\mu\nu}} + \sum_{n,J} f^2_{[\phi\phi]_{n,J}} G^s_{[\phi\phi]_{n,J}} + \sum_{\tau>\Delta_{\text{gap}}} f^2_{\Delta,J} G^s_{\Delta,J}, \tag{3.21}$$

where f_O is the OPE coefficient, and $[\phi\phi]$ are double-trace operators built from ϕ. Consider now a dispersive functional ω whose action on the four-point function vanishes. Applying it to the conformal block decomposition gives us

$$-\,\omega|_{\text{light}} = \sum_{\tau>\Delta_{\text{gap}}} f^2_{\Delta,J}\,\omega[G^s_{\Delta,J}], \tag{3.22}$$

where

$$\omega|_{\text{light}} \equiv \omega[G^s_1] + f_T^2 \omega[G^s_{T^{\mu\nu}}] + \sum_{n,J} f^2_{[\phi\phi]_{n,J}} \omega[G^s_{[\phi\phi]_{n,J}}]. \tag{3.23}$$

One can argue that $\omega|_{\text{light}}$ is determined by the Wilson coefficients of the low-energy EFT in AdS. Therefore, if we can find a functional ω such that

$$\omega[G^s_{\Delta,J}] \geq 0, \quad \tau > \Delta_{\text{gap}}, \tag{3.24}$$

then positivity of $f^2_{\Delta,J}$ implies that

$$-\omega|_{\text{light}} \geq 0, \tag{3.25}$$

which becomes an inequality on EFT Wilson coefficients.

To study the action of ω on heavy blocks, it is useful to consider two special limits.

- The “bulk point"/“flat space" limit is the regime of large Δ with $J/\Delta \ll 1$. As explained in (Simon Caron-Huot, Mazac, et al., 2021a), this corresponds to an AdS scattering process where the energy m and impact parameter β are given by

  $$m^2 \approx \Delta^2, \quad \beta \approx \frac{2J}{\Delta} \ll 1. \tag{3.26}$$

  The term “flat space" comes from the fact that the impact parameter β is much smaller than the AdS radius (which is 1 in our conventions).

- The Regge limit is the regime of large Δ, J with fixed ratio Δ/J. This corresponds to an AdS scattering process with impact parameter comparable to the AdS radius.

A necessary condition for a functional ω to be positive is that it should be positive in the flat space regime. In this regime, one can relate the action of ω on conformal blocks to the action of simple flat-space dispersion relations. For example,

$$\Psi_{k,\nu;f_k}[\Delta, J] = \frac{2m^2 - \nu^2}{m^2 - \nu^2} \frac{\mathcal{P}_J(1 - \frac{2\nu^2}{m^2})}{(m^2(m^2 - \nu^2))^{\frac{k}{2}}} \left(1 + O\left(\frac{J^2}{m^2}\right)\right), \tag{3.27}$$

where $\mathcal{P}_J$ is a Gegenbauer polynomial given by (3.18). On the left-hand side $\omega[\Delta, J]$ denotes the action of ω on a conformal block, rescaled by some positive factors:

$$\omega[\Delta, J] \equiv \frac{1}{q_{\Delta,J}} \frac{\omega[G^s_{\Delta,J}]}{2\sin^2(\pi\frac{\Delta-J-2\Delta_\phi}{2})}, \tag{3.28}$$

where

$$q_{\Delta,J} = \frac{1}{\pi p^{\text{MFT}}_{\Delta,J}} \frac{2n_J}{m^{2d-4}} \frac{\Gamma(\Delta-1)(2\Delta-d)}{\Gamma(\Delta-d+2)},$$

$$n_J = \frac{2^{d+1}\pi^{\frac{d-1}{2}}}{\Gamma(\frac{d-1}{2})}(J+1)_{d-3}(2J+d-2). \tag{3.29}$$

$p^{\text{MFT}}_{\Delta,J}$ is the OPE coefficient of the Mean Field Theory, whose expression can be found in (Fitzpatrick and Kaplan, 2012).

The functional $\Psi_{k,\nu;f_k}$ denotes a subtracted version of $\Psi_{k,\nu}$, where we insert an additional factor f_k into the integrand. As discussed below (3.4) this factor is needed to modify the behavior near the endpoints of the integral. For example, for $k = 2$, an appropriate subtraction factor is given by

$$f_{k=2}(u', v') = \frac{v' - u'}{u'v'}, \tag{3.30}$$

where u', v' are conformally-invariant cross-ratios,

$$u' = \frac{x_{12}^2 x_{34}^2}{x_{13}^2 x_{24}^2}, \quad v' = \frac{x_{14}^2 x_{23}^2}{x_{13}^2 x_{24}^2}. \tag{3.31}$$

We give subtraction factors for general k in section 3.3.

The right hand side of (3.27) is exactly the contribution of a state with mass m and spin J to the flat space scalar sum rule (3.19) after identifying $s = m^2, u = -\nu^2$. This guarantees that the flat space functionals with positive action on (3.19) can be uplifted to AdS and will give us a CFT functional with positive action on all blocks in the bulk-point limit ($\Delta \gg 1$).

As explained in (Simon Caron-Huot, Mazac, et al., 2021a), to obtain bounds on the bulk EFT Wilson coefficients, one must also ensure that the functional ω is positive outside the bulk point limit, in particular in the Regge regime (and other regimes if necessary). We leave an exploration of the Regge regime for four-point functions of spinning operators to future work. The goal in this work is to derive the bulk-point limit result (3.27) and its generalization to spinning operators from a saddle analysis of the spacetime integral.

Before we proceed, let us comment on a subtlety regarding (3.27). In Simon Caron-Huot, Mazac, et al., 2021a, (3.27) was derived (for a slightly different functional $C_{k,\nu}$ which is equivalent to $\Psi_{k,\nu}$ at large ν) for all $\nu \in [0, m)$. However, the derivation in this work will be in the limit where both ν and m are large (with fixed ratio).

(Therefore, sometimes we will also refer to the bulk-point limit as the $\nu, m \gg 1$ limit.) In Simon Caron-Huot, Mazac, et al., 2021a it was shown that in the scalar case, the regimes of finite ν and large-ν are continuously connected at large m. In other words, we can safely compute at large ν, and then later consider all $\nu \in [0, m)$. We expect the same to be true in the spinning case as well.

3.3 Heavy action from a spacetime saddle-point analysis

In this section, we define our functional in position space, and study its action on a conformal block $G_{\Delta,J}$ with large scaling dimension Δ. We will show that in the bulk point limit $\nu, \Delta \gg 1$, the integral completely localizes to a saddle point, and the heavy action can be obtained by evaluating conformally-invariant structures at the saddle. This allows us to derive a simple formula for the functional in the bulk point limit. We will first use this formula to reproduce the results summarized in section 3.2, and then write down the generalized functional for spinning operators.

Functionals as spacetime integrals

As explained in section 3.2, our starting point for the position space functional is the fact that the commutator of light-transformed operators vanishes,

$$\langle\Omega|O_4(x_4)[\mathbf{L}[O_3](x_0, z_3), \mathbf{L}[O_1](x_0, z_1)]O_2(x_2)|\Omega\rangle = 0. \tag{3.32}$$

To make sure the light transform integrals $\mathbf{L}[O_1]\mathbf{L}[O_3]$ converge, we also need the condition $J_1 + J_3 - 1 > J_0$, where J_0 is the Regge intercept (Kologlu et al., 2020). For the moment, let us assume this condition is satisfied, and we will come back to this issue later in section 3.3 and 3.3 by introducing subtraction factors.

We can integrate (3.32) against appropriate conformally-invariant structures to get different sum rules. We first consider the functional for scalar four-point functions. As we will see shortly, once we have derived this formula, the generalization to spinning operators will be obvious. For simplicity, we assume the external operators all have scaling dimension Δ_ϕ, but we will not impose that they are identical until section 3.3. Our functional is defined as

$$\Psi_{k,\nu}[\mathcal{G}] \equiv A_{k,\nu} \int_{\substack{2>4 \\ 0\approx 2,4}} \frac{d^d x_2 d^d x_4 d^d x_0 D^{d-2} z_0}{\mathrm{vol}(\widetilde{\mathrm{SO}}(d,2))} \langle 0|\phi_4(x_4^+)\mathbf{L}[O](x_0, z_0)\phi_2(x_2)|0\rangle^{-1}$$
$$\int D^{d-2} z_1 D^{d-2} z_3 \langle \widetilde{\mathcal{P}}_{\delta_1}(z_1)\widetilde{\mathcal{P}}_{\delta_3}(z_3)\mathcal{P}_\delta(z_0)\rangle \langle\Omega|\phi_4(x_4^+)[\mathbf{L}[\phi_3](x_0, z_3), \mathbf{L}[\phi_1](x_0, z_1)]\phi_2(x_2)|\Omega\rangle, \tag{3.33}$$

where the coefficient $A_{k,\nu}$ is given by

$$A_{k,\nu} = 2^{-8+4\Delta_\phi}\pi^{-2-\frac{d}{2}}e^{\pi\nu}\nu^{2+d-2k-4\Delta_\phi}\Gamma\left(\tfrac{d-2}{2}\right)\Gamma(\Delta_\phi)^2\Gamma\left(\Delta_\phi-\tfrac{d-2}{2}\right)^2. \tag{3.34}$$

The coefficient is chosen such that the heavy action of $\Psi_{k,\nu}$ agrees with the flat space sum rule. We have also applied $\mathcal{T}_4$ to the integrand for later convenience. The causality relations between the points are shown in figure 3.2a. In (3.33), $2>4$ indicates that x_2 is in the future lightcone of 4, and $0\approx 2,4$ indicates that x_0 is spacelike separated from x_2 and x_4.

Let us be explicit about the quantum numbers and structures in the definition (3.33). The operator $\mathcal{O}$ in the first line has scaling dimension $\Delta=\frac{d}{2}+i\nu$, and its spin is fixed by symmetry to be $J=-1$ (Hofman and J. Maldacena, 2008; Kologlu et al., 2021). The structure $\langle 0|\phi_4(x_4^+)\mathbf{L}[\mathcal{O}](x_0,z_0)\phi_2(x_2)|0\rangle^{-1}$ is a dual structure of a light transformed three-point function with respect to a Lorentzian three-point pairing,

$$\begin{aligned}&\Big(\langle\mathcal{O}_1\mathcal{O}_2\mathcal{O}\rangle,\langle\widetilde{\mathcal{O}}_1^\dagger\widetilde{\mathcal{O}}_2^\dagger\mathcal{O}^{S\dagger}\rangle\Big)_L\\ &\equiv\int_{\substack{2<1\\ x\approx1,2}}\frac{d^dx_1d^dx_2d^dxD^{d-2}z}{\mathrm{vol}(\widetilde{\mathrm{SO}}(d,2))}\langle\mathcal{O}_1(x_1)\mathcal{O}_2(x_2)\mathcal{O}(x,z)\rangle\langle\widetilde{\mathcal{O}}_1^\dagger(x_1)\widetilde{\mathcal{O}}_2^\dagger(x_2)\mathcal{O}^{S\dagger}(x,z)\rangle.\end{aligned} \tag{3.35}$$

The dual structure is defined by

$$\Big(\langle 0|\phi_4(x_4^+)\mathbf{L}[\mathcal{O}](x_0,z_0)\phi_2(x_2)|0\rangle^{-1},\langle 0|\phi_4(x_4^+)\mathbf{L}[\mathcal{O}](x_0,z_0)\phi_2(x_2)|0\rangle\Big)_L=1. \tag{3.36}$$

The explicit expression is (Kravchuk and Simmons-Duffin, 2018b)[6]

$$\begin{aligned}&\langle 0|\phi_4(x_4^+)\mathbf{L}[\mathcal{O}_{\Delta,J}](x_0,z_0)\phi_2(x_2)|0\rangle^{-1}\\ &=\frac{2^{2d-2}\Gamma(\frac{\Delta+J}{2})^2\,\mathrm{vol}(\mathrm{SO}(d-2))}{2\pi i\Gamma(\Delta+J-2)}\frac{(2z_0\cdot x_{40}x_{20}^2-2z_0\cdot x_{20}x_{40}^2)^{\Delta-d+1}}{(-x_{24}^2)^{\frac{\widetilde{\Delta}_2+\widetilde{\Delta}_4+\Delta-J-2d+2}{2}}(x_{02}^2)^{\frac{\widetilde{\Delta}_2+\Delta+J-\widetilde{\Delta}_4}{2}}(x_{02}^2)^{\frac{\widetilde{\Delta}_4+\Delta+J-\widetilde{\Delta}_2}{2}}}.\end{aligned} \tag{3.37}$$

In the second line of (3.33), $\langle\widetilde{\mathcal{P}}_{\delta_1}(z_1)\widetilde{\mathcal{P}}_{\delta_3}(z_3)\mathcal{P}_\delta(z_0)\rangle$ is a three-point structure of a fictitious $(d-2)$-dimensional Euclidean CFT on the celestial sphere, whose conformal symmetry is the Lorentz symmetry $\mathrm{SO}(d-1,1)$ of the original CFT. The polarizations z_i should be viewed as embedding space coordinates of this CFT_{d-2},

[6]Here, we choose the structures to be an analytic continuation from odd J, so the $(-1)^J$ factor in (Kravchuk and Simmons-Duffin, 2018b) becomes -1.

and $\mathcal{P}_\delta(z)$ is a primary with scaling dimension δ on the celestial sphere. In order for the integral (3.33) to be conformally-invariant, we must have $\delta = \frac{d-2}{2} + i\nu$. We also use the notation $\widetilde{\mathcal{P}}_{\delta_i} = \mathcal{P}_{d-2-\delta_i}$, and $\delta_i = \Delta_i - 1$, while $\widetilde{\delta_i} = d - 2 - \delta_i$ is the shadow dimension with respect to the $(d-2)$-dimensional fictitious CFT. The celestial three-point structure is given by

$$\langle \widetilde{\mathcal{P}}_{\delta_1}(z_1)\widetilde{\mathcal{P}}_{\delta_3}(z_3)\mathcal{P}_\delta(z_0)\rangle = \frac{1}{(-2z_1\cdot z_0)^{\frac{\delta+\widetilde{\delta}_1-\widetilde{\delta}_3}{2}}(-2z_3\cdot z_0)^{\frac{\delta+\widetilde{\delta}_3-\widetilde{\delta}_1}{2}}(-2z_1\cdot z_3)^{\frac{\widetilde{\delta}_1+\widetilde{\delta}_3-\delta}{2}}}. \tag{3.38}$$

Originally, the superconvergence sum rule (3.32) is parametrized by the positions and polarizations of the operators, subject to conformal invariance. By integrating it against the dual structure and celestial structure described above, we have transformed the statement of superconvergence into ν-space, which parametrizes the quantum numbers of the structures. In fact, one can also show that the condition $\Psi_{k,\nu}[\mathcal{G}] = 0$ is equivalent to (Kologlu et al., 2021)

$$C^-(\tfrac{d}{2} + i\nu, J = -1) = 0, \quad J_0 < -1, \tag{3.39}$$

where $C^-(\Delta, J)$ is the coefficient function computed by the Lorentzian inversion formula (Simon Caron-Huot, 2017; Simmons-Duffin, Stanford, and Witten, 2018), and encodes the analytic continuation of the CFT data from odd spin.

To further simplify the functional, let us focus on one term in the commutator $[\mathbf{L}[\phi_3], \mathbf{L}[\phi_1]]$ and consider

$$\begin{aligned}
\Psi_{k,\nu} &= \Psi^+_{k,\nu} - (1 \leftrightarrow 3),\\
\Psi^+_{k,\nu}[\mathcal{G}] &= A_{k,\nu}\int_{\substack{2>4\\0\approx 2,4}} \frac{d^dx_2 d^dx_4 d^dx_0 D^{d-2}z_0}{\mathrm{vol}(\widetilde{\mathrm{SO}}(d,2))}\langle 0|\phi_4(x_4^+)\mathbf{L}[O](x_0,z_0)\phi_2(x_2)|0\rangle^{-1}\\
&\quad \int D^{d-2}z_1 D^{d-2}z_3 \langle \widetilde{\mathcal{P}}_{\delta_1}(z_1)\widetilde{\mathcal{P}}_{\delta_3}(z_3)\mathcal{P}_\delta(z_0)\rangle\\
&\quad \langle\Omega|[\phi_4(x_4^+), \mathbf{L}[\phi_3](x_0,z_3)][\mathbf{L}[\phi_1](x_0,z_1), \phi_2(x_2)]|\Omega\rangle.
\end{aligned} \tag{3.40}$$

Note that since light-transformed operators annihilate the vacuum, we can rewrite the four-point function as a double commutator. Moreover, in (3.40), we can rewrite the integral over the two light transform directions z_1, z_3 as an integral over the positions of ϕ_1, ϕ_3 with additional delta function constraints (Chang, Kologlu, et al.,

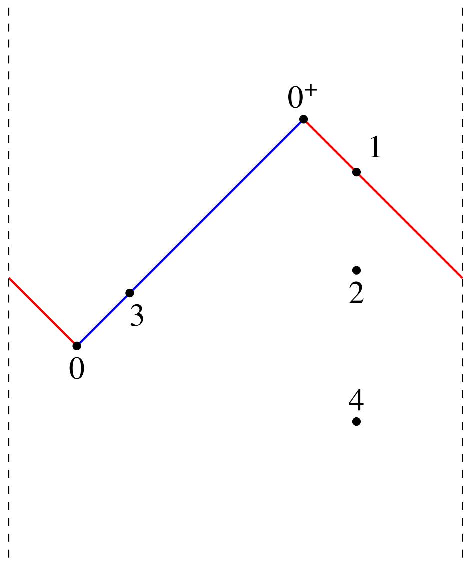

(a) Original configuration

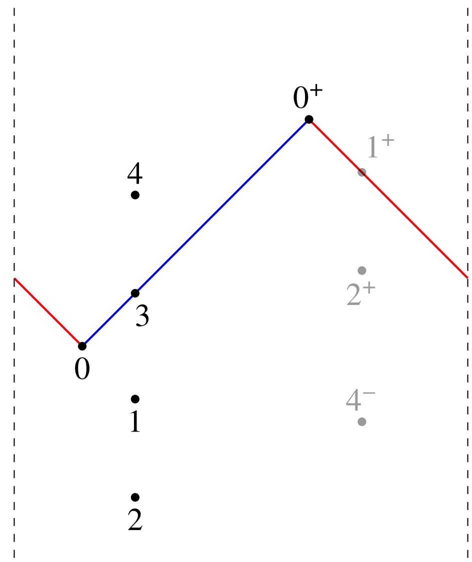

(b) Configuration after applying $\mathcal{T}$'s

Figure 3.2: Causality configuration of the functional. The left figure shows the configuration in the original definition (3.33). Points $1, 3$ both start from 0 and are integrated along two different null directions. The right figures shows the configuration after applying $\mathcal{T}_1^{-1}, \mathcal{T}_2^{-1}, \mathcal{T}_4$, which becomes $4 > 3 > 0 > 1 > 2$.

2022). Explicitly, this gives

$$\Psi^{+}_{k,\nu}[\mathcal{G}] = 4A_{k,\nu} \int_{\substack{2>4\\0\approx 2,4}} \frac{d^dx_1 d^dx_2 d^dx_3 d^dx_4 d^dx_0 D^{d-2}z_0}{\mathrm{vol}(\widetilde{\mathrm{SO}}(d,2))} \langle 0|\phi_4(x_4^+)\mathbf{L}[\mathcal{O}](x_0,z_0)\phi_2(x_2)|0\rangle^{-1}$$
$$\langle \widetilde{\mathcal{P}}_{\delta_1}(x_{10})\widetilde{\mathcal{P}}_{\delta_3}(x_{30})\mathcal{P}_{\delta}(z_0)\rangle \delta(x_{10}^2)\delta(x_{30}^2)\theta(x_{10})\theta(x_{30})\langle\Omega|[\phi_4(x_4^+),\phi_3(x_3)][\phi_1(x_1),\phi_2(x_2)]|\Omega\rangle, \tag{3.41}$$

where the theta-functions $\theta(x_{10})\theta(x_{30})$ indicate that x_{10} and x_{30} must be timelike and future-pointing. Finally, let us make a change of variables $x_1 \to x_1^+, x_2 \to x_2^+, x_4 \to x_4^-$. This makes the causality configuration equivalent to $4 > 3 > 0 > 1 > 2$ (see figure 3.2b), and we arrive at the expression

$$\Psi^{+}_{k,\nu}[\mathcal{G}] = 4A_{k,\nu} \int_{4>3>0>1>2} \frac{d^dx_1 d^dx_2 d^dx_3 d^dx_4 d^dx_0 D^{d-2}z_0}{\mathrm{vol}(\widetilde{\mathrm{SO}}(d,2))} .$$
$$\langle 0|\phi_4(x_4)\mathbf{L}[\mathcal{O}](x_0,z_0)\phi_2(x_2^+)|0\rangle^{-1}\langle \widetilde{\mathcal{P}}_{\delta_1}(x_{1^+0})\widetilde{\mathcal{P}}_{\delta_3}(x_{30})\mathcal{P}_{\delta}(z_0)\rangle$$
$$\delta(x_{1^+0}^2)\delta(x_{30}^2)\theta(x_{1^+0})\theta(x_{30})\langle\Omega|[\phi_4(x_4),\phi_3(x_3)][\phi_1(x_1^+),\phi_2(x_2^+)]|\Omega\rangle \tag{3.42}$$

Action on conformal blocks

Let us now apply the functional $\Psi^{+}_{k,\nu}$ to an s-channel conformal block $G^s_{\Delta,J}$ and study the action in the large Δ limit. In position space, the most useful expression for the block is the Lorentzian shadow representation (Polyakov, 1974), given by integrating a fifth point x_5 over a causal diamond $4 > 5 > 3$:

$$G^s_{\Delta,J} = \frac{1}{\beta_{\Delta,J}} \int_{4>5>3} d^d x_5 |\langle \phi_1 \phi_2 \mathcal{O}^{\mu_1 \cdots \mu_J}(x_5) \rangle| |\langle \widetilde{\mathcal{O}}^\dagger_{\mu_1 \cdots \mu_J}(x_5) \phi_3 \phi_4 \rangle|. \tag{3.43}$$

The external points should satisfy the causality constraint $1 > 2, 4 > 3$ with all other pairs of points spacelike-separated. On the right-hand side, the operator $\mathcal{O}$ has quantum numbers (Δ, J), and the quantum numbers of $\widetilde{\mathcal{O}}^\dagger$ are related to those of $\mathcal{O}$ by a shadow transform and Hermitian conjugate:[7]

$$\begin{aligned} \widetilde{\mathcal{O}} &: (\Delta, \rho) \mapsto (d - \Delta, \rho^R), \\ \mathcal{O}^\dagger &: (\Delta, \rho) \mapsto (\Delta, \rho^\dagger = (\rho^R)^*). \end{aligned} \tag{3.44}$$

In (3.43), we contract the indices of the exchanged operator $\mathcal{O}_5$. This is more natural for our purpose because the spin of the inserted block corresponds to spin of the exchanged massive particle in flat space, and hence we are only interested in the integer-spin case.[8] Moreover, later we will find a correspondence between blocks and flat space partial waves, which also come from contracting the indices of spin-J tensors. The shadow coefficient $\beta_{\Delta,J}$ in (3.43) in the scalar case is given by

$$\beta_{\Delta,J} = \frac{(-1)^J 2^{J-1} \pi^{\frac{d-2}{2}} \Gamma(\Delta + 2 - d) \Gamma(\frac{J+\Delta}{2})^2 \Gamma(\frac{\Delta+2-d-J}{2})^2}{\Gamma(\Delta + \frac{2-d}{2}) \Gamma(J + \Delta) \Gamma(\Delta + 2 - d - J)}. \tag{3.45}$$

For the three-point structures in (3.43), the notation $|\langle \ldots \rangle|$ means that all the x_{ij}'s in the denominator should come with absolute values (see appendix 3.A for definitions). In our case, the correct interpretation of the absolute-valued structures is in terms of a double commutator,

$$\begin{aligned} &\langle \Omega | [\phi_4(x_4), \phi_3(x_3)] [\phi_1(x_1), \phi_2(x_2)] | \Omega \rangle^s_{\Delta,J} \\ &= \frac{-2(2 \sin^2(\pi \frac{\Delta - J - 2\Delta_\phi}{2}))}{\beta_{\Delta,J}} \int_{4>5>3} d^d x_5 |\langle \phi_1 \phi_2 \mathcal{O}^{\mu_1 \cdots \mu_J}(x_5) \rangle| |\langle \widetilde{\mathcal{O}}^\dagger_{\mu_1 \cdots \mu_J}(x_5) \phi_3 \phi_4 \rangle|, \end{aligned} \tag{3.46}$$

where the left hand side denotes the contribution from the $G^s_{\Delta,J}$ block to the double commutator. Each commutator gives $2i \sin(\pi \frac{\Delta - J - 2\Delta_\phi}{2})$ from the difference of

[7] In the case where ρ is a traceless symmetric tensor representation with spin J, we have $\rho^R = \rho = (\rho^R)^*$.

[8] This is in contrast to the continuous-spin version of the Lorentzian shadow representation given in (Kravchuk and Simmons-Duffin, 2018b) that involves integrating over the polarization vector of the exchanged operator.

two phase factors, so we have an additional $-2(2\sin^2(\pi\frac{\Delta-J-2\Delta_\phi}{2}))$ factor, which is accounted for on the right-hand side.

In our calculation, we will use absolute-valued structures as convenient notation in intermediate steps, and replace them with commutators at the end as appropriate. For example, for the structure $|\langle\phi_1(x_1)\phi_2(x_2)\mathcal{O}(x_5)\rangle|$, which has causality relation $5 \approx (1 > 2)$, we have the following identity:

$$\langle 0|\mathcal{O}(x_5)[\phi_1(x_1),\phi_2(x_2)]|0\rangle = 2i\sin(\pi\frac{\Delta-J-2\Delta_\phi}{2})|\langle\phi_1(x_1)\phi_2(x_2)\mathcal{O}(x_5)\rangle|, \quad 5\approx(1>2), \tag{3.47}$$

where the left-hand side is a commutator of the standard Wightman structure. For the other structure $|\langle\widetilde{\mathcal{O}}^\dagger(x_5)\phi_3\phi_4\rangle|$, this identity is not well-defined due to the additional phase factors from x_{45}^2, x_{35}^2. However, in the final formula for the heavy action, we will be able to apply the above identity to both structures, enabling us to remove absolute values and write the final formula in terms of standard Wightman structures.

We can now plug the Lorentzian shadow representation into our functional. In the functional (3.42), the external points of the four-point function are $1^+, 2^+, 3, 4$ with the condition $4 > 3 > 0 > 1 > 2$, so the causality configuration agrees with the Lorentzian shadow representation (3.43). See also figure 3.2b. Therefore, using (3.43), the action of $\Psi^+_{k,\nu}$ on a conformal block can be written

$$\begin{aligned}\Psi^+_{k,\nu}[G^s_{\Delta,J}] =& \frac{-8(2\sin^2(\pi\frac{\Delta-J-2\Delta_\phi}{2}))A_{k,\nu}}{\beta_{\Delta,J}}\int_{4>5>3>0>1>2}\frac{d^dx_1d^dx_2d^dx_3d^dx_4d^dx_5d^dx_0D^{d-2}z_0}{\mathrm{vol}(\widetilde{\mathrm{SO}}(d,2))}\\ &\times\langle 0|\phi_4\mathbf{L}[\mathcal{O}](x_0,z_0)\phi_{2^+}|0\rangle^{-1}\langle\widetilde{\mathcal{P}}_{\delta_1}(x_{1^+0})\widetilde{\mathcal{P}}_{\delta_3}(x_{30})\mathcal{P}_\delta(z_0)\rangle\\ &\times\delta(x_{1^+0}^2)\delta(x_{30}^2)\theta(x_{1^+0})\theta(x_{30})|\langle\phi_{1^+}\phi_{2^+}\mathcal{O}^{\mu_1\cdots\mu_J}(x_5)\rangle||\langle\widetilde{\mathcal{O}}^\dagger_{\mu_1\cdots\mu_J}(x_5)\phi_3\phi_4\rangle|.\end{aligned} \tag{3.48}$$

For brevity, we have used the short-hand notation $\phi_i = \phi_i(x_i), \phi_{i^+} = \phi_i(x_i^+)$.

Now we use conformal symmetry to gauge fix the integral. We will choose the gauge fixing in (Simon Caron-Huot, Mazac, et al., 2021a) and fix $x_1 + x_3$ to the origin, $x_{2^+} + x_{4^-}$ to spatial infinity, and x_5 to the unit time vector e. More precisely, we choose (see figure 3.3)

$$x_3 = -x_1 = y, \quad x_4 = -x_2 = \frac{x}{-x^2}, \quad x_5 = e, \quad x, y > 0. \tag{3.49}$$

For this gauge fixing, the stabilizer group is $\mathrm{SO}(d-1)$, and the Faddeev-Popov determinant is (Simon Caron-Huot, Mazac, et al., 2021a)

$$2^d(1+2x\cdot y+x^2y^2)(1-2x\cdot y+x^2y^2)(1-x^2y^2)^{d-2}. \tag{3.50}$$

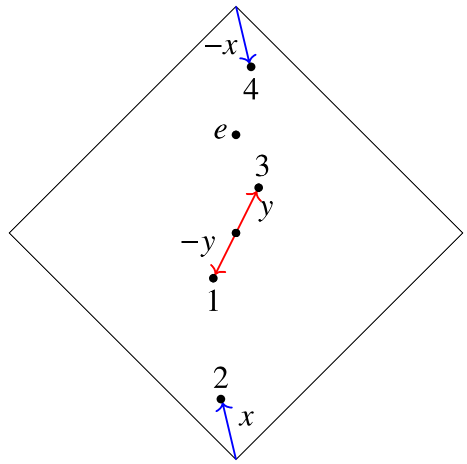

Figure 3.3: Our gauge fixing condition is $x_3 = -x_1 = y, x_4 = -x_2 = \frac{x}{-x^2}, x_5 = e$. The causality constraint is $4 > 5 > 3 > 0 > 1 > 2$.

After the gauge fixing, we obtain

$$\begin{aligned}\Psi^{+}_{k,\nu}[G^{s}_{\Delta,J}] =& \frac{-8(2\sin^2(\pi\frac{\Delta-J-2\Delta_\phi}{2}))A_{k,\nu}}{\beta_{\Delta,J}\,\mathrm{vol}(\mathrm{SO}(d-1))}\int \frac{d^dx d^dy d^dx_0 D^{d-2}z_0}{(-x^2)^{2d}} \\ &\times 2^d(1+2x\cdot y+x^2y^2)(1-2x\cdot y+x^2y^2)(1-x^2y^2)^{d-2} \\ &\times \langle 0|\phi_4 \mathbf{L}[\mathcal{O}](x_0,z_0)\phi_{2^+}|0\rangle^{-1}\langle \widetilde{\mathcal{P}}_{\delta_1}(x_{1^+0})\widetilde{\mathcal{P}}_{\delta_3}(x_{30})\mathcal{P}_{\delta}(z_0)\rangle \\ &\times \delta(x_{1^+0}^2)\delta(x_{30}^2)\theta(x_{1^+0})\theta(x_{30})|\langle\phi_{1^+}\phi_{2^+}\mathcal{O}^{\mu_1\cdots\mu_J}(x_5)\rangle||\langle\widetilde{\mathcal{O}}^{\dagger}_{\mu_1\cdots\mu_J}(x_5)\phi_3\phi_4\rangle|\Big|_{\mathrm{gauge-fixed}},\end{aligned} \tag{3.51}$$

where the last two lines should be evaluated in the gauge-fixed configuration (3.49).

The integral over z_0 can also be fixed using $\mathrm{SO}(d-1)$ invariance. After integrating over x, y, x_0, the remaining vectors in the integrand of (3.51) are z_0 and e. Homogeneity of z_0 then implies the z_0-integral must be of the form

$$\int D^{d-2}z_0\,(-2z_0\cdot e)^{2-d} = \frac{\pi^{\frac{d-2}{2}}\Gamma(\frac{d-2}{2})}{\Gamma(d-2)}. \tag{3.52}$$

Thus, we can eliminate the z_0-integral by setting z_0 to be a fixed null vector z_0^*, and then introduce a factor

$$(-2z_0^*\cdot e)^{d-2}\frac{\pi^{\frac{d-2}{2}}\Gamma(\frac{d-2}{2})}{\Gamma(d-2)}. \tag{3.53}$$

Let us introduce lightcone coordinate $x = (u, v, \vec{x}_\perp)$, where $x^2 = -uv + \vec{x}_\perp^2$, and choose $z_0^* = (1,0,\vec{0})$. Then (3.51) becomes

$$\begin{aligned}\Psi^+_{k,\nu}[G^s_{\Delta,J}] =& \frac{-8(2\sin^2(\pi\frac{\Delta-J-2\Delta_\phi}{2}))A_{k,\nu}}{\beta_{\Delta,J}\,\mathrm{vol}(\mathrm{SO}(d-1))}\frac{\pi^{\frac{d-2}{2}}\Gamma(\frac{d-2}{2})}{\Gamma(d-2)}\int\frac{d^dxd^dyd^dx_0}{(-x^2)^{2d}}\\ &\times 2^d(1+2x\cdot y+x^2y^2)(1-2x\cdot y+x^2y^2)(1-x^2y^2)^{d-2}\\ &\times\langle 0|\phi_4\mathbf{L}[O](x_0,z_0^*)\phi_{2^+})|0\rangle^{-1}\langle\widetilde{\mathcal{P}}_{\delta_1}(x_{1^+0})\widetilde{\mathcal{P}}_{\delta_3}(x_{30})\mathcal{P}_\delta(z_0^*)\rangle\\ &\times\delta(x^2_{1^+0})\delta(x^2_{30})\theta(x_{1^+0})\theta(x_{30})|\langle\phi_{1^+}\phi_{2^+}O^{\mu_1\cdots\mu_J}(x_5)\rangle||\langle\widetilde{O}^\dagger_{\mu_1\cdots\mu_J}(x_5)\phi_3\phi_4\rangle|\Big|_{\text{gauge}-\text{fixed}}.\end{aligned} \tag{3.54}$$

Saddle point analysis

We now study the action $\Psi^+_{k,\nu}[G^s_{\Delta,J}]$ in the bulk-point limit, where we take both ν and Δ to be large (and $\Delta\sim m$). To study the large ν, large Δ limit of (3.54), we will consider the factors that depend exponentially on ν and Δ and look for a saddle point. The important factors in (3.54) are given by

$$\begin{aligned}&\left(\frac{(2z_0\cdot x_{40}x^2_{20}-2z_0\cdot x_{20}x^2_{40})^2(2x_{10}\cdot x_{30})}{(-x^2_{24})(-x^2_{40})(-x^2_{20})(2z_0\cdot x_{10})(-2z_0\cdot x_{30})}\right)^{\frac{i\nu}{2}}\left(\frac{(-x^2_{35})(-x^2_{45})(-x^2_{12})}{(-x^2_{15})(-x^2_{25})(-x^2_{34})}\right)^{\frac{m}{2}}\Bigg|_{\text{gauge}-\text{fixed},z_0=z_0^*}\\ &=e^{f_{\nu,m}(x,y,x_0)},\end{aligned} \tag{3.55}$$

where the function $f_{\nu,m}(x,y,x_0)$ is given by

$$\begin{aligned}f_{\nu,m}(x,y,x_0) =& \frac{i\nu}{2}\log\left(\frac{4(z_0^*\cdot x(1+x^2x_0^2)-2z_0^*\cdot x_0x^2x\cdot x_0)^2(-y^2)}{(-x^2)(1-2x\cdot x_0+x^2x_0^2)(1+2x\cdot x_0+x^2x_0^2)(z_0^*\cdot(y-x_0))(z_0^*\cdot(y+x_0))}\right)\\ &+\frac{m}{2}\log\left(\frac{(e-x)^2(e-y)^2}{(e+x)^2(e+y)^2}\right).\end{aligned} \tag{3.56}$$

The integral we have to consider in the bulk-point limit then takes the form

$$\int d^dxd^dyd^dx_0\delta((y+x_0)^2)\delta((y-x_0)^2)\theta(y-x_0)\theta(y+x_0)e^{f_{\nu,m}(x,y,x_0)}g(x,y,x_0), \tag{3.57}$$

where $g(x,y,x_0)$ are all the factors that do not depend exponentially on ν and m in the integrand of (3.54).

To find the location of the saddle, it is convenient to consider lightcone coordinates

$$x=(u_x,v_x,\vec{x}_\perp),\quad y=(u_y,v_y,\vec{y}_\perp),\quad x_0=(u,v,\vec{y}_0). \tag{3.58}$$

Let us also define

$$\widetilde{t}_0=\frac{1}{2}\left(\frac{u}{u_y}+\frac{v}{v_y}-2\frac{\vec{y}_0\cdot\vec{y}_\perp}{u_yv_y}\right),\quad \widetilde{x}_0=\frac{1}{2}\left(\frac{u}{u_y}-\frac{v}{v_y}\right). \tag{3.59}$$

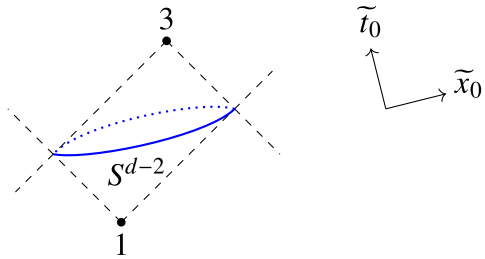

Figure 3.4: The two delta functions $\delta(x_{10}^2)\delta(x_{30}^2)$ force x_0 to be on an S^{d-2} (the blue curves). The directions of the variables $\widetilde{t}_0, \widetilde{x}_0$ defined in (3.59) are also indicated.

In our functional, there are two delta functions $\delta(x_{1^+0}^2)\delta(x_{30}^2)$ in the integrand due to the light transforms. These delta functions restrict x_0 to lie on the intersection of the past lightcone of x_3 and the future lightcone of x_1. So, the x_0-integral is forced to be on an S^{d-2}, as shown by figure 3.4. In terms of the variables defined above, the delta functions will localize $\widetilde{t}_0$ and $|\vec{y}_0|$ to be

$$\widetilde{t}_0 = 0, \quad |\vec{y}_0|^2 = \frac{u_y v_y (u_y v_y (1 - \widetilde{x}_0^2) - \vec{y}_\perp^2)}{u_y v_y - (\vec{n}_0 \cdot \vec{y}_\perp)^2}, \tag{3.60}$$

where $\vec{n}_0 = \vec{y}_0 / |\vec{y}_0|$ is the unit vector in the $\vec{y}_0$ direction. The remaining integral over S^{d-2} then becomes an integral over $\widetilde{x}_0 \in [-(1 - \frac{\vec{y}_\perp^2}{u_y v_y})^{\frac{1}{2}}, (1 - \frac{\vec{y}_\perp^2}{u_y v_y})^{\frac{1}{2}}]$ and $\vec{n}_0 \in S^{d-3}$. After going to lightcone coordinates and removing the delta functions, (3.57) becomes

$$\frac{(u_y v_y)^{\frac{d-2}{2}}}{32} \int d\widetilde{x}_0 du_x dv_x du_y dv_y d\Omega_{\vec{n}_0} d^{d-2}\vec{x}_\perp d^{d-2}\vec{y}_\perp (u_y v_y - (\vec{n}_0 \cdot \vec{y}_\perp)^2)^{\frac{2-d}{2}} (u_y v_y (1 - \widetilde{x}_0^2) - \vec{y}_\perp^2)^{\frac{d-4}{2}}$$
$$\times e^{f_{\nu,m}(x,y,x_0)} g(x, y, x_0). \tag{3.61}$$

The large ν and large m limit localizes all the variables in the integral, except for $\vec{n}_0$. In fact, the $f_{\nu,m}$ function leads to sixteen different saddles at

$$x_0 = (0, 0, \vec{y}_0), \quad x = \left(-i\tfrac{m \pm \sqrt{m^2 - \nu^2}}{\nu}, i\tfrac{m \pm \sqrt{m^2 - \nu^2}}{\nu}, \vec{0}\right), \ y = \left(i\tfrac{m \pm \sqrt{m^2 - \nu^2}}{\nu}, -i\tfrac{m \pm \sqrt{m^2 - \nu^2}}{\nu}, \vec{0}\right), \tag{3.62}$$

where $|\vec{y}_0|^2 = -y^2$. Each saddle corresponds to a locus S^{d-3} parametrized by $\vec{n}_0$. To find the correct saddle approximation for the integral (3.61), we need to deform the integration contour into steepest descendant flows and see which saddle locus the contour goes through (see (Witten, 2011) for a pedagogical introduction). The analysis is essentially identical to (Simon Caron-Huot, Mazac, et al., 2021a), which also studies saddle point of x, y in the bulk-point limit. The result is that the dominant saddle depends on the relative size of ν and m. The case we will be particularly interested in is the region related to the flat space functional, where one considers $\nu \in [0, \Delta_{\text{gap}}]$ and $m > \Delta_{\text{gap}}$. In this case ($\nu < m$), the saddle locus that dominates the integral is given by

$$x_0 = (0, 0, \vec{y}_0), \quad x = \left(-i\tfrac{m-\sqrt{m^2-\nu^2}}{\nu}, i\tfrac{m-\sqrt{m^2-\nu^2}}{\nu}, \vec{0}\right), \; y = \left(i\tfrac{m-\sqrt{m^2-\nu^2}}{\nu}, -i\tfrac{m-\sqrt{m^2-\nu^2}}{\nu}, \vec{0}\right). \tag{3.63}$$

Expanding the function $f_{\nu,m}$ around the dominant saddle (3.63), we find

$$f_{\nu,m} = -\pi\nu + i\nu\log 2 - \frac{1}{2}\begin{pmatrix}\widetilde{x}_0 & u_x & v_x & u_y & v_y & \vec{x}_\perp & \vec{y}_\perp\end{pmatrix} M_{\nu,m,\vec{y}_0}\begin{pmatrix}\widetilde{x}_0 \\ u_x \\ v_x \\ u_y \\ v_y \\ \vec{x}_\perp \\ \vec{y}_\perp\end{pmatrix} + \ldots, \tag{3.64}$$

where $\ldots$ are higher-order terms in the expansion. The Hessian $M_{\nu,m,\vec{y}_0}$ has determinant

$$\mathrm{Det}M_{\nu,m,\vec{y}_0} = -\frac{i\nu^{6d+1}(m^2-\nu^2)^2(m-\sqrt{m^2-\nu^2})^{-4d}}{16m^4}. \tag{3.65}$$

Therefore, the large ν, large m limit of the integral (3.57) can be written as

$$\begin{aligned}&\lim_{\substack{\nu,m\gg 1\\ \nu<m}}\int d^dx d^dy d^dx_0 \delta((y+x_0)^2)\delta((y-x_0)^2)\theta(y-x_0)\theta(y+x_0)e^{f_{\nu,m}(x,y,x_0)}g(x,y,x_0)\\ =&\frac{\nu^{4-d}(m-\sqrt{m^2-\nu^2})^{d-4}}{32}\sqrt{\frac{(2\pi)^{2d+1}}{\mathrm{Det}M_{\nu,m,\vec{y}_0}}}e^{-\pi\nu}2^{i\nu}\int d\Omega_{\vec{n}_0}\, g(x,y,x_0)|_{\text{saddle}}\,,\end{aligned} \tag{3.66}$$

where saddle stands for the configuration (3.63). Furthermore, the function $g(x, y, x_0)$ evaluated at the saddle does not include any $(d-2)$-dimensional vectors other than $\vec{n}_0$, and hence the remaining integral over the S^{d-3} locus must be trivial. The final expression of the integral is then given by

$$\begin{aligned}&\lim_{\substack{\nu,m\gg 1\\ \nu<m}}\int d^dx d^dy d^dx_0 \delta((y+x_0)^2)\delta((y-x_0)^2)\theta(y-x_0)\theta(y+x_0)e^{f_{\nu,m}(x,y,x_0)}g(x,y,x_0)\\ =&\frac{e^{i\frac{\pi}{4}}(2\pi)^{d+\frac{1}{2}}m^2\nu^{-4d+\frac{7}{2}}(m-\sqrt{m^2-\nu^2})^{3d-4}}{8(m^2-\nu^2)}\,\mathrm{vol}(S^{d-3})\; e^{f_{\nu,m}(x,y,x_0)}g(x,y,x_0)\Big|_{\text{saddle}}\,,\end{aligned} \tag{3.67}$$

where we have plugged in the Hessian determinant and used the fact that $e^{-\pi\nu}2^{i\nu}$ comes from evaluating $e^{f_{\nu,m}(x,y,x_0)}$ at the saddle.

Now, we can compare (3.67) and the functional (3.54) and find the expression for $\Psi^{+}_{k,\nu}[G^{s}_{\Delta,J}]$ in the bulk-point limit. From the above saddle analysis, we see that the integral in the bulk-point limit can be obtained by simply evaluating the integrand at the saddle and multiplying by the additional factors coming from the Jacobian and Hessian. This implies that in the bulk-point limit, the calculation of the heavy action of our functional can be simplified to evaluating conformally-invariant structures in the saddle configuration (3.63), which leads to

$$\begin{aligned}
&\lim_{\substack{\nu,m\gg 1\\ \nu<m}} \frac{\Psi^{+}_{k,\nu}[G^{s}_{\Delta,J}]}{-2(2\sin^2(\pi\frac{\Delta-J-2\Delta_\phi}{2}))}\\
&= A_{k,\nu}\frac{2^{\frac{5}{2}+3d}\pi^{\frac{3d-1}{2}}e^{i\frac{\pi}{4}}m^{d+2}\nu^{\frac{7}{2}-4d}(m^2-\nu^2)^{\frac{d-2}{2}}(m-\sqrt{m^2-\nu^2})^{d-4}}{\beta_{\Delta,J}\Gamma\left(\frac{d-2}{2}\right)\mathrm{vol}(\mathrm{SO}(d-2))}\\
&\times\langle 0|\phi_4\mathbf{L}[\mathcal{O}](x_0,z_0^*)\phi_{2^+}|0\rangle^{-1}\langle\widetilde{\mathcal{P}}_{\delta_1}(x_{1^+0})\widetilde{\mathcal{P}}_{\delta_3}(x_{30})\mathcal{P}_{\delta}(z_0^*)\rangle\\
&\times|\langle\phi_{1^+}\phi_{2^+}\mathcal{O}^{\mu_1\cdots\mu_J}(x_5)\rangle||\langle\widetilde{\mathcal{O}}^{\dagger}_{\mu_1\cdots\mu_J}(x_5)\phi_3\phi_4\rangle|\Big|_{\text{saddle}}.
\end{aligned}\tag{3.68}$$

The saddle calculation done above involves computing the determinant of a $(2d+1)\times(2d+1)$ Hessian matrix. An alternative derivation of the above formula that can avoid this technically involved calculation is by first studying the large ν limit of the functional, and then use the result of the large m saddle analysis that was already done in (Simon Caron-Huot, Mazac, et al., 2021a). We describe this calculation in appendix 3.B.

The shadow coefficient

Finally, the remaining task is to study the shadow coefficient $\beta_{\Delta,J}$ in the large Δ limit. For the scalar case, its explicit expression is known and given by (3.45). For the spinning case, the shadow transform will involve mixing of different tensor structures and therefore the shadow coefficients become a matrix. In principle it can be computed using e.g., weight-shifting operators (Karateev, Kravchuk, and Simmons-Duffin, 2018). However, as we discuss below, it turns out that the shadow transform at large Δ also gets localized to a saddle. Hence, the shadow transform at large Δ becomes algebraic and the coefficients can again be computed by evaluating structures at the saddle configuration.

Let us demonstrate this idea by studying the shadow transform in the scalar case. We will derive a formula for $\beta_{\Delta,J}$ that reproduces the known answer (3.45). However, the advantage of this formula is that its generalization to the spinning case is almost trivial.

Considering the OPE limit of (3.43), we see that the shadow coefficient $\beta_{\Delta,J}$ should satisfy

$$\begin{aligned}&\frac{1}{\beta_{\Delta,J}}\int_{4>5>3} d^d x_5 \langle \mathcal{O}^{\dagger}_{\nu_1\cdots\nu_J}(x_6)\mathcal{O}^{\mu_1\cdots\mu_J}(x_5)\rangle|\langle \widetilde{\mathcal{O}}^{\dagger}_{\mu_1\cdots\mu_J}(x_5)\phi_3\phi_4\rangle|\\&=|\langle \mathcal{O}^{\dagger}_{\nu_1\cdots\nu_J}(x_6)\phi_3\phi_4\rangle|.\end{aligned} \tag{3.69}$$

Let us choose the external points x_3, x_4, x_6 to be

$$x_3 = y|_{\text{saddle}}, \quad x_4 = \frac{x}{-x^2}\Big|_{\text{saddle}}, \quad x_6 = (-e)^+, \tag{3.70}$$

where x, y are evaluated at the saddle configuration (3.63). With this choice of external points, we find that at large Δ, the integrand in (3.69) has a saddle point at exactly $x_5 = e$, which agrees with the saddle configuration of the original integral of the functional $\Psi^{+}_{k,\nu}$. After computing the determinant factor coming from the Gaussian integral, we obtain that in the large Δ limit, (3.69) becomes

$$\begin{aligned}&\lim_{\Delta\gg 1}\frac{2^d\pi^{\frac{d}{2}}\Delta^{-\frac{d}{2}}}{\beta_{\Delta,J}}\langle \mathcal{O}^{\dagger}_{\nu_1\cdots\nu_J}(x_6)\mathcal{O}^{\mu_1\cdots\mu_J}(x_5)\rangle|\langle \widetilde{\mathcal{O}}^{\dagger}_{\mu_1\cdots\mu_J}(x_5)\phi_3\phi_4\rangle|\Big|_{\substack{\text{saddle}\\ x_6=(-e)^+}}\\&=|\langle \mathcal{O}^{\dagger}_{\nu_1\cdots\nu_J}(x_6)\phi_3\phi_4\rangle|\Big|_{\substack{\text{saddle}\\ x_6=(-e)^+}}.\end{aligned} \tag{3.71}$$

To recap, we see that at large Δ, the shadow transform gets localized to a saddle point. Furthermore, with a good choice of external points $x_6 = (-e)^+$, we can make the saddle point location agree with the saddle configuration for the functional (3.63). We have also checked that (3.71) is consistent with the known scalar result (3.45).

To simplify the formula of the functional in the bulk-point limit given by (3.68), we need the combination $\frac{1}{\beta_{\Delta,J}}|\langle \phi_{1^+}\phi_{2^+}\mathcal{O}^{\mu_1\cdots\mu_J}(x_5)\rangle||\langle \widetilde{\mathcal{O}}^{\dagger}_{\mu_1\cdots\mu_J}(x_5)\phi_3\phi_4\rangle|$, which is different from the structure appearing in (3.71). To get the correct structure, let us first note that the two-point structure at the saddle $\langle \mathcal{O}^{\dagger\nu_1\cdots\nu_J}((-e)^+)\mathcal{O}^{\mu_1\cdots\mu_J}(e)\rangle$ can be viewed as an invertible matrix for the spin-J representation of the Lorentz group.[9] Therefore, we can define an inverse "r-tensor" that satisfies

$$r_{\Delta,J;\rho_1\cdots\rho_J}{}^{\nu_1\cdots\nu_J}\langle \mathcal{O}^{\dagger}_{\nu_1\cdots\nu_J}((-e)^+)\mathcal{O}^{\mu_1\cdots\mu_J}(e)\rangle = \delta_{\{\rho_1}{}^{\{\mu_1}\cdots\delta_{\rho_J\}}{}^{\mu_J\}} - \text{traces}. \tag{3.72}$$

[9] More generally, if $\mathcal{O}$ has representation ρ, it should be a map from ρ^* to $\rho^\dagger = (\rho^*)^R$.

Here, $\{\mu_1 \cdots \mu_J\}$ means we symmetrize the indices, and "−traces" means we subtract terms proportional to $\delta^{\mu_i \mu_j}$ and $\delta_{\rho_i \rho_j}$ to make the result traceless. Concretely, in this case $r_{\Delta,J}$ is given by a reflection in the time direction,

$$r_{\Delta,J;\rho_1\cdots\rho_J}{}^{\nu_1\cdots\nu_J} = (-1)^J 2^{-J+2\Delta} \left(\delta_{\{\rho_1}{}^{\{\nu_1} + 2e_{\{\rho_1} e^{\{\nu_1}\right) \cdots \left(\eta_{\rho_J\}}{}^{\nu_J\}} + 2e_{\rho_J\}} e^{\nu_J\}}\right) - \text{traces}. \tag{3.73}$$

By contracting both sides of (3.71) with $|\langle \phi_{1^+} \phi_{2^+} O^{\rho_1\cdots\rho_J}(x_5)\rangle| r_{\Delta,J;\rho_1\cdots\rho_J}{}^{\nu_1\cdots\nu_J}$, we obtain

$$\begin{aligned} &\lim_{\Delta\gg 1} \frac{1}{\beta_{\Delta,J}} |\langle \phi_{1^+}\phi_{2^+} O^{\mu_1\cdots\mu_J}(x_5)\rangle| |\langle \widetilde{O}^\dagger_{\mu_1\cdots\mu_J}(x_5)\phi_3\phi_4\rangle| \Big|_{\substack{\text{saddle} \\ x_6=(-e)^+}} \\ &= 2^{-d}\pi^{-\frac{d}{2}}\Delta^{\frac{d}{2}} \, |\langle \phi_{1^+}\phi_{2^+} O^{\mu_1\cdots\mu_J}(x_5)\rangle| r_{\Delta,J;\mu_1\cdots\mu_J}{}^{\nu_1\cdots\nu_J} |\langle O^\dagger_{\nu_1\cdots\nu_J}(x_6)\phi_3\phi_4\rangle| \Big|_{\substack{\text{saddle} \\ x_6=(-e)^+}} . \end{aligned} \tag{3.74}$$

The left hand side of the above equation now agrees with the structure in the formula (3.68). We can then plug this equation into (3.68) and find a formula without the shadow coefficient. We write down this final formula in the next subsection.

Finally, let us discuss a natural formula for the $r_{\Delta,\rho}$-tensor that will make it easier for us to generalize to the spinning case. It also makes it clear that the tensor depends on a choice of two-point structure convention. For a general representation ρ, the corresponding r-tensor is defined as

$$r_{\Delta,\rho;a'}{}^{\overline{b}} \langle O^\dagger_{\overline{b}}((-e)^+) O^a(e)\rangle = \delta^a{}_{a'}, \tag{3.75}$$

where the operator O has quantum numbers (Δ,ρ). Here, a, a' are the indices of the representations ρ, ρ^*, and $\overline{b}$ labels the indices of the reflected representation ρ^R and its dual $\rho^\dagger$. On the right-hand side, $\delta^a{}_{a'}$ is the identity matrix of the ρ representation (i.e., $\delta^a{}_{a'} T^{a'} = T^a$ for any tensor T with representation ρ).

Motivated by symmetry, we can write down an ansatz for the $r_{\Delta,\rho}$-tensor using the two-point function of the shadow operator $\widetilde{O}$,

$$r_{\Delta,\rho;a'}{}^{\overline{b}} = C_{\Delta,\rho} \langle \widetilde{O}^\dagger_{a'}(e) \widetilde{O}^{\overline{b}}((-e)^+)\rangle. \tag{3.76}$$

Plugging this ansatz into the definition of $r_{\Delta,\rho}$ and taking the trace, we obtain

$$C_{\Delta,\rho} \langle \widetilde{O}^\dagger_a(e) \widetilde{O}^{\overline{b}}((-e)^+)\rangle \langle O^\dagger_{\overline{b}}((-e)^+) O^a(e)\rangle = \delta^a{}_a = \dim(\rho). \tag{3.77}$$

We see that the unknown coefficient $C_{\Delta,\rho}$ in the ansatz can be expressed in terms of the dimension of the representation and a pairing of the two-point functions.

We define a natural Euclidean two-point pairing (Karateev, Kravchuk, and Simmons-Duffin, 2019),[10]

$$\begin{aligned}\frac{\left(\langle\widetilde{O}^{\dagger}\widetilde{O}\rangle,\langle O^{\dagger}O\rangle\right)}{\mathrm{vol}(\mathrm{SO}(1,1))} &= \int\frac{d^dx d^dy}{\mathrm{vol}(\mathrm{SO}(d+1,1))}\langle\widetilde{O}_a^{\dagger}(x)\widetilde{O}^{\overline{b}}(y)\rangle\langle O_{\overline{b}}^{\dagger}(y)O^a(x)\rangle,\\ &= \frac{1}{2^d\,\mathrm{vol}(\mathrm{SO}(d))\,\mathrm{vol}(\mathrm{SO}(1,1))}\langle\widetilde{O}_a^{\dagger}(0)\widetilde{O}^{\overline{b}}(\infty)\rangle\langle O_{\overline{b}}^{\dagger}(\infty)O^a(0)\rangle.\end{aligned} \tag{3.78}$$

Originally, in (3.77) we want to compute the pairing between Lorentzian two-point structures. Since the two points $e,(-e)^+$ are spacelike separated, the structures can be thought of as Euclidean two-point structures with distance $\sqrt{-(2e)^2}=2$, and we can replace the pairing with a Euclidean two-point pairing (3.78). Using the two-point pairing, one can then show that (3.77) gives

$$C_{\Delta,\rho} = \frac{2^d\dim(\rho)}{\mathrm{vol}(\mathrm{SO}(d))\left(\langle\widetilde{O}^{\dagger}\widetilde{O}\rangle,\langle O^{\dagger}O\rangle\right)}, \tag{3.79}$$

and the r-tensor can be written as

$$r_{\Delta,\rho;a'}{}^{\overline{b}} = \frac{2^d\dim(\rho)}{\mathrm{vol}(\mathrm{SO}(d))\left(\langle\widetilde{O}^{\dagger}\widetilde{O}\rangle,\langle O^{\dagger}O\rangle\right)}\langle\widetilde{O}_{a'}^{\dagger}(e)\widetilde{O}^{\overline{b}}((-e)^+)\rangle. \tag{3.80}$$

Scalar sum rules

Let us briefly summarize what we have done and write down the final formula for the scalar functional in the bulk-point limit. We started with the commutator of two light-transformed operators and wrote down a functional $\Psi_{k,\nu}$ ((3.33)) whose action on any physical four-point function vanishes. The functional integrates the four-point function against a specific kernel over the external points $x_{1,2,3,4}$ and internal variables x_0, z_0. Using the Lorentzian shadow representation of conformal blocks, we wrote down the action of the functional on blocks, with an additional internal point x_5 from the shadow representation. We then found that in the bulk-point limit ($\nu, m \gg 1$ with $\nu < m$), the integral gets completely localized to a saddle configuration (3.63). Furthermore we removed the shadow coefficient by introducing a final internal point x_6.

In the end, we obtain a formula for the action of the functional on a conformal block in the bulk-point limit. The formula is given by a known coefficient and a

[10]Compared to the definition in (Karateev, Kravchuk, and Simmons-Duffin, 2019), we have absorbed an infinite vol(SO(1, 1)) factor to make the pairing finite.

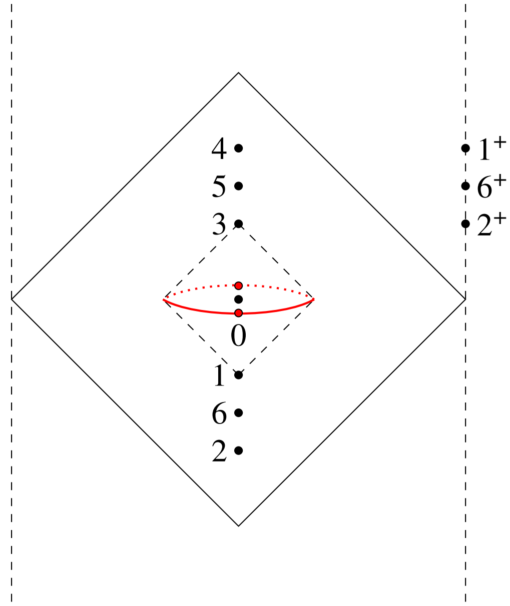

Figure 3.5: The bulk-point limit localizes the spacetime integral to a saddle locus that we call the scattering-crystal. The entire saddle satisfies the causality constraint $4 > 5 > 3 > 0 > 1 > 6 > 2$. The two delta functions restrict x_0 to be on an S^{d-2} shown by the red circle in the figure. The saddle locus further restricts x_0 to an S^{d-3}, which is represented by the two red dots (0-sphere). Points 5 and 6 are localized at $\pm e$. Points $1, 2, 3, 4$ are restricted to be timelike vectors, although in practice they have purely imaginary spatial components (see (3.81)).

product of conformally-invariant structures evaluated at a configuration that fixes all the positions and polarizations, $x_{0,1,2,3,4,5,6}, z_0$. In lightcone coordinates, the configuration is given by (see figure 3.5)

$$\begin{gathered}
x_3 = -x_1 = y, \quad x_4 = -x_2 = \frac{x}{-x^2}, \quad x_5 = e = (1, 1, \vec{0}), \quad x_6 = -e, \\
x = \left(-i\tfrac{m-\sqrt{m^2-\nu^2}}{\nu}, i\tfrac{m-\sqrt{m^2-\nu^2}}{\nu}, \vec{0}\right), \quad y = \left(i\tfrac{m-\sqrt{m^2-\nu^2}}{\nu}, -i\tfrac{m-\sqrt{m^2-\nu^2}}{\nu}, \vec{0}\right), \\
z_0 = (1, 0, \vec{0}), \quad x_0 = (0, 0, \vec{y}_0), \quad |\vec{y}_0|^2 = \frac{(m - \sqrt{m^2 - \nu^2})^2}{\nu^2}.
\end{gathered} \tag{3.81}$$

As we will show later, evaluating the conformal structures in this configuration reproduces the heavy action of a flat space sum rule and allows us to study the bulk scattering process. This is a generalization of the saddle point that leads to the *spacelike scattering* phenomenon in (Simon Caron-Huot, Mazac, et al., 2021a). We will call the configuration (3.81) the “scattering-crystal."

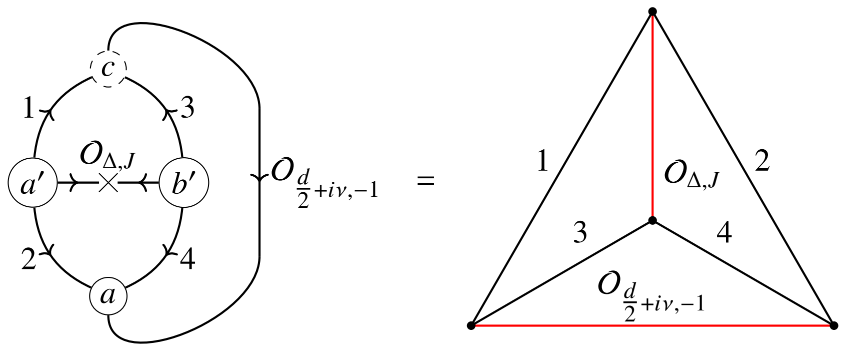

Figure 3.6: Our functional is a special $6j$ symbol (or a tetrahedron) where one of the three-point structures is a celestial structure. The cross in the left figure stands for the contraction of the $\langle\widetilde{\mathcal{O}}^\dagger\widetilde{\mathcal{O}}\rangle$ tensor. The flat space limit is the limit where the two red legs have large quantum numbers. (More precisely, the two legs have large scaling dimensions.)

By plugging (3.74) in (3.68) to remove the shadow coefficient, we find

$$\begin{aligned}
&\lim_{\substack{\nu,m\gg 1\\ \nu<m}} \frac{\Psi^+_{k,\nu}[G^s_{\Delta,J}]}{-2(2\sin^2(\pi\frac{\Delta-J-2\Delta_\phi}{2}))} \\
&= A_{k,\nu}\frac{2^{\frac{5}{2}+2d}\pi^{d-\frac{1}{2}}e^{i\frac{\pi}{4}}m^{\frac{3d}{2}+2}\nu^{\frac{7}{2}-4d}(m^2-\nu^2)^{\frac{d-2}{2}}(m-\sqrt{m^2-\nu^2})^{d-4}}{\Gamma\left(\frac{d-2}{2}\right)\mathrm{vol}(\mathrm{SO}(d-2))} \\
&\times\langle 0|\phi_4\mathbf{L}[\mathcal{O}](x_0,z_0)\phi_{2^+}|0\rangle^{-1}\langle\widetilde{\mathcal{P}}_{\delta_1}(x_{1^+0})\widetilde{\mathcal{P}}_{\delta_3}(x_{30})\mathcal{P}_\delta(z_0)\rangle \\
&\times|\langle\phi_{1^+}\phi_{2^+}\mathcal{O}^{\mu_1\cdots\mu_J}(x_5)\rangle|r_{\Delta,J;\mu_1\cdots\mu_J}{}^{\nu_1\cdots\nu_J}|\langle\mathcal{O}^\dagger_{\nu_1\cdots\nu_J}(x_6^+)\phi_3\phi_4\rangle|\Big|_{\text{scattering-crystal}}\,.
\end{aligned} \tag{3.82}$$

A nice feature of the scattering-crystal is that both structures with absolute values satisfy the identity (3.47) in this configuration. Therefore, we can replace those structures with commutators of standard Wightman structures, and remove the $-2((2\sin^2(\pi\frac{\Delta-J-2\Delta_\phi}{2}))$ factor on the left-hand side. Moreover, by applying the natural formula for the r-tensor given by (3.80), we arrive at the final formula for the action of the scalar functional in the bulk-point limit:[11]

$$
\begin{aligned}
&\lim_{\substack{\nu,m\gg 1\\ \nu<m}} \Psi^{+}_{k,\nu}[G^{s}_{\Delta,J}]\\
&= A_{k,\nu}\frac{2^{\frac{5}{2}+2d}\pi^{d-\frac{1}{2}}e^{i\frac{\pi}{4}}m^{\frac{3d}{2}+2}\nu^{\frac{7}{2}-4d}(m^2-\nu^2)^{\frac{d-2}{2}}(m-\sqrt{m^2-\nu^2})^{d-4}}{\Gamma\left(\frac{d-2}{2}\right)\mathrm{vol}(\mathrm{SO}(d-2))}\frac{2^d\dim(\rho)}{\mathrm{vol}(\mathrm{SO}(d))}\\
&\times\langle 0|\phi_4\mathbf{L}[O](x_0,z_0)\phi_{2^+}|0\rangle^{-1}\langle\widetilde{\mathcal{P}}_{\delta_1}(x_{1^+0})\widetilde{\mathcal{P}}_{\delta_3}(x_{30})\mathcal{P}_{\delta}(z_0)\rangle\\
&\times\left.\frac{\langle 0|[\phi_{1^+},\phi_{2^+}]O^{\mu_1\cdots\mu_J}(x_5)|0\rangle\langle\widetilde{O}^{\dagger}_{\mu_1\cdots\mu_J}(x_5)\widetilde{O}^{\nu_1\cdots\nu_J}(x_6^+)\rangle\langle 0|O^{\dagger}_{\nu_1\cdots\nu_J}(x_6^+)[\phi_4,\phi_3]|0\rangle}{\left(\langle\widetilde{O}^{\dagger}\widetilde{O}\rangle,\langle O^{\dagger}O\rangle\right)}\right|_{\text{scattering-crystal}}.
\end{aligned}
\tag{3.83}
$$

This formula can be viewed as a kind of $6j$ symbol, or equivalently a tetrahedron formed by gluing conformal three-point structures (see figure 3.6). Compared to the usual $6j$ symbol (Liu et al., 2019), in our case one of the three-point structures becomes a celestial structure, which originally comes from setting one of the legs to have $J=-1$. Furthermore, the bulk-point limit, which reproduces the flat space functional, corresponds to setting two of the legs to have large quantum numbers. In this limit, one of them has large and positive dimension $\Delta\gg 1$ and the other one has dimension $\frac{d}{2}+i\nu$ with $\nu\gg 1$. For usual $6j$ symbols in the classical limit, where all legs have large quantum number, they can be computed as the volume of a tetrahedron (Murakami and Yano, 2005). It would be interesting to see if there is a similar argument for the bulk-point limit of our functional.

Before using this formula, we still need to address two more issues. First, note that the original functional $\Psi_{k,\nu}$ in (3.33) is given by

$$\Psi_{k,\nu}=\Psi^{+}_{k,\nu}-(1\leftrightarrow 3). \tag{3.84}$$

Therefore, when we apply $\Psi_{k,\nu}$ to a four-point function of identical operators, which is manifestly symmetric under $(1\leftrightarrow 3)$, we will get a trivial sum rule since its action on each conformal block is simply zero. The second issue is about the convergence in the Regge limit discussed below (3.32). For external scalars, in order for the light transforms to converge, we need the Regge intercept to satisfy $J_0<-1$, while for non-perturbative CFTs we only know that $J_0\leq 1$ (Hartman, Jain, and Kundu, 2016; Simon Caron-Huot, 2017; Kologlu et al., 2020).

[11] To keep track of $(-1)^J$ factors, we should clarify our convention for $\langle 0|O^{\dagger}(x_6)[\phi_4,\phi_3]|0\rangle$. Our convention is that it should be the analytic continuation of (3.204) with $1\to 3, 2\to 4, 3\to 6$.

It turns out that both issues can be resolved by introducing a “subtraction factor" to the functional, that is, we consider a more general functional

$$\Psi_{k,\nu,f}[\mathcal{G}] = \Psi^{+}_{k,\nu}[f(u',v')\mathcal{G}] - (1 \leftrightarrow 3), \tag{3.85}$$

where $f(u',v')$ is a meromorphic function of the conformally-invariant cross-ratios u', v' defined in (3.31). Note that the kernel of $\Psi_{k,\nu,f}$ is again manifestly antisymmetric under $1 \leftrightarrow 3$. On the other hand, points 1 and 3 are always spacelike in the range of integration of the functional, which comes from the light transforms. Therefore, causality/crossing guarantees that any physical correlator $\mathcal{G}$ should be symmetric under $1 \leftrightarrow 3$ in the integral, and the action of the general functional $\Psi_{k,\nu,f}$ should vanish on physical four-point functions. Additionally, by choosing subtraction factors that are antisymmetric under $1 \leftrightarrow 3$, which swaps u' and v', we can get nontrivial sum rules for identical external scalars, meaning its action on each conformal block is nonzero. Furthermore, by restricting to subtraction factors with nice behaviors in the Regge limit, we can make sure the integral of the functional is convergent in the Regge limit.

For the scalar case, a nice choice of subtraction factors with the above properties is[12]

$$f_k^{\text{scalar}}(u',v') = \begin{cases} \frac{v'-u'}{(u'v')^{\frac{k+2}{4}}} & k \equiv 2 \bmod 4 \\ \frac{(v'-u')^3-(v'-u')}{4(u'v')^{\frac{k+4}{4}}} & k \equiv 0 \bmod 4 \end{cases}, \qquad k = 2,4,6,\ldots. \tag{3.87}$$

At the scattering-crystal locus, these subtraction factors become

$$f_k^{\text{scalar}}(u',v')\big|_{\text{scattering-crystal}} = -\nu^{2k+2}\frac{(2m^2-\nu^2)}{m^2(m^2-\nu^2)}\frac{1}{(m^2(m^2-\nu^2))^{\frac{k}{2}}}. \tag{3.88}$$

Note that this satisfies $f_k^{\text{scalar}}(u',v') = -f_k^{\text{scalar}}(v',u')$. In the Regge limit, the subtraction factor increases the effective Regge spin of the kernel by $k+1$. (One can see this from the large-m scaling of (3.88).) Therefore, the condition from convergence in the Regge limit becomes $J_0 < k$, which is indeed true for any $k \geq 2$.

[12] The $k \equiv 2 \bmod 4$ case follows straightforwardly from the discussion in appendix D of (Simon Caron-Huot, Mazac, et al., 2021a). The other case can be motivated by taking the large-ν limit of (D.12) in the same paper, and using the identity

$$\left((v'-u')^3 + \frac{3}{d-8}(v'-u')\right)G_{d-1,\frac{2-d}{2}+i\nu} \sim 8G_{d-5,\frac{2-d}{2}+i\nu}, \quad \nu \to \infty. \tag{3.86}$$

Using the subtraction factors (3.87), we can then write down nontrivial sum rules for identical scalars,

$$\Psi_{k,\nu,f_k^{\text{scalar}}}[\mathcal{G}_{\phi\phi\phi\phi}] = 0. \tag{3.89}$$

Its action on a single s-channel block is given by

$$\Psi_{k,\nu,f_k^{\text{scalar}}}[G^s_{\Delta,J}] = 2\Psi^+_{k,\nu}[f_k^{\text{scalar}}(u',v')G^s_{\Delta,J}]. \tag{3.90}$$

In the bulk-point limit, since the subtraction factors do not have any ν and m dependence, the formula (3.83) gets modified to

$$\begin{aligned}
&\lim_{\substack{\nu,m\gg 1\\ \nu<m}} \Psi_{k,\nu,f_k^{\text{scalar}}}[G^s_{\Delta,J}] \\
&= A_{k,\nu}\frac{2^{\frac{7}{2}+2d}\pi^{d-\frac{1}{2}}e^{i\frac{\pi}{4}}m^{\frac{3d}{2}+2}\nu^{\frac{7}{2}-4d}(m^2-\nu^2)^{\frac{d-2}{2}}(m-\sqrt{m^2-\nu^2})^{d-4}}{\Gamma\left(\frac{d-2}{2}\right)\mathrm{vol}(\mathrm{SO}(d-2))}\frac{2^d\dim(\rho)}{\mathrm{vol}(\mathrm{SO}(d))} \\
&\times \langle 0|\phi_4\mathbf{L}[\mathcal{O}](x_0,z_0)\phi_{2^+}|0\rangle^{-1}\langle\widetilde{\mathcal{P}}_{\delta_1}(x_{1^+0})\widetilde{\mathcal{P}}_{\delta_3}(x_{30})\mathcal{P}_{\delta}(z_0)\rangle f_k^{\text{scalar}}(u',v') \\
&\times \left.\frac{\langle 0|[\phi_{1^+},\phi_{2^+}]\mathcal{O}^{\mu_1\cdots\mu_J}(x_5)0|\rangle\langle\widetilde{\mathcal{O}}^\dagger_{\mu_1\cdots\mu_J}(x_5)\widetilde{\mathcal{O}}^{\nu_1\cdots\nu_J}(x_6^+)\rangle\langle 0|\mathcal{O}^\dagger_{\nu_1\cdots\nu_J}(x_6^+)[\phi_4,\phi_3]|0\rangle}{\left(\langle\widetilde{\mathcal{O}}^\dagger\widetilde{\mathcal{O}}\rangle,\langle\mathcal{O}^\dagger\mathcal{O}\rangle\right)}\right|_{\text{scattering-crystal}}.
\end{aligned} \tag{3.91}$$

We can then evaluate the structures and and the subtraction factor at the scattering-crystal locus to find an explicit expression. Moreover, for symmetric traceless tensors, the pairing $\frac{\mathrm{vol}(\mathrm{SO}(d))}{2^d\dim(\rho)}\left(\langle\widetilde{\mathcal{O}}^\dagger\widetilde{\mathcal{O}}\rangle,\langle\mathcal{O}^\dagger\mathcal{O}\rangle\right)$ becomes 4^{-d} (Karateev, Kravchuk, and Simmons-Duffin, 2019). After combining all the factors and writing the result in terms of the "heavy action" defined in (3.28), we obtain

$$\lim_{\substack{\nu,m\gg 1\\ \nu<m}} \Psi_{k,\nu,f_k^{\text{scalar}}}[\Delta,J] = \frac{2m^2-\nu^2}{m^2-\nu^2}\frac{\mathcal{P}_J(1-\frac{2\nu^2}{m^2})}{(m^2(m^2-\nu^2))^{\frac{k}{2}}}. \tag{3.92}$$

As reviewed in section 3.2, this is precisely the heavy state contribution of the flat space sum rule for scalars.

Spinning sum rules

We are now ready to write down the sum rules for spinning operators. The above analysis for the bulk-point limit can be generalized straightforwardly. A spinning functional can be defined by

$$\Psi^{(a),(c)}_{k,\nu,\lambda'}[\mathcal{G}] \equiv$$
$$\int_{\substack{2>4\\0\approx 2,4}} \frac{d^dx_2 d^dx_4 d^dx_0 D^{d-2}z_0}{\mathrm{vol}(\widetilde{\mathrm{SO}}(d,2))} \left(\langle 0|\mathcal{O}_4(x_4^+)\mathbf{L}[\mathcal{O}](x_0,z_0)\mathcal{O}_2(x_2)|0\rangle^{(a)}\right)^{-1}. \tag{3.93}$$
$$\int D^{d-2}z_1 D^{d-2}z_3 \langle \widetilde{\mathcal{P}}^{\dagger}_{\delta_1,\lambda_1}(z_1)\widetilde{\mathcal{P}}^{\dagger}_{\delta_3,\lambda_3}(z_3)\mathcal{P}_{\delta,\lambda'}(z_0)\rangle^{(c)}$$
$$\langle\Omega|\mathcal{O}_4(x_4^+)[\mathbf{L}[\mathcal{O}_3](x_0,z_3),\mathbf{L}[\mathcal{O}_1](x_0,z_1)]\mathcal{O}_2(x_2)|\Omega\rangle$$

Compared to the scalar case (3.33), the main difference is that the operators $\mathcal{O}$ and $\mathcal{P}_{\delta,\lambda'}$ can have more complicated representations, and there are multiple allowed dual structures and celestial structures.

Moreover, in the spinning case we do not include any coefficient in front of the integral. In the scalar case, there is a natural choice for this coefficient $A_{k,\nu}$, which is the factor needed to exactly reproduce the action of flat space sum rule (3.92). However, as we will see in the next section, for spinning operators, the CFT sum rules and flat space sum rules are related by a matrix. Since there is no natural choice for the overall factor, we do not include a factor in our definition of the spinning functional.

Let us introduce some notation to describe spinning operators. A spinning operator with $\mathrm{SO}(d-1,1)$ representation ρ can be described by a Young diagram with rows of length $(m_1, m_2, \ldots, m_n)$, where $n = \lfloor \frac{d}{2} \rfloor$. We will also use the notation $\rho = (J,\lambda)$, where $J = m_1$ is the spin, and $\lambda = (m_2,\ldots,m_n)$ specifies an $\mathrm{SO}(d-2)$ representation (which we sometimes call the "transverse" representation). We also define $j = m_2$ to be the transverse spin of the operator.

In (3.93), the external operators have quantum numbers $(\Delta_i, J_i, \lambda_i)$, and the operator $\mathcal{O}$ in the first line has quantum numbers $(\frac{d}{2}+i\nu, J_1+J_3-1, \lambda')$. In the second line, the celestial operators, which are primary operators that live on the celestial sphere, also carry $\mathrm{SO}(d-2)$ representations. $\widetilde{\mathcal{P}}^{\dagger}_{\delta_1,\lambda_1}$ and $\widetilde{\mathcal{P}}^{\dagger}_{\delta_3,\lambda_3}$ have the same $\mathrm{SO}(d-2)$ representations as the transverse representations of the external operators $\mathcal{O}_1, \mathcal{O}_3$, and $\mathcal{P}_{\delta,\lambda'}$ have the same transverse representation as $\mathcal{O}$. Note that the $\mathrm{SO}(d-1,1)$ indices of the ρ_2, ρ_4 representations, and the $\mathrm{SO}(d-2)$ indices of $\lambda_1, \lambda_3, \lambda'$ are implicitly contracted in (3.93).

In addition to the ν variable, the spinning functional also depends on a choice of $\mathrm{SO}(d-2)$ representation λ'. Moreover, the functional has two tensor structure labels $(a), (c)$. The first label (a) corresponds to the tensor structure of the spinning dual structure, defined as

$$\left(\left(\langle 0|O_4(x_4^+)\mathbf{L}[O](x_0,z_0)O_2(x_2)|0\rangle^{(a)}\right)^{-1}, \langle 0|O_4(x_4^+)\mathbf{L}[O](x_0,z_0)O_2(x_2)|0\rangle_{(b)}\right)_L = \delta^a_b. \tag{3.94}$$

The allowed number of labels (a) is the number of continuous-spin structures of $\langle O_2 O_4 O\rangle$, which is given by (Kravchuk and Simmons-Duffin, 2018a; Kologlu et al., 2021)

$$\left(\lambda' \otimes \left(\mathrm{Res}^{\mathrm{SO}(d-1,1)}_{\mathrm{SO}(d-2)} \rho_2 \otimes \rho_4\right)\right)^{\mathrm{SO}(d-2)}, \tag{3.95}$$

where Res^G_H denotes the restriction of a representation of G to its subgroup H, and $(\dots)^H$ denotes the number of H-singlets. The second tensor structure label (c) corresponds to the structures of a celestial three-point function with $\mathrm{SO}(d-2)$ representation $\lambda_1, \lambda_3, \lambda'$. The number of those structures is (Kravchuk and Simmons-Duffin, 2018a)

$$\left(\mathrm{Res}^{\mathrm{SO}(d-2)}_{\mathrm{SO}(d-3)} \lambda_1 \otimes \lambda_3 \otimes \lambda'\right)^{\mathrm{SO}(d-3)}. \tag{3.96}$$

Combining (3.95) and (3.96), we see that given the representations of the external operators, the allowed choice of the transverse representation λ' is

$$\left\{\lambda' | \lambda' \in \mathrm{Res}^{\mathrm{SO}(d-1,1)}_{\mathrm{SO}(d-2)} \rho_2 \otimes \rho_4, \left(\mathrm{Res}^{\mathrm{SO}(d-2)}_{\mathrm{SO}(d-3)} \lambda_1 \otimes \lambda_3 \otimes \lambda'\right)^{\mathrm{SO}(d-3)} \neq 0\right\}. \tag{3.97}$$

In section 3.4, we will give the set of allowed λ''s for some concrete examples.

Similar to the scalar case, commutativity of the light-transformed operators implies

$$\Psi^{(a),(c)}_{k,\nu,\lambda'}[\mathcal{G}] = 0, \quad J_1 + J_3 - 1 > J_0. \tag{3.98}$$

Again, this condition can be equivalently written in terms of the $C^{\pm}_{ab}(\Delta, \rho)$ coefficient function,

$$C^{(-1)^{J_1+J_3-1}}_{ab}\left(\tfrac{d}{2} + i\nu, J_1 + J_3 - 1, \lambda'\right) = 0, \quad J_1 + J_3 - 1 > J_0, \tag{3.99}$$

where a is the same tensor structure label of the functional (3.93), which corresponds to the structures of the $O_2 \times O_4$ OPE. On the other hand, b is a subset of the structures of the $O_1 \times O_3$ OPE that have the same counting rule as the celestial structures (3.96) (see (Chang, Kologlu, et al., 2022) for more details).

The spinning heavy action

We now derive a formula for the heavy action of the spinning functional in the bulk-point limit, similar to the scalar case (3.83). For simplicity, in what follows we assume the external operators are symmetric traceless tensors with spin J_e, and they all have scaling dimensions Δ_e. By rewriting the light transforms in (3.93), the spinning functional can be written as

$$\Psi^{(a),(c)}_{k,\nu,\lambda'} = \Psi^{+(a),(c)}_{k,\nu,\lambda'} - (1 \leftrightarrow 3), \tag{3.100}$$

and

$$\begin{aligned}
&\Psi^{+(a),(c)}_{k,\nu,\lambda'}[\mathcal{G}] \\
&= 4\int_{4>3>0>1>2} \frac{d^dx_1 d^dx_2 d^dx_3 d^dx_4 d^dx_0 D^{d-2}z_0}{\mathrm{vol}(\widetilde{\mathrm{SO}}(d,2))}\delta(x^2_{1^+0})\delta(x^2_{30})\theta(x_{1^+0})\theta(x_{30}) \\
&\times \left(\langle 0|\mathcal{O}_4(x_4)\mathbf{L}[\mathcal{O}](x_0,z_0)\mathcal{O}_2(x_2^+)|0\rangle^{(a)}\right)^{-1} \langle \widetilde{\mathcal{P}}^\dagger_{\delta_1,\lambda_1}(x_{1^+0})\widetilde{\mathcal{P}}^\dagger_{\delta_3,\lambda_3}(x_{30})\mathcal{P}_{\delta,\lambda'}(z_0)\rangle^{(c)} \\
&\times \langle\Omega|[\mathcal{O}_4(x_4),\mathcal{O}_3(x_3,x_{30})][\mathcal{O}_1(x_1^+,x_{1^+0}),\mathcal{O}_2(x_2^+)]|\Omega\rangle.
\end{aligned} \tag{3.101}$$

Note that the polarizations of $\mathcal{O}_1, \mathcal{O}_3$ are fixed to be x_{30}, x_{1^+0} (which are null vectors due to the delta functions in the integrand). This is because of the light transforms $\mathbf{L}[\mathcal{O}_3]\mathbf{L}[\mathcal{O}_1]$ in (3.93).

To study the action of $\Psi^{+(a),(c)}_{k,\nu,\lambda'}$ on a conformal block, we again use the Lorentzian shadow representation of the block and consider the bulk-point limit, in which $\Delta \sim m$ and $\nu, m \gg 1, \nu < m$. To perform the saddle point analysis, we separate the integrand into a quickly-varying part and slowly-varying part. Crucially, in the bulk-point limit, the quickly-varying part of the integrand is the same as the scalar case! To see why, recall that the factor in the scalar case is given by (3.55), and it comes from powers of $x^2_{ij}, z_0 \cdot x_{10}, z_0 \cdot x_{30}, x_{10} \cdot x_{30}$, and $V_{0,24}$ in the conformally-invariant structures in the integrand. For spinning structures, the powers of these factors will only differ by integer values that depend on the representations and choice of tensor structures, and hence they do not matter in the $\nu, m \gg 1$ limit. Since the quickly-varying part in the scalar and spinning cases are identical, the saddle point analysis for the spinning case is identical to what we did in section 3.3. As a result, the formula in the scalar case immediately generalizes to the spinning case, and by rewriting (3.83) we obtain that the formula in the spinning case is given by

$$\lim_{\substack{\nu,m\gg 1\\ \nu<m}} \Psi^{+(a),(c)}_{k,\nu,\lambda'}[G^{s}_{\Delta,\rho,(a'b')}]$$
$$= \frac{2^{\frac{5}{2}+2d}\pi^{d-\frac{1}{2}}e^{i\frac{\pi}{4}}m^{\frac{3d}{2}+2}\nu^{\frac{7}{2}-4d}(m^2-\nu^2)^{\frac{d-2}{2}}(m-\sqrt{m^2-\nu^2})^{d-4}}{\Gamma\left(\frac{d-2}{2}\right)\mathrm{vol}(\mathrm{SO}(d-2))}\frac{2^d\dim(\rho)}{\mathrm{vol}(\mathrm{SO}(d))}\times$$
$$\left(\langle 0|\mathcal{O}_4(x_4)\mathbf{L}[\mathcal{O}](x_0,z_0)\mathcal{O}_2(x_2^+)|0\rangle^{(a)}\right)^{-1}\langle\widetilde{\mathcal{P}}^{\dagger}_{\delta_1,\lambda_1}(x_{1^+0})\widetilde{\mathcal{P}}^{\dagger}_{\delta_3,\lambda_3}(x_{30})\mathcal{P}_{\delta,\lambda'}(z_0)\rangle^{(c)}\times$$
$$\left.\frac{\langle 0|[\mathcal{O}_1(x_{1^+},x_{1^+0}),\mathcal{O}_2(x_{2^+})]\mathcal{O}(x_5)|0\rangle_{(a')}\langle\widetilde{\mathcal{O}}^{\dagger}(x_5)\widetilde{\mathcal{O}}(x_6^+)\rangle\langle 0|\mathcal{O}^{\dagger}(x_6^+)[\mathcal{O}_4(x_4),\mathcal{O}_3(x_3,x_{30})]|0\rangle_{(b')}}{\left(\langle\widetilde{\mathcal{O}}^{\dagger}\widetilde{\mathcal{O}}\rangle,\langle\mathcal{O}^{\dagger}\mathcal{O}\rangle\right)}\right|_{\substack{\text{scattering-}\\ \text{crystal}}},$$
(3.102)

where (a'), (b') are the three-point tensor structure labels of the block. The formula should be evaluated at the same "scattering-crystal" as the scalar case, given by (3.81), and we have implicitly contracted all the $\mathrm{SO}(d-1,1)$ indices of ρ_2,ρ_4,ρ and the $\mathrm{SO}(d-2)$ indices of $\lambda_1,\lambda_3,\lambda'$.

Subtraction factors

To finish the discussion of spinning sum rules, let us give the subtraction factors that should be used in the spinning case. We consider a more general functional

$$\Psi^{(a),(c)}_{k,\nu,\lambda',f}[\mathcal{G}] = \Psi^{+(a),(c)}_{k,\nu,\lambda'}[f(u',v')\mathcal{G}] - (1\leftrightarrow 3). \qquad (3.103)$$

As discussed in section 3.3, to have nontrivial sum rules for identical external operators, the kernel of the $\Psi^{+(a),(c)}_{k,\nu,\lambda'}$ functional times the subtraction factor $f(u',v')$ should be antisymmetric under $(1\leftrightarrow 3)$. For the spinning functionals, the signature under swapping 1 and 3 depends on the transverse representation λ'. We will focus on the case where the external operators are symmetric traceless tensors, so the allowed λ' satisfying the selection rule (3.97) should be a symmetric traceless tensor itself (as an $\mathrm{SO}(d-2)$ representation). Therefore, the spinning functionals in this case are labeled by an integer j', which is the transverse spin. Due to the celestial structure $\langle\widetilde{\mathcal{P}}_1\widetilde{\mathcal{P}}_3\mathcal{P}_{\delta,j'}\rangle$, the functional $\Psi^{+(a),(c)}_{k,\nu,j'}$ has signature $(-1)^{j'}$ under $(1\leftrightarrow 3)$. Therefore, the nontrivial spinning sum rules are given by

$$\Psi^{+(a),(c)}_{k,\nu,j'}[f^{(-1)^{j'}}(u',v')\mathcal{G}] = 0, \qquad (3.104)$$

where the subtraction factors should satisfy

$$f^{\pm}(v',u') = \mp f^{\pm}(u',v'). \qquad (3.105)$$

We find that for external operators with spin J_e, the subtraction factors with even j' can be chosen to be

$$f^{+}_{k;J_e}(u',v') = \begin{cases} \frac{v'-u'}{(u'v')^{\frac{k-2J_e+2}{4}}} & k \equiv 2J_e + 2 \bmod 4 \\ \frac{(v'-u')^3-(v'-u')}{4(u'v')^{\frac{k-2J_e+4}{4}}} & k \equiv 2J_e \bmod 4 \end{cases}, \qquad k = 2,4,6,\dots, \tag{3.106}$$

which reduces to the scalar case (3.87) when $J_e = 0$. On the other hand, for odd j' we have

$$f^{-}_{k;J_e}(u',v') = \begin{cases} -\frac{1}{(u'v')^{\frac{k-2J_e+1}{4}}} & k \equiv 2J_e + 3 \bmod 4 \\ -\frac{(u'-v')^2-1}{4(u'v')^{\frac{k-2J_e+3}{4}}} & k \equiv 2J_e + 1 \bmod 4 \end{cases}, \qquad k = 3,5,7,\dots. \tag{3.107}$$

When evaluating these subtraction factors at the scattering crystal (3.81), we find

$$\begin{aligned} f^{+}_{k;J_e}(u',v')\Big|_{\text{scattering-crystal}} &= -\nu^{2(k-2J_e+1)}\frac{(2m^2-\nu^2)}{m^2(m^2-\nu^2)}\frac{1}{(m^2(m^2-\nu^2))^{\frac{k-2J_e}{2}}}, \quad k = 2,4,6,\dots, \\ f^{-}_{k;J_e}(u',v')\Big|_{\text{scattering-crystal}} &= -\nu^{2(k-2J_e)}\frac{\nu^2}{m^2(m^2-\nu^2)}\frac{1}{(m^2(m^2-\nu^2))^{\frac{k-2J_e-1}{2}}}, \quad k = 3,5,7,\dots. \end{aligned} \tag{3.108}$$

From the flat space point of view, the expressions for the subtraction factors at the saddle are precisely what we need. We expect that functionals with even j' are related to the $s \leftrightarrow t$ symmetric part of the flat space amplitude. Therefore, the corresponding flat space sum rule should have a factor

$$\left(\frac{1}{s} + \frac{1}{s+u}\right)\frac{1}{(s(s+u))^{\frac{k}{2}}} = \frac{2s+u}{s(s+u)}\frac{1}{(s(s+u))^{\frac{k}{2}}}. \tag{3.109}$$

On the other hand, functionals with odd j' should be related to the $s \leftrightarrow t$ antisymmetric part, and the corresponding flat space sum rule should have the factor

$$\left(\frac{1}{s} - \frac{1}{s+u}\right)\frac{1}{(s(s+u))^{\frac{k}{2}}} = \frac{u}{s(s+u)}\frac{1}{(s(s+u))^{\frac{k}{2}}}. \tag{3.110}$$

Under the identification $s = m^2, u = -\nu^2$, we see that these expressions agree with $f^{\pm}_{k;J_e}(u',v')$ at the saddle. We make this connection more precise in section 3.4.

Finally, let us explain the allowed range of k in (3.106) and (3.107). In the Regge limit, the subtraction factor f^+ changes the Regge spin by $k - 2J_e + 1$, and f^- changes the Regge spin by $k - 2J_e$. Therefore, for the integral of the functional to be convergent, we must have $k > J_0$ for even j' and $k - 1 > J_0$ for odd j'. For non-perturbative CFTs, we have $J_0 \leq 1$. So, we should choose $k \geq 2$ for even j' and $k \geq 3$ for odd j'. As we will show in the next section, k also agrees with the Regge spin of the corresponding flat space sum rule.

Normally, introducing subtraction factors comes with a price that the action of the functional becomes non-vanishing on finitely many light double-traces (Simon Caron-Huot, Mazac, et al., 2021b). However, if J_e is large enough, sometimes we can have subtraction factors that make the Regge behavior of the kernel worse. For these unsubtracted sum rules, the action on all double-traces will remain zero. On the flat space side, the EFT series of the corresponding flat space sum rule should automatically truncate, since there is no denominator in the integrand. As an example, for $J_e = 2$ (which corresponds to flat space gravitons), we have two such subtraction factors from $k = 2, k = 3$. Their expressions at the saddle are given by

$$\begin{aligned} f^{+}_{k=2;J_e=2}(u',v')\Big|_{\text{scattering-crystal}} &= -\nu^{-2}(2m^2 - \nu^2), \\ f^{-}_{k=3;J_e=2}(u',v')\Big|_{\text{scattering-crystal}} &= 1. \end{aligned} \tag{3.111}$$

These unsubtracted sum rules for gravitons will be given in section 3.4.

3.4 Flat space interpretation

We now discuss the flat space interpretation of the CFT sum rules derived in the previous section. On the flat space side, we are mainly interested in sum rules of photons and gravitons, which are dual to conserved operators on the CFT side. Our goal is to relate the CFT heavy action formula (3.102) to the heavy state contribution of the flat space sum rule. The heavy action formula consists of a block part (fourth line of (3.102)) from the block insertion, and a kernel part (third line of (3.102)) from the kernel of the functional. We will be able to understand both of them in flat space. Throughout the discussion, we will study the photon case in detail and explain how to match the CFT result and the flat space result. For the graviton case, we simply give the final relation between CFT sum rules and flat space sum rules.

Hereafter, we use D to denote the spacetime dimension of flat space, and $d = D - 1$ is the spacetime dimension of the CFT.

Conservation at large Δ

The flat space limit of a dispersive functional corresponds to an AdS scattering process where the incoming particles are boosted to high energies. Our main interest is in massless particles like photons and gravitons, which are dual to conserved CFT operators. In this highly boosted limit, conservation will substantially simplify the dictionary that we find. We expect that for external massive particles, it is most natural to use the goldstone equivalence theorem to break them into massless excitations, and use our dictionary for each excitation.

We first note that the conservation condition for CFT three-point structures simplifies when one of the operator dimensions Δ becomes large. For a three point function $\langle O_1(x_1, z_1) O_2(x_2, z_2) O_3(x_3, z_3)\rangle$, with O_1 conserved we can write its conservation condition as

$$0 = \partial_{\mu_1} \langle O_1^{\mu_1\cdots\mu_J}(x_1) O_2(x_2, z_2) O_3(x_3, z_3)\rangle. \tag{3.112}$$

We claim that at large $\Delta = \Delta_3$ this simplifies to

$$v^{\mu_1}_{1,23} \langle O_{1;\mu_1\cdots\mu_J} O_2 O\rangle = 0, \tag{3.113}$$

where

$$v^{\mu}_{1,23} = \frac{1}{2}\partial_1^{\mu} \log \frac{x_{12}^2}{x_{13}^2} = \frac{x_{12}^{\mu} x_{13}^2 - x_{13}^{\mu} x_{23}^2}{x_{12}^2 x_{13}^2}. \tag{3.114}$$

To see why, we can isolate the Δ dependence in the three-point structure:

$$\langle O_1^{\mu_1\cdots\mu_J}(x_1) O_2(x_2, z_2) O_3(x_3, z_3)\rangle = \left(\frac{x_{12}^2}{x_{13}^2 x_{23}^2}\right)^{\Delta/2} \times (\cdots), \tag{3.115}$$

where $(\cdots)$ does not depend exponentially on Δ. Applying the conservation condition (3.112), the leading contribution in the large-Δ limit comes from the prefactor in (3.115), which gives (3.113).

Let us check this claim in the explicit example $\langle JJO\rangle$, where J is a spin-1 conserved operator, and O is a symmetric traceless tensor. Before imposing conservation, the general three-point function $\langle JJO\rangle$ in the embedding space (using the conventions in (3.211)) is given by

$$\begin{aligned}&\langle J(X_1, Z_1) J(X_2, Z_2) O(X_3, Z_3)\rangle \\ &= \frac{c_1(-2V_3)^{J-2} H_{23} H_{13} + c_2 H_{12} (-2V_3)^J + c_3 V_2 H_{13} (-2V_3)^{J-1} + c_4 V_1 H_{23} (-2V_3)^{J-1} + c_5 V_1 V_2 (-2V_3)^J}{X_{12}^{\frac{\Delta_1+\Delta_2-\Delta+2-J}{2}} X_{13}^{\frac{\Delta_1-\Delta_2+\Delta+J}{2}} X_{23}^{\frac{-\Delta_1+\Delta_2+\Delta+J}{2}}}.\end{aligned} \tag{3.116}$$

Let us now impose the conservation condition (3.112). Starting with $\langle JJO\rangle$, we can see that $\partial_{X_1} \cdot \mathcal{D}_{Z_1} \langle JJO\rangle$ transforms like $\langle \phi JO\rangle$. It therefore has two independent structures; one proportional to V_2 and one proportional to H_{23}. These must independently vanish. Furthermore, we get two more equations from imposing that J_2 be conserved. If however we impose $\Delta_1 = d-1 = \Delta_2$ as required for a conserved spin 1 operator, we see that only 3 of these equations are independent. Imposing them and denoting $\Delta_3 = \Delta$ we get

$$\begin{aligned}
(4-2d-J+\Delta)c_1 + 4Jc_2 + 2c_3 + 2(d-1+\Delta)c_4 &= 0,\\
(2J+2\Delta)c_2 + (2(d-1)+J-\Delta)c_3 + 2(d-1+\Delta)c_5 &= 0,\\
(4-2d-J+\Delta)c_1 + 4Jc_2 + 2(d-1+\Delta)c_3 + 2c_4 &= 0,\\
(2J+2\Delta)c_2 - (2(d-1)+J-\Delta)c_4 + 2(d-1+\Delta)c_5 &= 0.
\end{aligned} \tag{3.117}$$

As mentioned above, of these four equations, only 3 are linearly independent. We can then take the large Δ limit to get

$$c_1 - 2c_4 = 0 \quad 2c_2 + c_4 + 2c_5 = 0 \quad c_3 + c_4 = 0. \tag{3.118}$$

One can then verify that this is the same as (3.113), which is equivalent to demanding that in the embedding space

$$\begin{aligned}
V_1 \cdot D_{Z_1}\langle \mathcal{O}_1(X_1,Z_1)\mathcal{O}_2(X_2,Z_2)\mathcal{O}(X,Z)\rangle &= 0.\\
V_2 \cdot D_{Z_2}\langle \mathcal{O}_1(X_1,Z_1)\mathcal{O}_2(X_2,Z_2)\mathcal{O}(X,Z)\rangle &= 0,
\end{aligned} \tag{3.119}$$

where V_i^A is the usual embedding space structure V_i defined in (3.206) with Z_i^A stripped off, and $D_{Z_i}^A = \left(\frac{d}{2} - 1 + Z_i \cdot \partial_{Z_i}\right)\partial_{Z_i}^A - \frac{1}{2}Z_i^A \partial_{Z_i}^2$ is the Todorov/Thomas operator (Costa, Joao Penedones, et al., 2011).

Importantly, the simplified conservation condition (3.113) is algebraic. It allows us to describe the conserved operator using a boundary polarization vector with one fewer degree of freedom, which will be necessary for writing a simple correspondence between boundary and bulk polarizations.

CFT 3-point structures and flat space 3-point amplitudes

Our goal now is to interpret the last line of (3.102) in flat space language. The conformal three-point structures will become three-point amplitudes, and their contractions will become a partial wave. Recall that the partial wave decomposition of a spinning flat space amplitude is given by (Simon Caron-Huot, Li, et al., 2023b)

$$\mathcal{M}(s,u) = s^{\frac{4-D}{2}} \sum_\rho n_\rho^{(D)} \sum_{ab} (a_\rho(s))_{ab} \pi_{\rho,(ab)}, \tag{3.120}$$

where ρ is an irrep of $\mathrm{SO}(d)$, a, b represent the three-point structures (see below), and $n_\rho^{(D)} = \frac{2^{d+1}(2\pi)^{d-1}\dim\rho}{\mathrm{vol}\, S^{d-1}}$ is a normalization factor. This is a generalization of the scalar partial wave decomposition (3.17), where instead of the Gegenbauer polynomial $\mathcal{P}_J$ we now have a more general partial wave $\pi_{\rho,(ab)}$.

The partial wave $\pi_{\rho,(ab)}$ transforms in the representation ρ of the $\mathrm{SO}(d)$ group that stabilizes $P^\mu = p_1^\mu + p_2^\mu$. It can be obtained by gluing two vertices,

$$\pi_{\rho,(ab)} \equiv (\overline{v}_b(n', e_3, e_4), v_a(n, e_1, e_2)), \tag{3.121}$$

where the pairing $(\ldots, \ldots)$ represents the contraction of $\mathrm{SO}(d)$ indices, and $\overline{f}(x) = f(x^*)^*$ is Schwarz reflection. The vertex $v_a(n, e_1, e_2)$ is a three-point amplitude of two massless particles and a massive particle. The massive particle has momentum P^μ and transforms in the representation ρ under the little group $\mathrm{SO}(d)$. We use a to label different independent vertices, and we define n^μ and e_i^μ as

$$n^\mu = \frac{p_1^\mu - p_2^\mu}{\sqrt{(p_1 - p_2)^2}}, \quad e_i^\mu = \epsilon_i^\mu - p_i^\mu \frac{\epsilon_i \cdot P}{p_i \cdot P}. \tag{3.122}$$

They satisfy $n \cdot e_i = e_i^2 = 0, n^2 = 1$. The other vertex can be defined in the same way with momenta p_3^μ, p_4^μ.

Let us demonstrate how to obtain vertices $v_a(n, e_1, e_2)$ from CFT structures by studying the example of photon scattering. As we saw in the previous section, for a CFT three-point function between two conserved spin one currents and an operator with large Δ, conservation places a simple constraint on the allowed three point structures. For example, when O is a traceless symmetric tensor, we have

$$\begin{aligned}&\langle J_1(X_1, Z_1) J_2(X_2, Z_2) O(X_5, Z_5)\rangle \\ &= \frac{c_1(-2V_5)^{J-2} H_{25} H_{15} + c_2 H_{12}(-2V_5)^J + c_3 V_2 H_{15}(-2V_5)^{J-1} + c_4 V_1 H_{25}(-2V_5)^{J-1} + c_5 V_1 V_2 (-2V_5)^J}{X_{12}^{\frac{2d-\Delta-J}{2}} X_{15}^{\frac{\Delta+J}{2}} X_{25}^{\frac{\Delta+J}{2}}}.\end{aligned} \tag{3.123}$$

At large Δ, conservation demands that we have no terms proportional to V_1 or V_2. Moreover, at the saddle configuration of (3.102) we find

$$-v_{1,25}|_{\mathrm{saddle}} = v_{2,51}|_{\mathrm{saddle}} = v_{3,46}|_{\mathrm{saddle}} = -v_{4,63}|_{\mathrm{saddle}} = e, \tag{3.124}$$

where e is the unit vector in the time direction. Therefore, if we choose the polarization vectors z_1, z_2 for the conserved currents to have no time component, the conserved structures of $\langle JJO\rangle$ at large Δ will satisfy

$$\begin{aligned}
\langle J_1 J_2 O\rangle^{(1)}_{\text{saddle},z_i=(0,z_i^x,\vec{z}_{i\perp})} &= \left.\frac{(-2V_5)^{J-2}H_{15}H_{25}}{X_{12}^{\frac{2d-\Delta-J}{2}}X_{15}^{\frac{\Delta+J}{2}}X_{25}^{\frac{\Delta+J}{2}}}\right|_{\text{saddle},z_i=(0,z_i^x,\vec{z}_{i\perp})}, \\
\langle J_1 J_2 O\rangle^{(2)}_{\text{saddle},z_i=(0,z_i^x,\vec{z}_{i\perp})} &= \left.\frac{(-2V_5)^{J}H_{12}}{X_{12}^{\frac{2d-\Delta-J}{2}}X_{15}^{\frac{\Delta+J}{2}}X_{25}^{\frac{\Delta+J}{2}}}\right|_{\text{saddle},z_i=(0,z_i^x,\vec{z}_{i\perp})}.
\end{aligned} \tag{3.125}$$

We would like to interpret these expressions in such a way that they give rise to flat-space three-point vertices. We can describe the possible vertices using the formalism of (S. Chakraborty et al., 2020; Simon Caron-Huot, Li, et al., 2023b). The two massless spin-1 particles have momenta p_1 and p_2, as well as polarizations e_1 and e_2. We additionally have the momentum of the third particle $p_3 := P = p_1 + p_2$ and another Lorentz invariant quantity $n \propto p_1 - p_2$. We have the freedom to normalize n, and to shift the polarizations e_i by p_i. As the third particle is massive, we can go to its rest frame and parameterize its momentum as $P = (m, 0, \cdots, 0)$. We can then use the symmetry of our saddle point to find the flat space kinematics.

Since the vertices are tensors with $\mathrm{SO}(d)$ indices, we can introduce index free notation and contract the indices with polarization vectors $w_1, w_2, \ldots \in \mathbb{C}^d$ for each row of the Young diagram. For example, if ρ is a symmetric traceless tensor, we have a single polarization vector w_1, and from these quantities we can build two three-point amplitudes:

$$\begin{aligned}
v^{(1)}_{\gamma\gamma J}(n, e_1, e_2) &= (n\cdot w_1)^{J-2}(e_1\cdot w_1)(e_2\cdot w_1), \\
v^{(2)}_{\gamma\gamma J}(n, e_1, e_2) &= (n\cdot w_1)^{J}(e_1\cdot e_2).
\end{aligned} \tag{3.126}$$

These two amplitudes should correspond to (3.125) through the appropriate dictionary.

Our saddle point (3.81) defines an $\mathrm{SO}(d-1) \subset \mathrm{SO}(d,2)$ subgroup that fixes the locations of the operators J_1, J_2, O. The vector $v^{\mu}_{5,12}$ points along the direction preserved by this $\mathrm{SO}(d-1)$ at the location of O. In the bulk, there is a corresponding $\mathrm{SO}(d-1)$ that preserves n. Thus it is natural to impose

$$(z_5\cdot v_{5,12})^J \leftrightarrow (w_1\cdot n)^J. \tag{3.127}$$

The left-hand side is the projection of the polarization of O along the $\mathrm{SO}(d-1)$-invariant direction, while the right-hand side is the projection of the polarization of the massive particle along the $\mathrm{SO}(d-1)$-invariant direction.

Therefore we should impose $p_1^\mu - p_2^\mu \propto (0, v^\mu_{5,12})$. Evaluating this on the saddle (3.81) we find $n^\mu = (0, \frac{\sqrt{m^2-\nu^2}}{m}, \frac{\nu}{m}, 0, \cdots, 0)$, while we can choose the momenta of the scattering process to be:

$$\begin{aligned} p_1 =& \frac{1}{2}(m, \sqrt{m^2-\nu^2}, \nu, 0, \ldots, 0), \qquad p_2 = \frac{1}{2}(m, -\sqrt{m^2-\nu^2}, -\nu, 0, \ldots, 0), \\ p_3 =& \frac{1}{2}(m, \sqrt{m^2-\nu^2}, -\nu, 0, \ldots, 0), \quad p_4 = \frac{1}{2}(m, -\sqrt{m^2-\nu^2}, \nu, 0, \ldots, 0). \end{aligned} \tag{3.128}$$

Here, p_1, p_2 are incoming and p_3, p_4 are outgoing.

It now remains to parameterize the bulk polarization vectors e_1, e_2, w_1 in terms of CFT polarization vectors z_1, z_2, z_5 to get (3.125) to agree with (3.126). Our CFT polarizations can be expressed as

$$z_1 = (0, z_1^x, \vec{z}_{1\perp}), \quad z_2 = (0, z_2^x, \vec{z}_{2\perp}), \quad z_5 = (z_5^t, z_5^x, \vec{z}_{5\perp}), \tag{3.129}$$

where we've explicitly set the time component of z_1 and z_2 to be zero, in accordance with (3.124). Meanwhile, we can express the bulk polarizations as

$$e_1^\mu = e_1^n n_\perp^\mu + (0,0,0,\vec{e}_{1\perp}), \quad e_2^\mu = e_2^n n_\perp^\mu + (0,0,0,\vec{e}_{2\perp}), \quad w_1^\mu = (0, w_1^t, w_1^x, \vec{w}_{1\perp}), \tag{3.130}$$

where $n_\perp^\mu$ is a vector perpendicular to n^μ, given by

$$n_\perp^\mu = (0, -\tfrac{\nu}{m}, \tfrac{\sqrt{m^2-\nu^2}}{m}, 0, \ldots, 0). \tag{3.131}$$

As we argued above, the SO$(d-1)$ singlets should match between CFT and flat space. In particular, this imposes

$$\begin{aligned} \frac{H_{15}}{X_{15}}\bigg|_{\text{saddle}} &\leftrightarrow e_1 \cdot w_1, \quad & \frac{H_{25}}{X_{25}}\bigg|_{\text{saddle}} &\leftrightarrow e_2 \cdot w_1, \\ \frac{H_{12}}{X_{12}}\bigg|_{\text{saddle}} &\leftrightarrow e_1 \cdot e_2, \quad & V_{5,12}\big|_{\text{saddle}} &\leftrightarrow -in \cdot w_1, \end{aligned} \tag{3.132}$$

which we can achieve by setting

$$z_1^x = e_1^n, \quad \vec{z}_{1\perp} = \vec{e}_{1\perp}, \quad z_2^x = -e_2^n, \quad \vec{z}_{2\perp} = \vec{e}_{2\perp}, \quad z_5^t = -iw_1^t, \quad z_5^x = w_1^x, \quad \vec{z}_5 = \vec{w}_{1\perp}. \tag{3.133}$$

Let us emphasize that even though we use a t superscript for the w_1^t component, it is actually a spatial direction in the bulk, while z_5^t is the time direction in the CFT.

This is why we need an i factor in their relation. Note also that the relation maps the condition $z_i^2 = 0$ to $e_i^2 = w_1^2 = 0$. If the Young diagram of the representation ρ has more than one row, then we need to introduce more polarization vectors for both the flat space vertex and the CFT three-point structure. The map between these polarizations is the same as the relation between z_5 and w_1 in (3.133).

The polarization map (3.133) turns each CFT three-point structure building block into an amplitude building block, and thus the CFT three-point structures naturally become flat space vertices.

Note that in the CFT sum rule (3.102), the three-point structures appear as commutators of Wightman functions. So we will use the commutator to define vertices, and divide by the $\sin(\ldots)$ factor from the commutator by hand. For the cases we consider in this paper (photons and gravitons), the Young diagram of the exchanged representation ρ has at most three rows. We will often write $\rho = (J, j, \widetilde{j})$ to denote the length of each row. For external operators $\mathcal{O}_1, \mathcal{O}_2$ with quantum numbers (Δ_i, J_i) and exchanged representation ρ, we define the vertices as[13]

$$
\begin{aligned}
&v_a(n, e_1, e_2, w_i) \\
&\equiv (-x_{12}^2)^{\frac{\Delta_1+\Delta_2}{2}} \left(\frac{x_{15}^2}{x_{25}^2}\right)^{\frac{\Delta_1-\Delta_2}{2}} \left. \frac{\langle 0|[\mathcal{O}_1(x_{1^+}, z_1), \mathcal{O}_2(x_{2^+}, z_2)]\mathcal{O}(x_5, z_5, \vec{w}_5)]|0\rangle_{(a)}}{2i(\sin(\pi\frac{\widetilde{\tau}_\rho - \Delta_1 - J_1 - \Delta_2 - J_2}{2}))} \right|_{\text{saddle},(3.133)},
\end{aligned}
\tag{3.134}
$$

where w_i on the left-hand side are the flat space polarizations, and $z_5, \vec{w}_5$ on the right-hand side are the CFT polarizations. The $2i(\sin(\pi\frac{\widetilde{\tau}_\rho - \Delta_1 - J_1 - \Delta_2 - J_2}{2}))$ factor comes from taking the commutator, and $\widetilde{\tau}_\rho = \Delta - J + j + \widetilde{j}$ for $\rho = (J, j, \widetilde{j})$.[14] We introduce the factor $(-x_{12}^2)^{\frac{\Delta_1+\Delta_2}{2}} \left(\frac{x_{15}^2}{x_{25}^2}\right)^{\frac{\Delta_1-\Delta_2}{2}}$ to remove factors of v.

As an example, we can apply the polarization map (3.133) to the $\langle JJ\mathcal{O}\rangle$ CFT

[13]Reference Li, 2021 presents a similar relation between flat space 3-point amplitudes and CFT 3-point structures, but with a different configuration of CFT positions and polarizations X_i, Z_i. We expect that our relation is equivalent up to a choice of conformal frame.

[14]We find this $\sin(\pi\frac{\widetilde{\tau}_\rho - \Delta_1 - J_1 - \Delta_2 - J_2}{2})$ factor by studying the commutator of (3.211). It would be interesting to determine what $\widetilde{\tau}_\rho$ should be for general ρ.

three-point structures (3.125). We get

$$
\begin{aligned}
&(-x_{12}^2)^{d-1}\left.\left\{\frac{\langle 0|[J(x_{1^+},z_1),J(x_{2^+},z_2)]O(x_5,z_5)|0\rangle_{(1,2)}}{2i\left(\sin(\pi\frac{\Delta-J-2d}{2})\right)}\right\}\right|_{\text{saddle},(3.133)} \\
&=-(-i)^J 2^J\left\{2^{-2}(n\cdot w_1)^{J-2}(e_1\cdot w_1)(e_2\cdot w_1),(n\cdot w_1)^J(e_1\cdot e_2)\right\}. \qquad (3.135)
\end{aligned}
$$

As expected, the result correctly reproduces the three-point amplitudes (3.126).

The other vertex $\overline{v}(n',e_3,e_4)$ can be defined using the $\langle O_3O_4O_6\rangle$ CFT three-point structure in a similar way. The polarization map is given by

$$
z_3^x=e_3^{n'},\quad \vec{z}_{3\perp}=\vec{e}_{3\perp},\quad z_4^x=-e_4^{n'},\quad z_{4\perp}=\vec{e}_{4\perp},\quad z_6^t=-iw_1^t,\quad z_6^x=w_1^x,\quad \vec{z}_6=\vec{w}_{1\perp}. \qquad (3.136)
$$

We again set the time component of z_3, z_4 to be zero, and

$$
e_3^\mu=e_3^{n'}n_\perp'^\mu+(0,0,0,\vec{e}_{3\perp}),\quad e_4^\mu=e_4^{n'}n_\perp'^\mu+(0,0,0,\vec{e}_{4\perp}),\quad w_1^\mu=(0,w_1^t,w_1^x,\vec{w}_{1\perp}), \qquad (3.137)
$$

where

$$
n_\perp'^\mu=(0,\tfrac{\nu}{m},\tfrac{\sqrt{m^2-\nu^2}}{m},0,\dots,0), \qquad (3.138)
$$

which is perpendicular to $n'^\mu=(0,\frac{\sqrt{m^2-\nu^2}}{m},-\frac{\nu}{m},0,\dots,0)\propto p_3^\mu-p_4^\mu$.

The definition of the $\overline{v}(n',e_3,e_4)$ is given by

$$
\begin{aligned}
&\overline{v}_b(-n',e_3,e_4,w_i) \\
&\equiv(-x_{34}^2)^{\frac{\Delta_3+\Delta_4}{2}}\left(\frac{x_{36}^2}{x_{46}^2}\right)^{\frac{\Delta_3-\Delta_4}{2}}\mathcal{I}_e^\rho\left.\frac{\langle 0|O^\dagger(x_{6^+},z_6,\vec{w}_6)[O_4(x_4,z_4),O_3(x_3,z_3)]|0\rangle_{(b)}}{2i(\sin(\pi\frac{\widetilde{\tau}_\rho-\Delta_3-J_3-\Delta_4-J_4}{2}))}\right|_{\text{saddle},(3.136)}. \qquad (3.139)
\end{aligned}
$$

On the right hand side, $\mathcal{I}_e^\rho$ is a tensor that reflects all the indices in the time direction. More precisely, for any tensor T with representation ρ, in the index-free notation we have

$$
(\mathcal{I}_e^\rho T)(z,\vec{w})=T(I_e\cdot z,I_e\cdot\vec{w}), \qquad (3.140)
$$

where $I_{e\ \nu}^{\mu}=\delta^\mu{}_\nu+2e^\mu e_\nu$ is the usual reflection in time direction.

Note that (3.139) gives a definition for $\overline{v}(-n',e_3,e_4)$ instead of $\overline{v}(n',e_3,e_4)$, which appears in the actual partial wave. This is to ensure that the two definitions (3.134) and (3.139) are consistent. In particular, one can show that the partial waves are always positive in the forward limit. Furthermore, the definitions for $v(n, e_1, e_2)$ and $\overline{v}(-n', e_3, e_4)$ are related by CRT symmetry on the CFT side. We give more details in appendix 3.C, in which we also write down the relation between the partial waves coming from CFT and the Young tableaux basis of (S. Chakraborty et al., 2020; Simon Caron-Huot, Li, et al., 2023b).

The appearance of $\mathcal{I}_e^\rho$ in (3.139) is due to the two-point structure $\langle\widetilde{O}^\dagger(e)\widetilde{O}((-e)^+)\rangle$ in the block part of the CFT sum rule (3.102). The effect of this two-point structure is a reflection of all the indices of O in the time direction with some overall factor. For a representation $\rho = (J, j, \widetilde{j})$, we find

$$\frac{2^d \dim(\rho)}{\mathrm{vol}(\mathrm{SO}(d))} \frac{\langle\widetilde{O}_a^\dagger(x_5)\widetilde{O}^{\overline{b}}(x_6^+)\rangle}{\left(\langle\widetilde{O}^\dagger\widetilde{O}\rangle, \langle O^\dagger O\rangle\right)}\Bigg|_{\text{saddle}} = 2^{-J+2\Delta}(-1)^{J-j+\widetilde{j}} R_\rho \left(\mathcal{I}_e^\rho\right)_a{}^{\overline{b}}, \tag{3.141}$$

where the lower index a and upper index $\overline{b}$ are indices in the dual ρ^* and reflected ρ^R representations respectively. As one can see from the left-hand side, the coefficient R_ρ depends on our convention of the two-point structure. For the two-point convention (3.207), we have

$$R_{\rho=(J,j,\widetilde{j})} = \frac{(j-\widetilde{j}+1)(J-j+1)(J-\widetilde{j}+2)}{(j+1)(J+1)(J+2)}. \tag{3.142}$$

This result can be obtained by using weight-shifting operators (Karateev, Kravchuk, and Simmons-Duffin, 2018) to derive a recursion relation of R_ρ. We give an example in appendix 3.C.

Using the momentum configuration and maps of polarizations discussed above, we can now write down the precise flat space interpretation of the block part of the CFT sum rule. Let us define

$$\begin{aligned}
\mathcal{B}_{\Delta,\rho,(a'b')} &= \frac{2^d \dim(\rho)}{\mathrm{vol}(\mathrm{SO}(d))}\times \\
&\frac{\langle 0|[O_1(x_{1^+}, z_1), O_2(x_{2^+}, z_2)]O(x_5)|0\rangle_{(a')}\langle\widetilde{O}^\dagger(x_5)\widetilde{O}(x_6^+)\rangle}{\left(\langle\widetilde{O}^\dagger\widetilde{O}\rangle, \langle O^\dagger O\rangle\right)}\times \\
&\langle 0|O^\dagger(x_6^+)[O_4(x_4, z_4), O_3(x_3, z_3)]|0\rangle_{(b')}\Big|_{\substack{\text{saddle,}\\ (3.133),(3.136)}}.
\end{aligned} \tag{3.143}$$

From the definitions (3.134), (3.139), and (3.141), we find

$$\begin{aligned}
&\frac{\mathcal{B}_{\Delta,\rho,(a'b')}}{-2(2\sin(\pi\frac{\widetilde{\tau}_\rho-\Delta_1-J_1-\Delta_2-J_2}{2})\sin(\pi\frac{\widetilde{\tau}_\rho-\Delta_3-J_3-\Delta_4-J_4}{2}))}\\
&= 2^{-J+2\Delta-\Delta_1-\Delta_2-\Delta_3-\Delta_4} m^{-\Delta_1-\Delta_2-\Delta_3-\Delta_4} \nu^{2(\Delta_1+\Delta_3)} \left(m-\sqrt{m^2-\nu^2}\right)^{-\Delta_1+\Delta_2-\Delta_3+\Delta_4} R_\rho \pi_{\rho,(a'b')},
\end{aligned} \tag{3.144}$$

where $\pi_{\rho,(a'b')}$ is the flat space partial wave (3.121) in the CFT three-point structure basis, and R_ρ is given by (3.142). Note that when turning the vertex $\overline{v}(-n', e_3, e_4)$ in (3.139) into $\overline{v}(n', e_3, e_4)$ to get the partial wave, we get a $(-1)^{J-j+\widetilde{j}}$ factor, which exactly cancels with the same factor in (3.141).

Recall that in the scalar case, where the exchanged operators are symmetric traceless tensors, we define a heavy action $\Psi[\Delta, J]$ in (3.28) by rescaling the action of the functional on the block by a positive factor. Relation (3.144) in fact suggests a way to generalize this definition to more general representation ρ. Since the other parts of the sum rule should not know about the exchanged quantum numbers of the inserted block, the heavy action should remove the m- and ρ-dependent factors that we don't expect to appear in the flat space answer, such as the R_ρ coefficient. For external operators with quantum numbers (Δ_i, J_i) and a general exchanged representation ρ, we define the large $\Delta \sim m$ heavy action $\Psi[\Delta, \rho]$ to be[15]

$$\begin{aligned}
\Psi[\Delta,\rho]_{(a'b')} \equiv & \frac{2^{J-2\Delta-\Delta_1-\Delta_2-\Delta_3-\Delta_4} m^{\Delta_1+\Delta_2+\Delta_3+\Delta_4-2-\frac{d}{2}}}{R_\rho}\\
&\times \frac{\Psi[G^s_{\Delta,\rho,(a'b')}]}{2\sin(\pi\frac{\widetilde{\tau}_\rho-\Delta_1-J_1-\Delta_2-J_2}{2})\sin(\pi\frac{\widetilde{\tau}_\rho-\Delta_3-J_3-\Delta_4-J_4}{2})}.
\end{aligned} \tag{3.145}$$

Kernels and the shock frame

We now consider the kernel part of our spinning sum rules. It is given by evaluating a celestial structure $\langle \widetilde{\mathcal{P}}_1 \widetilde{\mathcal{P}}_3 \mathcal{P}_{\delta,j'} \rangle$ and a dual structure $\langle 0|\mathcal{O}_4 \mathbf{L}[\mathcal{O}]\mathcal{O}_2|0\rangle^{-1}$ at the scattering-crystal. In the heavy action formula, we first evaluate these structures at the scattering crystal (3.81), and then we can use the maps of CFT and flat space polarizations (3.133), (3.136) to get the corresponding flat space answer. We claim that the resulting expression can be seen to correspond to a shockwave amplitude in flat space. The shockwave amplitude is defined as the amplitude of an elastic

[15] In the scalar case (3.28), the factor $q_{\Delta,J}$ in the heavy action definition comes from the OPE coefficient of Mean Field Theory. So, to find the analogous factor for more general external operators, one can consider the corresponding OPE coefficients in the Mean Field Theory. However, we do not do this in this paper, and the definition (3.145) is good enough for our purpose.

scattering of a probe particle X and two shockwave gravitons g^* (Kologlu et al., 2020),

$$g^*(p_1)X(p_2) \to g^*(p_3)X(p_4). \tag{3.146}$$

In our case, we will take the probe particle X to be a graviton. The two shockwave gravitons are dual to the two light transformed operators $\mathbf{L}[\mathcal{O}_1], \mathbf{L}[\mathcal{O}_3]$ in the CFT functional. A convenient choice of momenta for shockwave amplitudes is given by (in all incoming convention)

$$\begin{aligned} p_1^\mu &= p_{\overline{s}}\overline{s}^\mu + q_1^\mu, \qquad p_2^\mu = p_s s^\mu - q_3^\mu \\ p_3^\mu &= -p_{\overline{s}}\overline{s}^\mu + q_3^\mu, \quad p_4^\mu = -p_s s^\mu - q_1^\mu, \end{aligned} \tag{3.147}$$

where s^μ and $\overline{s}^\mu$ are two null directions, and the polarization of the shock gravitons should be in the $\overline{s}^\mu$ direction. The transverse momenta q_1^μ, q_3^μ are perpendicular to the null directions, and in order to make the external momenta on-shell, we must have $q_1^2 = q_3^2 = 0$. We will call the momentum configuration (3.147) the shock frame. More explicitly, let $D = d + 1$ be the spacetime dimension of the bulk, in the shock frame we have two null vectors $s^\mu, \overline{s}^\mu$ and $D - 2$ transverse unit vectors $v_{1;\perp}^\mu, v_{2;\perp}^\mu, \ldots, v_{D-2;\perp}^\mu$ satisfying

$$s^2 = \overline{s}^2 = s \cdot v_{i;\perp} = \overline{s} \cdot v_{i;\perp} = 0, \quad s \cdot \overline{s} = -2, \quad v_{i;\perp} \cdot v_{j;\perp} = \delta_{ij}. \tag{3.148}$$

In the previous subsection, we have shown that in order to match the blocks to flat space partial waves, we should choose the flat space momentum to be (3.128). The shock frame momenta (3.147) should also agree with these center of mass frame momenta (3.128). By relating the two frames, we obtain that in terms of the bulk Minkowski coordinates used in (3.128), the vectors in the shock frame can be written as

$$\begin{aligned} \overline{s}^\mu &= \left(\tfrac{\sqrt{m^2-\nu^2}}{m}, 1, 0, \tfrac{i\nu}{m}, 0, \ldots, 0\right) \\ s^\mu &= \left(\tfrac{\sqrt{m^2-\nu^2}}{m}, -1, 0, \tfrac{i\nu}{m}, 0, \ldots, 0\right) \\ v_{1;\perp}^\mu &= \left(\tfrac{i\nu}{m}, 0, 0, \tfrac{\sqrt{m^2-\nu^2}}{m}, 0, \ldots\right) \\ v_{2;\perp}^\mu &= (0, 0, 1, 0, 0, \ldots, 0) \\ v_{3;\perp}^\mu &= (0, 0, 0, 0, 1, 0, \ldots, 0) \\ &\vdots \\ v_{D-2;\perp}^\mu &= (0, 0, 0, 0, 0, 0, \ldots, 1), \end{aligned} \tag{3.149}$$

and

$$p_{\bar{s}} = p_s = \frac{\sqrt{m^2 - \nu^2}}{2}, \quad q_1^\mu = -\frac{i\nu}{2} v_{1;\perp}^\mu + \frac{\nu}{2} v_{2;\perp}^\mu, \quad q_3^\mu = \frac{i\nu}{2} v_{1;\perp}^\mu + \frac{\nu}{2} v_{2;\perp}^\mu. \tag{3.150}$$

One motivation for relating the CFT kernel to the shock frame is that we set the CFT polarization vectors z_1, z_3 to be x_{1^+0}, x_{30} in the CFT sum rule (3.102). Using the map of CFT and flat space polarizations (3.133),(3.136) derived in the previous subsection, we find that in flat space the two polarizations become (up to $e_i \sim e_i + \alpha p_i$ gauge redundancy)

$$x_{1^+0}|_{(3.133)} \sim i\frac{m(m - \sqrt{m^2 - \nu^2})}{\nu^2}\bar{s}^\mu, \qquad x_{30}|_{(3.136)} \sim i\frac{m(m - \sqrt{m^2 - \nu^2})}{\nu^2}\bar{s}^\mu, \tag{3.151}$$

where $\bar{s}^\mu$ is given by (3.149). We see that the polarizations of particles 1 and 3 should be set to the same null direction $\bar{s}^\mu$, which agrees with the fact that the two shock gravitons in the shockwave amplitude should have the same polarizations along the direction of the shock.

We can now discuss the CFT kernel in the shock frame. Explicitly, evaluating the celestial three-point structure at the saddle configuration gives

$$\begin{aligned} &\langle \widetilde{\mathcal{P}}^\dagger_{\delta_1}(x_{1^+0}) \widetilde{\mathcal{P}}^\dagger_{\delta_3}(x_{30}) \mathcal{P}_{\delta,j'}(z_0, w_0)\rangle\Big|_{\text{saddle}} \\ &= (-1)^{j'}(-i)^{-\delta} 2^{j'+\delta-\widetilde{\delta}_1-\widetilde{\delta}_3} \nu^{\widetilde{\delta}_1+\widetilde{\delta}_3}(m - \sqrt{m^2-\nu^2})^{-\widetilde{\delta}_1-\widetilde{\delta}_3}(\vec{n}_0 \cdot \vec{w}_{0\perp})^{j'}, \end{aligned} \tag{3.152}$$

where we have introduced a polarization $w_0 = (0, 0, \vec{w}_{0\perp})$ for the transverse indices of $\mathcal{P}_{\delta,j'}$, and $\vec{n}_0 = \vec{y}_0/|\vec{y}_0|$ is the unit vector in the transverse $\vec{y}_0$ direction in the scattering crystal (3.81).

For each transverse spin j', the celestial three-point function has a unique structure which gives (3.152) at the saddle. On the other hand, the dual structure $\langle 0|O_4 \mathbf{L}[O] O_2|0\rangle^{-1}$ can have multiple tensor structures. Moreover, they are subject to constraints from imposing conservation on O_2 and O_4. Interestingly, the space of allowed structures becomes easier to study when we just focus on the saddle configuration. This fact can be seen from the identity

$$- V_{2,40} V_{0,24}\big|_{\text{saddle}, z_i=(0,z_i^x,\vec{z}_{i\perp})} = H_{20}\big|_{\text{saddle}, z_i=(0,z_i^x,\vec{z}_{i\perp})}, \tag{3.153}$$

and a similar identity for $V_{4,02}$ and H_{40}. Note that we also set the time component of the polarizations to zero, which is due to the large-Δ conservation analysis in section

3.4. This identity allows us to just remove all $V_{2,40}, V_{4,02}$ structures when writing down the basis for the spinning dual structures. Additionally, it can be shown that the basis constructed without $V_{2,40}, V_{4,02}$ gives the correct number of independent tensor structures of continuous-spin three-point function of two conserved operators, which should be given by (Kravchuk and Simmons-Duffin, 2018a; Kologlu et al., 2021)

$$\left(\lambda' \otimes \mathrm{Res}^{\mathrm{SO}(d-1)}_{\mathrm{SO}(d-2)} \rho_2 \otimes \rho_4\right)^{\mathrm{SO}(d-2)}. \tag{3.154}$$

We give the argument for this statement in appendix 3.D, and also explain how to compute these spinning dual structures.

As an example, let us consider $j' = 0$. Focusing just on the spinning part of $\mathcal{O}_2, \mathcal{O}_4$, we see that the allowed structures should be

$$H_{20}^{J_2-n} H_{40}^{J_4-n} H_{24}^{n}, \tag{3.155}$$

where $n = 0, 1, \ldots, \min(J_2, J_4)$. The number of structures is $\min(J_2, J_4) + 1$, which agrees with (3.154).

We now study the four-photon example in detail, where all external operators should be conserved spin-1 currents. The selection rule (3.97) implies that the allowed values of transverse spin should be $j' = 0, 1, 2$. Using the algorithm explained in appendix 3.D, we obtain that the dual structures for $j' = 0$ in the large ν limit are given by (for $4 > 0 > 2^-$)

$$\begin{aligned}
&\left\{\left(\langle 0|J(X_4,Z_4)\mathbf{L}[\mathcal{O}](X_0,Z_0)J(X_2,Z_2)|0\rangle^{(1)}\right)^{-1}, \left(\langle 0|J(X_4,Z_4)\mathbf{L}[\mathcal{O}](X_0,Z_0)J(X_2,Z_2)|0\rangle^{(2)}\right)^{-1}\right\} \\
&= 2^{\frac{3d-5}{2}-i\nu} e^{-\frac{i\pi}{4}} \sqrt{\frac{\nu}{\pi}}\, \mathrm{vol}\, \mathrm{SO}(d-2) \frac{1}{X_{24}^{\frac{4-\Delta_F-J_F}{2}} X_{02}^{\frac{\Delta_F+J_F}{2}} (-X_{04})^{\frac{\Delta_F+J_F}{2}}} \\
&\times \left\{ \frac{16(d-1)}{d-2} (-2V_{0,42})^{J_F-2} H_{20}H_{40} + \frac{4}{d-2} (-2V_{0,42})^{J_F} H_{24}, \right. \\
&\qquad \left. \frac{4}{d-2} (-2V_{0,42})^{J_F-2} H_{20}H_{40} + \frac{1}{d-2} (-2V_{0,42})^{J_F} H_{24} \right\} + \ldots,
\end{aligned} \tag{3.156}$$

where $\Delta_F = d, J_F = \frac{2-d}{2} + i\nu$, and $\ldots$ are subleading terms at large ν. The first structure is dual to the light-transformed structure $\langle 0|J\mathbf{L}[\mathcal{O}]J|0\rangle$ with $H_{20}H_{40}$ (see (3.270)), and the second structure is dual to the one with H_{24}.

Then, the next step is to evaluate (3.156) at the saddle (after applying a $\mathcal{T}_2$ to (3.156) to make the causality configuration agree with the saddle). This will give us an expression that depends on the external polarizations z_2, z_4 (note that z_0 is fixed in (3.81)). For example, for the H_{24} structure, we have

$$\frac{H_{24}}{X_{24}}\bigg|_{\text{saddle},z_i=(0,z_i^x,\vec{z}_{i\perp})} = -z_2^x z_4^x + \vec{z}_{2\perp}\cdot\vec{z}_{4\perp}. \tag{3.157}$$

Using (3.133) and (3.136) to map this to flat space, we find

$$-z_2^x z_4^x + \vec{z}_{2\perp}\cdot\vec{z}_{4\perp} \longrightarrow -e_2^n e_4^{n'} + \vec{e}_{2\perp}\cdot\vec{e}_{4\perp} = e_{2\mu_2}e_{4\mu_4}\left(-n_\perp^{\mu_2}n_\perp'^{\mu_4} + \delta_\perp^{\mu_2\mu_4}\right). \tag{3.158}$$

Our goal is to rewrite this expression in the shock frame (3.149). Because of the gauge redundancy, we can shift everything that is contracted with e_2 by p_2. Furthermore, thanks to the momentum configuration we choose in section 3.4, we have $e_2\cdot p_1 = 0$, so we can also shift by p_1. Similarly, we can shift things that are contracted with e_4 by p_3, p_4. Using this, we can make a gauge choice to remove all the $s^\mu, \bar{s}^\mu$, and we find that the H_{24} structure mapped to the shock frame can be written as

$$\frac{H_{24}}{X_{24}}\bigg|_{\text{saddle},(3.133),(3.136)} = e_{2\mu_2}e_{4\mu_4}\left(\delta_{\perp;D-4}^{\mu_2\mu_4} - \frac{1}{\nu^2(m^2-\nu^2)^2}(\mathcal{V}_2^{\mu_2}\mathcal{V}_4^{\mu_4} + \mathcal{W}_2^{\mu_2}\mathcal{W}_4^{\mu_4})\right), \tag{3.159}$$

where we define

$$\begin{aligned}
\mathcal{V}_2^{\mu_2} &= m^2 q_1^{\mu_2} + (m^2-\nu^2)q_3^{\mu_2},\\
\mathcal{V}_4^{\mu_4} &= (m^2-\nu^2)q_1^{\mu_4} + m^2 q_3^{\mu_4},\\
\mathcal{W}_2^{\mu_2} &= m^2 q_1^{\mu_2} - (m^2-\nu^2)q_3^{\mu_2},\\
\mathcal{W}_4^{\mu_4} &= (m^2-\nu^2)q_1^{\mu_4} - m^2 q_3^{\mu_4}.
\end{aligned} \tag{3.160}$$

The momenta q_1^μ, q_3^μ are given by (3.149), (3.150), and $\delta_{\perp;D-4}^{\mu_2\mu_4}$ is the metric in the $(D-4)$-dimensional transverse space spanned by $v_{3;\perp}^\mu, \dots, v_{D-2;\perp}^\mu$. Similarly, the structure with $H_{20}H_{40}$ becomes

$$\frac{H_{20}H_{40}}{X_{20}X_{40}}\bigg|_{\text{saddle},(3.133),(3.136)} = \frac{1}{4\nu^2(m^2-\nu^2)}e_{2\mu_2}e_{4\mu_4}\mathcal{V}_2^{\mu_2}\mathcal{V}_4^{\mu_4}. \tag{3.161}$$

Using (3.156), (3.159), and (3.161), we can then obtain the flat space kernels for the two $j'=0$ dual structures.

For nonzero j', we also need to contract the transverse indices carried by $\mathcal{O}$ in the dual structure and $\mathcal{P}_{\delta,j'}$ in the celestial structure. Let us define

$$\begin{aligned}
\mathcal{K}_{\nu,j'}^{4\gamma,(a)} = &\left(\langle 0|J(x_4,z_4)\mathbf{L}[\mathcal{O}_{j'}](x_0,z_0)J(x_{2^+},z_2)|0\rangle^{(a)}\right)^{-1}\\
&\langle\widetilde{\mathcal{P}}_{\delta_J}^\dagger(x_{1^+0})\widetilde{\mathcal{P}}_{\delta_J}^\dagger(x_{30})\mathcal{P}_{\delta,j'}(z_0)\rangle\,\Big|_{\substack{\text{saddle},(3.133),\\(3.136),\,\nu\to\infty}},
\end{aligned} \tag{3.162}$$

where $\nu \to \infty$ indicates that we take the leading term at large ν. The results for the four-photon kernels are given by

$$\begin{aligned}
\mathcal{K}^{4\gamma,(1)}_{\nu,j'=0} &= \frac{K^{4\gamma}_\nu}{2} e_{2\mu_2} e_{4\mu_4} \left((\mathcal{V}_2^{\mu_2}\mathcal{V}_4^{\mu_4} + \mathcal{W}_2^{\mu_2}\mathcal{W}_4^{\mu_4} - \nu^2(m^2-\nu^2)^2 \delta^{\mu_2\mu_4}_{\perp;D-4}) - (D-2)\mathcal{V}_2^{\mu_2}\mathcal{V}_4^{\mu_4} \right), \\
\mathcal{K}^{4\gamma,(2)}_{\nu,j'=0} &= \frac{K^{4\gamma}_\nu}{8} e_{2\mu_2} e_{4\mu_4} \left(\mathcal{W}_2^{\mu_2}\mathcal{W}_4^{\mu_4} - \nu^2(m^2-\nu^2)^2 \delta^{\mu_2\mu_4}_{\perp;D-4} \right), \\
\mathcal{K}^{4\gamma,(1)}_{\nu,j'=1} &= K^{4\gamma}_\nu e_{2\mu_2} e_{4\mu_4} \mathcal{W}_2^{\mu_2}\mathcal{V}_4^{\mu_4}, \\
\mathcal{K}^{4\gamma}_{\nu,j'=2} &= -\frac{4K^{4\gamma}_\nu}{(D-1)} e_{2\mu_2} e_{4\mu_4} \left(\mathcal{W}_2^{\mu_2}\mathcal{W}_4^{\mu_4} + \frac{\nu^2(m^2-\nu^2)^2}{D-4} \delta^{\mu_2\mu_4}_{\perp;D-4} \right),
\end{aligned} \tag{3.163}$$

where

$$K^{4\gamma}_\nu = \frac{2^{-\frac{d}{2}+i\nu} e^{-\pi\nu} m^{-d} \nu^{-4+3d} (m^2-\nu^2)^{-2-\frac{d}{2}} (m-\sqrt{m^2-\nu^2})^{2-d}}{d-2}. \tag{3.164}$$

Note that for $j' = 1$ there are two tensor structures (see (3.211)). However, they are just related by $2 \leftrightarrow 4$, and as we will see later, kernels that are related by $2 \leftrightarrow 4$ will give the same sum rule, so we just include one of the structures here.

Finally, let us comment on the symmetry properties of the kernel. On the CFT side, the celestial three-point structure has a stabilizer group $\mathrm{SO}(d-3)$, which is also the stabilizer group of the scattering crystal (3.81). In the shock frame, this group becomes the $\mathrm{SO}(D-4)$ that fixes the shockwave amplitude momenta (3.147), and the group only rotates in the $v^\mu_{3;\perp}, \ldots, v^\mu_{D-2;\perp}$ directions. On the other hand, for the continuous-spin dual structure we can choose a conformal frame to fix all three points to be on the same line, and fix the continuous-spin polarization vector in a null direction. The configuration should be fixed by an $\mathrm{SO}(d-2)$, and the transverse spin j' is a representation of this group. In flat space, this should correspond to an $\mathrm{SO}(D-3)$. From the expressions of the kernels (3.163), it is not clear what this $\mathrm{SO}(D-3)$ should be. It turns out that (at least in the Regge limit) the group can be understood as the rotation group that fixes the $s^\mu, \bar{s}^\mu, v^\mu_{2;\perp}$ shock frame vectors. To see this we will first need to study how to apply the kernels (3.163) to four-photon amplitudes and write down the full sum rules for photons. We will therefore explain this $\mathrm{SO}(D-3)$ group and the meaning of transverse spin in the bulk in section 3.4.

Review: flat space sum rules for photons

After understanding how to map each part of the CFT bulk-point limit formula (3.102) to flat space, we can now derive the dictionary between CFT and flat space sum rules for photons and gravitons. Let us first review flat space sum rules for photons (S. Caron-Huot, n.d.; Simon Caron-Huot, Li, et al., 2023b). The graviton sum rules will be considered in section 3.4.

The four-photon amplitude $\mathcal{M}_{4\gamma}(p_i, \epsilon_i)$ is a function of photon momenta p_i and polarizations ϵ_i for $i = 1,2,3,4$. They should satisfy $p_i^2 = p_i \cdot \epsilon_i = \epsilon_i^2 = 0$ and $\epsilon_i \sim \epsilon_i + \# p_i$. In general, the amplitude can be written as a sum of Lorentz-invariant polynomials of p_i, ϵ_i times functions of Mandelstam variables defined in (3.16). Depending on the choice of the polynomials, sometimes the functions of Mandelstam variables can develop spurious poles. It turns out that there exists a "local module" such that the amplitude won't have any spurious poles (Chowdhury, Gadde, et al., 2020). Namely, an amplitude that is a polynomial can always be written as generators of the local module times polynomials of Mandelstam variables.

To describe the generators of the local module, let us introduce some basic building blocks,[16]

$$
\begin{aligned}
H_{ij} &= F^{\mu}_{i\nu} F^{\nu}_{j\mu}, & H_{ijk} &= F^{\mu}_{i\nu} F^{\nu}_{j\sigma} F^{\sigma}_{k\mu}, \\
H_{ijkl} &= F^{\mu}_{i\nu} F^{\nu}_{j\sigma} F^{\sigma}_{k\rho} F^{\rho}_{l\mu}, & V_{i,jk} &= p_{k\mu} F^{\mu}_{i\nu} p^{\nu}_{j},
\end{aligned}
\tag{3.165}
$$

where $F^{\mu}_{i\nu} = p^{\mu}_i \epsilon_{i\nu} - \epsilon^{\mu}_i p_{i\nu}$. We also define

$$
\begin{aligned}
X_{ijkl} &= H_{ijkl} - \frac{1}{4} H_{ij} H_{kl} - \frac{1}{4} H_{ik} H_{jl} - \frac{1}{4} H_{il} H_{jk}, \\
S &= V_{1,24} H_{234} + V_{2,31} H_{341} + V_{3,42} H_{412} + V_{4,13} H_{123}.
\end{aligned}
\tag{3.166}
$$

Then, the four-photon amplitude can be written as

$$
\mathcal{M}_{4\gamma}(s,u) = \left(H_{14} H_{23} \mathcal{M}^{(1)}_{4\gamma}(s,u) + X_{1243} \mathcal{M}^{(2)}_{4\gamma}(s,u) + \text{permutations} \right) + S \mathcal{M}^{(3)}_{4\gamma}(s,t),
\tag{3.167}
$$

where $\mathcal{M}^{(1)}_{4\gamma}, \mathcal{M}^{(2)}_{4\gamma}$ are symmetric in their two arguments, and $\mathcal{M}^{(3)}_{4\gamma}$ is symmetric under all permutations of s, t, u.

To write down dispersion relations for $\mathcal{M}_{4\gamma}(s,u)$, we need to study how the polarization structures behave in the fixed-u Regge limit, where we take $s \to \infty$. This will tell us how many subtractions we should have in the dispersion relations. Moreover, for fixed-u sum rules it is useful to separately consider structures that are symmetric

[16] We are using V and H for the building blocks of both CFT tensor structures and flat space amplitudes. We hope the meaning of the notations will be clear from the context and this won't cause too much confusion.

and antisymmetric under $s \leftrightarrow t$. The polarization structures in the Regge limit scale as (Simon Caron-Huot, Li, et al., 2023b)

$$H_{12}, H_{14} \sim s, \quad H_{13} \sim s^0, \quad X_{1234}, X_{1243} - X_{1324} \sim s, \quad X_{1243} + X_{1324} \sim s^2, \quad S \sim s^2, \tag{3.168}$$

where other structures can be obtained by permutations.

The amplitude itself $\mathcal{M}_{4\gamma}$ satisfies boundedness and analyticity properties due to unitarity and causality (Simon Caron-Huot, Mazac, et al., 2021c; Simon Caron-Huot, Mazac, et al., 2021a; Simon Caron-Huot, Li, et al., 2023a; Häring and Zhiboedov, 2022). As shown by Häring and Zhiboedov, 2022, for a suitably smeared amplitude,

$$\mathcal{M}_\Psi(s) \equiv \int_0^M dp \Psi(p) \mathcal{M}(s, -p^2), \tag{3.169}$$

along any complex direction of s it should satisfy

$$|\mathcal{M}_\Psi(s)|_{s\to\infty} \leq s \times \text{constant}. \tag{3.170}$$

The Regge behaviors (3.168), (3.170) then combine to give boundedness conditions on each coefficient function $\mathcal{M}^{(i)}$. For example, since $X_{1243} - X_{1324} \sim s$ in the Regge limit, $\mathcal{M}^{(2)}(s,u) - \mathcal{M}^{(2)}(t,u)$ can't grow faster than s^0 in the Regge limit. Performing this analysis for all the structures, we can then determine the subtractions needed for the dispersion relation of each coefficient $\mathcal{M}^{(i)}$. The complete list of flat space fixed-u sum rules for photons is given by

$$\begin{aligned}
\left\{C^{+(1,2,3,4,5)}_{4\gamma;k,u}\right\} &= -\oint_\infty \frac{ds}{4\pi i}\frac{1}{(-st)^{\frac{k}{2}}}\Big\{(s-t)\mathcal{M}^{(1,2)+}_{4\gamma}(s,u), (s-t)\left(\tfrac{-u}{2}\right)\mathcal{M}^{(3)}_{4\gamma}(s,t), \\
&\qquad\qquad \mathcal{M}^{(2)-}_{4\gamma}(s,u), \tfrac{(s-t)}{(-st)}\mathcal{M}^{(1)}_{4\gamma}(s,t)\Big\}, \quad k = 2,4,\ldots, \\
\left\{C^{-(1,2)}_{4\gamma;k,u}\right\} &= -\oint_\infty \frac{ds}{4\pi i}\frac{1}{(-st)^{\frac{k-1}{2}}}\Big\{\mathcal{M}^{(1)-}_{4\gamma}(s,u), \tfrac{(s-t)}{(-st)}\mathcal{M}^{(2)}_{4\gamma}(s,t)\Big\}, \quad k = 3,5,\ldots,
\end{aligned} \tag{3.171}$$

where we have used the notation $\mathcal{M}^{(i)\pm}(s,u) = \mathcal{M}^{(i)}(s,u) \pm \mathcal{M}^{(i)}(t,u)$. For later convenience, we introduce an additional $\frac{-u}{2}$ factor for $\mathcal{M}^{(3)}_{4\gamma}$. This would also make all the sum rules have the same power counting since the S structure has one more $p_i \cdot p_j$ compared to the other structures. The parameter k is the Regge spin of the sum rule. A sum rule with Regge spin k would be convergent if the amplitude $\mathcal{M}$ satisfies $\mathcal{M}/s^k \to 0$ in the Regge limit.

At low energy, the amplitude can be computed by an EFT with cutoff M. To derive bounds from the dispersion relations, one can deform the contour in (3.171) and separate the contributions from high energy $s \geq M^2$ and low energy $s < M^2$. Our main focus is the high energy part, where one decomposes the amplitude into SO(d) partial waves and imposes unitarity.

When applying the dispersion relations (3.171) to the partial wave expansion (3.120), for each sum rule C we can write its heavy contribution as

$$\left\langle C[m^2, \rho]_{(ab)} \right\rangle , \tag{3.172}$$

where $\langle \cdots \rangle$ is a heavy average defined as

$$\langle \cdots \rangle = \frac{1}{\pi} \sum_{\rho} n_{\rho}^{(D)} \sum_{ab} \int_{M^2}^{\infty} \frac{dm^2}{m^2} m^{4-D} \operatorname{Im}(a_{\rho}(s))_{ab} \, (\cdots) \, . \tag{3.173}$$

For example, for the $C^{+(1)}_{4\gamma;k,u}$ sum rule in (3.171), we have

$$C^{+(1)}_{4\gamma;k,u}[m^2, \rho]_{(ab)} = \frac{2m^2 + u}{m^2 + u} \frac{1}{[m^2(m^2 + u)]^{\frac{k-2}{2}}} \pi^{(1)}_{\rho,(ab)}(m^2, u), \tag{3.174}$$

where we have decomposed the partial wave into different polarization structures similar to (3.167), so $\pi^{(1)}_{\rho,(ab)}$ is the $H_{14}H_{23}$ component of the partial wave.

This dictionary we obtain below in sections 3.4 and 3.4 will be a relation between the action of CFT sum rules on conformal blocks in the bulk-point limit (3.102) and the action of flat space sum rules on partial waves (3.172). This will allow us to find CFT sum rules with positive action on conformal blocks with large Δ straightforwardly from the flat space result.

From CFT to flat space for photons

Now, we combine the discussion about the block/partial wave in section 3.4 and the discussion about the kernel/shockwave amplitude in section 3.4 to write down the relation between four-photon flat space sum rules and the bulk-point limit of our CFT sum rules.

When combining the two parts, we first have to understand how to contract the indices of the external operators. Recall that in the CFT functional, the polarizations z_1, z_3 are set to be $z_1 = x_{1^+0}, z_3 = x_{30}$. As discussed in 3.4, this implies that in the bulk, we should set $e_1^{\mu} = e_3^{\mu} = i\frac{m(m-\sqrt{m^2-\nu^2})}{\nu^2}\bar{s}^{\mu}$. For 2 and 4, we have to contract the indices of the kernel and the block. Note that we have chosen the CFT polarization vectors to have no time component. In the bulk, this means that e_2 has no time and n^μ components (see (3.130)), and similarly e_4^μ has no time and n'^μ components. Let us consider the following index contraction in the CFT sum rule:

$$(z_2^x K^x + \vec{z}_{2\perp} \cdot \vec{K}_\perp) \odot (z_2^x G^x + \vec{z}_{2\perp} \cdot \vec{G}_\perp), \tag{3.175}$$

where $K^x, \vec{K}_\perp$ are from the kernel and $G^x, \vec{G}_\perp$ are from the block, and the symbol $\odot$ represents the index contraction. For spin-1, it is simply stripping off the z_2's and contracting both sides, and we see that after the index contraction, we should get $K^x G^x + \vec{K}_\perp \cdot \vec{G}_\perp$. On the other hand, mapping (3.175) to the bulk, we have

$$\begin{aligned}
&(-e_2^n K^x + \vec{e}_{2\perp} \cdot \vec{K}_\perp) \odot (-e_2^n G^x + \vec{e}_{2\perp} \cdot \vec{G}_\perp)\\
=&e_{2\mu_2}(-n_\perp^{\mu_2} K^x + \delta_\perp^{\mu_2 i} \vec{K}_{\perp i}) \odot e_{2\rho_2}(-n_\perp^{\rho_2} G^x + \delta_\perp^{\rho_2 i} \vec{G}_{\perp i})\\
=&e_{2\mu_2} K^{\mu_2} \odot e_{2\rho_2} G^{\rho_2},
\end{aligned} \tag{3.176}$$

where K^{μ_2} is $-n_\perp^{\mu_2} K^x + \delta_\perp^{\mu_2 i} \vec{K}_{\perp i}$ up to a shift by $p_1^{\mu_2}, p_2^{\mu_2}$ and similarly for G^{ρ_2}. For example, in the $j' = 2$ kernel given by (3.163) we have $K^{\mu_2} \propto m^2 q_1^{\mu_2} - (m^2 - \nu^2) q_3^{\mu_2}$. To correctly reproduce $K^x G^x + \vec{K}_\perp \cdot \vec{G}_\perp$, we should perform a polarization sum in e_2 using[17]

$$e_{2\mu_2} e_{2\rho_2} \to \eta_{\mu_2\rho_2} - \frac{p_{1\mu_2} p_{2\rho_2} + p_{1\rho_2} p_{2\mu_2}}{p_1 \cdot p_2}. \tag{3.177}$$

Then, we obtain

$$K^{\mu_2} G^{\rho_2} \left(\eta_{\mu_2\rho_2} - \frac{p_{1\mu_2} p_{2\rho_2} + p_{1\rho_2} p_{2\mu_2}}{p_1 \cdot p_2} \right) = K^x G^x + \vec{K}_\perp \cdot \vec{G}_\perp \tag{3.178}$$

In summary, for the flat space sum rules we should set the polarizations e_1, e_3 to be proportional to $\bar{s}$, and perform polarization sums for e_2, e_4. More precisely,

$$\begin{aligned}
e_{1\mu} = e_{3\mu} &= i\frac{m(m - \sqrt{m^2 - \nu^2})}{\nu^2} \bar{s}_\mu,\\
e_{2\mu_2} e_{2\rho_2} \to \eta_{\mu_2\rho_2} - \frac{p_{1\mu_2} p_{2\rho_2} + p_{1\rho_2} p_{2\mu_2}}{p_1 \cdot p_2}, &\quad e_{4\mu_4} e_{4\rho_4} \to \eta_{\mu_4\rho_4} - \frac{p_{3\mu_4} p_{4\rho_4} + p_{3\rho_4} p_{4\mu_4}}{p_3 \cdot p_4}.
\end{aligned} \tag{3.179}$$

To study how the spinning CFT sum rules are mapped to flat space, we first start with the heavy action formula (3.102). Then, we further decompose the conformal block $G^s_{\Delta,\rho}$ into independent four-point tensor structures. Namely, we want to consider

$$\Psi^{+(a)}_{k,\nu,j'}[G^s_{\Delta,\rho,(a'b'),I} Q^I], \tag{3.180}$$

[17] For a general polarization ϵ_2, p_1 can be replaced with any null vector q. However, here we have chosen the polarization to satisfy the condition $e_2 \cdot p_1 = e_2 \cdot p_2 = 0$, so the correct choice here is $q = p_1$.

where Q^I is a basis of CFT four-point structures. We will choose the CFT four-point structures such that under the polarization maps (3.133),(3.136), they get mapped to the generators of the local module of the four-photon amplitude. Namely, the four-point structures satisfy

$$Q^I\big|_{\text{saddle},(3.133),(3.136)} = \frac{16}{\nu^4}\left\{H_{14}H_{23}, H_{13}H_{24}, H_{12}H_{34}, X_{1243}, X_{1234}, X_{1324}, \frac{2}{\nu^2}S\right\}, \tag{3.181}$$

where the structures on the right hand side is the basis of polarization structures of the four-photon amplitude introduced in section 3.4. We give the explicit expressions of Q^I's in appendix 3.E.

We can now apply the polarization map (3.133),(3.136) to the right hand side of the heavy action formula (3.102). From the previous discussions, we know that the kernel part should become $\mathcal{K}^{(a)}_{\nu,j'}$ defined in (3.162) and it acts on the four-point tensor structures Q^I's through (3.179). For the block part, by (3.143), (3.144), it should turn into four-photon partial waves which are further decomposed in four-point structures. In summary, we have

$$\begin{aligned}
&\lim_{\substack{\nu,m\gg 1\\ \nu<m}} \frac{\Psi^{+(a)}_{k,\nu,j'}[G^s_{\Delta,\rho,(a'b')}]}{-2(2\sin^2(\pi\frac{\tilde{\tau}_\rho-2d}{2}))}\\
&= \frac{2^{\frac{5}{2}+2d}\pi^{d-\frac{1}{2}}e^{i\frac{\pi}{4}}m^{\frac{3d}{2}+2}\nu^{\frac{7}{2}-4d}(m^2-\nu^2)^{\frac{d-2}{2}}(m-\sqrt{m^2-\nu^2})^{d-4}}{\Gamma\left(\frac{d-2}{2}\right)\mathrm{vol}(\mathrm{SO}(d-2))}\\
&\times \mathcal{K}^{(a)}_{\nu,j'}[Q^I]\\
&\times 2^{-J+2m-4d+4}m^{-4d+4}\nu^{4d-4}R_\rho\pi^I_{\rho,(a'b')}.
\end{aligned} \tag{3.182}$$

Our remaining task is to evaluate the above expression explicitly. We perform the polarization sum of $\mathcal{K}^{(a)}_{\nu,j'}[Q^I]$ using (3.163), (3.179), and also insert the subtraction factors $f^{(-1)^{j'}}_{k;J_e}$ given by (3.106), (3.107) with $J_e = 1$. Finally, by comparing the result with the heavy state contribution of the four-photon flat space sum rules (3.171), we obtain the dictionary between the four-photon CFT and flat space sum rules.

$$\lim_{\substack{\Delta,\nu\gg 1\\ \nu<m}} \begin{pmatrix} \Psi^{(1)}_{4\gamma;k,\nu,j'=0;f^+_{k;Je=1}}[\Delta,\rho] \\ \Psi^{(2)}_{4\gamma;k,\nu,j'=0;f^+_{k;Je=1}}[\Delta,\rho] \\ \Psi_{4\gamma;k,\nu,j'=2;f^+_{k;Je=1}}[\Delta,\rho] \end{pmatrix} = \frac{1}{A^{4\gamma}_{k,\nu}} M^+_{4\gamma} \begin{pmatrix} C^{+(1)}_{4\gamma;k,-\nu^2}[m^2,\rho] \\ C^{+(2)}_{4\gamma;k,-\nu^2}[m^2,\rho] \\ C^{+(3)}_{4\gamma;k,-\nu^2}[m^2,\rho] \end{pmatrix}, \quad k = 2,4,= \ldots,$$
$$\lim_{\substack{\Delta,\nu\gg 1\\ \nu<m}} \left(\Psi^{(1)}_{4\gamma;k,\nu,j'=1;f^-_{k;Je=1}}[\Delta,\rho]\right) = \frac{1}{A^{4\gamma}_{k,\nu}} M^-_{4\gamma} \left(C^{-(1)}_{4\gamma;k,-\nu^2}[m^2,\rho]\right), \quad k = 3,5,\ldots, \tag{3.183}$$

where $A^{4\gamma}_{k,\nu}$ is

$$A^{4\gamma}_{k,\nu} = 2^{5d-3-2j'} e^{\pi\nu} \pi^{1-d} \nu^{6-3d-2k} \Gamma(\tfrac{d}{2}). \tag{3.184}$$

The two matrices $M^+_{4\gamma}, M^-_{4\gamma}$ are our main results. They are given by

$$M^+_{4\gamma} = \begin{pmatrix} -4(D-2) & -2(D-4) & 0 \\ -1 & -\frac{D-4}{2} & (D-3) \\ \frac{2}{(D-1)} & -\frac{1}{(D-1)} & 0 \end{pmatrix},$$
$$M^-_{4\gamma} = \left(2\right). \tag{3.185}$$

The left-hand side of the dictionary is written as the heavy action defined by (3.145), and the right hand side is the heavy state contribution given by e.g., (3.174). The dictionary should be true for all tensor structures of the block/partial wave, so we suppress their labels $(a'), (b')$ in (3.183). Moreover, since $(-1)^{j'}$ gives the signature of the integrand under $1 \leftrightarrow 3$, or equivalently $s \leftrightarrow t$, we can separately consider the CFT sum rules with even/odd j' and the flat space sum rules that are symmetric/antisymmetric under $s \leftrightarrow t$. On the CFT side, k is a parameter of the functional and the subtraction factor, which controls the behavior of the integrand in the Regge limit. On the flat space side, the same k gives the Regge spin of the sum rule.

We also notice that the all the CFT sum rules correspond to the “lowest-subtracted" flat space sum rules, meaning that they have the minimal number of subtractions (for a given Regge spin) among all the sum rules in (3.171). (In other words, their corresponding polarization structures grow the fastest in the Regge limit.) Interestingly, upon setting $e_1 = e_3$ to be along the $\bar{s}^\mu$ direction following (3.179), we find that the only four-photon amplitude structures that are still non-vanishing are the ones that appear in the lowest subtracted sum rules. It would be nice to better understand why this happens.

Transverse spin of sum rules

By construction, our CFT sum rules are labeled by a transverse spin j'. As discussed below the dictionary (3.183), the signature $(-1)^{j'}$ tells us if the flat space sum rule is symmetric or antisymmetric under $s \leftrightarrow t$. However, j' is a representation of $\mathrm{SO}(d-2)$, so it should encode more information than just a signature. On the CFT side, the transverse spin appears in the dual structure $\left(\langle 0|\mathcal{O}_4(x_4)\mathbf{L}[\mathcal{O}](x_0,z_0)\mathcal{O}_2(x_2^+)\rangle^{(a)}\right)^{-1}$, and j' can be realized as a representation of the $\mathrm{SO}(d-2)$ group that stabilizes the saddle configuration of x_{2^+}, x_4, x_0, z_0. On the flat space side, this should correspond to an $\mathrm{SO}(D-3)$. What is this $\mathrm{SO}(D-3)$ in flat space? Moreover, in the dictionary (3.183), (3.185), each CFT sum rule with a fixed j' gets mapped to a linear combination of the coefficient functions $\mathcal{M}_{4\gamma}^{(i)}$. How can we interpret this linear combination as having a transverse spin j' directly in flat space?

We find that the simplest way to understand transverse spin in flat space is by considering the fixed-u Regge limit in the shock frame (3.149). First, note that in the Regge limit, the $\mathcal{V}, \mathcal{W}$ vectors defined in (3.160) become $\mathcal{V}^\mu \sim q_1^\mu + q_3^\mu = \nu v_{2;\perp}^\mu$, $\mathcal{W}^\mu \sim q_1^\mu - q_3^\mu = -i\nu v_{1;\perp}^\mu$. Therefore, the four kernels in (3.163) become

$$
\begin{aligned}
\mathcal{K}^{4\gamma,(1)}_{j'=0}\Big|_{\text{Regge}} &\propto e_{2\mu_2}e_{4\mu_4}\left((D-3)v_{2;\perp}^{\mu_2}v_{2;\perp}^{\mu_4} + v_{1;\perp}^{\mu_2}v_{1;\perp}^{\mu_4} + \delta_{\perp;D-4}^{\mu_2\mu_4}\right),\\
\mathcal{K}^{4\gamma,(2)}_{j'=0}\Big|_{\text{Regge}} &\propto e_{2\mu_2}e_{4\mu_4}\left(v_{1;\perp}^{\mu_2}v_{1;\perp}^{\mu_4} + \delta_{\perp;D-4}^{\mu_2\mu_4}\right),\\
\mathcal{K}^{4\gamma,(1)}_{j'=1}\Big|_{\text{Regge}} &\propto e_{2\mu_2}e_{4\mu_4}v_{1;\perp}^{\mu_2}v_{2;\perp}^{\mu_4},\\
\mathcal{K}^{4\gamma}_{j'=2}\Big|_{\text{Regge}} &\propto e_{2\mu_2}e_{4\mu_4}\left(v_{1;\perp}^{\mu_2}v_{1;\perp}^{\mu_4} - \frac{v_{1;\perp}^{\mu_2}v_{1;\perp}^{\mu_4} + \delta_{\perp;D-4}^{\mu_2\mu_4}}{D-3}\right).
\end{aligned}
\tag{3.186}
$$

From the expression of the kernels in the Regge limit, we see that the $\mathrm{SO}(D-3)$ that realizes the transverse spin in flat space should be the stabilizer group of $s, \bar{s}, v_{2;\perp}$, and $v_{1;\perp}^{\mu_2}v_{1;\perp}^{\mu_4} + \delta_{\perp;D-4}^{\mu_2\mu_4}$ is the metric of the corresponding $(D-3)$-dimensional space. In fact, we can see this more clearly by studying the four-photon amplitude in the Regge limit. To make the action of the $\mathrm{SO}(D-3)$ more manifest, we can parametrize the polarizations as

$$
\begin{aligned}
e_2^\mu &= e_{2s}s^\mu + e_{2\bar{s}}\bar{s}^\mu + e_{2+}v_{2;\perp}^\mu + z_2^\mu,\\
e_4^\mu &= e_{4s}s^\mu + e_{4\bar{s}}\bar{s}^\mu + e_{4+}v_{2;\perp}^\mu + z_4^\mu,
\end{aligned}
\tag{3.187}
$$

where z_2^μ, z_4^μ are $(D-3)$-dimensional vectors that transform under the $\mathrm{SO}(D-3)$ group. Using transversality $p_2 \cdot e_2 = 0$ and the gauge redundancy $e_2 \sim e_2 + \#p_2$, we can express $e_{2s}, e_{2\bar{s}}$ in terms of e_{2+}, z_2 and the shock frame momenta (and similarly for e_4). Therefore, we can parametrize the polarizations using e_{2+}, e_{4+} and z_2, z_4.

We now take the four-point amplitude and set $e_1 = e_3 = i\frac{m(m-\sqrt{m^2-\nu^2})}{\nu^2}\bar{s}$ as required by our functional. As mentioned above, after this step only the polarization structures that appear in the lowest-subtracted sum rules are non-vanishing. We then take the Regge limit and consider the leading term. With the parametrization (3.187), we find

$$
\begin{aligned}
\mathcal{M}_{4\gamma}^{\text{Regge}} = {}& \frac{m^2\nu^2(D-1)}{8}\left(\tfrac{2}{D-1}\mathcal{M}^{(1)+}(s,u) - \tfrac{1}{D-1}\mathcal{M}^{(2)+}(s,u)\right)E_{24,j'=2}^{4\gamma} \\
&+ \frac{im^2\nu^2}{8}\left(2\mathcal{M}^{(1)-}(s,u)\right)E_{24,j'=1}^{4\gamma} \\
&- \frac{m^2\nu^2}{4(D-3)}\left(-\mathcal{M}^{(1)+}(s,u) - \tfrac{D-4}{2}\mathcal{M}^{(2)+}(s,u) + (D-3)\tfrac{\nu^2}{2}\mathcal{M}^{(3)}\right)E_{24,j'=0}^{4\gamma,(1)} \\
&- \frac{m^2\nu^2}{16(D-3)}\left(-4(D-2)\mathcal{M}^{(1)+}(s,u) - 2(D-4)\mathcal{M}^{(2)+}(s,u)\right)E_{24,j'=0}^{4\gamma,(2)},
\end{aligned}
\tag{3.188}
$$

where each $E_{24,j'}^{4\gamma}$ is a tensor built from e_2, e_4 that transforms as a spin-j' representation under the $\mathrm{SO}(D-3)$ group. They are defined as

$$
\begin{aligned}
E_{24,j'=2}^{4\gamma} &= z_2\cdot v_{1;\perp}z_4\cdot v_{1;\perp} - \frac{z_2\cdot z_4}{D-3}, \qquad & E_{24,j'=1}^{4\gamma} &= e_{4+}z_2\cdot v_{1;\perp} - e_{2+}z_4\cdot v_{1;\perp}, \\
E_{24,j'=0}^{4\gamma,(1)} &= z_2\cdot z_4 - e_{2+}e_{4+}, & E_{24,j'=0}^{4\gamma,(2)} &= e_{2+}e_{4+}.
\end{aligned}
\tag{3.189}
$$

We see that by decomposing $\mathcal{M}_{4\gamma}^{\text{Regge}}$ into different representations under $\mathrm{SO}(D-3)$, the linear combinations of the coefficient functions exactly agree with the ones in the dictionary (3.185). In other words, we can write $\mathcal{M}_{4\gamma}^{\text{Regge}}$ as

$$
\begin{aligned}
\mathcal{M}_{4\gamma}^{\text{Regge}} = {}& \left(-\tfrac{m^2\nu^2}{4(D-3)}E_{24,j'=0}^{4\gamma,(1)} \quad -\tfrac{m^2\nu^2}{16(D-3)}E_{24,j'=0}^{4\gamma,(2)} \quad \tfrac{m^2\nu^2(D-1)}{8}E_{24,j'=2}^{4\gamma}\right)M_{4\gamma}^{+}\begin{pmatrix}\mathcal{M}^{(1)+}(s,u)\\ \mathcal{M}^{(2)+}(s,u)\\ \frac{\nu^2}{2}\mathcal{M}^{(3)}(s,t)\end{pmatrix} \\
&+ \left(\tfrac{im^2\nu^2}{8}E_{24,j'=1}^{4\gamma}\right)M_{4\gamma}^{-}\left(\mathcal{M}^{(1)-}(s,u)\right),
\end{aligned}
\tag{3.190}
$$

where $M_{4\gamma}^{+}, M_{4\gamma}^{-}$ are the matrices in the dictionary (3.185).

Another way to see why we get the same matrices that appear in the dictionary is that under the polarization sum, the pairing between the Regge limit kernels (3.186) and the spin-j' tensors (3.189) form a diagonal matrix.

For the $j' = 0$ case, there are two different tensors structures. By comparing $E^{(1)}_{j'=0}, E^{(2)}_{j'=0}$ and the CFT structures that give the two kernels for $j' = 0$, we can even write down a dictionary between the embedding space CFT structures and spin-j' tensors:

$$H_{20}H_{40} \leftrightarrow e_{2+}e_{4+}, \quad H_{24} \leftrightarrow z_2 \cdot z_4 - e_{2+}e_{4+}. \tag{3.191}$$

A similar dictionary between CFT structures and polarization structures in a conformal frame is also given in (Kravchuk and Simmons-Duffin, 2018a).

Sum rules for gravitons

In this section we give the dictionary between the CFT sum rules and flat space sum rules for gravitons. We first review the flat space graviton sum rules.

The local module of the graviton amplitude has 29 generators, and 28 of them can be constructed from taking products of the photon generators defined in section 3.4. The remaining generator $\mathcal{G}$ can be written as the Gram determinant of all dot products between $(p_1, p_2, p_3, e_1, e_2, e_3, e_4)$. The general four-graviton amplitude in generic spacetime dimension ($D \geq 8$) takes the form (Chowdhury, Gadde, et al., 2020)

$$\begin{aligned}
\mathcal{M}_{4g}(s,u) =& \mathcal{G}\mathcal{M}^{(1)}_{4g}(s,u) + S^2\mathcal{M}^{(10)}_{4g}(s,u) \\
&+ \Big(H_{14}^2H_{23}^2\mathcal{M}^{(2)}_{4g}(s,u) + H_{12}H_{13}H_{24}H_{34}\mathcal{M}^{(3)}_{4g}(s,u) \\
&\quad + H_{14}H_{23}(X_{1243} - X_{1234} - X_{1324})\mathcal{M}^{(4)}_{4g}(s,u) + X_{1243}^2\mathcal{M}^{(6)}_{4g}(s,u) \\
&\quad + X_{1234}X_{1324}\mathcal{M}^{(7)}_{4g}(s,u) + H_{14}H_{23}S\mathcal{M}^{(8)}_{4g}(s,u) \\
&\quad + X_{1243}S\mathcal{M}^{(9)}_{4g}(s,u) + \text{triplet permutations} \Big) \\
&+ H_{12}H_{34}X_{1243}\mathcal{M}^{(5)}_{4g}(s,u) + \text{sextuplet permutations}.
\end{aligned} \tag{3.192}$$

The functions that multiply the polarization structures $\mathcal{G}$ and S^2 are symmetric under all permutations of s, t, u, and the ones with "triplet permutations" are symmetric in their two arguments. For the $\mathcal{M}^{(5)}$ function one should include all six permutations.

By repeating the analysis of the Regge limit behavior reviewed in section 3.4, one can obtain the dispersion relations for the graviton amplitude. There are 19 independent fixed-u sum rules with even Regge spin k and are symmetric under $s \leftrightarrow t$ (Simon Caron-Huot, Li, et al., 2023b). Similar to the photon case, the number of subtractions for a given Regge spin of these sum rules can be different. In the dictionary for photons, we see that our CFT sum rules all correspond to the lowest-subtracted flat space sum rules. This turns out to be true for gravitons as well. For graviton sum rules with even Regge spin, 7 of them are the lowest-subtracted. They are given by

$$\left\{C^{+(1-7)}_{4g;k,u}\right\} = -\oint_\infty \frac{ds}{4\pi i}\frac{(s-t)}{(-st)^{\frac{k-2}{2}}}\left\{\mathcal{M}^{(3)}_{4g}(s,t), \left(\tfrac{-u}{2}\right)^2\mathcal{M}^{(10)}_{4g}(s,t), \mathcal{M}^{(2,5)+}_{4g}(s,u),\right.$$
$$\left.\left(\tfrac{-u}{2}\right)\mathcal{M}^{(8,9)+}_{4g}(s,u), \mathcal{M}^{(6)+}_{4g}(s,u)+\mathcal{M}^{(7)}_{4g}(s,t)\right\}, \quad k=2,4,\dots. \tag{3.193}$$

For the remaining 12 sum rules that have higher number of subtractions, see appendix A of (Simon Caron-Huot, Li, et al., 2023b). We again use the notation $\mathcal{M}^{(i)\pm}(s,u) = \mathcal{M}^{(i)}(s,u) \pm \mathcal{M}^{(i)}(t,u)$, and rescale some of the sum rules by $\left(\frac{-u}{2}\right)$ to make all of them have the same power counting.

For graviton sum rules with odd Regge spin, there are 10 independent sum rules, and 3 of them are the lowest-subtracted,

$$\left\{C^{-(1-3)}_{4g;k,u}\right\} = -\oint_\infty \frac{ds}{4\pi i}\frac{1}{(-st)^{\frac{k-3}{2}}}\left\{\mathcal{M}^{(2,5)-}_{4g}(s,u), \left(\tfrac{-u}{2}\right)\mathcal{M}^{(8)-}_{4g}(s,u)\right\}, \quad k=3,5,\dots. \tag{3.194}$$

When performing the CFT analysis for gravitons, all the discussions in section 3.4 and 3.4 can be generalized straightforwardly. In particular, we can also obtain a simple relation similar to (3.144) that relates the block part of the four-stress-tensor functional to the four-graviton partial waves, which include 20 different cases in total (S. Chakraborty et al., 2020; Simon Caron-Huot, Li, et al., 2023b). Moreover, we can obtain the graviton kernels that are similar to (3.163). The number of independent kernels are 3 for $j'=0$, 2 for $j'=1$, 3 for $j'=2$, 1 for $j'=3$, 1 for $j'=4$. Therefore, we have 7 even j' and 3 odd j' sum rules in total, and they indeed agree with the number of “lowest-subtracted" flat space graviton sum rules that are symmetric or antisymmetric under $s \leftrightarrow t$ given in (3.193) and (3.194).

Finally, the only remaining difference in the graviton case is that instead of (3.179), the rules for polarization sum of e_2, e_4 become

$$e_i^\mu e_i^\nu e_i^\alpha e_i^\beta \to \frac{1}{2}\left(P^{\mu\alpha}_{e_i}P^{\nu\beta}_{e_i} + P^{\nu\alpha}_{e_i}P^{\mu\beta}_{e_i}\right) - \frac{1}{D-2}P^{\mu\nu}_{e_i}P^{\alpha\beta}_{e_i}, \quad i=2,4, \tag{3.195}$$

where

$$\begin{aligned} P^{\mu\nu}_{e_2} &= \eta^{\mu\nu} - \frac{p_1^\mu p_2^\nu + p_1^\nu p_2^\mu}{p_1\cdot p_2}, \\ P^{\mu\nu}_{e_4} &= \eta^{\mu\nu} - \frac{p_3^\mu p_4^\nu + p_3^\nu p_4^\mu}{p_3\cdot p_4}. \end{aligned} \tag{3.196}$$

Our final dictionary for gravitons is given by

$$
\begin{aligned}
\lim_{\substack{\Delta,\nu\gg1\\ \nu<m}}\begin{pmatrix}\Psi^{(1)}_{4g;k,\nu,j'=0;f^+_{k;J_e=2}}[\Delta,\rho]\\ \Psi^{(2)}_{4g;k,\nu,j'=0;f^+_{k;J_e=2}}[\Delta,\rho]\\ \Psi^{(3)}_{4g;k,\nu,j'=0;f^+_{k;J_e=2}}[\Delta,\rho]\\ \Psi^{(1)}_{4g;k,\nu,j'=2;f^+_{k;J_e=2}}[\Delta,\rho]\\ \Psi^{(2)}_{4g;k,\nu,j'=2;f^+_{k;J_e=2}}[\Delta,\rho]\\ \Psi^{(3)}_{4g;k,\nu,j'=2;f^+_{k;J_e=2}}[\Delta,\rho]\\ \Psi_{4g;k,\nu,j'=4;f^+_{k;J_e=2}}[\Delta,\rho]\end{pmatrix} &= \frac{1}{A^{4g}_{k,\nu}}M^+_{4g}\begin{pmatrix}C^{+(1)}_{4g;k,-\nu^2}[m^2,\rho]\\ C^{+(2)}_{4g;k,-\nu^2}[m^2,\rho]\\ C^{+(3)}_{4g;k,-\nu^2}[m^2,\rho]\\ C^{+(4)}_{4g;k,-\nu^2}[m^2,\rho]\\ C^{+(5)}_{4g;k,-\nu^2}[m^2,\rho]\\ C^{+(6)}_{4g;k,-\nu^2}[m^2,\rho]\\ C^{+(7)}_{4g;k,-\nu^2}[m^2,\rho]\end{pmatrix}, \quad k=2,4,=\dots,\\
\lim_{\substack{\Delta,\nu\gg1\\ \nu<m}}\begin{pmatrix}\Psi^{(1)}_{4g;k,\nu,j'=1;f^-_{k;J_e=2}}[\Delta,\rho]\\ \Psi^{(2)}_{4g;k,\nu,j'=1;f^-_{k;J_e=2}}[\Delta,\rho]\\ \Psi^{(1)}_{4g;k,\nu,j'=3;f^-_{k;J_e=2}}[\Delta,\rho]\end{pmatrix} &= \frac{1}{A^{4g}_{k,\nu}}M^-_{4g}\begin{pmatrix}C^{-(1)}_{4g;k,-\nu^2}[m^2,\rho]\\ C^{-(2)}_{4g;k,-\nu^2}[m^2,\rho]\\ C^{-(3)}_{4g;k,-\nu^2}[m^2,\rho]\end{pmatrix}, \quad k=3,5,=\dots,
\end{aligned}
\tag{3.197}
$$

where the coefficient $A^{4g}_{k,\nu}$ is

$$
A^{4g}_{k,\nu}=2^{5d+3-2j'}e^{\pi\nu}\pi^{1-d}\nu^{2-3d-2k}\Gamma(\tfrac{d+2}{2}),
\tag{3.198}
$$

and the two matrices are given by

$$
\begin{aligned}
M^+_{4g} &= \begin{pmatrix}
16(D-4)(D-2) & 0 & 16D(D+2) & 8(D-4)D & 0 & 0 & 4(D-4)(D-2)\\
16 & 0 & 16D & 2\left(D^2-3D-2\right) & -4(D-2)(D-1) & -2(D-4)(D-1) & 2\left(D^2-6D+7\right)\\
2 & (D-3)(D-1) & 2 & \frac{D-3}{2} & 1-D & -\frac{1}{2}(D-4)(D-1) & \frac{1}{4}\left(D^2-6D+7\right)\\
-\frac{8D}{D+1} & 0 & \frac{8(D+2)}{D+1} & -\frac{4}{D+1} & 0 & 0 & \frac{2}{D+1}\\
-\frac{32}{D+1} & 0 & -\frac{32(D+2)}{D+1} & \frac{16}{D+1} & 0 & 0 & \frac{4(D-1)}{D+1}\\
-\frac{8}{D+1} & 0 & -\frac{8}{D+1} & -\frac{D-3}{D+1} & 2 & -1 & \frac{D-1}{D+1}\\
\frac{24}{(D+1)(D+3)} & 0 & \frac{24}{(D+1)(D+3)} & -\frac{12}{(D+1)(D+3)} & 0 & 0 & \frac{6}{(D+1)(D+3)}
\end{pmatrix},\\
M^-_{4g} &= \begin{pmatrix}
-16(D+2) & 4(D-4) & 0\\
-8 & (D-3) & 2(D-1)\\
\frac{24}{D+1} & \frac{6}{D+1} & 0
\end{pmatrix}.
\end{aligned}
\tag{3.199}
$$

Finally, the transverse spin analysis done in section 3.4 can also be performed in the graviton case. In this case we have transverse spin up to $j'=4$. As an example, let us consider the spin-4 tensor which is defined as

$$
E^{4g}_{24,j'=4}=(z_2\cdot v_{1;\perp})^2(z_4\cdot v_{1;\perp})^2-\text{traces}.
\tag{3.200}
$$

When we isolate the spin-4 part of the four-graviton amplitude in the Regge limit (and after setting e_1, e_3 to be in the $\overline{s}$ direction), we obtain

$$\mathcal{M}_{4g}^{\text{Regge}} = \frac{m^4\nu^4}{64}\Big(4\mathcal{M}^{(3)}(s,t) + 4\mathcal{M}^{(2)+}(s,u) - 2\mathcal{M}^{(5)+}(s,u) \\ +\mathcal{M}^{(6)+}(s,u) + \mathcal{M}^{(7)}(s,t)\Big) E^{4g}_{24,j'=4} + \dots, \tag{3.201}$$

where $\dots$ are other terms with $j' < 4$. Indeed, we see that the linear combination of the coefficient functions agrees with the dictionary (3.199) (the last row of M^{+}_{4g}).

3.5 Discussion

In this work, we studied a basis of CFT dispersive sum rules for spinning operators. The basis was constructed using the fact that the commutator of two null-integrated operators on the same null plane vanishes, also known as superconvergence. Using the Lorentzian shadow representation of conformal blocks, we expressed the action of our sum rule on a conformal block as an integral over spacetime. We showed that in the bulk point limit, where ν (parameter of the sum rule) and Δ (dimension of the block) both become large, the spacetime integral gets completely localized to a “scattering-crystal." This enabled us to derive a simple formula for the block action of our sum rule in the bulk point limit, generalizing the results in (Simon Caron-Huot, Mazac, et al., 2021a) to the spinning case.

The main result of this paper is a dictionary between the block action of CFT sum rules in the bulk point limit and the heavy state contribution of flat space sum rules. We fixed the dictionary by exploring flat space interpretations for the inserted block and the kernel in the simple formula of the CFT sum rule. We showed that CFT three-point structures at the saddle form a natural basis for the flat space three-point amplitudes, allowing the inserted block to be directly related to flat space partial waves in this basis. On the other hand, the kernels of the sum rule can be interpreted as actions on shockwave amplitudes in flat space. Combining the two results, we derived the dictionary between our CFT sum rules and the flat space sum rules for photons and gravitons.

By construction, the CFT sum rules are labeled by a transverse spin j'. Through the dictionary, this gives a basis of flat space sum rules each labeled by a transverse spin (an SO$(D-3)$ representation). This SO$(D-3)$ stabilizes the shock directions and the momentum transfer $p_1 + p_3$ of the shockwave amplitude, and the transverse spin of each sum rule can be realized by studying the amplitude in the Regge limit.

However, from the flat space perspective, it remains unclear how this “transverse spin basis" is useful in practice. It would be interesting to explore this further.

So far, we have only found a dictionary that relates CFT sum rules to some of the known flat space sum rules. In particular, we only get sum rules that have the fewest subtractions. As discussed in 3.4, to get other sum rules we have to leave the configuration where the polarizations of the shock gravitons are along the shock direction. In CFT this condition comes from setting the polarizations of the light-transformed operators $\mathcal{O}_1, \mathcal{O}_3$ to be the null vectors x_{10}, x_{30}. Therefore, it is conceivable that new sum rules can be obtained by studying null-integrated operators that are not integrated along their polarizations. Equivalently, we can consider taking derivatives of the light transformed operators. Schematically, we would like to find a differential operator $\mathcal{D}$ such that

$$\mathcal{D}_{x,z_1,z_3}\mathbf{L}[\mathcal{O}_1](x,z_1)\mathbf{L}[\mathcal{O}_3](x,z_3) \tag{3.202}$$

is a conformal primary at x. These conformally-invariant differential operators have interesting connections to reducible representations of the conformal group (João Penedones, Trevisani, and Yamazaki, 2016). We hope to address this problem in future.

Our construction of spinning CFT sum rules is an important step toward lifting the flat space gravitational bounds in (Simon Caron-Huot, Li, et al., 2023b) to AdS/CFT. It provides functionals with positive action on conformal blocks with large Δ and fixed J. In order to complete the bootstrap argument, there are still several remaining tasks. First, as discussed above, we have to construct the additional CFT sum rules that give rise to the other flat space sum rules which cannot be written in terms of the shock amplitudes. Second, one also needs to check the positivity of the sum rules in the Regge limit, where Δ and J are both large. Finally, one has to derive a similar dictionary that relates the low energy EFT contribution of the CFT and flat space sum rules. In the scalar case (Simon Caron-Huot, Mazac, et al., 2021a), the light contribution analysis also involves a saddle point. Therefore we expect we should be able to generalize it to the spinning case by arguments similar to section 3.3. Once these calculations are done, one can then derive bounds on the higher derivative corrections of gravitational AdS EFTs in terms of the large CFT gap. These bounds would give a sharp form of the HPPS conjecture (Heemskerk et al., 2009) at the level of four-point functions of stress tensors.

It would be interesting to also test the HPPS conjecture beyond four-point functions using superconvergence. For instance, one could consider commutators of light-transformed operators in a multi-point correlation function. In flat space, we expect this should correspond to commutators of multiple shockwaves. Another interesting direction is studying superconvergence in a thermal state by using the folded light transform contour from (Simon Caron-Huot, 2023).

In Simon Caron-Huot, Mazac, et al., 2021a, it was shown that superconvergence sum rules also exist at $J = -2, -4, \ldots$. In these sum rules, one integrates a commutator against derivatives of delta functions, which again constrains the two operators in the commutator to be spacelike separated. It would be interesting to find spinning versions of these sum rules.

In flat space, unitarity additionally imposes an upper bound on the spectral density. This condition has been used in the context of EFT amplitudes through primal bootstrap methods (Chiang et al., 2022; Chen, Fitzpatrick, and Karateev, 2022). However, it is not clear what the corresponding CFT statement is. To understand how this upper bound is realized in CFT, our dictionary will be an important ingredient.

Crossing-symmetric dispersion relations in flat space (Sinha and Zahed, 2021; Chowdhury, Ghosh, et al., 2022) have also proven valuable in studying dispersive bounds on EFTs. They have the advantage of making low-energy crossing almost trivial to impose, and are more well-behaved when including loop EFT corrections (Li, 2023). Analogous CFT dispersion relations have been established in Mellin space (Gopakumar, Sinha, and Zahed, 2021), and crossing-symmetric dispersion relations in position space were recently studied in (Bissi and Sinha, 2023). We expect that position space methods will be more straightforward to generalize to spinning case.

Including loop EFT corrections often makes the forward limit in flat space divergent (Bellazzini, Elias Miró, et al., 2021; Bellazzini, Riembau, and Riva, 2022). Consequently, one has to consider a limited set of sum rules that give weaker positivity bounds. On the other hand, loop corrections in AdS are automatically regularized by R_{AdS}. By computing the loop contributions from summing over double-trace exchanged operators (Aharony, Alday, et al., 2017; Meltzer, E. Perlmutter, and Sivaramakrishnan, 2020; Meltzer and Sivaramakrishnan, 2020), one should be able to obtain finite loop corrections to the tree-level AdS bounds.

3.A Conventions for two-point and three-point structures

In this appendix, we summarize the conventions for the conformally-invariant structures we use in the main text.

For standard two-point and three-point structures, we use

$$\begin{aligned}\langle \mathcal{O}(x_1,z_1)\mathcal{O}(x_2,z_2)\rangle &= \frac{(2z_1\cdot I(x_{12})\cdot z_2)^J}{x_{12}^{2\Delta}},\\ I^\mu{}_\nu(x) &= \delta^\mu{}_\nu - \frac{2x^\mu x_\nu}{x^2},\end{aligned}\tag{3.203}$$

and

$$\langle \phi_1(x_1)\phi_2(x_2)\mathcal{O}(x_3,z_3)\rangle = \frac{(2z_3\cdot x_{23}x_{13}^2 - 2z_3\cdot x_{13}x_{23}^2)^J}{(x_{12}^2)^{\frac{\Delta_1+\Delta_2-\Delta+J}{2}}(x_{13}^2)^{\frac{\Delta_1+\Delta+J-\Delta_2}{2}}(x_{23}^2)^{\frac{\Delta_2+\Delta+J-\Delta_1}{2}}}.\tag{3.204}$$

In the embedding space, the standard structures can be written as

$$\begin{aligned}\langle \mathcal{O}(X_1,Z_1)\mathcal{O}(X_2,Z_2)\rangle &= \frac{(2H_{12})^J}{X_{12}^{\Delta+J}},\\ \langle \phi_1(X_1)\phi_2(X_2)\mathcal{O}(X_3,X_3)\rangle &= \frac{(-2V_{3,12})^J}{X_{12}^{\frac{\Delta_1+\Delta_2-\Delta-J}{2}}X_{13}^{\frac{\Delta_1+\Delta+J-\Delta_2}{2}}X_{23}^{\frac{\Delta_2+\Delta+J-\Delta_1}{2}}},\end{aligned}\tag{3.205}$$

where

$$\begin{aligned}X_{ij} &= -2X_i\cdot X_j,\\ V_{i,jk} &= \frac{Z_i\cdot X_j X_i\cdot X_k - Z_i\cdot X_k X_i\cdot X_j}{X_j\cdot X_k},\\ H_{ij} &= -2(Z_i\cdot Z_j X_i\cdot X_j - Z_i\cdot X_j Z_j\cdot X_i).\end{aligned}\tag{3.206}$$

We also need the structures with more complicated representations. In the main text, the most complicated case will be when $\mathcal{O}_1, \mathcal{O}_2$ are symmetric traceless tensors with spins J_1, J_2, and $\mathcal{O}$ has representation ρ whose Young diagram has three rows of length $(J, j, \widetilde{j})$. Our convention for the two-point structure is

$$\langle \mathcal{O}(X_1,Z_1,W_1,\widetilde{W}_1)\mathcal{O}(X_2,Z_2,W_2,\widetilde{W}_2)\rangle = \frac{(2H_{12})^{J-j}(2Y_{12})^{j-\widetilde{j}}(2\widetilde{Y}_{12})^{\widetilde{j}}}{X_{12}^{\Delta+J}}.\tag{3.207}$$

For the additional two rows of the Young diagram, we introduce two null polarization vectors $W_i, \widetilde{W}_i$ with the conditions

$$\begin{aligned}&X_i\cdot W_i = Z_i\cdot W_i = X_i\cdot\widetilde{W}_i = Z_i\cdot\widetilde{W}_i = W_i\cdot\widetilde{W}_i = 0,\\ &W_i \sim W_i + \#X_i + \#Z_i,\\ &\widetilde{W}_i \sim \widetilde{W}_i + \#X_i + \#Z_i + \#W_i.\end{aligned}\tag{3.208}$$

The structures $Y_{12}, \widetilde{Y}_{12}$ are index contractions of the antisymmetrization of the embedding space vectors $X_i, Z_i, W_i, \widetilde{W}_i$. Let us introduce the notation

$$[V_1, V_2, \ldots, V_n] \cdot [W_1, W_2, \ldots, W_n] \equiv \sum_{\sigma \in S_n} \mathrm{sgn}(\sigma) V_{1\alpha_1} V_{2\alpha_2} \ldots V_{n\alpha_n} W_1^{\alpha_{\sigma(1)}} W_2^{\alpha_{\sigma(2)}} \ldots W_n^{\alpha_{\sigma(n)}}. \tag{3.209}$$

Then, the structures $Y_{12}, \widetilde{Y}_{12}$ are defined as

$$\begin{aligned} Y_{ij} &= -2[X_i, Z_i, W_i] \cdot [X_j, Z_j, W_j], \\ \widetilde{Y}_{ij} &= -2[X_i, Z_i, W_i, \widetilde{W}_i] \cdot [X_j, Z_j, W_j, \widetilde{W}_j]. \end{aligned} \tag{3.210}$$

One can check that subject to the conditions (3.208), (3.207) is the only conformally-invariant structure with the correct homogeneity of the embedding space vectors. We have chosen the two-point convention such that (3.207) itself is Rindler positive.

For three-point structures, we have

$$\begin{aligned} &\langle \mathcal{O}_1(X_1, Z_1) \mathcal{O}_2(X_2, Z_2) \mathcal{O}(X_3, Z_3, W_3, \widetilde{W}_3) \rangle^{(a)} \\ &= \frac{(-2V_{3,12})^{m_3} V_{1,23}^{m_1} V_{2,31}^{m_2} H_{12}^{n_{12}} H_{13}^{n_{13}} H_{23}^{n_{23}} (-2U_{3,12})^{k_{31}} (-2U_{3,21})^{k_{32}} (-2\widetilde{U}_{3,12})^{\widetilde{j}}}{X_{12}^{\frac{\Delta_1+J_1+\Delta_2+J_2-\Delta-J-j-\widetilde{j}}{2}} X_{13}^{\frac{\Delta_1+J_1+\Delta+J+j+\widetilde{j}-\Delta_2-J_2}{2}} X_{23}^{\frac{\Delta_2+J_2+\Delta+J+j+\widetilde{j}-\Delta_1-J_1}{2}}}, \end{aligned} \tag{3.211}$$

where the tensor structure is labeled by the nonnegative integers m_i, n_{ij}, k_{ij}, subject to the constraints

$$\begin{aligned} m_1 + n_{12} + n_{13} + k_{31} &= J_1 - \widetilde{j}, \\ m_2 + n_{12} + n_{23} + k_{32} &= J_2 - \widetilde{j}, \\ m_3 + n_{13} + n_{23} &= J - j, \\ k_{31} + k_{32} &= j - \widetilde{j}. \end{aligned} \tag{3.212}$$

The structures $U_{i,jk}, \widetilde{U}_{i,jk}$ are defined as

$$\begin{aligned} U_{i,jk} &= \frac{X_{ij}}{X_{jk}} [X_i, Z_i, W_i] \cdot [X_j, Z_j, X_k], \\ \widetilde{U}_{i,jk} &= \frac{X_{ij} X_{ik}}{X_{jk}} [X_i, Z_i, W_i, \widetilde{W}_i] \cdot [X_j, Z_j, X_k, Z_k]. \end{aligned} \tag{3.213}$$

When writing the Lorentzian shadow representation of the block (e.g., (3.43)), we need to use the three-point structures with absolute values. Also, note that the two structures in (3.43) have different causality configurations. Their explicit expressions are given by

$$
\begin{aligned}
|\langle\phi_1(x_1)\phi_2(x_2)O(x_5,z_5)\rangle| &= \frac{(2z_5\cdot x_{25}x_{15}^2 - 2z_5\cdot x_{15}x_{25}^2)^J}{(-x_{12}^2)^{\frac{\Delta_1+\Delta_2-\Delta+J}{2}}(x_{15}^2)^{\frac{\Delta+J+\Delta_1-\Delta_2}{2}}(x_{25}^2)^{\frac{\Delta+J+\Delta_2-\Delta_1}{2}}}, \quad 1>2, 5\approx 1,2 \\
|\langle\phi_3(x_3)\phi_4(x_4)O(x_5,z_5)\rangle| &= \frac{(2z_5\cdot x_{45}x_{35}^2 - 2z_5\cdot x_{35}x_{45}^2)^J}{(-x_{43}^2)^{\frac{\Delta_4+\Delta_3-\Delta+J}{2}}(-x_{45}^2)^{\frac{\Delta+J+\Delta_4-\Delta_3}{2}}(-x_{35}^2)^{\frac{\Delta+J+\Delta_3-\Delta_4}{2}}}, \quad 4>5>3.
\end{aligned}
\tag{3.214}
$$

From the expression of $|\langle\phi_1(x_1)\phi_2(x_2)O(x_5,z_5)\rangle|$, one can explicitly verify the identity (3.47).

In the definition of the functional (3.93), we introduce a celestial three-point structure. This structure is a standard three-point structure in a Euclidean $(d-2)$-dimensional CFT, where z_i are viewed as the embedding space coordinates. Therefore, we can get this structure by taking the d-dimensional three-point structure in (3.205) and make the replacement $X_i \to z_i, Z_i \to w_i$. This gives

$$
\langle\mathcal{P}_{\delta_1}(z_1)\mathcal{P}_{\delta_2}(z_2)\mathcal{P}_{\delta,j}(z,w)\rangle = \frac{(4w\cdot z_1 z\cdot z_2 - 4w\cdot z_2 z\cdot z_1)^j}{(-2z_1\cdot z)^{\frac{\delta_1+\delta+j-\delta_2}{2}}(-2z_2\cdot z)^{\frac{\delta_2+\delta+j-\delta_1}{2}}(-2z_1\cdot z_2)^{\frac{\delta_1+\delta_2-\delta+j}{2}}}.
\tag{3.215}
$$

Finally, in the functional we also use a dual structure $\langle 0|O_4\mathbf{L}[O]O_{2^+}|0\rangle^{-1}$, which should be a continuous-spin structure. In particular, we are interested in the structure with the causality constraint $4>0>2$. We define the standard continuous-spin structure with this configuration as

$$
\begin{aligned}
&\langle 0|\phi_4(x_4)O(x_0,z_0)\phi_2(x_2^+)|0\rangle \\
&= \frac{(2z_0\cdot x_{40}x_{20}^2 - 2z_0\cdot x_{20}x_{40}^2)^J}{(-x_{24}^2)^{\frac{\Delta_2+\Delta_4-\Delta+J}{2}}(-x_{02}^2)^{\frac{\Delta+J+\Delta_2-\Delta_4}{2}}(-x_{04}^2)^{\frac{\Delta+J+\Delta_4-\Delta_2}{2}}}, \quad 4>0>2.
\end{aligned}
\tag{3.216}
$$

In the embedding space, it is given by

$$
\begin{aligned}
&\langle 0|\phi_4(X_4)O(X_0,Z_0)\phi_2(X_2^+)|0\rangle \\
&= \frac{(-2V_{0,42}(-X_{24}))^J}{(-X_{24})^{\frac{\Delta_2+\Delta_4-\Delta+J}{2}}(-X_{02})^{\frac{\Delta+J+\Delta_2-\Delta_4}{2}}(-X_{04})^{\frac{\Delta+J+\Delta_4-\Delta_2}{2}}}, \quad 4>0>2.
\end{aligned}
\tag{3.217}
$$

Note that the combination $-2V_{0,42}(-X_{24})$ is always positive due to the causality constraint $4>0>2$. The actual dual structure will be the above structure with the replacement $\Delta\to J+d-1, J\to\Delta-d+1, \Delta_i\to\widetilde{\Delta}_i$, multiplied by a computable prefactor. In the scalar case, it is given by (3.37). We discuss the spinning case in more detail in appendix 3.D.

3.B Heavy action formula from the large ν limit

In the main text of this paper we have taken the large ν limit of the kernel and large Δ limit of the block at the same time. However, in this appendix we compute the large ν limit independently. Taking the large ν limit of the kernel alone will slightly differ from taking Δ and ν limits simultaneously. Recall that when we perform the gauge fixing, we also fix a fifth point x_5 coming from the conformal block we want to act the functional on. If we just study the action of the functional on a general four-point function, we can again use conformal symmetry to fix x_1+x_3 to the origin and $x_{2^+}+x_{4^-}$ to spatial infinity, and since we don't have a fifth point, the stabilizer group is generated by Lorentz transformations and dilatations. We can then use Lorentz transformation to fix all four points to be on the same plane. After performing the large ν analysis (which will be done below), one can then obtain a kernel that only depends on the cross ratios (see (3.237)). Therefore, we can undo the gauge fixing and go back the the bulk-point gauge fixing again, and then the rest of the calculation is the same as (Simon Caron-Huot, Mazac, et al., 2021a).

We now want to take the large ν limit of

$$\Psi^{+}_{k,\nu}[\mathcal{G}] = 4A_{k,\nu}\int_{4>3>0>1>2}\frac{d^dx_1d^dx_2d^dx_3d^dx_4d^dx_0D^{d-2}z_0}{\mathrm{vol}(\widetilde{\mathrm{SO}}(d,2))}\langle 0|\phi_4(x_4)\mathbf{L}[O](x_0,z_0)\phi_2(x_2^+)|0\rangle^{-1}$$
$$\langle\widetilde{\mathcal{P}}_{\delta_1}(x_{1^+0})\widetilde{\mathcal{P}}_{\delta_3}(x_{30})\mathcal{P}_{\delta}(z_0)\rangle\delta(x_{1^+0}^2)\delta(x_{30}^2)\theta(x_{1^+0})\theta(x_{30})\langle\Omega|[\phi_4(x_4),\phi_3(x_3)][\phi_1(x_1^+),\phi_2(x_2^+)]|\Omega\rangle. \tag{3.218}$$

The only ν dependence is in dual and celestial structures, and so we need only focus on

$$\int d^dx_0D^{d-2}z\langle 0|\phi_4(x_4)\mathbf{L}[O](x_0,z_0)\phi_2(x_2^+)|0\rangle^{-1}\delta(x_{1^+0}^2)\delta(x_{30}^2)$$
$$\times\langle\mathcal{P}_{\delta}(z)\mathcal{P}_{\widetilde{\delta}_1}(x_{1^+0})\mathcal{P}_{\widetilde{\delta}_3}(x_{30})\rangle(-x_{13}^2)^{\widetilde{\Delta}_\phi}(-x_{24}^2)^{\widetilde{\Delta}_\phi}, \tag{3.219}$$

which we can rewrite using the explicit expression for the dual structure (3.37) which gives us

$$\int d^dx_0D^{d-2}z\times\langle\mathcal{P}_{\delta}(z)\mathcal{P}_{\widetilde{\delta}_1}(x_{1^+0})\mathcal{P}_{\widetilde{\delta}_3}(x_{30})\rangle(-x_{13}^2)^{\widetilde{\Delta}_\phi}(-x_{24}^2)^{\widetilde{\Delta}_\phi}\delta(x_{1^+0}^2)\delta(x_{30}^2)$$
$$\frac{(2z_0\cdot x_{40}x_{20}^2-2z_0\cdot x_{20}x_{40}^2)^{\Delta-d+1}}{(-x_{24}^2)^{\frac{\widetilde{\Delta}_2+\widetilde{\Delta}_4+\Delta-J-2d+2}{2}}(x_{02}^2)^{\frac{\widetilde{\Delta}_2+\Delta+J-\widetilde{\Delta}_4}{2}}(x_{02}^2)^{\frac{\widetilde{\Delta}_4+\Delta+J-\widetilde{\Delta}_2}{2}}}, \tag{3.220}$$

where we have dropped the overall coefficient in (3.37). It will be useful to notice that the dual structure has the form $\langle\widetilde{\phi}(x_4)O^F(x_0,z_0)\widetilde{\phi}(x_2)\rangle$, which is a three-point function of two scalars with shadow dimensions $\widetilde{\Delta}_\phi = d - \Delta_\phi$, and a third operator with $(\Delta_F, J_F) = (J + d - 1, \Delta - d + 1)$, where J and Δ are the dimension and spin of the light transformed operator. In particular we will focus on the limit $J_F = 2 - d + \delta = \frac{2-d}{2} + i\nu$, $\nu \to \infty$.

From the analysis in the cross-ratio space (Simon Caron-Huot, Mazac, et al., 2021a), we know that in the bulk-point limit x and y will get fixed to saddle points of the form

$$x = (u_x, v_x, \vec{0}), \qquad y = (u_y, v_y, \vec{0}), \tag{3.221}$$

and therefore we can just study the large ν limit for this particular x and y using the gauge fixing procedure described above.

Let us choose the coordinates of x_0 and z to be $x_0 = (u, v, \vec{y}_0)$, $z = (1, \vec{y}_z^2, \vec{y}_z)$. In the integrand, the J_F dependent factors are (we replace δ with $J_F + d - 2$ as well as Δ with $J_F + d - 1$)

$$\begin{aligned}
&\langle 0|\widetilde{\phi}_4(x_4) O^F(x_0, z)\widetilde{\phi}_2(x_2^+)|0\rangle\langle \mathcal{P}_\delta(z)\mathcal{P}_{\widetilde{\delta}_1}(x_{1^+0})\mathcal{P}_{\widetilde{\delta}_3}(x_{30})\rangle \\
=&\frac{(-2V_{0,24})^{J_F}}{(x_{2^+4}^2)^{\frac{2\widetilde{\Delta}_\phi - d+2-J_F}{2}}(-x_{40}^2)^{\frac{d-2+J_F}{2}}(x_{2^+0}^2)^{\frac{d-2+J_F}{2}}}\times \\
&\qquad\frac{1}{(-2z\cdot x_{1^+0})^{\frac{d-2+J_F}{2}}(-2z\cdot x_{30})^{\frac{d-2+J_F}{2}}(-2x_{1^+0}\cdot x_{30})^{\frac{2\widetilde{\delta}_\phi - d+2-J_F}{2}}}.
\end{aligned} \tag{3.222}$$

Note that we have the delta functions $\delta(x_{1^+0}^2)\delta(x_{30}^2)$, and therefore $-2x_{1^+0}\cdot x_{30} = (x_{1^+0} - x_{30})^2 = x_{1^+3}^2$.

The two delta functions can be written as

$$\delta(x_{1^+0}^2)\delta(x_{30}^2) = \delta((u+u_y)(v+v_y) - \vec{y}_0^2)\delta(-(u-u_y)(v-v_y) + \vec{y}_0^2). \tag{3.223}$$

In terms of $\widetilde{t}_0, \widetilde{x}_0$ defined in (3.59) (in this case we have $\vec{y}_\perp = 0$), the delta functions fix $\widetilde{t}_0 = 0$ and $r_0 \equiv |\vec{y}_0| = (u_y v_y(1-\widetilde{x}_0^2))^{\frac{1}{2}}$. The Jacobian relating $\widetilde{t}_0, \widetilde{x}_0$ and u, v is given by $du dv = 2u_y v_y d\widetilde{t}_0 d\widetilde{x}_0$. This gives (for any function $f(u, v, \vec{y}_0)$)

$$\begin{aligned}
&\frac{1}{2}\int du dv d^{d-2}\vec{y}_0\, \delta(-(u-u_y)(v-v_y) + \vec{y}_0^2)\delta((u+u_y)(v+v_y) - \vec{y}_0^2) f(u, v, \vec{y}_0) \\
=&\int d\widetilde{x}_0 d\Omega_{\vec{n}_0}\frac{(u_y v_y(1-\widetilde{x}_0^2))^{\frac{d-4}{2}}}{8} f(\widetilde{t}_0 = 0, \widetilde{x}_0, r_0 = (u_y v_y(1-\widetilde{x}_0^2))^{\frac{1}{2}}, \Omega_{\vec{n}_0}),
\end{aligned} \tag{3.224}$$

where $\vec{n}_0$ is the unit vector in the $\vec{y}_0$ direction.

After removing the delta functions, (3.219) becomes

$$\int d\widetilde{x}_0 d\Omega_{\vec{n}_0} d^{d-2}\vec{y}_z \frac{(u_y v_y(1-\widetilde{x}_0^2))^{\frac{d-4}{2}}}{8} \frac{2^{-J_F}}{(-x_{2^+4^-}^2)^{\frac{2\widetilde{\Delta}_\phi-d+2-J_F}{2}}(x_{4^-0}^2)^{\frac{d-2}{2}}(x_{2^+0}^2)^{\frac{d-2}{2}}}\times$$
$$\frac{1}{(-2z\cdot x_{1^+0})^{\frac{d-2}{2}}(-2z\cdot x_{30})^{\frac{d-2}{2}}(-2x_{1^+0}\cdot x_{30})^{\frac{2\widetilde{\delta}_\phi-d+2-J_F}{2}}} e^{J_F\times h(\widetilde{x}_0,\vec{y}_z,\Omega_{\vec{n}_0})}(4u_y v_y)^{(d-\Delta_\phi)}(\tfrac{4}{u_x v_x})^{(d-\Delta_\phi)},$$
(3.225)

where the function $h(\widetilde{x}_0,\vec{y}_z,\Omega_{\vec{n}_0})$ is given by

$$\begin{aligned} & h(\widetilde{x}_0,\vec{y}_z,\Omega_{\vec{n}_0}) \qquad (3.226)\\ &= \log\left(\frac{1}{u_x}+\frac{\vec{y}_z^2}{v_x}-u_y v_y(1-\widetilde{x}_0^2)(v_x+u_x\vec{y}_z^2)-u_x v_y^2\widetilde{x}_0^2-u_y^2 v_x\widetilde{x}_0^2\vec{y}_z^2+2(u_y v_x-v_y u_x)\widetilde{x}_0\vec{y}_0\cdot\vec{y}_z\right)\\ &\quad -\frac{1}{2}\log\Big((v_y(1-\widetilde{x}_0)-2\vec{y}_0\cdot\vec{y}_z+u_y(1+\widetilde{x}_0)\vec{y}_z^2)(v_y(1+\widetilde{x}_0)+2\vec{y}_0\cdot\vec{y}_z u_y(1-\widetilde{x}_0)\vec{y}_z^2)\Big)\\ &\quad -\frac{1}{2}\log\left(\frac{(1-u_y v_y u_x v_x-(u_y v_x-v_y u_x)\widetilde{x}_0)(1-u_y v_y u_x v_x+(u_y v_x-u_x v_y)(1-\widetilde{x}_0))}{u_x^2 v_x^2}\right). \end{aligned}$$
(3.227)

We find that at large J_F, the integral has two saddle loci: one at $\widetilde{x}_0=0,\vec{y}_z=0$ and one at $\widetilde{x}_0=0,\vec{y}_z=\infty$. Namely,

$$\begin{aligned} \frac{\partial}{\partial\widetilde{x}_0}h(\widetilde{x}_0,\vec{y}_z,\Omega_{\vec{n}_0})\Big|_{\widetilde{x}_0\to0,\vec{y}_z\to0} &= \frac{\partial}{\partial\vec{y}_z}h(\widetilde{x}_0,\vec{y}_z,\Omega_{\vec{n}_0})\Big|_{\widetilde{x}_0\to0,\vec{y}_z\to0}=0\\ \frac{\partial}{\partial\widetilde{x}_0}h(\widetilde{x}_0,\vec{y}_z,\Omega_{\vec{n}_0})\Big|_{\widetilde{x}_0\to0,\vec{y}_z\to\infty} &= \frac{\partial}{\partial\vec{y}_z}h(\widetilde{x}_0,\vec{y}_z,\Omega_{\vec{n}_0})\Big|_{\widetilde{x}_0\to0,\vec{y}_z\to\infty}=0. \end{aligned} \qquad (3.228)$$

Let us first consider the locus at $\widetilde{x}_0=\vec{y}_z=0$. We will see what the other saddle should give shortly. Expanding $h(\widetilde{x}_0,\vec{y}_z,\Omega_{\vec{n}_0})$ around $\widetilde{x}_0=\vec{y}_z=0$, we get

$$\begin{aligned} h(\widetilde{x}_0,\vec{y}_z,\Omega_{\vec{n}_0}) &\approx -\log\left(\frac{v_y}{v_x}\right)+\frac{(1+u_y^2v_x^2-2u_xu_yv_xv_y)(1-u_x^2v_y^2)}{2(1-u_yv_yu_xv_x)^2}\widetilde{x}_0^2\\ &\quad +\frac{2(1-u_x^2v_y^2)}{v_y(1-u_yv_yu_xv_x)}\widetilde{x}_0\vec{y}_0\cdot\vec{y}_z+\frac{2v_x(\vec{y}_0\cdot\vec{y}_z)^2-v_y(u_yv_x-v_yu_x)\vec{y}_z^2}{v_xv_y^2}+\dots\\ &= -\log\left(\frac{v_y}{v_x}\right)+\frac{1}{2}\begin{pmatrix}\widetilde{x}_0 & \vec{y}_z\end{pmatrix}M_{\vec{y}_0}\begin{pmatrix}\widetilde{x}_0\\ \vec{y}_z\end{pmatrix}. \end{aligned} \qquad (3.229)$$

Alternatively, one can also choose to not integrate $\widetilde{t}_0$, $|\vec{y}_0|$ and keep the delta functions. Then the function h will also depend on $\widetilde{t}_0$ and $|\vec{y}_0|$, and one can show that there are saddle loci at $\widetilde{t}_0 = \widetilde{x}_0 = 0, \vec{y}_z = 0, \infty$. We can then expand h around the saddle locus and use the delta functions to fix $\widetilde{t}_0$ and $|\vec{y}_0|$. This calculation should give the same result.

Now let us compute the saddle integral in (3.225). By rotational invariance, the determinant of the Hessian $M_{\vec{y}_0}$ in (3.229) does not depend on the direction of $\vec{y}_0$, so we can pick a direction that makes computing the determinant simple. For example, $\vec{y}_0 = |\vec{y}_0|(1, 0, \dots, 0)$. We then find

$$\mathrm{Det}M_{\vec{y}_0} = \frac{2^{d-2}(1-u_y^2 v_x^2)(1-v_y^2 u_x^2)(v_y u_x - u_y v_x)^{d-2}}{(v_x v_y)^{d-2}(1-u_y v_y u_x v_x)^2}. \tag{3.230}$$

One also has to check the sign of each eigenvalue of $\mathrm{Det}M_{\vec{y}_0}$ in order to get the correct phase in the saddle integral. We find that for $v_y u_x - u_y v_x > 0$, all eigenvalues are positive, and for $v_y u_x - u_y v_x < 0$, one eigenvalue is positive and the other $d-2$ eigenvalues are negative. Both cases turn out to give the same result, so let us assume $v_y u_x - u_y v_x > 0$ here. The saddle integral in (3.225) is then given by

$$\begin{aligned} &\int d\widetilde{x}_0 d^{d-2}\vec{y}_z \, (\cdots) \, e^{J_F \times h(\widetilde{x}_0, \vec{y}_z, \Omega_{\vec{n}_0})} \\ &\approx (\cdots)\,|_{\widetilde{x}_0 \to 0, \vec{y}_z \to 0} \times \left(\frac{v_x}{v_y}\right)^{J_F} e^{\frac{i\pi}{2}(d-1)} J_F^{-\frac{d-1}{2}} \sqrt{\frac{(2\pi)^{d-1}}{\mathrm{Det}M_{\vec{y}_0}}} + \dots, \end{aligned} \tag{3.231}$$

where $(\cdots)$ are the other factors in the integrand of (3.225), and $\dots$ are subleading terms at large J_F. Evaluating the remaining factors on the saddle locus $\widetilde{x}_0 = 0, \vec{y}_z = 0$, we obtain

$$\begin{aligned} &(4u_y v_y)^{(d-\Delta_\phi)} \left(\tfrac{4}{u_x v_x}\right)^{(d-\Delta_\phi)} \int d\Omega_{\vec{n}_0} \frac{(u_y v_y)^{\frac{d-4}{2}}}{8} \left(\frac{v_x}{v_y}\right)^{J_F} e^{\frac{i\pi}{2}(d-1)} J_F^{-\frac{d-1}{2}} \sqrt{\frac{(2\pi)^{d-1}}{\mathrm{Det}M_{\vec{y}_0}}} \times \\ &\left.\frac{2^{-J_F}}{(-x_{2^+4^-}^2)^{\frac{2\widetilde{\Delta}_\phi - d + 2 - J_F}{2}} (x_{4^-0}^2)^{\frac{d-2}{2}} (x_{2^+0}^2)^{\frac{d-2}{2}}} \frac{1}{(-2z\cdot x_{1^+0})^{\frac{d-2}{2}} (-2z\cdot x_{30})^{\frac{d-2}{2}} (-2x_{1^+0}\cdot x_{30})^{\frac{2\widetilde{\delta}_\phi - d + 2 - J_F}{2}}}\right|_{\widetilde{x}_0 \to 0, \vec{y}_z \to 0} \\ &= 2^{-\frac{9}{2}+2d+J_F} \pi^{\frac{d-1}{2}} \mathrm{vol}(S^{d-3}) e^{\frac{i\pi}{2}(d-1)} J_F^{-\frac{d-1}{2}} \times \\ &\quad \frac{(v_y u_x)^{\frac{d-2-J_F}{2}} (u_y v_x)^{\frac{J_F}{2}+d-2} (v_y u_x - u_y v_x)^{\frac{2-d}{2}} (1-u_y v_y u_x v_x)^{3-d}}{\sqrt{(1-u_y^2 v_x^2)(1-v_y^2 u_x^2)}}. \end{aligned} \tag{3.232}$$

We can write the result in terms of the conformally-invariant cross-ratios r and η defined as

$$u' = \frac{(1-2r\eta+r^2)^2}{16r^2}, \quad v' = \frac{(1+2r\eta+r^2)^2}{16r^2}, \tag{3.233}$$

where u', v' are defined in (3.31). In terms of r, η, the u-channel Regge limit corresponds to $r \longrightarrow 0$ with fixed η. In our gauge fixing, they are given by

$$r = |x||y| = (u_y v_y u_x v_x)^{\frac{1}{2}}, \qquad \eta = -\frac{x \cdot y}{|x||y|} = \frac{v_y u_x + u_y v_x}{2(u_y v_y u_x v_x)^{\frac{1}{2}}}. \tag{3.234}$$

Then, in terms of r, η, (3.232) becomes

$$2^{-\frac{9}{2}+2d+J_F} \pi^{\frac{d-1}{2}} \operatorname{vol}(S^{d-3}) e^{\frac{i\pi}{4}(d-1)} \nu^{-\frac{d-1}{2}} \frac{(1-r^2)^{3-d} r^{d-2} w^{-i\nu} (w - \frac{1}{w})^{\frac{2-d}{2}}}{((1+r^2)^2 - 4r^2\eta^2)^{\frac{1}{2}}}, \tag{3.235}$$

where we have used $J_F = \frac{2-d}{2} + i\nu$ and $\eta = \frac{w+1/w}{2}$. One can then notice that the leading large ν behavior is similar to

$$\mathcal{P}_{\frac{2-d}{2}+i\nu}\left(\frac{w+1/w}{2}\right) \sim \frac{\Gamma(d-2)}{\Gamma(\frac{d-2}{2})} \frac{\nu^{\frac{2-d}{2}}}{(w-1/w)^{\frac{d-2}{2}}} \left(e^{-\frac{i\pi}{4}(d-2)} w^{i\nu} + e^{\frac{i\pi}{4}(d-2)} w^{-i\nu}\right), \quad \nu \to \infty, |w| > 1. \tag{3.236}$$

In particular, the second term agrees with (3.235), and the first term comes from the other saddle locus. Therefore, after including both saddle loci, the integral (3.225) becomes

$$2^{-\frac{9}{2}+2d+J_F} \pi^{\frac{d-1}{2}} e^{\frac{i\pi}{4}} \operatorname{vol}(S^{d-3}) \nu^{-\frac{1}{2}} \frac{\Gamma(\frac{d-2}{2})}{\Gamma(d-2)} \frac{(1-r^2)^{3-d} r^{d-2}}{((1+r^2)^2 - 4r^2\eta^2)^{\frac{1}{2}}} \mathcal{P}_{\frac{2-d}{2}+i\nu}(\eta). \tag{3.237}$$

The expression we start with, (3.219), is essentially the shadow representation of the conformal block $G^{\widetilde{\Delta}_\phi}_{\frac{d}{2}+i\nu, J=-1}$, where one of the three-point structures becomes a celestial structure and delta functions due to setting $J = -1$ (Chang, Kologlu, et al., 2022). What we have shown here is that its large ν limit is given by (3.237). Although the same result can be obtained in the cross-ratio space using the Casimir equation (Kravchuk and Simmons-Duffin, 2018b), we believe that the above calculation from saddle point can be more straightforwardly generalized to spinning operators. Since $G^{\widetilde{\Delta}_\phi}_{\frac{d}{2}+i\nu, J=-1}$ is exactly the kernel appearing in the Lorentzian inversion formula for $C(\Delta = \frac{d}{2} + i\nu, J = -1)$, the calculation here could also be helpful for understanding the OPE data at large Δ (Mukhametzhanov and Zhiboedov, 2019).

Finally, to reproduce the heavy action formula, we can take the conformally-invariant expression (3.237) and plug it back in (3.218). Similar to the main text, we can then study its action on conformal block and choose the gauge fixing (3.49), which introduces the Faddeev-Popov factor (3.50). This gives (3.51) with the kernel part replaced with (3.237). Combining with the subtraction factors (3.87), we find that we get an integral of the form

$$\int d^dxd^dy \frac{r^{k+d-1}(1-r^4)\eta}{((1+r^2)^2-4r^2\eta^2)^{\frac{k+1}{2}}} \times \\ \frac{1}{(-x^2)^{2d}} \frac{1}{(-x_{12}^2)^{\widetilde{\Delta}_\phi}(-x_{34}^2)^{\widetilde{\Delta}_\phi}} |\langle \phi_{1^+}\phi_{2^+}O^{\mu_1\cdots\mu_J}(x_5)\rangle||\langle \widetilde{O}^\dagger_{\mu_1\cdots\mu_J}(x_5)\phi_3\phi_4\rangle|\Big|_{\text{gauge-fixed}}. \tag{3.238}$$

The only difference between this integral and the one considered in Simon Caron-Huot, Mazac, et al., 2021a (see (3.25) and (3.37)) is a factor of η, which becomes 1 in the bulk-point limit. One can further check that the overall factors also agree. Hence, the calculation in Simon Caron-Huot, Mazac, et al., 2021a implies that we recover the same heavy action formula (3.92).

3.C Details on matching partial waves

In this appendix, we give some more details on the partial wave discussion in section 3.4.

Partial waves in monomial basis

In the main text, we define the vertices $v(n, e_1, e_2)$ directly from evaluating the CFT three-point structures at the saddle and applying the polarization map. From the flat space perspective, it is more convenient to define the vertices as monomials, which can be easily expressed using Young tableaux, as given in (Simon Caron-Huot, Li, et al., 2023b). Furthermore, the bootstrap calculation done in (Simon Caron-Huot, Li, et al., 2023b) also uses the monomial basis (up to a Gram-Schmidt procedure to convert it into a orthonormal basis). The dictionary found in the main text tells us that we can take the flat space functional found in (Simon Caron-Huot, Li, et al., 2023b) and construct a positive CFT functional with positive action on heavy blocks. If we want to further study the OPE coefficients in the bootstrap calculation, we will need to know the relation between the two different bases.

One can find the relation between the two bases by explicitly evaluating the CFT three-point structures at the saddle for all the exchanged representations ρ in the photon and graviton case (see (Simon Caron-Huot, Li, et al., 2023b) for a complete list). It turns out that there is a clear map between the building blocks of CFT three-point tensor structures and the building blocks of the monomial basis, given by columns of the Young tableaux. We find that the map between the structures of

$\langle O_1 O_2 O_5 \rangle$ and $v(n, e_1, e_2)$ is given by

$$
\begin{aligned}
&\begin{array}{|c|}\hline n\\\hline\end{array} \leftrightarrow [X_5, Z_5] \cdot [X_1, X_2], && e_1 \cdot e_2 \leftrightarrow [X_1, Z_1] \cdot [X_2, Z_2], \\
&\begin{array}{|c|}\hline e_1\\\hline n\\\hline\end{array} \leftrightarrow [X_5, Z_5, W_5] \cdot [X_1, Z_1, X_2], && \begin{array}{|c|}\hline e_2\\\hline n\\\hline\end{array} \leftrightarrow [X_5, Z_5, W_5] \cdot [X_2, Z_2, X_1], \\
&\begin{array}{|c|}\hline e_1\\\hline e_2\\\hline n\\\hline\end{array} \leftrightarrow [X_5, Z_5, W_5, \widetilde{W}_5] \cdot [X_1, Z_1, X_2, Z_2],
\end{aligned}
\tag{3.239}
$$

where we use the notation (3.209) for the CFT structures. The Young tableaux columns represent the antisymmetrization of the vectors in the boxes (see (Simon Caron-Huot, Li, et al., 2023b) for the precise definition). For example,

$$
\begin{array}{|c|}\hline e_1\\\hline n\\\hline\end{array} = e_1 \cdot w_1 n \cdot w_2 - n \cdot w_1 e_1 \cdot w_2, \tag{3.240}
$$

where w_1, w_2 are the polarizations of the vertex. Both sides of the map agree up to an overall factor after one evaluates the CFT structure at the scattering-crystal configuration (3.81) and applies the polarization map (3.133).

The map given in (3.239) allows us to unambiguously relate the structure labels of the two bases, and we find that the partial waves computed in the two bases are related by

$$
\pi^{\mathrm{CFT}}_{\rho,(a'b')} = 2^{2J-2j-n^{a'}_{15}-n^{a'}_{25}-n^{b'}_{36}-n^{b'}_{46}} (-1)^{n^{a'}_{12}+n^{a'}_{25}+n^{b'}_{34}+n^{b'}_{46}} \pi^{\mathrm{tableaux}}_{\rho,(a'b')}, \tag{3.241}
$$

where $n^{a'}_{15}$ counts the number of H_{15} of the (a') tensor structure, and other $n^{a'}_{ij}, n^{b'}_{ij}$ are defined similarly (see (3.211)). Note that the above relation is true for each a', b'. Alternatively, one can think of the factor relating the two partial waves as two diagonal matrices that rescale the vertices.

We also see that this change of basis preserves the positivity of the partial wave actions, so we can reuse the positive functional in the monomial basis. In the forward limit, where $n = n'$, $e_3 = e_1^*$, $e_4 = e_2^*$, the partial wave in the monomial basis is positive (or positive semi-definite for multiple tensor structures) by construction. In the CFT basis, (3.241) implies that the partial wave is also positive. (Note that if we instead define $\overline{v}(n', e_3, e_4)$ in (3.139), then the partial wave wouldn't be positive in the forward limit.)

Polarization map and CRT symmetry

We now explain why the two definitions of vertices (3.134), (3.139) are consistent with each other. In particular, we will show that by using the definition of $v(n, e_1, e_2)$ and the CRT symmetry, we can recover the definition of $\overline{v}(-n', e_3, e_4)$.

For any CFT, there is an anti-unitary CRT symmetry J satisfying $J^2 = 1$, and it acts on local operators as (assuming the operator is bosonic)

$$J\mathcal{O}(x,z)J^{-1} = \mathcal{O}^\dagger(\overline{x},\overline{z}^*), \tag{3.242}$$

where $\overline{x} = (-x^0, -x^1, x^2, \ldots)$ (and similarly for $\overline{z}^*$) is a Rindler reflection. Since J is anti-unitary, any CFT correlation function should satisfy

$$\langle \mathcal{O}_1(x_1,z_1)\cdots\mathcal{O}_n(x_n,z_n)\rangle = \langle \mathcal{O}_1^\dagger(\overline{x}_1,\overline{z}_1^*)\cdots\mathcal{O}_n^\dagger(\overline{x}_n,\overline{z}_n^*)\rangle^*, \tag{3.243}$$

where we have applied a CRT to each operator.

More generally, as explained in (Kologlu et al., 2020), for any spacelike points A and B, one can define two Rindler wedges $B > x > A^-$ and $A > x > B^-$. Then, there exists a Rindler conjugation J_{AB} that exchanges the two wedges. Explicitly,

$$J_{AB}(X) = X - 2\frac{X\cdot X_A}{X_A\cdot X_B}X_B - 2\frac{X\cdot X_B}{X_A\cdot X_B}X_A. \tag{3.244}$$

It turns out that if we choose A to be the future infinity and B^- to be the origin, under the corresponding Rindler conjugation J_{AB} we have $3 \to 1^+, 4 \to 2^+, 6^+ \to 5$ in the scattering crystal configuration (3.81). Therefore, using this J_{AB}, one might expect

$$\langle 0|\mathcal{O}^\dagger(x_{6^+},z_6)\mathcal{O}_4(x_4,z_4)\mathcal{O}_3(x_3,z_3)|0\rangle\big|_{\text{saddle}} \overset{?}{=} \langle 0|\mathcal{O}(x_5,\overline{z}_6^*)\mathcal{O}_4^\dagger(x_{2^+},\overline{z}_4^*)\mathcal{O}_3^\dagger(x_{1^+},\overline{z}_3^*)|0\rangle^*\Big|_{\text{saddle}}. \tag{3.245}$$

This is however too fast. A funny feature of our saddle configuration is that although the points $x_{1,2,3,4}$ are timelike, they all have purely imaginary spatial components. The correct way to think about this should be we first consider e.g. $x_3 = (u_y, v_y, 0)$ for real u_y, v_y, and at the end analytically continue to $u_y \to -i\frac{m-\sqrt{m^2-\nu^2}}{\nu}, v_y \to i\frac{m-\sqrt{m^2-\nu^2}}{\nu}$. To take into account the fact that there are imaginary spatial components, we should apply an additional reflection to them, which can then be shifted to act on the polarizations. In summary, the correct CRT relation becomes

$$\begin{aligned}&\langle 0|\mathcal{O}^\dagger(x_{6^+},z_6)\mathcal{O}_4(x_4,z_4)\mathcal{O}_3(x_3,z_3)|0\rangle\big|_{\text{saddle}}\\ &= \langle 0|\mathcal{O}(x_5,I_e\cdot z_6^*)\mathcal{O}_4^\dagger(x_{2^+},I_e\cdot z_4^*)\mathcal{O}_3^\dagger(x_{1^+},I_e\cdot z_3^*)|0\rangle^*\Big|_{\text{saddle}},\end{aligned} \tag{3.246}$$

where the polarizations are reflected only in the time direction. Since (3.246) is simply a statement about the CFT structures at the saddle configuration, we can explicitly verify that it is true for different representations ρ.

Using the CRT relation (3.246), we can write

$$
\begin{aligned}
&(-x_{34}^2)^{\frac{\Delta_3+\Delta_4}{2}}\left(\frac{x_{36}^2}{x_{46}^2}\right)^{\frac{\Delta_3-\Delta_4}{2}} \mathcal{I}_e^{\rho} \left.\frac{\langle 0|\mathcal{O}^\dagger(x_{6^+},z_6)[\mathcal{O}_4(x_4,z_4),\mathcal{O}_3(x_3,z_3)]|0\rangle_{(b)}}{2i(\sin(\pi\frac{\widetilde{\tau}_\rho-\Delta_3-J_3-\Delta_4-J_4}{2}))}\right|_{\text{saddle}} \\
&= (-x_{12}^2)^{\frac{\Delta_3+\Delta_4}{2}}\left(\frac{x_{15}^2}{x_{25}^2}\right)^{\frac{\Delta_3-\Delta_4}{2}} \left.\frac{\langle 0|[\mathcal{O}_3(x_{1^+},z_3^*),\mathcal{O}_4(x_{2^+},z_4^*)]\mathcal{O}(x_5,z_6^*)|0\rangle_{(b)}^*}{-2i(\sin(\pi\frac{\widetilde{\tau}_\rho-\Delta_3-J_3-\Delta_4-J_4}{2}))}\right|_{\text{saddle}}.
\end{aligned}
\tag{3.247}
$$

We assume there is only one polarization z_6 for simplicity, but the argument for more polarizations $\vec{w}_6$ is the same. We have also imposed conservation to set the time components of z_3, z_4 to zero. So, $I_e\cdot z_3 = z_3, I_e\cdot z_4 = z_4$, and the reflection tensor $\mathcal{I}_e^{\rho}$ cancels with the I_e acting on z_6. The additional minus sign in the denominator comes from changing the operator order in the commutator.

Since the positions are now at x_{1^+}, x_{2^+}, x_5, we can use the definition (3.134) for $v(n,e_1,e_2)$ (although now it is a vertex for external particles with spin J_3, J_4). We can then write (3.247) as

$$
\begin{aligned}
&(-x_{34}^2)^{\frac{\Delta_3+\Delta_4}{2}}\left(\frac{x_{36}^2}{x_{46}^2}\right)^{\frac{\Delta_3-\Delta_4}{2}} \mathcal{I}_e^{\rho} \left.\frac{\langle 0|\mathcal{O}^\dagger(x_{6^+},z_6)[\mathcal{O}_4(x_4,z_4),\mathcal{O}_3(x_3,z_3)]|0\rangle_{(b)}}{2i(\sin(\pi\frac{\widetilde{\tau}_\rho-\Delta_3-J_3-\Delta_4-J_4}{2}))}\right|_{\text{saddle}} \\
&= v(n, z_3^{x*}n_\perp+\vec{z}^{\,*}_{3\perp}, -z_4^{x*}n_\perp+\vec{z}^{\,*}_{4\perp}, w_1=(0,iz_6^{t*},z_6^{x*},\vec{z}^{\,*}_{6\perp}))^*.
\end{aligned}
\tag{3.248}
$$

When contracting the indices of the vertex $\overline{v}$, we should contract the polarizations after taking the complex conjugate. So, using $(v\cdot z)^* = v^*\cdot z^*$, we can write the above equation as a Schwarz reflection,

$$
\begin{aligned}
&(-x_{34}^2)^{\frac{\Delta_3+\Delta_4}{2}}\left(\frac{x_{36}^2}{x_{46}^2}\right)^{\frac{\Delta_3-\Delta_4}{2}} \mathcal{I}_e^{\rho} \left.\frac{\langle 0|\mathcal{O}^\dagger(x_{6^+},z_6)[\mathcal{O}_4(x_4,z_4),\mathcal{O}_3(x_3,z_3)]|0\rangle_{(b)}}{2i(\sin(\pi\frac{\widetilde{\tau}_\rho-\Delta_3-J_3-\Delta_4-J_4}{2}))}\right|_{\text{saddle}} \\
&= \overline{v}(n, z_3^{x}n_\perp+\vec{z}_{3\perp}, -z_4^{x}n_\perp+\vec{z}_{4\perp}, w_1=(0,-iz_6^{t},z_6^{x},\vec{z}_{6\perp})).
\end{aligned}
\tag{3.249}
$$

Rotational invariance demands that the vertex should just contain dot products of the polarizations and n^μ. Thus we are free to apply a reflection to all the vectors since it leaves the dot products invariant. In the bulk Minkowski coordinates $(t^{\text{bulk}}, x_1^{\text{bulk}}, x_2^{\text{bulk}}, \ldots)$, we will apply a reflection in the x_1^{bulk} direction. This will send $n^\mu \to -n'^\mu, n_\perp^\mu \to n_\perp'^\mu$. (See section 3.4 for their expressions in Minkowski coordinates.) After this reflection, we finally arrive at

$$
\begin{aligned}
&(-x_{34}^2)^{\frac{\Delta_3+\Delta_4}{2}}\left(\frac{x_{36}^2}{x_{46}^2}\right)^{\frac{\Delta_3-\Delta_4}{2}} \mathcal{I}_e^\rho \left.\frac{\langle 0|\mathcal{O}^\dagger(x_{6^+},z_6)[\mathcal{O}_4(x_4,z_4),\mathcal{O}_3(x_3,z_3)]|0\rangle_{(b)}}{2i(\sin(\pi\frac{\widetilde{\tau}_\rho-\Delta_3-J_3-\Delta_4-J_4}{2}))}\right|_{\text{saddle}}\\
&=\overline{v}(-n',z_3^x n'_\perp+\vec{z}_{3\perp},-z_4^x n'_\perp+\vec{z}_{4\perp},w_1=(0,iz_6^t,z_6^x,\vec{z}_{6\perp})), \qquad (3.250)
\end{aligned}
$$

which agrees with the $\overline{v}(-n',e_3,e_4)$ definition (3.139) and the polarization map (3.136).

Computing R_ρ

In the main text, we claim that

$$
\frac{2^d\dim(\rho)}{\mathrm{vol}(\mathrm{SO}(d))}\left.\frac{\langle\widetilde{\mathcal{O}}_a^\dagger(x_5)\widetilde{\mathcal{O}}^{\overline{b}}(x_6^+)\rangle}{\left(\langle\widetilde{\mathcal{O}}^\dagger\widetilde{\mathcal{O}}\rangle,\langle\mathcal{O}^\dagger\mathcal{O}\rangle\right)}\right|_{\text{saddle}} = 2^{-J+2\Delta}(-1)^{J-j+\widetilde{j}}R_\rho\left(\mathcal{I}_e^\rho\right)_a{}^{\overline{b}}, \qquad (3.251)
$$

where the R_ρ coefficient is given by (3.142). Here, we give a derivation for (3.142) in the case where $\rho=(J,j)$.

By the two-point pairing definition (3.78), we can rewrite the left-hand side of the above equation as

$$
\dim(\rho)\frac{\langle\widetilde{\mathcal{O}}_a^\dagger(e)\widetilde{\mathcal{O}}^{\overline{b}}((-e)^+)\rangle}{\langle\widetilde{\mathcal{O}}_{a'}^\dagger(e)\widetilde{\mathcal{O}}^{\overline{b}'}((-e)^+)\rangle\langle\mathcal{O}^{a'}(e)\mathcal{O}_{\overline{b}'}^\dagger((-e)^+)\rangle}. \qquad (3.252)
$$

It is not hard to see that both the shadow two-point $\langle\widetilde{\mathcal{O}}^\dagger\widetilde{\mathcal{O}}\rangle$ and the two-point structure $\langle\mathcal{O}^\dagger\mathcal{O}\rangle$ are proportional to the reflection tensor $\mathcal{I}_e^\rho$. However, the coefficient R_ρ should only depend on the convention of the two-point structure $\langle\mathcal{O}^\dagger\mathcal{O}\rangle$. From (3.207), we get

$$
\begin{aligned}
&\langle\mathcal{O}^\dagger(e,z_5,w_5,\widetilde{w}_5)\mathcal{O}((-e)^+,z_6,w_6,\widetilde{w}_6)\rangle\\
&\quad=2^{J-2\Delta}(-1)^{J-j+\widetilde{j}}\widehat{I}_e^\rho(z_5,w_5,\widetilde{w}_5;z_6,w_6,\widetilde{w}_6), \qquad (3.253)
\end{aligned}
$$

where

$$
\begin{aligned}
&\widehat{I}_e^\rho(z_5,w_5,\widetilde{w}_5;z_6,w_6,\widetilde{w}_6)\\
&=(z_6\cdot I_e\cdot z_5)^{J-j}\left(\sum_{\sigma\in S_2}z_{6\alpha_1}w_{6\alpha_2}I_e^{\alpha_1}{}_{\beta_1}I_e^{\alpha_2}{}_{\beta_2}z_5^{\beta_{\sigma(1)}}w_5^{\beta_{\sigma(2)}}\right)^{j-\widetilde{j}}\\
&\times\left(\sum_{\sigma\in S_3}z_{6\alpha_1}w_{6\alpha_2}\widetilde{w}_{6\alpha_3}I_e^{\alpha_1}{}_{\beta_1}I_e^{\alpha_2}{}_{\beta_2}I_e^{\alpha_3}{}_{\beta_3}z_5^{\beta_{\sigma(1)}}w_5^{\beta_{\sigma(2)}}\widetilde{w}_5^{\beta_{\sigma(3)}}\right)^{\widetilde{j}}, \qquad (3.254)
\end{aligned}
$$

where $I^{\mu}_{e\ \nu} = \delta^{\mu}{}_{\nu} + 2e^{\mu}e_{\nu}$, and we have introduced polarization vectors $z, w, \widetilde{w}$ for the three rows of the Young diagram of ρ. By comparing (3.251), (3.252), (3.253), and using the fact that $\left(\mathcal{I}^{\rho}_{e}\right)_{a}{}^{\overline{b}}\left(\mathcal{I}^{\rho}_{e}\right)^{a}{}_{\overline{b}} = \dim\rho$, we obtain

$$\mathcal{I}^{\rho}_{e} = R_{\rho}\widehat{I}^{\rho}_{e}. \tag{3.255}$$

This implies

$$(\widehat{I}^{\rho}_{e})_{a}{}^{\overline{b}}(\widehat{I}^{\rho}_{e})^{a}{}_{\overline{b}} = R_{\rho}^{-2}\dim\rho. \tag{3.256}$$

Now, let us specialize to $\rho = (J, j)$ and compute $(\widehat{I}^{\rho}_{e})_{a}{}^{\overline{b}}(\widehat{I}^{\rho}_{e})^{a}{}_{\overline{b}}$. The main idea is that we can use weight-shifting operators to derive a recursion relation (Karateev, Kravchuk, and Simmons-Duffin, 2018; Karateev, Kravchuk, and Simmons-Duffin, 2019). In particular, we will use

$$\begin{aligned}
\mathcal{D}^{0+\mu}_{z,w}\Big|_{J,j} &= (j-J)w^{\mu} + z^{\mu} z\cdot\frac{\partial}{\partial w},\\
\mathcal{D}^{0-\mu}_{z,w}\Big|_{J,j} &= \left((-J-d+4-j)\delta^{\mu}{}_{\nu} + z^{\mu}\frac{\partial}{\partial z^{\nu}}\right)\left((d-6+2j)\frac{\partial}{\partial w_{\nu}} - w^{\nu}\partial_{w}^{2}\right),
\end{aligned} \tag{3.257}$$

where $\mathcal{D}^{0+}_{z,w}$ increases the transverse spin j by 1 and $\mathcal{D}^{0-}_{z,w}$ decreases j by 1. These operators are the weight-shifting operators of the $\mathrm{SO}(d-1,1)$ group in the vector representation (Karateev, Kravchuk, and Simmons-Duffin, 2018). Using them, we can build a “bubble diagram,"

$$\mathcal{D}^{0+}_{z_5,w_5}\cdot\mathcal{D}^{0-}_{z_5,w_5}\widehat{I}^{\rho}_{e}(z_5,w_5;z_6,w_6) = j(d-6+2j)(J+j+d-4)(J-j+2)\widehat{I}^{\rho}_{e}(z_5,w_5;z_6,w_6). \tag{3.258}$$

Furthermore, one can perform crossing on a weight-shift operator and move it to the other leg of $\widehat{I}_{e}$,

$$\mathcal{D}^{0-\mu}_{z_5,w_5}\widehat{I}^{\rho}_{e}(z_5,w_5;z_6,w_6) = \frac{j(d-6+2j)(J+j+d-4)}{J-j+1}\mathcal{D}^{0+\mu}_{z_6,w_6}\widehat{I}^{\rho'}_{e}(z_5,w_5;z_6,w_6), \tag{3.259}$$

where $\rho' = (J, j-1)$. Combining the above two equations, we get

$$\widehat{I}^{\rho}_{e}(z_5,w_5;z_6,w_6) = \frac{1}{(J-j+1)(J-j+2)}\mathcal{D}^{0+}_{z_5,w_5}\cdot\mathcal{D}^{0+}_{z_6,w_6}\widehat{I}^{\rho'}_{e}(z_5,w_5;z_6,w_6). \tag{3.260}$$

Our goal is to compute the index contraction of two $\widehat{I}_e^{\rho}$ tensors. Using (3.260) we can rewrite it as the index contraction of $\mathcal{D}^{0+}_{z_5,w_5} \cdot \mathcal{D}^{0+}_{z_6,w_6}\widehat{I}_e^{\rho'}$ and $\widehat{I}_e^{\rho}$. Then, we can "integrate by parts" to move the weight-shifting operators to act on $\widehat{I}_e^{\rho}$. More precisely, let us denote the index contraction by a pairing $(\cdots,\cdots)$. Then the integration by parts relation is

$$\left(\mathcal{D}^{0+\mu}_{z,w}\widehat{I}_e^{\rho'}, \widehat{I}_e^{\rho}\right) = \frac{J-j+2}{j(d-6+2j)(J+j+d-4)}\left(I_e^{\rho'}, \mathcal{D}^{0-\mu}_{z,w} I_e^{\rho}\right). \tag{3.261}$$

Note that this relation is different from the one given in (Karateev, Kravchuk, and Simmons-Duffin, 2019). This is simply because they are adjoint relations with respect to different pairings. To obtain the adjoint with respect to index contraction, a simple way is to use the identity of the $\mathcal{D}^{(h)}$ operator given in (Simon Caron-Huot, Li, et al., 2023b). (Note that the $\mathcal{D}^{0-}$ operator defined here is just a special case of $\mathcal{D}^{(h)}$ with $h = 2$.)

The adjoint relation enables us to turn the computation into the index contraction of $\widehat{I}_e^{\rho'}$ and $\mathcal{D}^{0-}_{z_5,w_5} \cdot \mathcal{D}^{0-}_{z_6,w_6}\widehat{I}_e^{\rho}$, which then becomes the contraction of two $\widehat{I}_e^{\rho'}$'s. Together with (3.256), this gives the recursion relation

$$R_\rho^{-2} \dim\rho = \frac{(j+d-5)(2j+d-4)(J-j+2)(J+j+d-3)}{j(2j+d-6)(J-j+1)(J+j+d-4)} R_{\rho'}^{-2} \dim\rho'. \tag{3.262}$$

The relation between $\dim\rho$ and $\dim\rho'$ can be obtained from standard formula (Kravchuk, 2018; Karateev, Kravchuk, and Simmons-Duffin, 2019), or from the recursion relation for the Plancherel measure of the $\mathrm{SO}(d-1,1)$ Lorentz group (Karateev, Kravchuk, and Simmons-Duffin, 2019). Eventually, we get

$$\frac{R^2_{\rho'=(J,j-1)}}{R^2_{\rho=(J,j)}} = \frac{(J-j+2)^2}{(J-j+1)^2}. \tag{3.263}$$

With the initial condition $R_{\rho=(J,0)} = 1$, this leads to (3.142) in the $\widetilde{j} = 0$ case.

3.D Dual structures at large ν

In this appendix, we discuss how to compute the dual structure $\left(\langle 0|\mathcal{O}_4 \mathbf{L}[\mathcal{O}]\mathcal{O}_2|0\rangle^{(a)}\right)^{-1}$ that appears in the kernel of the functional. In particular, we are interested in the large ν limit, where ν parametrizes the scaling dimension of $\mathcal{O}$ as $\Delta = \frac{d}{2} + i\nu$.

Light transform at large dimension

To understand the dual structure, we should first study the light transform of the three-point function $\langle 0|\mathcal{O}_4\mathcal{O}\mathcal{O}_2|0\rangle$, and then consider its Lorentzian three-point pairing. Hence, let us first consider the light transform $\mathbf{L}[O]$ in the limit where O has large scaling dimension. Recall that the light transformed three-point function is given by

$$\langle 0|O_4\mathbf{L}[O_{\Delta,J,\lambda'}](X_0,Z_0)O_2|0\rangle = \int d\alpha\, \langle 0|O_4 O_{\Delta,J,\lambda'}(Z_0-\alpha X_0,-X_0)O_2|0\rangle \tag{3.264}$$

We will focus on the case $4>0>2^-$ and consider the limit $\Delta=\frac{d}{2}+i\nu$, $\nu\to\infty$. In this limit, we see that the quickly varying part of the integrand is

$$e^{-\frac{i\nu}{2}(\log(-2(Z_0-\alpha X_0)\cdot X_2)+\log(-2(Z_0-\alpha X_0)\cdot X_4))}, \tag{3.265}$$

which implies that the integral has a saddle point at

$$\alpha_* = \frac{2X_0\cdot X_2 Z_0\cdot X_4 + 2X_0\cdot X_4 Z_0\cdot X_2}{X_{02}X_{04}}. \tag{3.266}$$

As one can check, this point is spacelike from both 2 and 4. Therefore, the light transform gets localized to the point in the middle of the region that is spacelike from 2 and 4.

Expanding the quickly varying part around α_*, we find that the saddle integral we have to do is

$$\int d\alpha\, e^{\frac{i\nu}{2}\left(\frac{X_{02}X_{04}}{V_{0,24}X_{24}}\right)^2(\alpha-\alpha_*)^2} = e^{-\frac{3i\pi}{4}}\sqrt{\frac{2\pi}{\nu}}\frac{(-V_{0,42})X_{24}}{X_{02}(-X_{04})}. \tag{3.267}$$

The phase factor $e^{-\frac{3i\pi}{4}}$ comes from deforming the contour to a steepest descent contour. We show the steepest descent flow and the deformed contour in figure 3.7. The contour passes through the saddle point with angle $-\frac{3\pi}{4}$, and hence we have the $e^{-\frac{3i\pi}{4}}$ factor in (3.267). Also, note that when taking $\left(\frac{X_{02}X_{04}}{V_{0,42}X_{24}}\right)^2$ out of the square root, we have to make sure all factors are positive. In summary, the above analysis implies that the large Δ limit of $\langle 0|O_4\mathbf{L}[O_{\Delta,J}](X_0,Z_0)O_2|0\rangle$ should be given by

$$\lim_{\substack{\Delta=\frac{d}{2}+i\nu\\ \nu\gg 1}}\langle 0|O_4\mathbf{L}[O_{\Delta,J,\lambda'}](X_0,Z_0)O_2|0\rangle = e^{-\frac{3i\pi}{4}}\sqrt{\frac{2\pi}{\nu}}\frac{(-V_{0,42})X_{24}}{X_{02}(-X_{04})}\langle 0|O_4 O_{\Delta,J,\lambda'}(Z_0-\alpha_* X_0,-X_0)O_2|0\rangle. \tag{3.268}$$

Furthermore, we can study how each building block of the three-point structure transforms under $X_0\to Z_0-\alpha_* X_0$, $Z_0\to -X_0$. We will focus on the structures that

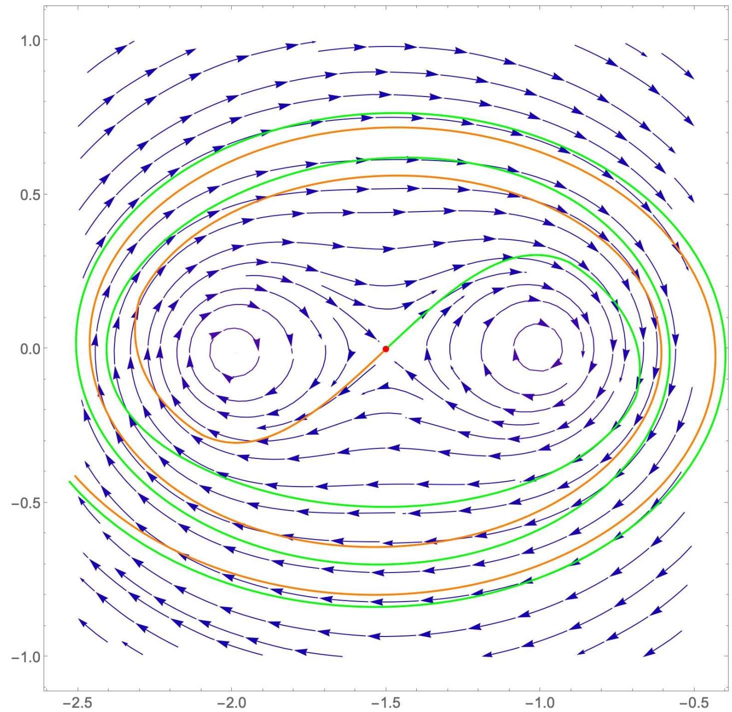

Figure 3.7: The steepest descent flow of the saddle integral (3.267). The red point is the saddle point. We show the deformed contour passing through the saddle in green and orange. The green part starts at infinity, goes in the opposite direction of the flow, and gradually spirals in toward the saddle. Along the green contour, the integrand keeps increasing and reaches maximum at the saddle point. It passes through the saddle point along a direction that is rotated by $e^{-\frac{3\pi i}{4}}$ relative to the real axis. After passing through the saddle point, the contour (in orange) goes in the same direction as the flow and gradually spirals out to infinity. The integrand at infinity goes as $\alpha^{-i\nu}$, so by making the contour spiral many times clockwise at infinity, we ensure that the contribution $\alpha^{-i\nu} \propto e^{2\pi\nu \arg(\alpha)}$ can be made arbitrarily small.

appear when λ' has a single row of length j'. We find

$$\begin{aligned} X_{02} &\to \frac{(-V_{0,42})X_{24}}{-X_{04}}, \quad V_{2,04} \to -\left(V_{2,04} + \frac{H_{20}}{V_{0,42}}\right), \quad U_{0,24} \to \frac{(-V_{0,42})X_{24}}{(-X_{04})X_{02}} U_{0,24}, \\ X_{04} &\to \frac{(-V_{0,42})X_{24}}{X_{02}}, \quad V_{4,20} \to -\left(V_{4,20} + \frac{H_{40}}{V_{0,42}}\right), \quad U_{0,42} \to \frac{(-V_{0,42})X_{24}}{X_{04}X_{02}} U_{0,42}, \end{aligned} \tag{3.269}$$

and all other structures are invariant (assuming O_2 and O_4 have no transverse spin). Therefore, starting with the three-point structure (3.211), its light transform at large

Δ is given by

$$\lim_{\substack{\Delta=\frac{d}{2}+i\nu \\ \nu\gg 1}} \langle 0|O_4 \mathbf{L}[O_{\Delta,J,j'}](X_0,Z_0,W_0)O_2|0\rangle = 2^{\Delta+J-1}e^{-\frac{3i\pi}{4}}\sqrt{\frac{2\pi}{\nu}}$$
$$\times \frac{(-2V_{0,42})^{1-\Delta-J+m_0}\left(-V_{2,04}-\frac{H_{20}}{V_{0,42}}\right)^{m_2}\left(-V_{4,20}-\frac{H_{40}}{V_{0,42}}\right)^{m_4} H_{24}^{n_{24}}H_{02}^{n_{02}}H_{04}^{n_{04}}(-2U_{0,24})^{k_{02}}(2U_{0,42})^{k_{04}}}{X_{24}^{\frac{\Delta_2+J_2+\Delta_4+J_4-2+\Delta+J-j'}{2}}(-X_{04})^{\frac{\Delta_4+J_4+2-\Delta-J+j'-\Delta_2-J_2}{2}}X_{02}^{\frac{\Delta_2+J_2+2-\Delta-J+j'+\Delta_2+J_2}{2}}}. \tag{3.270}$$

The result can also be written as

$$2^{\Delta+J-1}e^{-\frac{3i\pi}{4}}\sqrt{\frac{2\pi}{\nu}}\langle 0|O_4 O^L(X_0,Z_0,W_0)O_2|0\rangle\Big|_{V_{2,04}\to-\left(V_{2,04}+\frac{H_{20}}{V_{0,42}}\right),V_{4,20}\to-\left(V_{4,20}+\frac{H_{40}}{V_{0,42}}\right),U_{0,42}\to-U_{0,42}}, \tag{3.271}$$

where the operator O^L has quantum numbers $(1-J,1-\Delta,j')$.

Computation of light transform of general spinning three-point functions has been discussed in (Kologlu et al., 2020) for general Δ (see eq. (5.69)). One can check that the above result agrees with the large Δ_1 limit of the result in (Kologlu et al., 2020), which contains an Appell F_2. The Appell F_2 function in this limit will simplify and lead to the replacement rule $V_{2,04}\to-\left(V_{2,04}+\frac{H_{20}}{V_{0,42}}\right)$, $V_{4,20}\to-\left(V_{4,20}+\frac{H_{40}}{V_{0,42}}\right)$ given above.

We also need to understand how to impose conservation condition. In section 3.4, we study the conservation condition when the exchanged operator O has large dimension. Here, after the light transform, the dimension and spin are swapped, and therefore we have to instead consider conservation at large spin. However, the strategy in both cases are the same. We should identify the quickly-varying part of the three-point structure and take its derivative. By taking a x_4-derivative of the Δ-dependent factor of (3.270), we find that the conservation condition $\partial_{x_4}\langle O_4 O O_2\rangle = 0$ after the light transform becomes equivalent to

$$\left(V_{4,20}+\frac{H_{40}}{V_{0,42}}\right)_A D_{Z_4}^A\langle 0|O_4\mathbf{L}[O]O_2|0\rangle = 0, \tag{3.272}$$

where A is an embedding space index, and its meaning as a subscript is that we should take the structures $V_{4,20}$, H_{40} and strip off the Z_4. $D_{Z_4}^A$ is the Todorov/Thomas operator (Costa, Joao Penedones, et al., 2011). This condition is perfectly consistent with the original large Δ conservation (3.113) and the replacement rule from the light transform given by (3.269).

Dual structures

To get the dual structures, we can start with a standard basis of continuous-spin three-point structures $\langle 0|\widetilde{\mathcal{O}}_4^\dagger \mathcal{O}^F \widetilde{\mathcal{O}}_2^\dagger|0\rangle^{(a)}$ by adding spinning structures to the scalar convention (3.217) following (3.211). The quantum numbers of $\widetilde{\mathcal{O}}_2^\dagger, \widetilde{\mathcal{O}}_4^\dagger$ are $(d-\Delta_2, J_2)$ and $(d-\Delta_4, J_4)$. For $\mathcal{O}^F$, we should have $(\Delta_F, J_F) = (J+d-1, \Delta-d+1)$, where $\Delta = \frac{d}{2}+i\nu$ and $J = J_1+J_3-1$ depends on the spin of the external operators. The actual dual structures should be given by

$$\left(\langle 0|\mathcal{O}_4\mathbf{L}[\mathcal{O}]\mathcal{O}_2|0\rangle^{(a)}\right)^{-1} = \alpha^{(a)}{}_{(b)}\langle 0|\widetilde{\mathcal{O}}_4^\dagger \mathcal{O}^F \widetilde{\mathcal{O}}_2^\dagger|0\rangle^{(b)}, \tag{3.273}$$

and our goal is to find the coefficients $\alpha^{(a)}{}_{(b)}$.

Following the definition of dual structures (3.94), we have

$$\alpha^{(a)}{}_{(b)}\left(\langle 0|\widetilde{\mathcal{O}}_4^\dagger \mathcal{O}^F \widetilde{\mathcal{O}}_2^\dagger|0\rangle^{(b)}, \langle 0|\mathcal{O}_4\mathbf{L}[\mathcal{O}]\mathcal{O}_2|0\rangle_{(c)}\right)_L = \delta^a_c, \tag{3.274}$$

which gives

$$\begin{aligned}\alpha^{(a)}{}_{(b)} &= \left(\langle 0|\widetilde{\mathcal{O}}_4^\dagger \mathcal{O}^F \widetilde{\mathcal{O}}_2^\dagger|0\rangle^{(b)}, \langle 0|\mathcal{O}_4\mathbf{L}[\mathcal{O}]\mathcal{O}_2|0\rangle_{(a)}\right)_L^{-1}\\ &=2^{2d-2}\,\mathrm{vol}(\mathrm{SO}(d-2))\left(\langle 0|\widetilde{\mathcal{O}}_4^\dagger(0^+)\mathcal{O}^F(\infty,z_0^*)\widetilde{\mathcal{O}}_2^\dagger(e)|0\rangle^{(b)}\langle 0|\mathcal{O}_4(0^+)\mathbf{L}[\mathcal{O}](\infty,z_0^*)\mathcal{O}_2(e)|0\rangle_{(a)}\right)^{-1},\end{aligned} \tag{3.275}$$

where the in the second line we have used the conformal group to fixed all the points to the configuration $x_4 = 0^+, x_2 = e, x_0 = \infty$ and $z_0 = (1,1,\vec{0})$ (in lightcone coordinates). The prefactor $2^{2d-2}\,\mathrm{vol}(\mathrm{SO}(d-2))$ comes from the Faddeev-Popov determinant and volume of the stabilizer group of the gauge-fixed configuration (Kravchuk and Simmons-Duffin, 2018b).

Then, the calculation of dual structures is now reduced to evaluating the continuous-spin basis and the light transformed structures in this standard configuration. Since the continuous-spin basis can be obtained from (3.217), (3.211), and the light transformed structures at large ν are given by (3.270), the dual structures at large ν can be computed straightforwardly using (3.275).

Lastly, when we impose conservation on the external operators $\mathcal{O}_2, \mathcal{O}_4$, the dual structures get a gauge redundancy due to the conservation equations. At large ν, the statement becomes

$$\langle 0|\mathcal{O}_4\mathbf{L}[\mathcal{O}]\mathcal{O}_2|0\rangle^{-1} \sim \langle 0|\mathcal{O}_4\mathbf{L}[\mathcal{O}]\mathcal{O}_2|0\rangle^{-1} + \left(V_{4,20}+\frac{H_{40}}{V_{0,42}}\right)(\ldots) + \left(V_{2,04}+\frac{H_{20}}{V_{0,42}}\right)(\ldots). \tag{3.276}$$

The idea is that whenever we have a $\left(V_{4,20} + \frac{H_{40}}{V_{0,42}}\right)$ factor, we can always integrate it by parts in the pairing (Karateev, Kravchuk, and Simmons-Duffin, 2019) and get the large-ν conservation equation (3.272). The argument for the other factor is similar. Fortunately, thanks to the identity (3.153), when we evaluate the structures at the saddle and set the time component of the external polarizations to zero, the result is independent of this gauge redundancy.

In summary, to compute the dual structures for conserved external operators, we can use the gauge redundancy to remove all the V_i structures for the external operators and simply consider a basis with just the H_{i0}, H_{ij} structures, as stated in section 3.4. We can then use (3.275) to compute the dual structure coefficients, where the label (b) only includes continuous-spin structures without the V_i's, and (a) are the conserved structures. These two structures both have the same counting given by (3.154).

3.E CFT four-point structures

In this appendix, we give the expressions of the CFT four-point structures that we use in the main text. In particular, they should satisfy (3.181). From the group-theoretic counting argument (Kravchuk and Simmons-Duffin, 2018a), we already know that the number of CFT four-point structures should agree with the number of flat space polarization structures.

$$
\begin{aligned}
H^{CFT}_{ijk} &= [X_i, Z_i]^{A_1A_2}[X_j, Z_j]^{A_2A_3}[X_k, Z_k]^{A_3A_1}, \\
H^{CFT}_{ijkl} &= [X_i, Z_i]^{A_1A_2}[X_j, Z_j]^{A_2A_3}[X_k, Z_k]^{A_3A_4}[X_l, Z_l]^{A_4A_1}, \\
X^{CFT}_{ijkl} &= H^{CFT}_{ijkl} - \frac{1}{4}\left(H^{CFT}_{14}H^{CFT}_{23} + H^{CFT}_{13}H^{CFT}_{24} + H^{CFT}_{12}H^{CFT}_{34}\right), \\
S^{CFT} &= V^{CFT}_{1,24}H^{CFT}_{234} + V^{CFT}_{2,31}H^{CFT}_{341} + V^{CFT}_{3,42}H^{CFT}_{412} + V^{CFT}_{4,13}H^{CFT}_{123}, \qquad (3.277)
\end{aligned}
$$

where A_i are embedding space indices, and $[X, Z]^{AB} = X^A Z^B - X^B Z^A$. The superscript CFT is to distinguish the CFT structure and the flat space structure, and V^{CFT}, H^{CFT}_{ij} are given in (3.206). Then, we find

$$
\begin{aligned}
&\{H^{CFT}_{14}H^{CFT}_{23}, H^{CFT}_{13}H^{CFT}_{24}, H^{CFT}_{12}H^{CFT}_{34}, X^{CFT}_{1243}, X^{CFT}_{1234}, X^{CFT}_{1324}, S^{CFT}\}\big|_{\text{saddle},(3.133),(3.136)} \\
=&\frac{16}{\nu^4}\left\{H_{14}H_{23}, H_{13}H_{24}, H_{12}H_{34}, X_{1243}, X_{1234}, X_{1324}, \frac{2}{\nu^2}S\right\}. \qquad (3.278)
\end{aligned}
$$

Thus, we choose the left hand side of the above equation to be our four-point structure basis Q^I in the main text.

The CFT four-point structures we choose all have homogeneity 1 for all $X_{1,2,3,4}$, $Z_{1,2,3,4}$. Under the map of polarizations, they reproduce the expected amplitude structures, with the correct Regge behavior. The additional factors of ν should not be a big issue since we can absorb them into the prefactors. The only different case is that we have to introduce a $\frac{2}{\nu^2}$ factor for the S structure. This is reasonable from dimensional analysis since the S structure has an additional $p_i \cdot p_j$. It also seems to suggest that from the CFT point of view, $\frac{2}{\nu^2}S$ is a more natural choice for the structure.

For the four-graviton case, the construction given above can be easily generalized. The only four-graviton flat space structure that can't be written in terms of H_{ij}, X_{ijkl}, S is the Gram determinant of all dot products between $(p_1, p_2, p_3, e_1, e_2, e_3, e_4)$, which we write as $\mathcal{G}_{p_1,p_2,p_3,e_1,e_2,e_3,e_4}$. Even though this structure does not appear in the graviton sum rule dictionary given in section 3.4 as it grows more slowly in the Regge limit, let us still give the corresponding CFT structure for completeness. The corresponding CFT structure can be written as

$$X_{24}\left(\frac{X_{14}X_{34}}{X_{12}X_{23}}\right)^{\frac{1}{2}}\mathcal{G}_{X_1,X_2,X_3,Z_1,Z_2,Z_3,Z_4} - (\ldots)\mathcal{G}_{X_1,X_2,X_3,Z_1,Z_2,Z_3,X_4}. \tag{3.279}$$

This structure is manifestly invariant under $Z_i \to Z_i + \#X_i$ thanks to properties of determinant. The only exception is the $Z_4 \to Z_4 + \#X_4$ gauge redundancy. This is why we introduce the second term, and $(\ldots)$ is a factor that fixes homogeneity. The structure is constructed such that its homogeneity is the same as the other structures (has homogeneity 1 for all X_i, Z_i). When evaluating the above expression at the saddle and applying the polarization map, we find that the second term vanishes, and we have

$$X_{24}\left(\frac{X_{14}X_{34}}{X_{12}X_{23}}\right)^{\frac{1}{2}}\mathcal{G}_{X_1,X_2,X_3,Z_1,Z_2,Z_3,Z_4}\Bigg|_{\text{saddle},(3.133),(3.136)} = \frac{256}{\nu^6}\mathcal{G}_{p_1,p_2,p_3,e_1,e_2,e_3,e_4}. \tag{3.280}$$

So, (3.279) should be the correct CFT four-point structure that gives $\mathcal{G}_{p_1,p_2,p_3,e_1,e_2,e_3,e_4}$.

Chapter 4

DE SITTER LIGHT RAY OPERATORS

4.1 Introduction

For over a quarter century we have known that our universe is undergoing accelerated expansion (S. Perlmutter et al., 1998; Riess et al., 1998), and that its far future may well be described by de Sitter space. Despite this, our knowledge of quantum field theory (QFT) in de Sitter space is in a much more primitive state than that of its other maximally symmetric counterparts, Minkowski and AdS spaces. There are at least two interesting complications that make QFT in de Sitter space subtle. The first is the lack of clearly defined Lorentzian observables, since there is no precisely defined S-matrix.[1] The second is the presence of infrared (IR) divergences (Green, 2023; Ford, 1985; Polyakov, 2012; Seery, 2010; Burgess et al., 2010; Rajaraman, 2010; Marolf and Morrison, 2010; Cohen and Green, 2020; Premkumar, 2024) (see (Akhmedov, Moschella, and Popov, 2019; Hu, 2018) for reviews), which are manifest in loop corrections but can often even appear at tree level in the form of secular growth.

There are regimes in which some of these questions are answered, partially resolved, or mitigated. The inflationary regime is one such example. It is naturally associated with a "meta-observer" who has access to all of the future conformal boundary $\mathscr{I}^+$, and the questions of interest are formulated in the vicinity of $\mathscr{I}^+$ (see the reviews (Achúcarro et al., 2022; Baumann et al., 2024) and references therein for such topics). This is not the regime we focus on in this work. Instead, we are interested in the perspective of a "bulk observer" and in the observables that are meaningful for such an observer. The motivation for this is two-fold: first, this is a very plausible description of the far future of our own universe; second, observers and their associated horizons are ubiquitous features in curved spacetimes. There has been substantial recent work taking the observer and their horizons as a starting point in general spacetimes, notably (Chandrasekaran et al., 2023). From this perspective, our focus on de Sitter space can be viewed as the study of the simplest such universe. The advantage is that de Sitter is a maximally symmetric spacetime

[1] For recent attempts to define S-matrix–like observables in de Sitter space, we refer the reader to (Albrychiewicz and Neiman, 2021; Melville and Pimentel, 2024b; Donath and Pajer, 2024; Melville and Pimentel, 2024a; Kristiano et al., 2025).

and shares familiar features, such as homogeneity, isotropy and even local timelike Killing fields, while nevertheless realizing a QFT that is organized in a rather different way from its Minkowski counterpart.

We can orient ourselves in such a spacetime by asking what kind of information an observer could, in principle, have access to. A natural class of such observables one could consider are *light-ray operators*. In Minkowski space these operators formalize many of the physical measurements performed by real-world particle detectors; they can be made IR finite, and are well defined even in the absence of an S-Matrix, as is the case in conformal field theories (CFTs).

Light-ray operators have two different origins. The first is their role as energy flux operators in particle physics (Sveshnikov and Tkachov, 1996; Korchemsky and Sterman, 1999) (for a detailed historical overview see (Moult and Zhu, 2025)), and the second is their appearance in the context of gravity as the central object in the average null energy condition (ANEC) (Tipler, 1978). The ANEC operator has been central to many important results even in flat-space QFTs, for example in constraining the behavior of renormalization group (RG) flows (Hartman, Kundu, and Tajdini, 2017; Hartman and Grégoire Mathys, 2024b; Hartman and Grégoire Mathys, 2023; Hartman and Grégoire Mathys, 2024a). Energy flux operators, on the other hand, have long been powerful tools in collider physics as manifestly IR-safe observables, and have been used in some of the most precise determinations of the strong coupling α_s (Hayrapetyan et al., 2024). Hofman and Maldacena Hofman and J. Maldacena, 2008 showed that expectation values of these idealized detectors can be written as integrals of correlation functions of local operators. This then not only gave rise to a resurgence in interest in energy flux operators in particle physics (Moult and Zhu, 2025), but also expanded it to a much wider field. Their construction in terms of local correlation functions allows these operators to be studied in CFTs, which do not admit an S-matrix. CFTs have been shown to possess a particularly rich space of light-ray operators: any local irrep of the conformal group integrated along a null ray is another such irrep, known as its *light transform* (Kravchuk and Simmons-Duffin, 2018b). Moreover, in the operator product expansion (OPE) of any two light transformed operators there exists an even larger class of light-ray operators, which themselves cannot be the light transform of a local operator, but rather live on Regge trajectories associated with the light transform of a local operator (Kologlu et al., 2021). In interacting theories, these Regge trajectories get renormalized to account for IR divergences, giving rise to a family of theory-dependent, IR-safe detector operators (Simon Caron-Huot, Kologlu, et al., 2023).

In summary, to address theories in de Sitter space that do not admit an S-matrix, we will focus on a class of observables that do not require an S-matrix, and yet model real-world measurements. In Minkowski space there exists a systematic framework for rendering such operators IR safe, but we will not attempt to implement the corresponding IR analysis in de Sitter here, leaving this to future work.

To address the question of systematically constructing appropriate light-ray operators in de Sitter space, we begin in section 4.2 by introducing the relevant coordinate systems. We describe four-dimensional de Sitter space first as an embedding into the hyperbolic embedding space $\mathbb{R}^{1,4}$ in section 4.2, then into the null embedding space $\mathbb{R}^{2,4}$ in section 4.2, before realizing its conformal completion on the Lorentzian cylinder in section 4.2. In section 4.3 we review the simplest light-ray operator in Minkowski space, namely the null integral of the stress tensor (defined on the future null infinity of Minkowski space $\mathscr{I}^+_{\mathrm{M}}$), and emphasize its different *equivalent* incarnations as an energy flux operator, an angular contribution to the Hamiltonian, the ANEC operator, and the light transform of the stress tensor. In section 4.4, we systematically classify the de Sitter analogs of these light-ray operators, which leads to a richer set of *inequivalent*, observer-dependent constructions. In section 4.4 we explicitly compute matrix elements of these four distinct de Sitter light-ray operators in the free conformal theory, and show how these manifest the expected symmetry and positivity properties outlined in section 4.4. Finally, in section 4.5 we summarize our results and conclude with a discussion of open questions and future directions suggested by this framework.

4.2 de Sitter space: coordinate systems and tilings

In this section, we primarily set up conventions and definitions for the various coordinate systems that will be used to define d-dimensional de Sitter (dS_d) space. Our focus will be on four dimensional de Sitter space dS_4, whose Ricci scalar R is given by $R = 12H^2$, with H being the Hubble constant. We will introduce the following three coordinate spaces that are relevant to our analysis:

1. *intrinsic* coordinates on dS_4, denoted by lowercase Latin and Greek letters $(t, x, \tau, \theta, \ldots)$,

2. the *hyperbolic embedding space* $\mathbb{R}^{1,4}$, denoted by uppercase Latin letters with Greek indices $(X^\mu, Z^\nu, \ldots)$, and

3. the *null embedding space* $\mathbb{R}^{2,4}$, denoted by uppercase Latin and Greek letters with Latin indices $(X^A, Z^B, \Xi^C, \ldots)$.

Intrinsic dS$_4$

In Lorentzian signature, dS$_4$ is a maximally symmetric spacetime of constant positive curvature, with isometry group $SO(1,4)$. In global coordinates, it is described by the metric

$$\mathrm{d}s^2 = \ell^2(-\mathrm{d}\zeta^2 + \cosh^2\zeta\, \mathrm{d}\Omega_3^2)\,, \tag{4.1}$$

where $\zeta \in \mathbb{R}$ and $\mathrm{d}\Omega_3^2 = \mathrm{d}\theta^2 + \sin^2\theta\, \mathrm{d}\Omega_2^2$ is the standard round metric on the 3-sphere S^3 (depicted by the Penrose diagram in Figure 4.1), while the radius of curvature ℓ is determined by the Hubble constant $\ell = H^{-1}$. In what follows, it will be convenient for us to set $H = \ell = 1$ and consequently all quantities will be measured in units of H (or equivalently in units of ℓ^{-1}). It will be crucial for our analysis to adopt an observer's point of view, thus breaking the homogeneity of global dS$_4$. To that end, we will work with the doubled Penrose diagram, whose left and right edges are identified, and with the observer's worldline placed at the center of the diagram as shown in Figure 4.2.

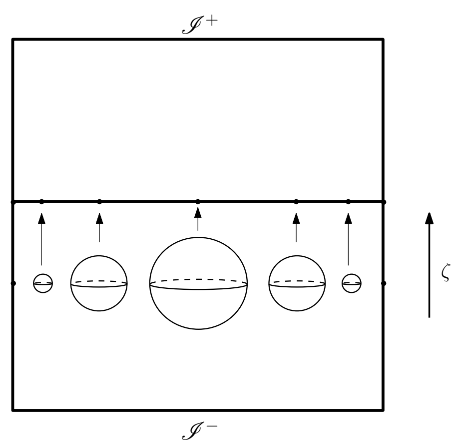

Figure 4.1: The usual Penrose diagram for global dS$_4$ space. Each horizontal slice represents a 3-sphere S^3. At $\zeta = 0$, the spatial slice is a 3-sphere S^3 of unit radius (in units of H^{-1}), which grows hyperbolically toward $\mathscr{I}^\pm$, where it becomes infinitely large. Each point on such a slice represents a two-sphere S^2 that expands toward the center of the diagram and shrinks to a point at the left and right edges. The observer is conventionally placed on the left, at the South Pole.

EPP/CPP Poincaré patches. We will now focus on two coordinate systems that break the homogeneity of global dS$_4$ due to the presence of such an observer. The

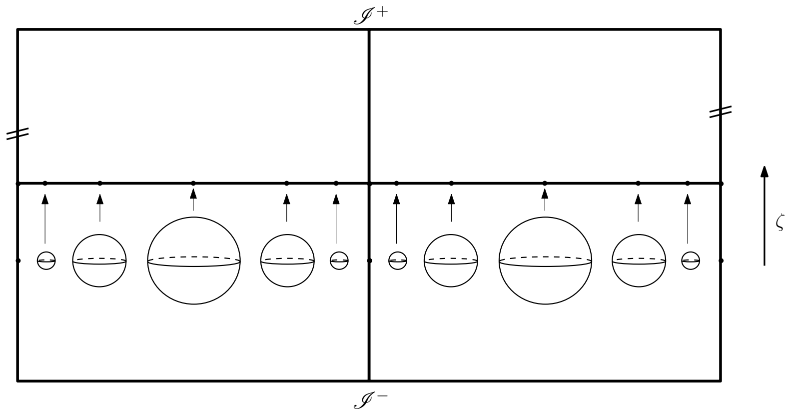

Figure 4.2: It will be more useful for our purposes to adopt the observer's point of view. We therefore place the observer at the center and work with the doubled Penrose diagram, where the left and right edges are identified.

first of these is the Poincaré patch(es), which cover one half of global dS_4 and admits spatial slices of $\mathbb{R}^3$. The geometry features a time-dependent scale factor that grows exponentially in the *expanding* Poincaré patch (EPP) and shrinks exponentially in the *contracting* Poincaré patch (CPP), corresponding to the two complementary halves of global dS_4. The metric in both these patches can be compactly expressed by

$$\mathrm{d}s^2 = -\mathrm{d}t^2 + e^{\pm 2t}\,\mathrm{d}\vec{x}^2 \,, \tag{4.2}$$

where $t \in \mathbb{R}$ and $\mathrm{d}\vec{x}^2$ is the Euclidean metric on $\mathbb{R}^3$, with $\pm$ denoting the metric on the EPP/CPP respectively. There is a useful class of coordinates on these patches known as *conformal* coordinates. Setting $\mp\eta = e^{\mp t}$, the metric in (4.2) in both the Poincaré patches attains the same form

$$\mathrm{d}s^2 = \frac{-\mathrm{d}\eta^2 + \mathrm{d}\vec{x}^2}{\eta^2} \,. \tag{4.3}$$

As shown in Figure 4.3, these patches are bounded by a null horizon $\mathscr{H}^\pm$ and an infinitely large spatial S^3. In the case of the CPP, this S^3 is in the past/early-time boundary $\mathscr{I}^-$ and the null horizon $\mathscr{H}^+$ bounds its future. In the EPP, the infinitely large spatial S^3 is in the future/late-time boundary $\mathscr{I}^+$ and $\mathscr{H}^-$ bounds its past.

Static patch. We now consider *static patch* coordinates, which can be seen as the intersection between the two Poincaré patches, and is consequently bounded by the CPP horizon $\mathscr{H}^+$ in the future and by the EPP horizon $\mathscr{H}^-$ in the past. The static patch metric is given by

$$\mathrm{d}s^2 = -(1 - r^2)\,\mathrm{d}\tau^2 + \frac{\mathrm{d}r^2}{(1 - r^2)} + r^2\mathrm{d}\Omega_2^2 \,, \tag{4.4}$$

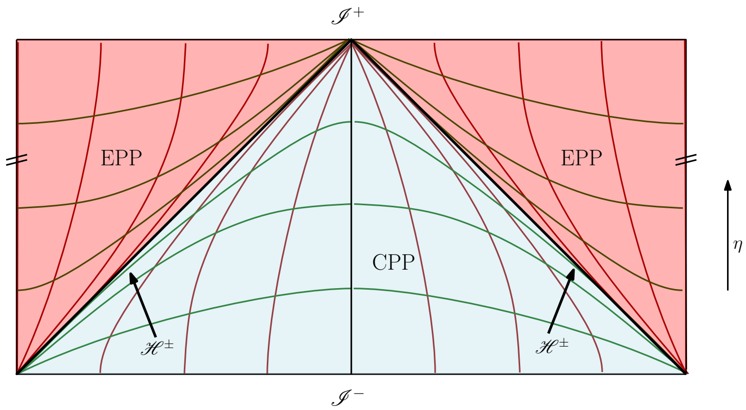

Figure 4.3: The Penrose diagram of dS space covered by the expanding (EPP) and contracting (CPP) Poincaré patches, with the observers worldline at the center of the CPP. The boundary between the patches is the $\mathscr{H}^+$ of the observer at the center of the CPP and the $\mathscr{H}^-$ of the observer at the center of the EPP.

where $0 < r < 1$ and $d\Omega_2^2$ is the standard round metric on the 2-sphere S^2. This metric is manifestly static as it is independent of the static patch time τ and is thereby endowed with a timelike Killing field ∂_τ, which simply points in the direction of τ. Both the past and the future cosmological/static patch horizons are at $r = 1$ and will be denoted by $\mathscr{H}_{\mathrm{SP}}^-$ and $\mathscr{H}_{\mathrm{SP}}^+$, respectively. For the observer at the center (situated at $r = 0$), $\mathscr{H}_{\mathrm{SP}}^\pm$ is a bifurcate Killing horizon for ∂_τ, and the bifurcation sphere is S^2 at the middle of the Penrose diagram, as shown in figure Figure 4.4.

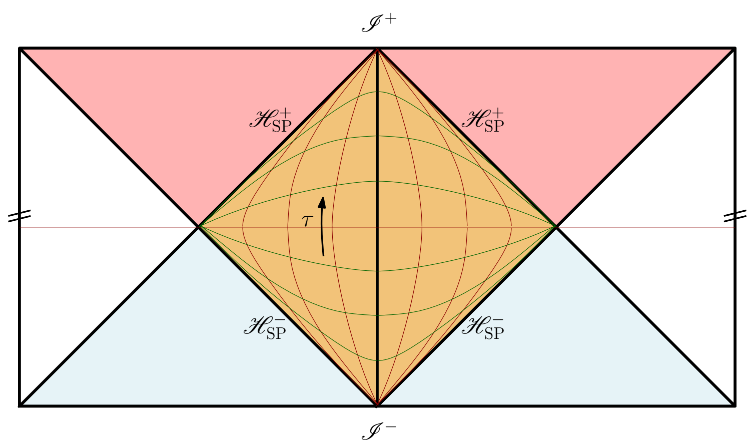

Figure 4.4: Static patch (gold) seen as the overlap between two Poincaré patches (red and blue). This is the causal patch of our observer at the center sitting at $r = 0$.

Hyperbolic Embedding Space

The hyperbolic embedding space arises when dS_4 is viewed (Figure 4.5) as a timelike hyperboloid living in five-dimensional Minkowski space $\mathbb{R}^{1,4}$

$$dS_4 = \{X \in \mathbb{R}^{1,4} : \eta_{\mu\nu} X^\mu X^\nu = 1\} , \tag{4.5}$$

where $\eta_{\mu\nu} = \mathrm{diag}(-1, 1, 1, 1, 1)$. It is worthwhile to think of this as a generalized

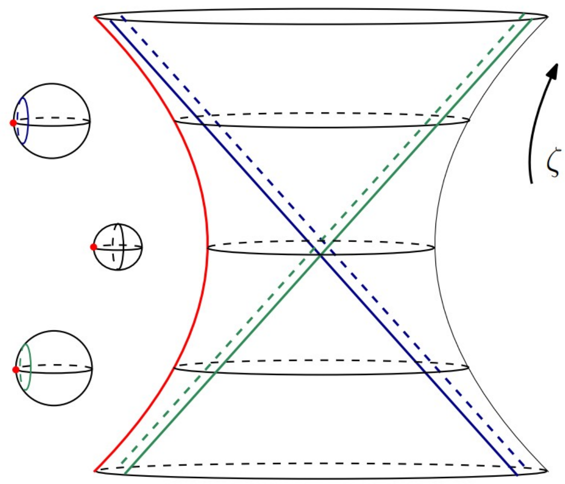

Figure 4.5: The embedding of dS_4 as a hyperboloid in $\mathbb{R}^{1,4}$. The observer sits at the South Pole (denoted by the red line on the left). Each horizontal cross-section represents a spatial S^3 slice of the global geometry. Two overlapping Poincaré patches define a static patch. The static patch always has the same size (of unit radius) but its portion of the overall global dS slice varies with ζ. At $\zeta = 0$ it coincides with the entire left half of the S^3. As the global S^3 slices grow away from $\zeta = 0$, the static patch remains a fixed-radius disk that occupies a decreasing fraction of the full sphere.

sphere as this suggests many ways to generalize intuitions from spheres. For example, if we consider the analytic continuation of dS_4 as defined in (4.5) to the 4-sphere S^4, then given any two points $X, Y \in S^4 \subset \mathbb{R}^5$ their inner product

$$\sigma \equiv X \cdot Y = \cos s \in [-1, 1] , \tag{4.6}$$

defines the so-called *embedding distance*, where s is the angle subtended by the great arc connecting the two points, or simply the *geodesic distance*. The embedding distance is a more natural object to work with since the $SO(5)$ isometry group of S^4 acts linearly on these embedding vectors and any dS invariant two-point function can be expressed in terms of the embedding distance. In a similar fashion, we can define the $SO(1,4)$ invariant *hyperbolic distance* between two points $x_i, x_j \in \mathrm{dS}_4$ as

$$h_{ij} \equiv \eta_{\mu\nu} X^\mu(x_i) X^\nu(x_j) \; . \tag{4.7}$$

Unlike the spherical case, the exact relationship between the hyperbolic and geodesic distances will depend on whether the two points are connected by a timelike, spacelike, or null geodesic. Hence the hyperbolic distance h depends on the geodesic distance s as

$$h_{ij}(s) = \begin{cases} \cosh s \in (1, \infty) & \text{if } s \text{ is timelike} \\ 1 & \text{if } s = 0 \\ \cos s \in [-1, 1) & \text{if } s \text{ is spacelike} \; . \end{cases} \tag{4.8}$$

There are also pairs of points in dS space for which h_{ij} is well defined, for example with $h_{ij} < -1$, but which are not connected by any real geodesic (see Figure 4.6). The regime $h_{ij} \to -\infty$ is often referred to as the cosmological limit, since it corresponds to taking both points to the late time boundary $\mathscr{I}^+$ while keeping their spatial separation fixed.

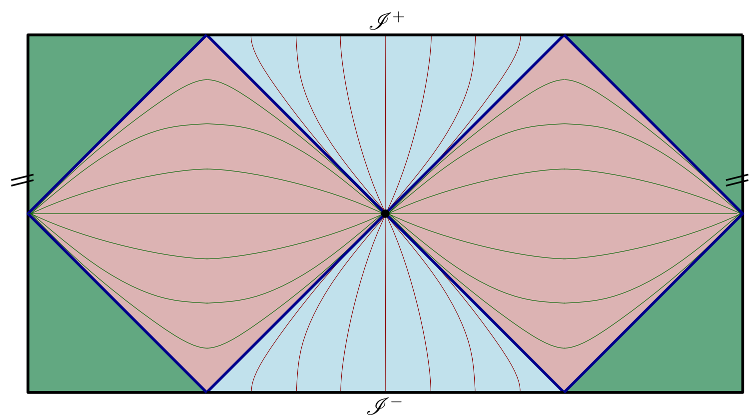

Figure 4.6: The observer at the center can travel along geodesics in any direction: timelike (shown in blue), spacelike (shown in red), or null in between. There also exist regions (shown in green) that cannot be reached from the origin by any geodesic.

We can also parameterize our tangent space $T(\mathrm{dS}_4) \subset T(\mathbb{R}^{1,4})$ in a very straightforward way. Given any point $X^\mu \in \mathrm{dS}_4$, its tangent space $T_X(\mathrm{dS}_4)$ is defined as

$$T_X(\mathrm{dS}_4) = \{ Y \in T_X(\mathbb{R}^{1,4}) : \eta_{\mu\nu} X^\mu Y^\nu = 0 \} \; . \tag{4.9}$$

This is analogous to the case of a sphere, in that the tangent space at a point X consists of all vectors in the ambient tangent space that are orthogonal to X itself.

In both cases, it is a consequence of the fact that $0 = \mathrm{d}(X \cdot X) = 2X^\mu \mathrm{d}X_\mu$. From this, it also follows that for every tensor field $H_{\mu_1 \ldots \mu_n}(X)$

$$X^{\mu_i} H_{\mu_1 \ldots \mu_n}(X) = 0 \ . \tag{4.10}$$

With an eye for later computations, it will also be useful to define the covariant derivative in hyperbolic embedding space as the projection of the partial derivative $\frac{\partial}{\partial X^\nu}$ onto dS by using the induced metric $G_{\mu\nu}$ as a projector in the manner

$$\nabla_\mu H_{\nu_1 \ldots \nu_l} = G^\nu_\mu G^{\delta_1}_{\nu_1} \cdots G^{\delta_l}_{\nu_l} \frac{\partial}{\partial X^\nu} H_{\delta_1 \ldots \delta_l} \ , \quad G_{\mu\nu} = \eta_{\mu\nu} - X^\mu X^\nu \ . \tag{4.11}$$

We are now in a position to parameterize points on this hyperbolic embedding space using any of the coordinate patches described in section 4.2. For example, we can parameterize the entire hyperboloid in terms of global dS_4 coordinates as

$$(X^0, X^4, X^1, X^2, X^3) = (\sinh \zeta, n_i \cosh \zeta) \ , \tag{4.12}$$

where $\vec{n}^2 = 1$ parametrizes the unit 3-sphere $S^3 \subset \mathbb{R}^4 \subset \mathbb{R}^{1,4}$. The hyperbolic distance between any two points can be expressed in terms of global dS_4 coordinates as

$$h_{ij} = -\sinh \zeta_i \sinh \zeta_j + n_i \cdot n_j \cosh \zeta_i \cosh \zeta_j \ . \tag{4.13}$$

This expression shows that when the two points differ only in their time coordinate, we have $h_{ij} = \cosh(\zeta_i - \zeta_j)$. If instead both points lie on the $\zeta = 0$ slice, then $h_{ij} = n_i \cdot n_j = \cos(\theta_i - \theta_j)$.

We can also parameterize portions of the hyperboloid using EPP/CPP coordinates

$$(X^0, X^4, X^1, X^2, X^3) = \left(\pm \sinh t + \frac{e^{\pm t}}{2} \vec{x}^2, \cosh t - \frac{e^{\pm t}}{2} \vec{x}^2, \frac{e^{\pm t}}{2} \vec{x} \right) \ , \tag{4.14}$$

where + is for the EPP, which covers the $X^0 + X^4 > 0$ half of the hyperboloid and $-$ is for the CPP covering the other $X^0 + X^4 < 0$ half. It should be emphasized that there is no unique way to choose these coordinate patches within dS space. In the construction above, we align the coordinates with an observer located at the origin, which, to maintain correspondence with global dS space, we take to be at $(X^0, X^4, X^1, X^2, X^3) = (0, 1, 0, 0, 0)$. Accordingly, we choose the embeddings of the EPP/CPP such that their origins coincide with that of the observer (see Figure 4.4). In this configuration, the two patches do not jointly cover the entire dS manifold but rather overlap, and their intersection corresponds to the static patch, which can be parametrized by

$$(X^0, X^4, X^1, X^2, X^3) = \left(\sqrt{1 - r^2} \sinh \tau, \sqrt{1 - r^2} \cosh \tau, r \widehat{\mathbf{n}} \right) \ , \tag{4.15}$$

where now $\widehat{\mathbf{n}}^2 = 1$ parametrizes the unit 2-sphere $\widehat{\mathbf{n}} \in S^2$.

Null Embedding Space

Given that dS_4 can be described as the hypersurface satisfying $\eta_{\mu\nu}X^\mu X^\nu = 1$ in the ambient space $\mathbb{R}^{1,4}$, we can equivalently view it as a projective null cone in $\mathbb{R}^{2,4}$. To make this manifest, let us rewrite the defining equation (4.5) as follows

$$\eta_{\mu\nu}X^\mu X^\nu - 1 = 0\,, \tag{4.16}$$

which can be expressed in the homogeneous form as

$$\eta_{AB}X^A X^B = 0\,, \tag{4.17}$$

where $X^A \in \mathbb{R}^{2,4}$ and one of the additional timelike coordinates is fixed to ± 1 such that

$$X^\mu = (X^0, X^4, X^1, X^2, X^3) \to X^A = (X^0, X^4, \pm 1, X^1, X^2, X^3)\,. \tag{4.18}$$

For later convenience, we relabel the null embedding coordinates as $(X^{-1}, X^4, X^0, X^1, X^2, X^3)$,[2] and we begin with the choice $X^0 = 1$ (we explore the other choice in section 4.2). This corresponds to a specific representative within the projective equivalence class, since the rescaling

$$X^A \to \lambda X^A\,, \qquad \lambda \in \mathbb{R}^+, \tag{4.19}$$

identifies the same point on the hyperboloid. With this choice in hand, all of the parameterizations introduced in section 4.2 carry over directly, with the same replacement applied to each. For instance, the EPP/CPP patches in this representation can be written as

$$(X^{-1}, X^4, X^0, X^1, X^2, X^3) = \left(\pm\sinh t + \frac{e^{\pm t}}{2}x^2, \cosh t - \frac{e^{\pm t}}{2}x^2, 1, \frac{e^{\pm t}}{2}\vec{x}\right)\,, \tag{4.20}$$

while the static patch can be written as

$$(X^{-1}, X^4, X^0, X^1, X^2, X^3) = \left(\sqrt{1-r^2}\sinh\tau, \sqrt{1-r^2}\cosh\tau, 1, r\widehat{\mathbf{n}}\right)\,. \tag{4.21}$$

Our notion of the hyperbolic distance (4.7) now becomes an $SO(2,4)$ invariant distance, which we can define as the *null embedding distance* Z_{ij} between two points $x_i, x_j \in \mathrm{dS}_4$ as follows

$$Z_{ij} \equiv \eta_{AB}X^A(x_i)X^B(x_j) = \eta_{\mu\nu}X^\mu(x_i)X^\nu(x_j) - 1 = h_{ij} - 1\,. \tag{4.22}$$

The tangent space $T_X(\mathrm{dS}_4)$ to a point X can be constructed as

$$T_X(\mathrm{dS}_4) = \{Y \in T_X(\mathbb{R}^{2,4}) : \eta_{AB}X^A Y^B = 0\}/Z - \lambda Z\,, \tag{4.23}$$

[2] We should point that the component X^{-1} should not be confused as the inverse of X^1!

where the orthogonality is a result of $X^2 = 0 \Rightarrow X \cdot \mathrm{d}X = 0$ in hyperbolic embedding space. The additional rescaling comes from the fact that the map $f : \mathbb{R}^{2,4} \to \mathbb{R}^{2,4}$ taking $X \to \lambda X$ is equivalent to the identity map. This map then induces the equality $Z \sim \lambda Z$ on the tangent space.

The advantage of these parameterizations, as we will soon elucidate, is that $\mathbb{R}^{2,4}$ provides the natural setting in which the conformal group acts linearly on dS_4. This same ambient space also furnishes the most convenient framework for describing the conformal action on four-dimensional Minkowski space. In the Minkowski case, this construction is commonly referred to as the embedding space formalism.

Embedding Space: Minkowski Edition

In this section, we briefly review the embedding space formalism (Dirac, 1936) in Minkowski space (for a more detailed discussion please refer to (Kravchuk and Simmons-Duffin, 2018b; Simmons-Duffin, 2023; Costa, Joao Penedones, et al., 2011)), which will set the stage for an analogous dS construction in the subsequent section. When studying a CFT in Minkowski space, there are several motivations for adopting the embedding space formalism. The first is the convenience that the conformal transformations act linearly in the embedding space. In addition, the embedding space and its tangent bundle provide a natural setting for exploring the representation theory of the conformal group. A more immediate motivation, however, is that Minkowski space itself is not closed under conformal transformations. The same is true in the Euclidean case, although there the issue is remedied by adding a single point at infinity, effectively compactifying the space into a sphere. In Lorentzian signature, by contrast, the asymptotic structure is richer as one must distinguish between spacelike, timelike, and null infinities. While spacelike (i^0) and timelike infinities ($i^\pm$) can each be represented by a single point, null infinity ($\mathscr{I}^\pm_{\mathrm{M}}$) requires entire surfaces. The minimal extension of Minkowski space that is closed under the conformal group is its conformal compactification, and the embedding space provides an explicit realization of this construction.

The standard way to embed Minkowski space is to start with the projective null cone in the six-dimensional embedding space $\mathbb{R}^{2,4}$. Let us introduce lightcone coordinates $X^\pm = X^{-1} \pm X^4$ such that the metric on the embedding space $\mathbb{R}^{2,4}$ is

$$X_A X^A = -X^+ X^- - (X^0)^2 + (X^1)^2 + (X^2)^2 + (X^3)^2 \,. \tag{4.24}$$

We can now identify a copy of $\mathbb{R}^{1,3}$ by making the gauge choice $X^+ = 1$, often called the Poincaré section.[3] Any point on the null cone with $X^+ > 0$ then admits a representative in this section. For a point $x^\mu \in \mathbb{R}^{1,3}$, its embedding as a null vector on this Poincaré section defined by $X^+ = 1$ then has the form

$$\text{Patch I}: \quad x^\mu \longrightarrow X^A(x) = (X^+, X^-, X^\mu) = (1, x^2, x^\mu) , \tag{4.25}$$

which is depicted by Patch I in Figure 4.7 (in blue) on the Lorentzian cylinder. Moreover, the induced metric on the Poincaré section is

$$\mathrm{d}X(x) \cdot \mathrm{d}X(x) = -\mathrm{d}t^2 + \mathrm{d}\vec{x}^2 = \mathrm{d}s^2_{\mathbb{R}_{1,3}} . \tag{4.26}$$

Furthermore, the null embedding distance between two points is expressed as

$$Z_{ij} \equiv X(x_i) \cdot X(x_j) = -\frac{1}{2}(x_i - x_j)^2 . \tag{4.27}$$

We can also describe the tangent space as given by (4.23) since Minkowski space is the same projective null cone, just parameterized differently. So given a point $x^\mu \in \mathbb{R}^{1,3}$ and a tangent vector w^μ at that point, we can describe its avatar $W^A(x, w)$ in the embedding space $\mathbb{R}^{2,4}$ as

$$W^A(x, w) = (0, 2w \cdot x, w^\mu) . \tag{4.28}$$

We have so far neglected the points with $X^+ = 0$, which correspond to the spacetime boundary $\mathscr{I}^+_\mathrm{M}$ of Minkowski space. The asymptotic regions can be parameterized by using these points directly. To see this, one can easily verify the fact that the leading term of the embedding vector $X^A(x)$ in taking $t \longrightarrow \infty$ (while keeping the spatial coordinates fixed) approaches $X_{i^+} = (0, -1, 0)$, which represents future timelike infinity i^+. Similarly, spatial infinity i^0 is represented by $X_{i^0} = (0, 1, 0)$, which is the direction obtained by taking $r \longrightarrow \infty$ (at fixed t). To identify $\mathscr{I}^+_\mathrm{M}$, consider any bulk point $x_0 = (t_0, r_0\widehat{\mathbf{n}})$ and a null direction $\bar{z} = (1, \widehat{\mathbf{n}})$, where $\widehat{\mathbf{n}} \in S^2$. Shooting a light-ray off in the $\bar{z}$ direction, we get

$$x(L) = x_0 + L\bar{z} = (t_0, r_0\widehat{\mathbf{n}}) + L\bar{z} = (t_0 + L, (r_0 + L)\widehat{\mathbf{n}}) , \tag{4.29}$$

which can be seen to approach $\mathscr{I}^+_\mathrm{M}$ as $L \longrightarrow \infty$[4]

$$\lim_{L\to\infty} X(x(L)) \longrightarrow L(0, 2\bar{z} \cdot x_0, \bar{z}^\mu) + \mathcal{O}(1) = L(0, 2(r_0 - t_0), 1, \widehat{\mathbf{n}}) + \mathcal{O}(1) . \tag{4.30}$$

[3] This is not to be confused with the Poincaré patches of dS_4 introduced earlier in section 4.2.

[4] One can verify that this approaches past null infinity $\mathscr{I}^-_\mathrm{M}$ if we instead take the limit $L \longrightarrow -\infty$.

Extracting the leading order term above, we obtain the parameterization of points on $\mathscr{I}^+_{\mathrm{M}}$

$$X_{\mathscr{I}^+_{\mathrm{M}}} = (0, 2(r_0 - t_0), 1, \widehat{\mathbf{n}}) \equiv (0, -\alpha, 1, \widehat{\mathbf{n}}) \ , \tag{4.31}$$

where the real parameter $\alpha = 2(t_0 - r_0)$ is twice[5] the retarded time. We see that these limiting points are naturally parameterized by $\mathbb{R} \times S^2$, as is expected for $\mathscr{I}^+_{\mathrm{M}}$.

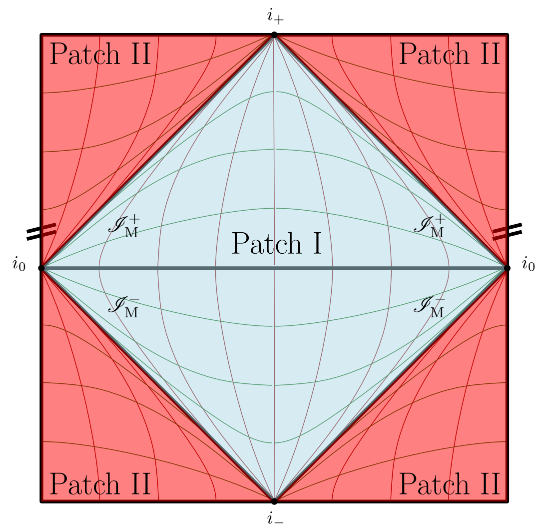

Figure 4.7: Two neighboring Minkowski patches on the Lorentzian cylinder shown in two dimensions, where their embedding coordinates differ by $X^+ = \pm 1$. From the perspective of Patch I, the surface $X^+ = 0$ coincides with $\mathscr{I}^+_{\mathrm{M}}$ with the spatial infinity $X_{i^0} = (0, 1, 0)$ and timelike infinity $X_{i^+} = (0, -1, 0)$ as its end points. The full Lorentzian cylinder is tiled by an infinite number of such Minkowski patches.

However, as we pass through $X^+ = 0$, we now reach the region with $X^+ < 0$, corresponding to points that cannot be connected to our previous Poincaré section by any positive rescaling. This defines a second copy of Minkowski space obtained by now choosing the section $X^+ = -1$, which we label as Patch II on the cylinder in Figure 4.7 (in red)

$$\text{Patch II}: \quad x^\mu \to X^A(x) = (X^+, X^-, X^\mu) = (-1, -x^2, -x^\mu) \ . \tag{4.32}$$

In fact, each point in Patch I can be mapped to a distinct point in Patch II through the transformation $X \to \mathcal{T} X = -X$. The transformation $\mathcal{T}$ is defined such that for a Minkowski point p, the point $\mathcal{T} p$ is obtained by shooting light rays in all possible future directions from p and finding the first point where they converge in the subsequent Minkowski patch. Together, these two patches can be viewed as

[5] This factor of 2 is unavoidable, since the metric carries an overall factor of $1/2$. There is no particularly good convention for where it should appear, so we simply adopt this choice.

neighboring Minkowski patches on the Lorentzian cylinder, the universal cover of the conformal compactification of Minkowski space. In other words, they live on the spacetime on which $\widetilde{SO}(2,4)$, the universal cover of the Lorentzian conformal group $SO(2,4)$, acts naturally. In fact, the full Lorentzian cylinder is tiled by an infinite number of such Minkowski patches.

Tiling the Lorentzian Cylinder with dS

One of the primary ways in which we will use the null embedding space is to relate different patches of dS space to regions of Minkowski space, allowing us to leverage results obtained in flat space within the dS context. The most useful of these relations is the one between the EPP/CPP and Minkowski space, which we alluded to above. Let us first start with the CPP metric (4.2) in the null embedding space, which was shown in (4.20) to take the form

$$X^A_{\text{CPP}} = (X^{-1}, X^4, X^0, X^1, X^2, X^3) = \left(-\sinh t + \frac{e^{-t}}{2}x^2, \cosh t - \frac{e^{-t}}{2}x^2, 1, \frac{e^{-t}}{2}\vec{x}\right) . \tag{4.33}$$

Making the choice $e^t = +\eta$, the metric becomes (4.3), which is simply the Minkowski metric $\mathbb{R}^{1,3}$ with Weyl factor η^{-1}. If we now examine the parameterization of the CPP in the null embedding space and introduce lightcone coordinates, as we did for Minkowski space, we find

$$(X^+, X^-, X^0, X^1, X^2, X^3) = \left(\frac{1}{\eta}, \frac{-\eta^2 + \vec{x}^2}{\eta}, 1, \frac{\vec{x}}{\eta}\right) = \frac{1}{\eta}X^A(x) \equiv X^A_{\text{CPP}}(\eta, \vec{x}) . \tag{4.34}$$

We see that the above is equivalent to the parameterization of a point $x^\mu \in \mathbb{R}^{1,3}$ (4.25) up to an overall factor of the Weyl factor η^{-1}. Also, the induced metric on the Poincaré section is the CPP metric

$$\mathrm{d}X_{\text{CPP}}(\eta, \vec{x}) \cdot \mathrm{d}X_{\text{CPP}}(\eta, \vec{x}) = \frac{-\mathrm{d}\eta^2 + \mathrm{d}\vec{x}^2}{\eta^2} , \tag{4.35}$$

along with the fact that the null embedding distance

$$Z_{ij} \equiv X_{\text{CPP}}(\eta_i, \vec{x}_i) \cdot X_{\text{CPP}}(\eta_j, \vec{x}_j) = -\frac{-(\eta_i - \eta_j)^2 + (\vec{x}_i - \vec{x}_j)^2}{2\eta_i\eta_j} , \tag{4.36}$$

is the same as the Minkowski result (4.27) up to overall Weyl factors, as expected. We can also now parameterize tangent space vectors, as we did in Minkowski space. At a point $x = (\eta, \vec{x})$, taking a tangent vector w^μ along that point is the same as (4.28)

$$W(x, w) = (0, 2w \cdot x, w^\mu) . \tag{4.37}$$

Now let us again consider shooting light-rays from a generic point $x_0 = (\eta_0, r_0\widehat{\mathbf{n}})$ in the bulk of the CPP coordinate patch directed along $\bar{z} = (1, \widehat{\mathbf{n}})$ toward the future CPP horizon $\mathscr{H}^+$. This null line is parameterized by

$$x(L) = (\eta_0, r_0\widehat{\mathbf{n}}) + L\bar{z} = (\eta_0 + L, (r_0 + L)\widehat{\mathbf{n}}) \ , \tag{4.38}$$

which in the null embedding space is described by

$$X_{\text{CPP}}(x(L)) = \left(\frac{1}{\eta_0 + L}, \frac{-(\eta_0 + L)^2 + (r_0 + L)^2}{\eta_0 + L}, 1, \frac{(r_0 + L)\widehat{\mathbf{n}}}{\eta_0 + L}\right) \ . \tag{4.39}$$

On taking the limit $L \to \infty$, we get

$$\lim_{L\to\infty} X_{\text{CPP}}(x(L)) = (0, 2x_0 \cdot \bar{z}, \bar{z}) = (0, 2(r_0 - \eta_0), 1, \widehat{\mathbf{n}}) \equiv (0, -\alpha, 1, \widehat{\mathbf{n}}) \ . \tag{4.40}$$

As a result, we can parameterize a point on the CPP horizon $\mathscr{H}^+$ by $\alpha \in \mathbb{R}$ and a unit vector $\widehat{\mathbf{n}} \in S^2$. Putting a minus sign in front of α ensures that taking the limit $r_0 \to \infty$ coincides with $\alpha \to -\infty$. This means that when we parameterize the points on the CPP horizon $\mathscr{H}^+$ as

$$X_{\mathscr{H}^+}(\alpha, \widehat{\mathbf{n}}) \equiv (0, -\alpha, 1, \widehat{\mathbf{n}}) \ , \tag{4.41}$$

α parametrizes a null line labeled by $\widehat{\mathbf{n}}$ with $\alpha = -\infty$ as the beginning of the null line. For now, notice that if we map the CPP to Minkowski as suggested by (4.3), then the CPP horizon $\mathscr{H}^+$ maps to $\mathscr{I}^+_{\text{M}}$ of Minkowski space.

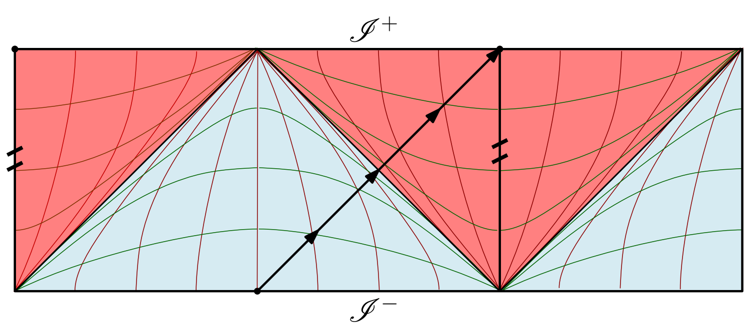

Figure 4.8: A null line going from the origin of one CPP (in blue), to that of a neighboring EPP (in red) on the Lorentzian cylinder. The two points in question are related by the transformation $X \to \mathcal{T}X = -X$.

However, unlike $\mathscr{I}^+_{\text{M}}$ of Minkowski space, as we approach the CPP horizon $\mathscr{H}^+$ ($\eta \to \infty$) we do not reach a spacetime boundary; this surface is a coordinate horizon, and one crosses smoothly into the EPP. If our null line $x(L)$ starts from the spatial origin in the CPP at $\eta = 0$, then it must end in the EPP at its spatial origin at its

$\eta = 0$, as shown in Figure 4.8. To see this, consider a curve as given by (4.38) and starting at $(\eta_0, r_0) = (0, 0)$

$$\left(\frac{1}{L}, 0, 1, \widehat{\mathbf{n}}\right) \equiv \left(-\beta, 0, 1, \widehat{\mathbf{n}}\right) \ , \tag{4.42}$$

with $\beta = -\frac{1}{L}$. Then, in the projective sense, as $\beta \to -\infty$ the curve approaches $(1, 0, 0, \vec{0})$, which is the origin of the CPP, while as $\beta = +\infty$ it approaches $(-1, 0, 0, \vec{0})$, which coincides with the origin of the EPP.

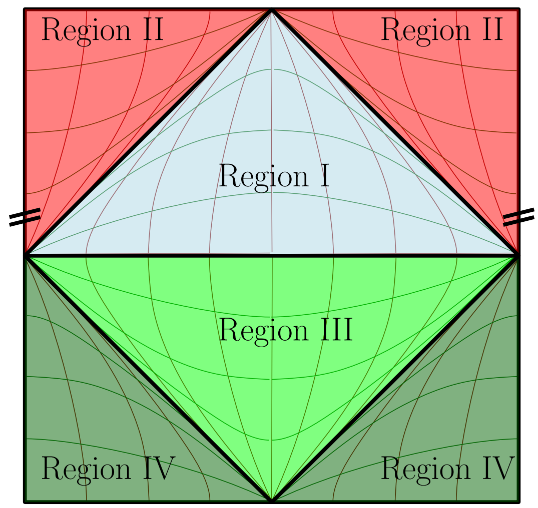

Figure 4.9: Two neighboring dS embeddings, and hence four associated Poincaré patches on the Lorentzian cylinder. Regions I and II are the CPP and EPP, respectively, of the dS patch labeled by $X^0 = +1$. Regions III and IV are the EPP and CPP, respectively, of the neighboring dS patch labeled by $X^0 = -1$. As in the Minkowski case, the full Lorentzian cylinder is tiled by an infinite sequence of dS embeddings, or equivalently by neighboring EPP/CPP pairs.

We can now use this more generally to tile the Lorentzian cylinder with dS embeddings, each one built from a corresponding pair of CPP and EPP regions. Let us begin with the CPP region already defined in (4.34). On the Lorentzian cylinder, this maps to the upper triangular region of Minkowski Patch I in Figure 4.7, which was labeled by $X^+ = +1$. On the Lorentzian cylinder tiled with copies of dS shown in Figure 4.9, we call this Region I of the dS embedding labeled by $X^0 = +1$

$$\text{Region I}: \quad X_{\text{CPP}} = \left(\frac{1}{\eta},\ \frac{-\eta^2 + \vec{x}^2}{\eta},\ 1,\ \frac{\vec{x}}{\eta}\right) = \frac{1}{\eta}\left(1,\ -\eta^2 + \vec{x}^2\ \eta,\ \vec{x}\right) \ , \quad \eta = e^t > 0\,.$$

Next, we move to the neighboring EPP region of the same dS embedding ($X^0 = +1$). We know that the conformal time η assumes negative values $\eta = -e^{-t}$ and on the Lorentzian cylinder maps to the (upper) Minkowski Patch II of Figure 4.7, which was labeled by $X^+ = -1$. We label this EPP region as Region II of the dS embedding labeled by $X^0 = +1$

$$\text{Region II}: \quad X_{\text{EPP}} = \left(\frac{1}{\eta},\ \frac{-\eta^2+\vec{x}^2}{\eta},\ 1,\ \frac{\vec{x}}{\eta}\right) = \frac{1}{|\eta|}\left(-1,\ \eta^2-\vec{x}^2,\ -\eta,\ -\vec{x}\right)\ ,\ \eta = -e^{-t} < 0\ ,$$

where we have factored out a positive Weyl factor since we need $X^+ = -1$. These two regions complete the tiling of the original dS embedding given by $X^0 = +1$.

Equivalently, if we describe the CPP of Region I with $X^+ = 1$, then the neighboring EPP is in the neighboring Region II with $X^+ = -1$ obtained by $X \to \mathcal{T}X = -X$.

Let us now continue our original CPP (Region I of Figure 4.9) to a new dS embedding now labeled by $X^0 = -1$. In this region, $\eta = -e^{-t}$, and on the Lorentzian cylinder maps to the lower triangular region of Minkowski Patch I of Figure 4.7, which was labeled by $X^+ = +1$. This defines a new EPP region of a new dS embedding, which we call Region III on the Lorentzian cylinder

$$\text{Region III}: \quad X_{\text{EPP}} = \left(-\frac{1}{\eta},\ \frac{\eta^2-\vec{x}^2}{\eta},\ -1,\ \frac{\vec{x}}{\eta}\right) = \frac{1}{|\eta|}\left(1,\ -\eta^2+\vec{x}^2,\ \eta,\ \vec{x}\right)\quad ,\quad \eta = -e^{-t} < 0\ .$$

We can now continue the above EPP to its neighboring CPP, which defines our final region on the cylinder. The conformal time in this region is positive $\eta = e^t$ and on the Lorentzian cylinder maps to the (lower) Minkowski Patch II of Figure 4.7, which was labeled by $X^+ = -1$. This defines the CPP region of the new dS embedding ($X^0 = -1$), which we call Region IV on the Lorentzian cylinder

$$\text{Region IV}: \quad X_{\text{CPP}} = \left(-\frac{1}{\eta},\ \frac{\eta^2-\vec{x}^2}{\eta},\ -1,\ \frac{\vec{x}}{\eta}\right) = \frac{1}{\eta}\left(-1,\ \eta^2-\vec{x}^2,\ -\eta,\ -\vec{x}\right)\quad ,\quad \eta = e^{t} > 0\ .$$

In summary, both Minkowski space and dS space admit conformal completions on the Lorentz-ian cylinder, described by the projective null cone in $\mathbb{R}^{2,4}$. For Minkowski space, each embedding is specified by a choice of X^+, while for dS space it is specified by a choice of X^0. The CPP of dS space is conformally related to the $t \geq 0$ half of Minkowski space, while the EPP is related to the $t \leq 0$ half. For example, the Region I CPP of the first dS embedding is conformally related to the $t \geq 0$ half of Minkowski space Patch I, while the Region III EPP of the second dS embedding is related to the $t \leq 0$ half of the same Minkowski Patch I. Thus, a complete embedding of dS overlaps two neighboring Minkowski embeddings, and, conversely, a complete embedding of Minkowski space overlaps two neighboring dS embeddings.

4.3 Minkowski light-ray operators: a quick primer

Light-ray operators arise naturally in many contexts in Minkowski space (Moult and Zhu, 2025), and many features have been generalized to spaces with Minkowski-like asymptotics (Herrmann, Kologlu, and Moult, 2024; Gonzo and Pokraka, 2021). Each of these constructions has its own generalizations, but perhaps the simplest and most instructive of these operators is the null integral of the stress tensor. In this section we will focus on this operator, review its definition, and briefly discuss its importance from various perspectives; much of this can be found in (Simmons-Duffin, 2023; Moult and Zhu, 2025; Hofman and J. Maldacena, 2008).

The energy flux operator. Let us begin with the most physical interpretation of a light-ray operator that one can realize in a flat-space QFT, the energy flux operator $\mathcal{E}(\widehat{\mathbf{n}})$ (Sveshnikov and Tkachov, 1996; Korchemsky and Sterman, 1999). $\mathcal{E}(\widehat{\mathbf{n}})$ measures the flux of energy through a point $\widehat{\mathbf{n}} \in S^2$, the celestial sphere, and can be expressed as the time integral of the stress tensor in the limit of large radius as

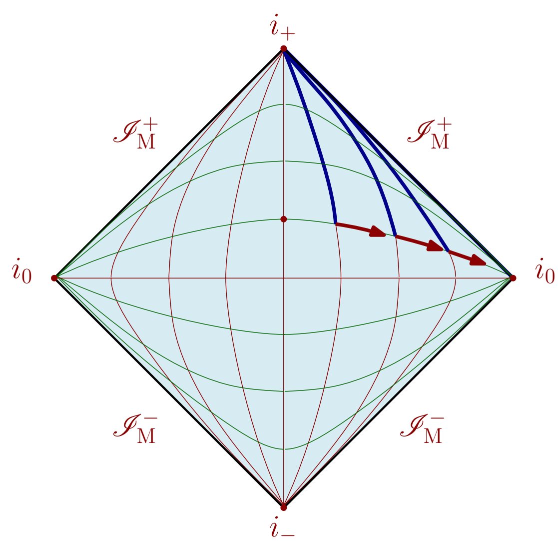

Figure 4.10: The energy flux operator $\mathcal{E}(\widehat{\mathbf{n}})$ in Minkowski space shown as a limiting procedure in two dimensions. A calorimeter (i.e. a stress-tensor insertion) placed at fixed radial distance r, integrated over all time, and then pushed out to $\mathscr{I}_{\mathrm{M}}^+$ as defined by the integral (4.43).

$$\mathcal{E}(\widehat{\mathbf{n}}) = \lim_{r\to\infty} r^2 \int_0^\infty \mathrm{d}t\, T_{i\nu}(t, r\widehat{\mathbf{n}})\, \widehat{\mathbf{n}}^i\, \xi^\nu \,, \tag{4.43}$$

where $\xi^\mu = (1, 0, 0, 0)$ is the timelike Killing vector, which becomes null at $\mathscr{I}_{\mathrm{M}}^+$. Thus, the operator $\mathcal{E}(\widehat{\mathbf{n}})$ can be thought of as placing a calorimeter (i.e. a stress tensor insertion) at some finite radial distance r from the spatial origin, with the interpretation that $r^2 T^0_i$ measures the local energy flux in the spatial $\widehat{\mathbf{n}}$ direction. Integrating over time collects all the radiation deposited at the point $\widehat{\mathbf{n}}$ on the celestial sphere. Finally, taking the limit of large radius (the factor r^2 ensures finiteness of the large radius limit $r \to \infty$), one pushes the calorimeter far away from the center of Minkowski space. As seen on the Penrose diagram in Figure 4.10, this ensures that the calorimeter asymptotes to future null infinity $\mathscr{I}^+_{\mathrm{M}}$.

Let us now try to express the integral (4.43) in a more covariant language utilizing the Minkowski embedding space $\mathbb{R}^{2,4}$ (section 4.2). The process of taking the large radius limit in (4.43) is a bit subtle, and it is convenient to introduce the null tangent vectors

$$z^\mu = (1, -\widehat{\mathbf{n}}) \,, \qquad \bar{z}^\mu = (1, \widehat{\mathbf{n}}) \,, \tag{4.44}$$

such that we can realize $\frac{1}{4}(z^\mu z^\nu - \bar{z}^\mu \bar{z}^\nu) T_{\mu\nu} = \widehat{\mathbf{n}}^i T^0_i$, which is the right-hand side of (4.43). Now considering the starting point of the integral to be $X^A(x) = (1, x^2, x^\mu)$, if we first take the $r \to \infty$ limit, we end up at $X_{i_0} = (0, 1, 0)$ and lose any time dependence. Instead, we should use retarded time $\alpha = 2(t - r)$ and take the $r \to \infty$ limit, while keeping α fixed. In the embedding space, if we express our null tangent space vectors $z, \bar{z}$ as suggested by (4.28), we can see that $Z(z)$ grows linearly in r in the large r limit, while $\overline{Z}(\bar{z})$ does not. We can therefore drop the $\bar{z}$ terms in the large r limit, which means that the integral is expressed as

$$\mathcal{E}(\widehat{\mathbf{n}}) = \lim_{r \to \infty} \frac{r^2}{8} \int_{-2r}^{\infty} \mathrm{d}\alpha \, Z^A Z^B T_{AB} \left(X \left(\frac{\alpha}{2} + r, r\widehat{\mathbf{n}} \right) \right) \,. \tag{4.45}$$

Equipped with this definition of energy flux operators, the natural observables to study are its correlation functions of the form

$$\langle \mathcal{E}(\widehat{\mathbf{n}}_1) \mathcal{E}(\widehat{\mathbf{n}}_2) \cdots \mathcal{E}(\widehat{\mathbf{n}}_n) \rangle \,, \tag{4.46}$$

which probe the angular distribution of energy and encode, for example, the jet structure produced in a given scattering event. We can compute this in a generic state $|\Psi\rangle$, created for example by local scalar ϕ operators by computing

$$\langle \Psi | \mathcal{E}(\widehat{\mathbf{n}}) | \Psi \rangle = \int \mathrm{d}^4 x_1 \mathrm{d}^4 x_2 \Psi^*(x_1) \Psi(x_2) \, \langle 0 | \phi^*(x_1) \mathcal{E}(\widehat{\mathbf{n}}) \phi(x_2) | 0 \rangle \,. \tag{4.47}$$

One can naturally generalize this to other integrals of measurable quantities, for example, one can consider higher moments of the energy deposited at a point in the celestial sphere, see (Simmons-Duffin, 2023) for example.

Angular contribution to the Hamiltonian. There is a complementary interpretation of $\mathcal{E}(\widehat{\mathbf{n}})$: it represents the angular distribution of a conserved charge. To see this, note that integrating $\mathcal{E}(\widehat{\mathbf{n}})$ over the celestial sphere at infinity, the $S^2 \subset \mathscr{I}^+_{\mathrm{M}}$, amounts to integrating the $T_{\mu\nu}\xi^\mu$ component of the stress tensor across a codimension-one surface at future null infinity $\mathscr{I}^+_{\mathrm{M}}$. This reproduces the total Hamiltonian

$$H = \int_{S^2} \mathrm{d}\Omega_2\, \mathcal{E}(\widehat{\mathbf{n}}) = \int_{\mathscr{I}^+_{\mathrm{M}}} \mathrm{d}\sigma^\nu\, T_{\mu\nu}\xi^\mu\,, \tag{4.48}$$

where $\mathrm{d}\Omega_2$ is the volume form on the 2-sphere, and after including the $\mathrm{d}\alpha$ measure along the null direction, $\mathrm{d}\sigma^\nu$ becomes the natural volume form on $\mathscr{I}^+_{\mathrm{M}}$. More generally, replacing $T^\mu_{\ \nu}\xi^\nu$ with an arbitrary conserved current J^μ defines analogous charge measuring operators, and integrating these over S^2 yields the corresponding conserved charge (Hofman and J. Maldacena, 2008).

The ANEC operator. Another important light-ray operator is the averaged null energy operator or simply, the ANEC[6] operator. The construction begins by choosing any complete achronal null geodesic γ in an arbitrary curved spacetime and integrating the stress tensor along its null direction. In Minkowski space, this takes the form

$$\mathcal{A}_{\mathrm{M}} = \int_\gamma \mathrm{d}\alpha\, T_{\mu\nu}z^\mu z^\nu\,, \tag{4.49}$$

where z^μ is the tangent to the curve γ.

The light transform. In CFTs there is another well-studied class of light-ray operators defined by a conformally invariant integral transform called the *light transform* (Kravchuk and Simmons-Duffin, 2018b). The light transform $\mathbf{L}$ maps any local primary operator of dimension and spin (Δ, J) to a corresponding nonlocal operator with dimension and spin $(1-J, 1-\Delta)$ by integrating it over a complete, affine, null geodesic. Consider a local operator O that lives in a representation labeled by (Δ, J). Then, given a null ray in the z direction passing through a point y, we can define its light transform as

$$\mathbf{L}[O](x,z) = \int_{-\infty}^{\infty} \mathrm{d}\alpha\, z^{\mu_1}\cdots z^{\mu_J} O_{\mu_1\cdots\mu_J}(y+\alpha z)\,, \tag{4.50}$$

[6]Of course, the ANEC operator is a somewhat unfortunate name, since it should be the ANE operator, or the operator that gives rise to the ANEC inequality. However, the ANEC operator has a good ring to it, and everyone else seems to do it, so why should we deprive ourselves.

where x is the point at the beginning of the null line, i.e. $x = y - \infty z$. In the case of the spin-2 stress tensor, the corresponding light transform can be written as

$$\mathbf{L}[T](x,z) = \int_{-\infty}^{\infty} \mathrm{d}\alpha \;\; z^\mu z^\nu T_{\mu\nu}(y + \alpha z) \; . \tag{4.51}$$

This is easier to interpret on the Lorentzian cylinder, where we can begin the null line in one Minkowski patch and end it in another, such that x is a genuine point in the interior of Minkowski space. Letting X be the corresponding point in the embedding space and Z the embedding space image of the null vector z, we can denote a spinning operator as $\mathcal{O}(X,Z) \equiv Z^A \cdots Z^B \mathcal{O}_{A\cdots B}(X)$. It was shown in Kravchuk and Simmons-Duffin, 2018b that the light transform of $\mathcal{O}$ can also be expressed compactly as

$$\mathbf{L}[\mathcal{O}](X,Z) = \int_{-\infty}^{\infty} \mathrm{d}\alpha \, \mathcal{O}\left(Z - \alpha X, -X\right) \; . \tag{4.52}$$

Following this, the light transform of the stress tensor is simply expressed as

$$\mathbf{L}[T](X,Z) = \int_{-\infty}^{\infty} \mathrm{d}\alpha \, T\left(Z - \alpha X, -X\right) \; . \tag{4.53}$$

Given two such light transformed local operators, their OPE contains more general light-ray operators that are not themselves obtained as the light transform of any local primary (Kologlu et al., 2021). Among these, the light transform of the stress tensor plays a distinguished role, since the stress tensor is universally present in every CFT. In holographic CFTs this operator acquires an additional interpretation: its bulk dual corresponds to a gravitational shockwave propagating along the associated null direction (Kologlu et al., 2020).

We have ostensibly considered four realizations of the simplest light-ray operator: i) the energy flux operator (4.45), ii) the angular contribution to the Hamiltonian (4.48), iii) the ANEC operator (4.49), and iv) the light transform of the stress tensor (4.51). In Minkowski space, the first two constructions are always represented by the same operator, but they do not in general coincide with the ANEC operator $\mathcal{A}_{\mathrm{M}}$ or with the light transform of the stress tensor $\mathbf{L}[T]$, since the latter are defined along any complete null geodesic, whereas the energy flux operator $\mathcal{E}(\widehat{\mathbf{n}})$ is not. However, when all of them are placed on $\mathscr{I}^+_{\mathrm{M}}$, the four constructions agree. Moreover, in a conformal theory $\mathscr{I}^+_{\mathrm{M}}$ is no longer a distinguished null surface, and in that case these four notions coincide for any complete null line. We can see this explicitly as follows. Let us begin with the light transform of the stress tensor given by (4.51), which is clearly equivalent to the ANEC operator given by (4.49), since the line

$y + \alpha z$ for null z, is an affine parameterized complete null geodesic. Now, to show that the energy flux operator $\mathcal{E}(\widehat{\mathbf{n}})$ is the light transform of the stress tensor $\mathbf{L}[T]$ on $\mathscr{I}^+_{\mathrm{M}}$ takes only a few more steps. In the large r limit (keeping α fixed), the leading term in X goes as

$$X \simeq r(0, -\alpha, \bar{z}) = r(Z_{i_0} - \alpha X_{i_0}) , \tag{4.54}$$

where $X_{i_0} = (0, 1, 0)$ and $Z_{i_0} = (0, 0, \bar{z})$. We can write the leading term of the null tangent vector Z as

$$Z \simeq -4r(0, 1, 0) = -4rX_{i_0} . \tag{4.55}$$

Substituting these into the definition (4.45) of the energy flux operator $\mathcal{E}(\widehat{\mathbf{n}})$ and taking the large r limit, we obtain

$$\begin{aligned}
\mathcal{E}(\widehat{\mathbf{n}}) &= \frac{1}{8} \lim_{r\to\infty} r^2 \int_{-2r}^{\infty} \mathrm{d}\alpha \; T(r(Z_{i_0} - \alpha X_{i_0}), -4rX_{i_0}) \\
&= \frac{1}{8} \lim_{r\to\infty} r^2 \int_{-2r}^{\infty} \mathrm{d}\alpha \; r^{-4}(4r)^2 T(Z_{i_0} - \alpha X_{i_0}, -X_{i_0}) \\
&= 2 \int_{-\infty}^{\infty} \mathrm{d}\alpha \; T(Z_{i_0} - \alpha X_{i_0}, -X_{i_0}) = 2\mathbf{L}[T](X_{i_0}, Z_{i_0}) ,
\end{aligned} \tag{4.56}$$

where in the first line we used the homogeneity in X and Z. So we can see that (up to the overall factor of 2), the energy flux operator $\mathcal{E}(\widehat{\mathbf{n}})$ is the light transform of the stress tensor $\mathbf{L}[T]$, with the integral starting at X_{i_0} and going along $\mathscr{I}^+_{\mathrm{M}}$. Therefore, the ANEC operator $\mathcal{A}_{\mathrm{M}}$, the light transform of the stress tensor $\mathbf{L}[T]$, and the energy flux operator $\mathcal{E}(\widehat{\mathbf{n}})$ are in fact the same operator when defined on $\mathscr{I}^+_{\mathrm{M}}$.

In summary, the simplest light-ray operator given by the null integral of the stress tensor along a complete null line in $\mathscr{I}^+_{\mathrm{M}}$ is simultaneously an energy flux operator, an angular contribution to the Hamiltonian, the ANEC operator, and, in conformal theories, the light transform of the stress tensor. Each of these perspectives suggests its own natural generalizations. From the conformal viewpoint one is led to consider arbitrary light transformed operators and the broader class of light-ray operators they generate, while from the detector viewpoint one may generalize to other conserved currents or to higher moments of their fluxes. In all cases, the energy flux operator provides the basic and most physical example, and its various interpretations open different doors to broader classes of similar operators.

4.4 De Sitter light-ray operators

We now turn towards the main question of our paper: what are the analogs of the energy flux operator as one passes from Minkowski to dS space? We will begin in section 4.4 by setting up our stage, which will be free scalar field theory in dS_4, and then note the specific properties of the conformal mass case. After appropriately defining the stress tensor, we will classify the four inequivalent generalizations of the energy flux operator in section 4.4. We will end in section 4.4 by explicitly computing matrix elements of the various detectors in the conformal theory.

Setup: scalar field theory in $\mathbf{dS}_4$

We consider a free scalar field theory in dS_4 described by the action

$$S = -\frac{1}{2}\int \mathrm{d}^4x\sqrt{-g}\left(g^{\mu\nu}\nabla_\mu\phi\nabla_\nu\phi + m^2\phi^2 + \xi R\phi^2\right) . \tag{4.57}$$

Working in dS_4, we will set $R = 12$ (in terms of the unit Hubble radius) and find it convenient to define an effective mass term μ^2 of the form

$$\mu^2 \equiv m^2 + 12\xi . \tag{4.58}$$

Now, the two-point Wightman function $\langle\phi(X)\phi(Y)\rangle$ in the dS invariant vacuum satisfies a hypergeometric differential equation, which is best expressed in the hyperbolic embedding space $\mathbb{R}^{1,4}$. Consequently, it is a function of solely the $SO(1,4)$ invariant hyperbolic distance $h = X\cdot Y$ defined in (4.7). Therefore, the two-point Wightman function is expressed simply as $\langle\phi(X)\phi(Y)\rangle = G(X\cdot Y) \equiv G(h)$, and it is defined by the differential equation

$$(\Box - \mu^2)G(h) = (1-h^2)G''(h) - 4hG'(h) - \mu^2 G(h) = 0 . \tag{4.59}$$

This has the solution

$$G(h) = \frac{\Gamma(\Delta)\Gamma(\bar{\Delta})}{(4\pi)^2\Gamma(2)}\,{}_2F_1\left(\Delta,\bar{\Delta},2;\frac{1+h}{2}\right) , \tag{4.60}$$

where the parameters $\Delta, \bar{\Delta}$ are defined as

$$\Delta = \frac{3}{2} + i\nu , \qquad \bar{\Delta} = \frac{3}{2} - i\nu , \qquad \nu = \sqrt{\mu^2 - \left(\frac{3}{2}\right)^2} . \tag{4.61}$$

Now, note that generically the hypergeometric function ${}_2F_1(a,b,c;(1+h)/2)$ can have singularities when $h = \{-1, 1, \infty\}$. Recalling relation (4.8), these singularities correspond to the following limits of the hyperbolic distance h (depicted also in Figure 4.11):

- $h = 1$: This is the lightcone singularity and occurs when the two points are coincident (or equivalently, the geodesic distance between them vanishes), i.e. $X\cdot Y = 1$.

- $h = -1$: This singularity corresponds to $X \cdot Y = -1$, which is the antipodal configuration on the sphere, meaning that the two points are maximally separated while still connected by a geodesic.

- $h \to \infty$: This singularity simply corresponds to the two points being asymptotically separated in a timelike direction.

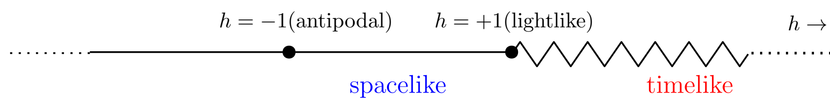

Figure 4.11: The three singularities of the ${}_2F_1$ function occur at $h = +1$ (lightlike separation), $h = -1$ (antipodal separation), and $h = +\infty$. The solid line indicates spacelike separated points with $h < 1$, while the zigzag line indicates timelike separated points with $h > 1$.

However, we choose[7] our solution $G(h)$ such that it only has singularities at $h = 1$ and $h = \infty$. The parameters[8] $\Delta, \bar{\Delta}$ are known as the scaling dimensions and they label the irreducible representations of the dS isometry group $SO(1,4)$. There are in general three classes of irreducible representations of $SO(1,4)$: i) the *principal series* corresponding to $\mu^2 > (3/2)^2$ for which $\Delta \in \mathbb{C}$, ii) the *complementary series* corresponding to $0 < \mu^2 < (3/2)^2$ for which $\Delta \in \mathbb{R}$ (but not integer valued), and iii) the *exceptional/discrete series* for which $\Delta \in \mathbb{N}$ assumes non-negative integer values (for a detailed introduction please refer to (Sun, 2024)).

Conformally coupled scalars

The label Δ is similar, but not identical, to the familiar m^2 in Minkowski space. The Wightman function exhibits different behavior for these distinct irreducible representations. In general, $G(h)$ develops a branch cut between its singularities at $h = 1$ and $h = \infty$. However, the analytic structure changes drastically in the special case of $\mu^2 = 2$ (or $\Delta = 1$), which corresponds to the *conformally coupled scalar*. In this case, the branch cut disappears and the Wightman two-point function is given by

$$G(h) = \frac{\Gamma(1)\Gamma(2)}{(4\pi)^2\Gamma(2)}\, {}_2F_1\left(1, 2, 2, \frac{1+h}{2}\right) = \frac{1}{(4\pi)^2}\frac{2}{1-h}\,. \tag{4.62}$$

[7] There is another class of solutions obtained by $h \to -h$, which arises from the $h \to -h$ symmetry of our hypergeometric differential equation (4.59). We do not take this as our solution since it does not have the lightcone singularity, but rather has its singularity at the antipode. For a more detailed discussion on this point, we refer the reader to (Einhorn and Larsen, 2003).

[8] In dS_4, they are related to one another by the shadow transform $\bar{\Delta} = 3 - \Delta$, as is evident from (4.61).

So far in this section, our discussion has been restricted to the usage of the hyperbolic embedding space $\mathbb{R}^{1,4}$. However, it will be more convenient to use the null embedding space $\mathbb{R}^{2,4}$. Recall from expression (4.22) that the null embedding distance Z is related to the hyperbolic distance h by $h = Z + 1$, with which the Wightman two-point function becomes

$$G(Z) = \frac{\Gamma(1)\Gamma(2)}{(4\pi)^2\Gamma(2)}\, {}_2F_1\left(1, 2, 2, \frac{2+Z}{2}\right) = -\frac{1}{(4\pi)^2}\frac{2}{Z} \, . \tag{4.63}$$

Using the expression (4.36), this becomes

$$G(Z) \equiv G(X_1, X_2) = \frac{1}{(4\pi)^2}\frac{4\eta_1\eta_2}{-(\eta_1-\eta_2)^2 + (\vec{x}_1 - \vec{x}_2)^2} \, , \tag{4.64}$$

which up to the Weyl factors $\eta_1\eta_2$, is the same as in flat space. In fact, since the Poincaré patches (EPP and CPP) of dS are Weyl equivalent to Minkowski space, as established in section 4.2, any correlation function of local CFT operators in dS space can be obtained from its flat-space counterpart by an appropriate Weyl rescaling via the Lorentzian cylinder.

The stress tensor

We now move to the computation of the stress tensor for free scalar fields in dS from the action (4.57). The classical stress tensor, defined by the relation

$$T_{\mu\nu}(x) = \frac{-2}{\sqrt{g}}\frac{\delta S}{\delta g^{\mu\nu}} \, , \tag{4.65}$$

is quadratic in the field and its derivatives, and can therefore be seen as the coincident point limit of a differential operator Θ acting on the fields at separated points. The quantum operator will be the same with the field replaced with operators, possibly up to corrections due to regularization. That is to say, we can express the classical stress tensor as

$$T_{\mu\nu}(x) = \lim_{y\to x} \Theta_{\mu\nu}(x,y)\phi(x)\phi(y) \, , \tag{4.66}$$

where the differential operator Θ takes the form

$$\Theta_{\mu\nu}(x,y) = (1-2\xi)\nabla_{\mu,x}\nabla_{\nu,y} - 2\xi\nabla_{\mu,y}\nabla_{\nu,y} + g_{\mu\nu}\left[\left(2\xi - \tfrac{1}{2}\right)\nabla_{\rho,x}\nabla^{\rho,y} + 2\xi\Box_x - \left(\tfrac{m^2}{2} + 3\xi\right)\right]. \tag{4.67}$$

In the quantum theory, one can just replace the field ϕ with the operator $\widehat{\phi}$ and define the stress tensor at an operational level by the limit (4.66). As it turns out, in the conformal case this operator is already finite. If the stress tensor is regularized using dimensional regularization, the resulting expression for the stress tensor is (the details of this derivation can be found in Appendix 4.A)

$$T_{\mu\nu}(x) = \lim_{\epsilon\to 0}\left(\lim_{y\to x}\Theta_{\mu\nu}(x,y)\phi(x)\phi(y) - \frac{1}{\epsilon}\frac{g_{\mu\nu}(x)}{32\pi^2}m^2(m^2+12\xi-2)\right). \tag{4.68}$$

The $1/\epsilon$ term vanishes both in the massless case, $m^2 = 0$, and in the conformal case, $m^2 + 12\xi \equiv \mu^2 = 2$. The operator is therefore finite in the case of conformally coupled scalars.

Classification of de Sitter light-ray operators

We now turn our attention to the construction of light-ray operators in dS space. First, we note that there is no obvious way to generalize the construction of light-ray operators in Minkowski space (discussed in section 4.3) straightforwardly to dS space. The kinematic configuration suggested by the detector picture in Minkowski space is clearly meaningless from the perspective of global dS_d space, as its spatial slices are $(d-1)$-spheres S^{d-1} and therefore have empty boundaries. On the other hand, the conformal boundaries $\mathscr{I}^\pm$ are spatial surfaces, and therefore cannot contain a null line. Instead, we must break global dS invariance and take the perspective of an observer. In other words, we take the asymptotics associated with that observer. The only natural null surfaces in dS are not located at the asymptotic conformal boundaries, but rather at the cosmological horizon of an observer. This aligns well with the idealized detector picture, since any signal or excitation placed outside an observer's horizon is, in principle, unrecoverable.

This still does not give us a unique construction. To see this, let us consider an observer sitting at some point in dS space, which we can naturally take to be the center of their static patch. They have in their vicinity a timelike Killing field, which provides them with a natural definition of energy. If we take the conserved charge associated with this Killing field and identify it as the Hamiltonian H, we may extract its angular contribution exactly as we did in Minkowski space with regards to the energy flux operator $\mathcal{E}(\widehat{\mathbf{n}})$ in (4.48). Denoting this static patch timelike Killing field by $\xi_S = \partial_\tau$, we have

$$H = \int_{S^3} \mathrm{d}\sigma^\nu\, T_{\mu\nu}\,\xi_S^\mu\,, \tag{4.69}$$

where the integral is performed over the $t=0$ spatial slice S^3, and $\mathrm{d}\sigma^\nu$ is the future directed normal volume form on S^3. We can now deform this surface up to the CPP horizon $\mathscr{H}^+$ as shown in Figure 4.12. In that case, (4.69) decomposes into an integral over the celestial sphere S^2 and a null direction labeled by α along which the

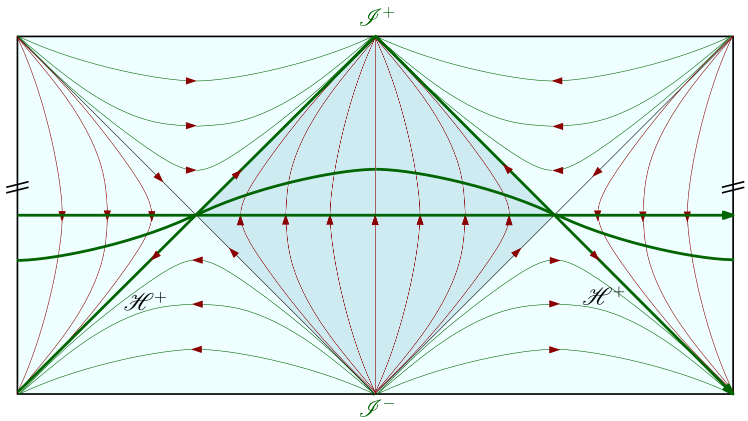

Figure 4.12: In this diagram, the thick green segments represent not just lines, but integrals over the suppressed orthogonal S^2 as well. The Hamiltonian may be evaluated on any of these Cauchy slices, whether on the $t = 0$ slice at the center, on the horizon $\mathscr{H}^+$, or on any interpolating surface in between. The full-horizon energy flux operator $\mathcal{E}_F(\widehat{\mathbf{n}})$ is defined on the entire CPP horizon $\mathscr{H}^+$.

tangent vector is $z^\mu = (1, -\widehat{\mathbf{n}})$. As a result of this, we can rewrite the Hamiltonian as

$$H = \int_{S^2} \mathrm{d}\Omega_2 \int_{-\infty}^{\infty} \mathrm{d}\alpha\, T_{\mu\nu}(\alpha, \widehat{\mathbf{n}})\, \xi_S^\mu\, z^\nu \equiv \int_{S^2} \mathrm{d}\Omega_2\, \mathcal{E}_F(\widehat{\mathbf{n}}) \ . \tag{4.70}$$

This defines our first dS light-ray operator as an integral over the entire CPP horizon $\mathscr{H}^+$, which we call the *full-horizon energy flux operator* $\mathcal{E}_F(\widehat{\mathbf{n}})$

$$\text{Full-horizon energy flux operator :} \qquad \mathcal{E}_F(\widehat{\mathbf{n}}) = \int_{-\infty}^{\infty} \mathrm{d}\alpha\, T_{\mu\nu}(\alpha, \widehat{\mathbf{n}})\, \xi_S^\mu\, z^\nu \ . \tag{4.71}$$

A nice feature of this construction is that under the Weyl map on the Lorentzian cylinder, the full-horizon energy flux operator (4.71) maps to an integral along the future null infinity $\mathscr{I}^+_{\mathrm{M}}$ of Minkowski space.

However, if we wish to follow the literal idealization of the Minkowski energy flux operator $\mathcal{E}(\widehat{\mathbf{n}})$ (recall Figure 4.10), we are led to a slightly different construction in dS space. Analogous to the construction of $\mathcal{E}(\widehat{\mathbf{n}})$, consider now placing a calorimeter at fixed radial distance and allowing it to flow along a timelike geodesic with $\tau \in [0, \infty)$ denoting the static patch time associated with the conserved charge we are calling the Hamiltonian. In the limit of large radial distance, we obtain a null line not over the full CPP horizon $\mathscr{H}^+$, but only over the portion of the horizon that intersects the static patch, as illustrated in Figure 4.13. This defines a second dS light-ray operator as an integral over the half CPP horizon or the static patch horizon $\mathscr{H}^+_{\mathrm{SP}}$, which we

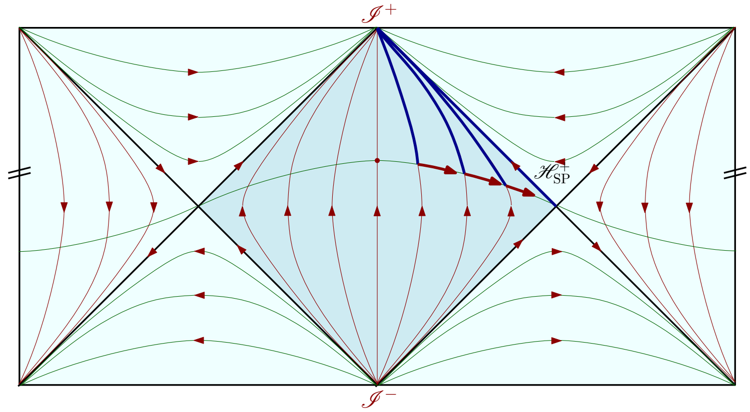

Figure 4.13: The observer sits at the center worldline, surrounded by their timelike Killing field. If they place a calorimeter at fixed radial distance and then move it out to the static patch horizon $\mathscr{H}^+_{\mathrm{SP}}$, the resulting dS light-ray operator $\mathcal{E}_S(\widehat{\mathbf{n}})$ is integrated over $\mathscr{H}^+_{\mathrm{SP}}$, which is half of the future CPP horizon $\mathscr{H}^+$.

call the *static patch/half-horizon energy flux operator* $\mathcal{E}_F(\widehat{\mathbf{n}})$

$$\text{Static patch/Half-horizon energy flux operator}: \quad \mathcal{E}_S(\widehat{\mathbf{n}}) = \int_0^\infty \mathrm{d}\alpha\, T_{\mu\nu}(\alpha, \widehat{\mathbf{n}})\, \xi^\mu_S\, z^\nu \,. \tag{4.72}$$

Note that when mapped to the Lorentzian cylinder, the above is an integral over half of $\mathscr{I}^+_{\mathrm{M}}$ and hence the integral (4.72) runs from $\alpha \in [0, \infty)$.

Now, neither of the above constructions, $\mathcal{E}_F(\widehat{\mathbf{n}})$ and $\mathcal{E}_S(\widehat{\mathbf{n}})$, yields the ANEC operator. For that, we require a different operator altogether, defined by integrating the stress tensor contracted with the tangent z^μ to the null line taken over a complete null geodesic and not the timelike Killing field ξ^μ_S. Taking this null line to lie along the CPP horizon $\mathscr{H}^+$, we can define a third dS light-ray operator called the *full-horizon ANEC operator*

$$\text{Full-horizon ANEC operator}: \quad \mathcal{A}_F(\widehat{\mathbf{n}}) = \int_{-\infty}^\infty \mathrm{d}\alpha\, T_{\mu\nu}(\alpha, \widehat{\mathbf{n}})\, z^\mu\, z^\nu \,. \tag{4.73}$$

This operator also implements the light transform of the dS stress tensor (4.66). To see this, we combine two facts: first, that the ANEC operator in Minkowski space (4.49) is precisely the light transform of the stress tensor (4.51); and second, that the light transform, is a conformally invariant transform and hence insensitive to Weyl rescalings. Therefore, these two operators carry over identically to the conformally related setting of dS space. Under the Weyl map from Minkowski space to the CPP (or Patch I) on the Lorentzian cylinder, the full-horizon ANEC operator $\mathcal{A}_F(\widehat{\mathbf{n}})$ is thus identified with the light transform of the dS stress tensor along the corresponding null generator.

Finally, there is an obvious fourth operator in the family: the analog of $\mathcal{A}_F(\widehat{\mathbf{n}})$, but restricted to an integral over only the future static patch horizon $\mathscr{H}^+_{\mathrm{SP}}$, in direct analogy with (4.72). Hence we call this light-ray operator as the *static patch/half-horizon ANEC-type operator* and list it below for the sake of completeness

$$\text{Static patch/Half-horizon ANEC-type operator}: \; \mathcal{A}_S(\widehat{\mathbf{n}}) = \int_0^\infty \mathrm{d}\alpha \, T_{\mu\nu}(\alpha, \widehat{\mathbf{n}}) \, z^\mu \, z^\nu \, . \tag{4.74}$$

Importantly, we note that the above detector has no natural interpretation in Minkowski space.

Symmetries and Full-Horizon Operators

In the spirit of the conformal collider framework (Hofman and J. Maldacena, 2008), it is natural to ask what kind of "measurements" our dS light-ray operators perform and which aspects of the theory they probe. Under the Weyl map from Minkowski space to dS conformal coordinates, the image of the timelike Killing field ∂_t in Minkowski space is the conformal Killing vector (CKV) field ∂_η associated to conformal time translation in dS space. Said differently, conformal time translations in the CPP (and EPP) are not true isometries of dS space, but rather they are conformal isometries. The corresponding dS light-ray operator is therefore naturally interpreted as the angular contribution to a conformally conserved charge. However, it is not appropriate to regard this charge as the energy, since it fails to be conserved in non-conformal theories. In this sense, the full-horizon dS light-ray operators, $\mathcal{E}_F(\widehat{\mathbf{n}})$ and $\mathcal{A}_F(\widehat{\mathbf{n}})$, are intimately tied to the symmetry structure of dS space: $\mathcal{E}_F(\widehat{\mathbf{n}})$ is associated with an ordinary spacetime isometry (i.e. static patch time translations) and can be viewed as the angular part of a conserved charge (i.e. the Hamiltonian), while $\mathcal{A}_F(\widehat{\mathbf{n}})$ is associated with a conformal isometry and represents the angular part of a conformally conserved charge.

Let Q_ξ and J_ξ denote either of the conserved charges and its associated currents. They are related by

$$Q_\xi = \int_\Sigma \mathrm{d}\Sigma_\mu J^\mu_\xi \, , \tag{4.75}$$

where the surface Σ is chosen to be the CPP horizon $\mathscr{H}^+$. Now, the action of the Lie derivative $\mathcal{L}_\xi$ along the associated Killing vector ξ on the two-point function is given by

$$\mathcal{L}_\xi(\langle\phi_1\phi_2\rangle) = i\left\langle\phi_1[Q_\xi,\phi_2]\right\rangle = i\int_\Sigma \mathrm{d}\Sigma_\mu \left\langle\phi_1[J^\mu_\xi,\phi_2]\right\rangle = i\int_\Sigma \mathrm{d}\Sigma_\mu \left\langle\phi_1 J^\mu_\xi \phi_2\right\rangle \, , \tag{4.76}$$

where in the final equality we have assumed that the dS vacuum is annihilated by the conserved current. Parameterizing the CPP horizon as before using (4.41), we can break up the integral on the right-hand side of (4.76) as

$$i\int_{\Sigma}\mathrm{d}\Sigma_\mu \left\langle \phi_1 J^\mu_\xi \phi_2 \right\rangle = i\int_{S^2}\mathrm{d}\Omega_2 \left\langle \phi_1 \int_{-\infty}^{\infty}\mathrm{d}\alpha\, z^\mu J^\mu_\xi \phi_2 \right\rangle = i\int_{S^2}\mathrm{d}\Omega_2 \left\langle \phi_1 O_F(\widehat{\mathbf{n}})\phi_2 \right\rangle \, , \tag{4.77}$$

where $O_F = \mathcal{E}_F, \mathcal{A}_F$. In section 4.4, we will explicitly verify this at the level of the matrix elements of the full-horizon operators in a theory of conformally coupled scalars.

Computation of matrix elements: the general setup

Having classified the various constructions of light-ray operators in dS space, we now turn to setting up the computation of their expectation values in generic quantum mechanical states. To begin our analysis of these operators, it is natural to start with their one-point functions. However, it is important to note that their one-point function vanishes in every theory on grounds of symmetry. $SO(1,4)$ invariance dictates that $\langle T_{\mu\nu}\rangle \sim g_{\mu\nu}$, and contracting this with two null vectors necessarily gives zero. Moreover, in order to evaluate these operators in a generic state, what we truly need are their matrix elements. Letting O denote any of the four operators introduced above, we want to compute

$$\langle\Psi|O|\Psi\rangle = \int \mathrm{d}^d x_1\, \mathrm{d}^d x_2 \sqrt{g(x_1)g(x_2)}\, \Psi^*(x_1)\Psi(x_2)\, \langle\phi(x_1)O\phi(x_2)\rangle \, . \tag{4.78}$$

Therefore, all we need are the matrix elements $\langle\phi(x_1)O\phi(x_2)\rangle$ where we will always fix the operator ordering via a suppressed $i\epsilon$. We want to express the operators $\mathcal{A}_{(F,S)}(\widehat{\mathbf{n}})$ and $\mathcal{E}_{(F,S)}(\widehat{\mathbf{n}})$ in coordinates adapted to their symmetries, namely conformal coordinates (4.3) and static patch coordinates (4.4), respectively. The two kinematic inputs that enter their definition are the location of the observer and the position of their horizon. However, both of these coordinate systems become singular at the horizon. The way to get around this is to work with the parameterization provided by the null embedding space $\mathbb{R}^{2,4}$, which treats the horizon in a nonsingular way.

To compute the matrix element $\langle\phi(X_1)O\phi(X_2)\rangle$, let us place the two scalar field insertions $\phi(X_1)$ and $\phi(X_2)$ at generic points X_1, X_2 in the interior of the CPP horizon. From (4.34), we know that these points are parameterized in the null embedding space by

$$X^A_{\mathrm{CPP}}(\eta_i,\vec{x}_i) = \frac{1}{\eta_i}\left(1, -\eta_i^2 + \vec{x}_i^{\,2}, \eta_i, \vec{x}_i\right) \, , \tag{4.79}$$

while the stress tensor sitting at a point X_0 on the CPP horizon $\mathscr{H}^+$ gets integrated along a null line on $\mathscr{H}^+$, which recall from (4.41) gets parameterized as

$$X_{\mathscr{H}^+}(\alpha, \widehat{\mathbf{n}}) = \left(0, -\alpha, 1, \widehat{\mathbf{n}}\right) \equiv X_0(\alpha, \widehat{\mathbf{n}}) \ . \tag{4.80}$$

This implies that the tangent vector to this null line is then given by

$$Z_{\mathscr{H}^+}(\alpha, \widehat{\mathbf{n}}) = \frac{\mathrm{d}X_0}{\mathrm{d}\alpha} = \left(0, -1, 0, \vec{0}\right) \equiv Z_0 \ , \tag{4.81}$$

where we note that this is simply a constant vector. We have to now consider the two bulk Killing fields and how they are denoted at the horizon $\mathscr{H}^+$. The first is the generator Ξ_S of static patch time translations $\tau \to \tau + a$, which when evaluated on the horizon is given by

$$\Xi_S\Big|_{\mathscr{H}^+} = (0, -\alpha, 0, \vec{0}) = \alpha Z_0 \ . \tag{4.82}$$

The second is the CKV field Ξ_C that generates conformal time translations $\eta \to \eta + a$. As discussed above, although this is not an isometry of dS space, it is a conformal isometry. When evaluated on the horizon, this CKV becomes

$$\Xi_C\Big|_{\mathscr{H}^+} = (0, -2, 0, \vec{0}) = 2Z_0 \ . \tag{4.83}$$

Thus, the matrix element $\langle \phi(X_1)\mathcal{A}_F(\widehat{\mathbf{n}})\phi(X_2)\rangle$ involves contracting the stress tensor $T_{\mu\nu}$ with two tangent vectors $z^\mu z^\nu$, and then integrating with measure $\mathrm{d}\alpha$ according to (4.73)

$$\langle \phi(X_1)\mathcal{A}_F(\widehat{\mathbf{n}})\phi(X_2)\rangle = 4\int_{-\infty}^{\infty} \mathrm{d}\alpha \ \langle \phi(X_1)T(X_0(\alpha, \widehat{\mathbf{n}}), Z_0)\phi(X_2)\rangle \ . \tag{4.84}$$

While the matrix element $\langle \phi(X_1)\mathcal{E}_F(\widehat{\mathbf{n}})\phi(X_2)\rangle$ involves contracting the stress tensor $T_{\mu\nu}$ with a tangent vector z^μ and a Killing vector ξ^μ_S, and then integrating with measure $\alpha\mathrm{d}\alpha$ according to (4.71)

$$\langle \phi(X_1)\mathcal{E}_F(\widehat{\mathbf{n}})\phi(X_2)\rangle = 2\int_{-\infty}^{\infty} \mathrm{d}\alpha \ \alpha \ \langle \phi(X_1)T(X_0(\alpha, \widehat{\mathbf{n}}), Z_0)\phi(X_2)\rangle \ . \tag{4.85}$$

Using the relations (4.66) and (4.67), the common integrand in the above expressions takes the following form in the null embedding space

$$\begin{aligned}\langle \phi(X_1)T(X_0, Z_0)\phi(X_2)\rangle &= \lim_{X_0'\to X_0} Z_0^A Z_0^B \Theta_{AB} \langle \phi(X_1)\phi(X_0)\phi(X_0')\phi(X_2)\rangle \\ &= 2(1-2\xi)X_1\cdot Z_0 X_2\cdot Z_0 G'(Z_{01})G'(Z_{02}) \\ &- 2\xi\left((X_1\cdot Z_0)^2 G''(Z_{01})G(Z_{02}) + (X_2\cdot Z_0)^2 G(Z_{01})G''(Z_{02})\right),\end{aligned} \tag{4.86}$$

where $G(Z_{0i}) \equiv G(X_0, X_i)$ is the Wightman two-point function given by (4.63). This amounts to a sum of products of hypergeometric functions, since derivatives of ${}_2F_1$ functions remain hypergeometric functions, albeit with shifted arguments. In generic scalar QFTs in dS_4, we have to perform the integrals in (4.86), which amounts to integrating products of ${}_2F_1$ functions. In general, such integrals do not admit known closed-form expressions. We can however, make some general statements based on the analytic properties of ${}_2F_1$ functions. If we let $k = 0, 1$ we can write all the integrals appearing in the matrix element $\langle \phi(X_1) O \phi(X_2) \rangle$ in the form

$$\int \mathrm{d}\alpha\, \alpha^k\, {}_2F_1\left(a, b, c; \frac{1}{2}\left(1 + \frac{\vec{x}_1 \cdot \widehat{\mathbf{n}}}{\eta_1} + \frac{\alpha}{2\eta_1}\right)\right) {}_2F_1\left(\tilde{a}, \tilde{b}, \tilde{c}; \frac{1}{2}\left(1 + \frac{\vec{x}_2 \cdot \widehat{\mathbf{n}}}{\eta_2} + \frac{\alpha}{2\eta_2}\right)\right), \tag{4.87}$$

where the arguments a, b, c and its tilde counterparts depend on the parameters $\Delta, \bar{\Delta}$. These integrals develop a singularity when the argument $\frac{1}{2}\left(1 + \frac{\vec{x}_i \cdot \widehat{\mathbf{n}}}{\eta_i} + \frac{\alpha}{2\eta_i}\right) = 1$, which corresponds to the lightcone of X_i intersecting the light-ray operator on the appropriate horizon. We can denote this point as $\alpha^*(X_i)$ as shown in Figure 4.14. This function has a branch cut in α that begins at $\alpha^*(X_i)$ and extends to ∞. For the half-horizon integrals $O_S = \mathcal{E}_S, \mathcal{A}_S$ where $\alpha \in [0, \infty)$, there is little additional simplification to be gained from this structure. However, for the full-horizon integrals $O_F = \mathcal{E}_F, \mathcal{A}_F$ we can rewrite the result as an integral over the discontinuity across the branch cut, starting at either $\alpha^*(X_i)$

$$\int_{\alpha^*(X_i)}^{\infty} \mathrm{d}\alpha\, \alpha^k\, \mathrm{Disc}\left[{}_2F_1\left(a, b, c; \frac{1}{2}\left(1 + \frac{\vec{x}_i \cdot \widehat{\mathbf{n}}}{\eta_i} + \frac{\alpha}{2\eta_i}\right)\right)\right] {}_2F_1\left(\tilde{a}, \tilde{b}, \tilde{c}; \frac{1}{2}\left(1 + \frac{\vec{x}_j \cdot \widehat{\mathbf{n}}}{\eta_j} + \frac{\alpha}{2\eta_j}\right)\right). \tag{4.88}$$

Interestingly, as long as at least one of the bulk points X_1, X_2 lies entirely within the static patch, the full-horizon operators becomes an integral that is entirely supported on $\mathscr{H}^+_{\mathrm{SP}}$, as shown in Figure 4.14.

Conformal de Sitter light-ray operators

So far, we have broadly classified the dS light-ray operators into four distinct types: the full-horizon operators $\mathcal{A}_F, \mathcal{E}_F$, and the static patch/half-horizon operators $\mathcal{A}_S, \mathcal{E}_S$. To compute matrix elements involving these operators, we found that one must evaluate integrals of the form (4.86), which require integrating products of hypergeometric ${}_2F_1$ functions and are, in general, quite complicated. However, we can obtain much better analytic control by restricting our attention to the case of conformally coupled scalars, for which the two-point function was shown in (4.63)

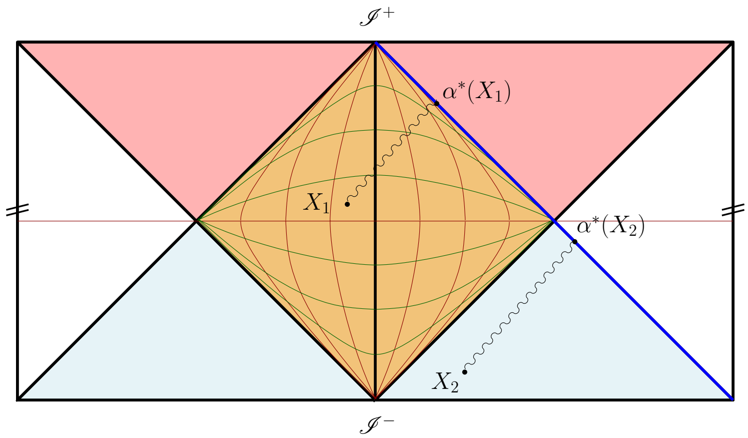

Figure 4.14: Two bulk points X_1, X_2 in dS space with their lightcones intersecting a full-horizon light-ray operator $O_F = \mathcal{E}_F, \mathcal{A}_F$ defined on the CPP horizon $\mathscr{H}^+$ (in blue). Since X_1 lies in the static patch, we can restrict the integral (4.87) to begin at its singularity, so that the entire contribution is constrained to lie along the static patch horizon $\mathscr{H}^+_{\text{SP}}$.

to take the simple form

$$G(Z_{0i}) \equiv G(X_0, X_i) = -\frac{1}{(4\pi)^2}\frac{2}{X_0 \cdot X_i} \,. \tag{4.89}$$

In that case, the common integrand in (4.86) simply reduces to the expression

$$\langle \phi(X_1) T(X_0, Z_0) \phi(X_2)\rangle = -\frac{1}{96\pi^4}\frac{(X_1 \cdot X_0 X_2 \cdot Z_0 - X_2 \cdot X_0 X_1 \cdot Z_0)^2}{(X_0 \cdot X_2)^3 (X_0 \cdot X_1)^3} \,. \tag{4.90}$$

One can check that this answer, up to numerical prefactors, is consistent with what is expected from conformal invariance (Kravchuk and Simmons-Duffin, 2018b). To better understand its singularity structure, let us consider the simple case where we place the two scalar operators at the two bulk points X_1, X_2 on the worldline of the observer. Using (4.36), the above expression can be written in the CPP conformal coordinates as

$$\langle \phi(\eta_1, \vec{x}_1 = 0)\, T(X_0(\alpha, \widehat{\mathbf{n}}), Z_0)\, \phi(\eta_2, \vec{x}_2 = 0)\rangle = -\frac{\eta_1\eta_2}{6\pi^4}\frac{(\eta_1 - \eta_2)^2}{(\alpha - 2\eta_1)^3(\alpha - 2\eta_2)^3} \,. \tag{4.91}$$

We see that this expression has two poles, each of third order, which appear when the integration contour crosses the lightcone of one of the bulk points. The overall factor of $\eta_1\eta_2$ in front can be understood as the Weyl factor of the two bulk operators, while the stress tensor located on the horizon has a Weyl factor that asymptotes to unity. Said differently, we are extracting the leading term in the limit $L \gg 1$, and the Weyl factor for the operator on the horizon is $O(L^{-1})$ (see (4.39)). When the scalar operators are placed at generic bulk points $x_i = (\eta_i, \vec{x}_i)$, the numerator is again the unique conformally invariant generalization of the expression above. The poles then merely shift to the new locations where the integration contour intersects the new lightcones of the bulk points

$$\langle\phi(\eta_1,\vec{x}_1)\, T(X_0(\alpha,\widehat{\mathbf{n}}), Z_0)\, \phi(\eta_2,\vec{x}_2)\rangle = -\frac{\eta_1\eta_2}{6\pi^4}\frac{z_{12}^2}{(\alpha+2z_1)^3(\alpha+2z_2)^3}\ , \tag{4.92}$$

where we have defined

$$z_i = \bar{z}\cdot x_i\ , \qquad z_{ij} = \bar{z}_i - \bar{z}_j\ , \tag{4.93}$$

with $\bar{z} = (1, \widehat{\mathbf{n}})$ as before.

Having analyzed the analytic structure of the common integrand, let us now perform the α-integration with the appropriate measure to compute matrix elements of the various dS light-ray operators. We begin with the full horizon ANEC operator $\mathcal{A}_F(\widehat{\mathbf{n}})$ defined in (4.73). Using (4.84) along with the result for the integrand (4.92), we obtain

$$\begin{aligned}\langle\phi(\eta_1,\vec{x}_1)\mathcal{A}_F(\widehat{\mathbf{n}})\phi(\eta_2,\vec{x}_2)\rangle &= -\frac{\eta_1\eta_2 z_{12}^2}{96\pi^4}\int_{-\infty}^{\infty}\frac{\mathrm{d}\alpha}{(\alpha+z_1)^3(\alpha+z_2)^3}\\ &= \frac{i}{(2\pi)^3}\frac{\eta_1\eta_2}{z_{12}^3}\ .\end{aligned} \tag{4.94}$$

Let us make two remarks on the above result. First, we can see in this an instantiation of ANEC positivity. If we place x_1 and x_2 at the same Lorentzian point x, while keeping their Euclidean time separation nonzero to maintain operator ordering, we obtain

$$\langle\phi^*(\eta,\vec{x})\mathcal{A}_F(\widehat{\mathbf{n}})\phi(\eta,\vec{x})\rangle = \frac{i}{(2\pi)^3}\frac{\eta^2}{(-i\epsilon)^3} > 0\ . \tag{4.95}$$

Second, in a conformal theory, we can recognize the quantity (4.94) as the integral of a conformally conserved current. We can show that it represents the angular contribution to the corresponding charge by integrating (4.94) over a two-sphere S^2 and comparing the result with the Lie derivative along the Killing flow of conformal time translations, as discussed in (4.76) and (4.77). In particular, for this CKV field ξ_C, we want to show that

$$\mathcal{L}_{\xi_C}(\langle\phi_1\phi_2\rangle) = i\int_{S^2}\mathrm{d}\Omega_2\ \langle\phi_1\mathcal{A}_F\phi_2\rangle\ . \tag{4.96}$$

The Lie derivative along the CKV field is not simply $\xi_C = \partial_{\eta_2}$. One could modify the Lie derivative to account for this explicitly, but a mathematically equivalent (and computationally simpler) approach is to evaluate both sides of (4.96) in flat space, where the corresponding Lie derivative is just ∂_{η_2}. Operationally, this amounts to dropping the $\eta_1\eta_2$ Weyl factors on both sides. In this frame, the Lie derivative reduces to a simple time derivative, and we obtain for the left-hand side

$$\mathcal{L}_{\xi_C}(\langle\phi_1\phi_2\rangle) = -\frac{1}{4\pi^2}\partial_{\eta_2}\frac{1}{-(\eta_1-\eta_2)^2+(\vec{x}_1-\vec{x}_2)^2} = -\frac{1}{2\pi^2}\frac{(\eta_1-\eta_2)}{(-(\eta_1-\eta_2)^2+(\vec{x}_1-\vec{x}_2)^2)^2}\,, \tag{4.97}$$

while the right-hand side of (4.96) evaluates to

$$\begin{aligned} i\int_{S^2}\mathrm{d}\Omega_2\,\langle\phi_1\mathcal{A}_F\phi_2\rangle &= -\frac{1}{(2\pi)^2}\int_0^\pi\frac{\sin\theta\mathrm{d}\theta}{(-\eta_1+\eta_2+|\vec{x}_1-\vec{x}_2|\cos\theta)^3} \\ &= -\frac{1}{2\pi^2}\frac{(\eta_1-\eta_2)}{(-(\eta_1-\eta_2)^2+(\vec{x}_1-\vec{x}_2)^2)^2}\,. \end{aligned} \tag{4.98}$$

Turning now to the case of the full-horizon energy flux operator $\mathcal{E}_F(\widehat{\mathbf{n}})$ defined in (4.71), we obtain its matrix element using the relations (4.85) and (4.92) to be

$$\begin{aligned} \langle\phi(\eta_1,\vec{x}_1)\mathcal{E}_F(\widehat{\mathbf{n}})\phi(\eta_2,\vec{x}_2)\rangle &= -\frac{\eta_1\eta_2 z_{12}^2}{96\pi^4}\int_{-\infty}^{\infty}\frac{\alpha\mathrm{d}\alpha}{(\alpha+z_1)^3(\alpha+z_2)^3} \\ &= \frac{i}{(2\pi)^3}\frac{\eta_1\eta_2}{z_{12}^3}\frac{z_1+z_2}{2}\,. \end{aligned} \tag{4.99}$$

For this result to be related to the static patch time translation symmetry generated by $\xi_S = \partial_{\tau_2}$, we have to now show that

$$\mathcal{L}_{\xi_S}(\langle\phi_1\phi_2\rangle) = i\int_{S^2}\mathrm{d}\Omega_2\,\langle\phi_1\mathcal{E}_F\phi_2\rangle\,. \tag{4.100}$$

To do this, we begin by rewriting the conformal two-point function (4.64) in static patch coordinates. We will do this in two steps. First, we express the conformal coordinates in a spherically symmetric form as $x_i = (\eta_i,\vec{x}_i) \to (\eta_i,\rho_i\widehat{\mathbf{n}}_i)$, and then change coordinates from conformal (η_i,ρ_i) to static patch (τ_i,r_i) via $\eta_i = e^{\tau_i}(1-r_i^2)^{-1/2}$ and $\rho_i = e^{\tau_i}r_i(1-r_i^2)^{-1/2}$. In these coordinates, the Lie derivative of the two-point function along the timelike Killing field $\xi_S = \partial_{\tau_2}$ takes the form

$$\begin{aligned} \mathcal{L}_{\xi_S}(\langle\phi_1\phi_2\rangle) &= -\frac{1}{8\pi^2}\partial_{\tau_2}\frac{1}{-1+\sqrt{1-r_1^2}\sqrt{1-r_2^2}\cosh(\tau_1-\tau_2)+r_1r_2\widehat{\mathbf{n}}_1\cdot\widehat{\mathbf{n}}_2} \\ &= -\frac{1}{8\pi^2}\frac{\sqrt{1-r_1^2}\sqrt{1-r_2^2}\sinh(\tau_1-\tau_2)}{(-1+\sqrt{1-r_1^2}\sqrt{1-r_2^2}\cosh(\tau_1-\tau_2)+r_1r_2\widehat{\mathbf{n}}_1\cdot\widehat{\mathbf{n}}_2)^2}\,, \end{aligned} \tag{4.101}$$

which we can now compare to the right-hand side of (4.100) by integrating it over S^2

$$
\begin{aligned}
i \int_{S^2} \mathrm{d}\Omega_2 \, \langle \phi_1 \mathcal{E}_F \phi_2 \rangle &= -\frac{\eta_1\eta_2}{16\pi^3} \int_{S^2} \mathrm{d}\Omega_2 \frac{z_1 + z_2}{z_{12}^3} = -\frac{\eta_1\eta_2}{16\pi^3} \int_{S^2} \mathrm{d}\Omega_2 \frac{-\eta_1 - \eta_2 + \widehat{\mathbf{n}} \cdot (\vec{x}_1 + \vec{x}_2)}{(-\eta_1 + \eta_2 + \widehat{\mathbf{n}} \cdot (\vec{x}_1 - \vec{x}_2))^3} \\
&= \frac{i\eta_1\eta_2}{4\pi^2} \frac{-\eta_2^2 + \vec{x}_2^2 + \eta_1^2 - \vec{x}_1^2}{(-(\eta_2 - \eta_1)^2 + (\vec{x}_2 - \vec{x}_1)^2)^2} \, . \qquad (4.102)
\end{aligned}
$$

Rewriting this in static patch coordinates, we recover exactly the expression in (4.101).

The matrix element for the static patch/half-horizon ANEC-type operator $\mathcal{A}_S(\widehat{\mathbf{n}})$ defined in (4.74) can similarly be computed to give

$$
\begin{aligned}
\langle \phi(\eta_1, \vec{x}_1) \mathcal{A}_S(\widehat{\mathbf{n}}) \phi(\eta_2, \vec{x}_2) \rangle &= -\frac{\eta_1\eta_2 z_{12}^2}{96\pi^4} \int_0^\infty \frac{\mathrm{d}\alpha}{(\alpha + z_1)^3 (\alpha + z_2)^3} \\
&= \frac{1}{192\pi^4} \frac{\eta_1\eta_2}{z_{12}^3} \left[\frac{(z_1^2 - z_2^2)(z_1^2 - 8 z_2 z_1 + z_2^2)}{z_1^2 z_2^2} + 12 \log\left(\frac{z_1}{z_2}\right) \right] ,
\end{aligned}
\tag{4.103}
$$

while the corresponding result for the static patch/half-horizon energy flux operator $\mathcal{E}_S(\widehat{\mathbf{n}})$ defined in (4.72) gives

$$
\begin{aligned}
\langle \phi(\eta_1, \vec{x}_1) \mathcal{E}_S(\widehat{\mathbf{n}}) \phi(\eta_2, \vec{x}_2) \rangle &= -\frac{\eta_1\eta_2 z_{12}^2}{96\pi^4} \int_0^\infty \frac{\alpha \mathrm{d}\alpha}{(\alpha + z_1)^3 (\alpha + z_2)^3} \\
&= \frac{1}{192\pi^4} \frac{\eta_1\eta_2}{z_{12}^3} \left[\frac{-z_{12}(z_1^2 + 10 z_1 z_2 + z_2^2)}{z_1 z_2} + 6(z_1 + z_2) \log\left(\frac{z_1}{z_2}\right) \right] .
\end{aligned}
\tag{4.104}
$$

We can see that the above matrix elements of both these half-horizon operators develop interesting new singularities at $z_i = 0$. The point $\alpha = 0$ that marks the beginning of the integration contour in both the integrals (4.103) and (4.104) is denoted in null embedding space as $X_{\mathscr{H}^+}(0, \widehat{\mathbf{n}}) = (0, 0, 1, \widehat{\mathbf{n}})$. Points in the bulk that are lightlike related to this point satisfy

$$
0 = X_i(\eta_i, \vec{x}_i) \cdot X_{\mathscr{H}^+}(0, \widehat{\mathbf{n}}) = -\eta_i + \vec{x}_i \cdot \widehat{\mathbf{n}} = z_i \, . \tag{4.105}
$$

The (logarithmic) branch cut at $z_i = 0$ thus reflects the fact that this is precisely the threshold at which the bulk points X_i become lightlike separated from the integration contour of the half-horizon operator in question. Hence the $z_i = 0$ point marks the transition between configurations where the contour does or does not intersect their lightcones.

4.5 Discussions and outlook

Historically, light-ray operators have been extensively studied in Minkowski space, primarily in the context of collider physics and more recently, in CFTs and extended to generic QFTs. There is by now a substantial body of work analyzing these operators from many different perspectives; see, for example, the review (Moult and Zhu, 2025) (and references therein). In Minkowski space, the energy flux operator $\mathcal{E}(\widehat{\mathbf{n}})$ is in some sense canonical: broader classes of light-ray operators can be constructed from it and naturally regarded as belonging to the same family. In this work, we have shown that an attempt to generalize these notions straightforwardly to dS space leads instead to a richer space of inequivalent constructions. The asymptotics of dS space, together with the structure of its isometry group, allow us to classify four distinct *observer-dependent* light-ray operators, as described in section 4.4. In the null embedding space $\mathbb{R}^{2,4}$, all of these can be written in the unified form

$$\mathcal{O}(\widehat{\mathbf{n}}) = 2^{2-k}\int_{\alpha_i}^{\infty} \mathrm{d}\alpha\, \alpha^k\, T_{AB}(X_0(\alpha,\widehat{\mathbf{n}}))Z_0^A Z_0^B\,, \tag{4.106}$$

where $X_0(\alpha,\widehat{\mathbf{n}})$ parametrizes points on the CPP horizon $\mathscr{H}^+$ (see (4.80)), and Z_0 is the tangent vector along a null line on $\mathscr{H}^+$ (4.81), while T_{AB} is the embedding space stress tensor in dS space. The four types of dS light-ray operators then correspond to different choices of the lower limit of the integral α_i and the constant $k = 0, 1$, as summarized in the table below.

Operator $\mathcal{O}(\widehat{\mathbf{n}})$	$\boldsymbol{\alpha_i}$	$\boldsymbol{k}$	**Horizon segment**	**Interpretation**
$\mathcal{E}_F(\widehat{\mathbf{n}})$	$-\infty$	1	CPP horizon $\mathscr{H}^+$	Full-horizon energy flux operator
$\mathcal{A}_F(\widehat{\mathbf{n}})$	$-\infty$	0	CPP horizon $\mathscr{H}^+$	Full-horizon ANEC operator
$\mathcal{E}_S(\widehat{\mathbf{n}})$	0	1	Static patch horizon $\mathscr{H}^+_{\mathrm{SP}}$	Static patch energy flux operator
$\mathcal{A}_S(\widehat{\mathbf{n}})$	0	0	Static patch horizon $\mathscr{H}^+_{\mathrm{SP}}$	Static patch ANEC-type operator

Table 4.1: A summary of the four types of dS light-ray operators classified in this work.

Having classified these dS light-ray operators, we then analyzed some of their matrix elements in the simplest possible setting, namely a theory of free, conformally coupled scalars in dS_4, as described in section 4.4. Our focus was deliberately restricted to the simplest operator in the most symmetric case, yet even in this regime the interplay between the horizon geometry, the Weyl map to Minkowski space, and the embedding space description already exhibits nontrivial structure. At the same time, many straightforward extensions of this analysis remain unexplored, and our results should be viewed as a first step toward a broader and systematically richer family of constructions, which we discuss below:

General masses and interacting theories. The most immediate extensions of our analysis involve departing from the conformal point to scalars with general mass and, subsequently, to interacting theories. In the present work we have already seen that generic scalar QFTs in dS_4 give rise to detector matrix elements expressed as integrals of products of ${}_2F_1$ functions, which in general have no known closed-form expressions (see discussion below (4.86)). It would be interesting to understand to what extent special values of the mass or perturbative interactions lead to simplifications, and whether there exist useful approximation schemes that render the space of dS light-ray correlators more tractable. Also, in fully interacting theories one also expects the OPE of these dS light-ray operators to become nontrivial, opening an additional direction for further study. This would then open the door to regularizing the IR divergences in a theory informed way, moving towards a dS analog of (Simon Caron-Huot, Kologlu, et al., 2023).

ANEC and positivity bounds. While we have shown an instantiation of positivity of the full horizon ANEC operator $\mathcal{A}_F(\widehat{\mathbf{n}})$ in (4.95), we leave the general proof of its positivity as future work. In Minkowski space, light ray operators have been used to constrain the space of QFTs by constraining Wilson coefficients (Kologlu et al., 2020; Simon Caron-Huot, Mazac, et al., 2021a; Chang, Landau, and Simmons-Duffin, 2025), and it would be desirable to similarly restrict the space of allowed theories in dS space. Our construction may provide a way to sharpen the positivity bounds of (Freytsis et al., 2023; Cordova, J. Maldacena, and Turiaci, 2017), and it would be interesting to explore how these dS light-ray operators interface with recent proposals for de Sitter S-matrix–like observables in different regimes.

Cosmological collider physics. In dS space the inflationary regime has been of great interest, in which the primary observables of interest are boundary correlators defined on $\mathscr{I}^+$ (Achúcarro et al., 2022; Baumann et al., 2024). As such, it would be interesting to ask what the operators defined in our work can tell us about cosmological collider physics. Although we have defined our operators using the observer's worldline, it can equally be defined by the origin or terminus of the worldline in $\mathscr{I}^\pm$, along with a choice of boost frame, and the point on the celestial sphere – all data already defined on $\mathscr{I}^\pm$. As such these operators can be entirely defined by their kinematic data on $\mathscr{I}^{\pm}$, and can be studied in that context. In Minkowski space, the energy flux operator $\mathcal{E}(\widehat{\mathbf{n}})$ in the collinear limit probes jet substructure (Moult and Zhu, 2025) and encodes detailed information about the UV theory. One might hope that suitable dS or cosmological analogs of $\mathcal{E}_F(\widehat{\mathbf{n}})$, or of the ANEC operator $\mathcal{A}_F(\widehat{\mathbf{n}})$, could probe the angular and frequency structure of late-time cosmological correlators in an analogous way.

Generic curved spacetimes and quantum gravity. Expanding on the previous direction, we note that the only kinematic input to our operators was the worldline of an observer and their associated horizons. These are well defined objects in generic curved spacetimes, with dS providing the simplest nontrivial example. As such, these operators capture the physics of physically realizable experiments in any curved spacetime. Moreover, these observables are well defined even in quantum gravity, as they are gravitationally dressed to the observer. In particular, the half-horizon operators, associated with the static patch of the observer, sit nicely within the framework of (Chandrasekaran et al., 2023), in which the generalized static patch serves as the largest regime associated to the algebra of an observer in any theory of quantum gravity.

Algebra of dS light-ray operators. Finally, it would be interesting to explore the algebraic structure of these dS light-ray operators. In Minkowski space, light-ray operators and their algebras are closely connected to asymptotic symmetries and to the structure of null infinity (Córdova and Shao, 2018; Korchemsky and Zhiboedov, 2021). Understanding these structures could help clarify the role of dS horizons and observer dependence in any putative notion of dS holography (Strominger, 2001; Anninos, Hartnoll, and Hofman, 2012; Susskind, 2021). We leave these questions, along with the many low hanging fruits outlined above, to future work.

4.A Regularizing the stress tensor

In this appendix, we will derive the regularized expression for the stress tensor (4.68). We will extract the divergent pieces of the stress tensor defined by the relations (4.66) and (4.67) using dimensional regularization. The stress tensor in this case only has one divergence, coming from its definition via point splitting. In general, interacting theories will have more divergences, but in this simple case there is only one. Additionally, even this divergence will never be an issue for us since, as we will show, the divergence is proportional to the metric; as such, when contracted with two null vectors, the divergence is zero. Another way of saying this is that the stress tensor is always a sum of two irreducible representations, the symmetric traceless part and the trace. Light-ray operators are sensitive to the traceless component while the divergence is only in the trace. Nonetheless, as we are using this operator, we include its regularization.

Let us begin by considering the insertion of the stress tensor into some generic correlation function in the following manner

$$\Big\langle O(z_1)\cdots T_{\mu\nu}(x)\cdots O(z_n)\Big\rangle = \lim_{y\to x}\Theta_{\mu\nu}(x,y)\,\langle O(z_1)\cdots\phi(y)\phi(x)\cdots O(z_n)\rangle\ , \tag{4.107}$$

where we have used the defining relation (4.66). In the free theory, for any value of the mass parameter μ^2, the fact that correlation functions factorize into Wick pairs ensures that the above correlator has a particularly simple form. If we consider the correlation function before the Θ operator acts on it, it decomposes into a sum of Wick contractions. Among these terms, some will have points x and y each contracted with distinct points z_i; such contributions do not generate any short-range singularity intrinsic to the definition of the stress tensor. The remaining terms, in which x and y contract with one another, will produce ultraviolet divergences. However, in this case, the Θ operator acts only on that two-point function, and so the stress tensor factorizes out as follows

$$\begin{aligned}\lim_{y\to x}\Theta_{\mu\nu}(x,y)\,&\langle O(z_1)\cdots\phi(y)\phi(x)\cdots O(z_n)\rangle\\ &=\lim_{y\to x}\Theta_{\mu\nu}(x,y)\,[\langle\phi(y)\phi(x)\rangle]\,\langle O(z_1)\cdots O(z_n)\rangle + \text{finite}\\ &=\Big\langle T_{\mu\nu}(x)\Big\rangle\,\langle O(z_1)\cdots O(z_n)\rangle + \text{finite}\ .\end{aligned} \tag{4.108}$$

Therefore, the divergent part of the correlator is simply the divergence of the one-point function of the stress tensor itself, which we now address.

The calculations involving the stress tensor will be carried out in the hyperbolic embedding space following (Pethybridge and Schaub, 2022). The Θ operator given in (4.67) can be defined in the hyperbolic embedding space $\mathbb{R}^{1,4}$ using the covariant derivative (4.11). Let us consider the action of the Θ operator on a generic function f of the hyperbolic distance $h \equiv X\cdot Y$. In the coincident limit $h\to 1$, we obtain

$$U^A V^B \Theta_{AB}(X,Y)[f(h)]|_{h\to 1} = -\frac{1}{2}U\cdot V((m^2+6\xi)f(1)+2f'(1))\ , \tag{4.109}$$

where we have assumed that $U, V \in T_{X,Y}(\mathbb{R}^{1,4})$ are in the tangent space, such that $U \cdot X = V \cdot X = 0$. Consequently, we can write

$$\langle T_{\mu\nu}\rangle_\epsilon = -\frac{1}{2} U \cdot V((m^2 + 6\xi)G_\epsilon(1) + 2G'_\epsilon(1)) \,, \tag{4.110}$$

where G_ϵ is the $1/\epsilon$ divergence of the Wightman two-point function. So to regularize the stress tensor, we need to find the $1/\epsilon$ divergence of $G(h)|_{h=1}$ and $G'(h)|_{h=1}$. Note that identifying and subtracting the divergence in $G(h)$ is, in effect, the regularization of the ϕ^2 operator.

Divergence of $G(h)|_{h=1}$

We will follow the conventions and normalizations of (P. Chakraborty and Stout, 2023). To extract the divergence of $G(h)$, we begin by examining the propagator G_E in Euclidean[9] dS_d, which is simply the d-sphere S^d. The key feature of this propagator is that it serves as the Green's function of the Klein-Gordon operator

$$G_E(x, y) = (-\Box_x + \mu^2)^{-1} \,, \tag{4.111}$$

where $\mu^2 \equiv m^2 + 12\xi$ as before. We can solve this explicitly on the d-sphere S^d using hyperspherical harmonics

$$G_E(\sigma) = \frac{\Gamma(\alpha)}{2\pi^{\alpha+1}} \sum_{J=0}^{\infty} \frac{J + \alpha}{J(J + 2\alpha) + \mu^2} C_J^\alpha(\sigma) \,, \tag{4.112}$$

where $\alpha = (d - 1)/2$, σ is the Euclidean embedding distance defined in (4.6), and C_J^α is a Legendre function of the first kind (a Gegenbauer polynomial if $J \in \mathbb{Z}$). In the coincident limit $\sigma = 1$, one has the relation

$$C_J^\alpha(1) = \frac{\Gamma(J + 2\alpha)}{\Gamma(J + 1)\Gamma(2\alpha)} \,, \tag{4.113}$$

which gives

$$G_E(\sigma)|_{\sigma=1} = \frac{\Gamma(\alpha)}{2\pi^{\alpha+1}\Gamma(2\alpha)} \sum_{J=0}^{\infty} \frac{J + \alpha}{J(J + 2\alpha) + \mu^2} \frac{\Gamma(J + 2\alpha)}{\Gamma(J + 1)} \,. \tag{4.114}$$

We can simplify the expressions further by writing the denominator factor as

$$\begin{aligned} \frac{1}{J(J + 2\alpha) + \mu^2} = \frac{1}{(J - h_+)(J - h_-)} &= \frac{\partial}{\partial \mu^2}[\log(J - h_+) + \log(J - h_-)] \\ &= \frac{\partial}{\partial \mu^2}\frac{\partial}{\partial s}[(J - h_-)^s + (J - h_+)^s]\bigg|_{s=0} \,. \end{aligned} \tag{4.115}$$

[9] To extract the short-distance singularity, it does not matter if one is in Lorentzian or Euclidean signature.

This gives us the following expression for the propagator in the coincident limit

$$G_E(\sigma)|_{\sigma=1} = \frac{\Gamma(\alpha)}{4\pi^{\alpha+1}\Gamma(2\alpha)}\frac{\partial}{\partial\mu^2}\frac{\partial}{\partial s}\sum_{\pm}\sum_{J=0}^{\infty}(2J+2\alpha)\frac{\Gamma(J+2\alpha)}{\Gamma(J+1)}(J-h_\pm)^s|_{s=0}\,. \tag{4.116}$$

We will begin by regulating the expression $\sum_{J=0}^{\infty}(2J+2\alpha)\frac{\Gamma(J+2\alpha)}{\Gamma(J+1)}(J-a)^s$, where a is a placeholder for $h_\pm$. We expand the summand in powers of J and isolate the term that produces a logarithmic divergence, which we will fix using dimensional regularization. Equivalently, this procedure amounts to expanding the sum in terms of zeta functions, in which case the only singularity arises from the pole of $\zeta(1)$

$$\sum_{J=0}^{\infty}(2J+2\alpha)\frac{\Gamma(J+2\alpha)}{\Gamma(J+1)}(J-a)^s = \alpha_0\sum_J J^{d-1+s}+\cdots+\beta\sum_J J^{d-5+s}+\cdots\,, \tag{4.117}$$

where β marks the coefficient multiplying $\zeta(1)$, and all the coefficients depend on a, d, and s. We will make use of the fact that

$$\frac{\partial}{\partial s}\beta(a,d,s)\sum_J^{\infty} J^{-1-\epsilon+s}\bigg|_{s=0} = \frac{\beta(a,d,0)}{\epsilon^2}+\frac{1}{\epsilon}\frac{\partial\beta(a,d,0)}{\partial s}+O(1)\,, \tag{4.118}$$

is the only $1/\epsilon$ pole and we can ignore all other terms. So it remains for us to find $\beta(a,d,s)$, which we can easily do since we have the explicit expression for everything involved. We can then expand around $\epsilon = 0$ and keep the first two terms

$$\begin{aligned}\beta(a,d,s) = \frac{1}{2880}\big(&-240d^7+15d^8+d^6(1670-120as)+24d^5(-277+50as)\\&-120d^3(217-96as+16a^2(-1+s)s)+5d^4(3307-1008as+72a^2(-1+s)s)\\&+48d(-274+215as-80a^2(-1+s)s+20a^3s(2-3s+s^2))\\&-20d^2(-1249+750as-198a^2(-1+s)s+24a^3s(2-3s+s^2))\\&+240(12-12as+6a^2(-1+s)s-2a^3s(2-3s+s^2)+a^4s(-6+11s-6s^2+s^3))\big)\,.\end{aligned} \tag{4.119}$$

By inspection, we can see that every factor of a in the above expression appears multiplied by s. Thus, when we set $s = 0$, all dependence on a drops out, and in particular no terms proportional to μ^2 survive. Differentiating with respect to μ^2 therefore annihilates these contributions. Consequently, we only need to retain the $O(1)$ part of β'. This can be done explicitly, after which we simply replace a with $h_\pm$ and differentiate with respect to μ^2. This finally gives us in $d = 4$

$$\frac{\partial}{\partial\mu^2}\sum_{\pm}\frac{1}{\epsilon}\frac{\partial\beta(h_\pm,4,0)}{\partial s} = \frac{2-\mu^2}{\epsilon}\,. \tag{4.120}$$

Reinstating an overall normalization factor, we finally extract the $1/\epsilon$ to be

$$\frac{2-\mu^2}{8\pi^2}\frac{1}{\epsilon}\,. \tag{4.121}$$

Divergence of $G'(h)|_{h=1}$

To extract the divergence of the derivative of the propagator $G'_E(\sigma)$, we now need to differentiate with respect to σ, which is straightforward given that we have the relation

$$\frac{\partial}{\partial\sigma}C_J^\alpha(\sigma) = 2\alpha C_{J-1}^{\alpha+1}(\sigma)\,. \tag{4.122}$$

Using the above, we obtain

$$\begin{aligned} G'_E(\sigma)|_{\sigma=1} &= \frac{\Gamma(\alpha)}{2\pi^{\alpha+1}}\sum_{J=0}^{\infty}\frac{J+\alpha}{J(J+2\alpha)+\mu^2}2\alpha C_{J-1}^{\alpha+1}(\sigma=1) \\ &= \frac{\Gamma(\alpha)}{2\pi^{\alpha+1}}\sum_{J=0}^{\infty}\frac{2\alpha(J+\alpha)}{J(J+2\alpha)+\mu^2}\frac{\Gamma(J+2\alpha+1)}{\Gamma(J)\Gamma(2(\alpha+1))}\,. \end{aligned} \tag{4.123}$$

We can now repeat the same procedure as in the previous appendix 4.A to extract the $1/\epsilon$ divergence of $G'(\sigma)$. After all is said and done, we obtain

$$\frac{\mu^2(\mu^2-2)}{32\pi^2}\frac{1}{\epsilon}\,. \tag{4.124}$$

Combining (4.121) and (4.124) into the relation (4.110), we can now express the divergence of the stress tensor as

$$-\frac{1}{2}U\cdot V((\mu^2-6\xi)G_\epsilon(1)+2G'_\epsilon(1)) = U\cdot V\frac{m^2(m^2+12\xi-2)}{32\pi^2}\frac{1}{\epsilon}\,. \tag{4.125}$$

For both the conformal case $m^2+12\xi=\mu^2=2$, and for the massless case $m^2=0$, the $1/\epsilon$ contribution vanishes and there are no divergences.

We note, of course, that in the conformal case the one-point function of the stress tensor vanishes identically, since by symmetry it is proportional to the metric, and is therefore proportional to its trace, which vanishes in a conformal theory. However, even when the stress tensor is inserted alongside other operators and is no longer proportional to the metric, the divergence still vanishes.

BIBLIOGRAPHY

Achúcarro, Ana et al. (Mar. 2022). "Inflation: Theory and Observations". In: arXiv: 2203.08128 [astro-ph.CO].

Adams, Allan et al. (2006). "Causality, analyticity and an IR obstruction to UV completion". In: *JHEP* 0610, p. 014. DOI: 10.1088/1126-6708/2006/10/014. arXiv: hep-th/0602178 [hep-th].

Afkhami-Jeddi, Nima et al. (2017). "Einstein gravity 3-point functions from conformal field theory". In: *JHEP* 12, p. 049. DOI: 10.1007/JHEP12(2017)049. arXiv: 1610.09378 [hep-th].

Aguilera-Damia, Jeremias et al. (2026). "de Sitter Vacua & pUniverses". In: arXiv: 2605.02883 [hep-th].

Aharonov, Y., A. Komar, and Leonard Susskind (1969). "Superluminal behavior, causality, and instability". In: *Phys. Rev.* 182, pp. 1400–1403. DOI: 10.1103/PhysRev.182.1400.

Aharony, Ofer, Luis F. Alday, et al. (2017). "Loops in AdS from Conformal Field Theory". In: *JHEP* 07, p. 036. DOI: 10.1007/JHEP07(2017)036. arXiv: 1612.03891 [hep-th].

Aharony, Ofer, Steven S. Gubser, et al. (2000). "Large N field theories, string theory and gravity". In: *Phys. Rept.* 323, pp. 183–386. DOI: 10.1016/S0370-1573(99)00083-6. arXiv: hep-th/9905111.

Akhmedov, E. T., U. Moschella, and F. K. Popov (2019). "Characters of different secular effects in various patches of de Sitter space". In: *Phys. Rev. D* 99.8, p. 086009. DOI: 10.1103/PhysRevD.99.086009. arXiv: 1901.07293 [hep-th].

Albrychiewicz, Emil and Yasha Neiman (2021). "Scattering in the static patch of de Sitter space". In: *Phys. Rev. D* 103.6, p. 065014. DOI: 10.1103/PhysRevD.103.065014. arXiv: 2012.13584 [hep-th].

Anninos, Dionysios, Tarek Anous, and Alejandro Rios Fukelman (2024). "De Sitter at all loops: the story of the Schwinger model". In: *JHEP* 08, p. 155. DOI: 10.1007/JHEP08(2024)155. arXiv: 2403.16166 [hep-th].

Anninos, Dionysios, Sean A. Hartnoll, and Diego M. Hofman (2012). "Static Patch Solipsism: Conformal Symmetry of the de Sitter Worldline". In: *Class. Quant. Grav.* 29, p. 075002. DOI: 10.1088/0264-9381/29/7/075002. arXiv: 1109.4942 [hep-th].

Arkani-Hamed, Nima, Tzu-Chen Huang, and Yu-tin Huang (2021). "The EFT-Hedron". In: *JHEP* 05, p. 259. DOI: 10.1007/JHEP05(2021)259. arXiv: 2012.15849 [hep-th].

Baumann, Daniel et al. (2024). "Snowmass White Paper: The Cosmological Bootstrap". In: *SciPost Phys. Comm. Rep.* 2024, p. 1. DOI: 10.21468/SciPostPhysCommRep.1. arXiv: 2203.08121 [hep-th].

Belin, Alexandre, Diego M. Hofman, and Gregoire Mathys (2019). "Einstein gravity from ANEC correlators". In: arXiv: 1904.05892 [hep-th].

Bellazzini, Brando, Joan Elias Miró, et al. (2021). "Positive moments for scattering amplitudes". In: *Phys. Rev. D* 104.3, p. 036006. DOI: 10.1103/PhysRevD.104.036006. arXiv: 2011.00037 [hep-th].

Bellazzini, Brando, Marc Riembau, and Francesco Riva (2022). "IR side of positivity bounds". In: *Phys. Rev. D* 106.10, p. 105008. DOI: 10.1103/PhysRevD.106.105008. arXiv: 2112.12561 [hep-th].

Birrell, N. D. and P. C. W. Davies (1982). *Quantum Fields in Curved Space*. Cambridge University Press.

Bissi, Agnese and Aninda Sinha (2023). "Positivity, low twist dominance and CSDR for CFTs". In: *SciPost Phys.* 14.4, p. 083. DOI: 10.21468/SciPostPhys.14.4.083. arXiv: 2209.03978 [hep-th].

Bros, J., H. Epstein, and U. Moschella (1998). "Analyticity properties and thermal effects for general quantum field theory on de Sitter space-time". In: *Commun. Math. Phys.* 196, pp. 535–570. arXiv: gr-qc/9801099.

Bros, J. and U. Moschella (1996). "Two-point Functions and Quantum Fields in de Sitter Universe". In: *Rev. Math. Phys.* 8, pp. 327–391. arXiv: gr-qc/9511019.

Bunch, T. S. and P. C. W. Davies (1978). "Quantum field theory in de Sitter space: renormalization by point-splitting". In: *Proc. Roy. Soc. Lond. A* 360, pp. 117–134. DOI: 10.1098/rspa.1978.0060.

Burgess, C. P. et al. (2010). "Breakdown of Semiclassical Methods in de Sitter Space". In: *JCAP* 10, p. 017. DOI: 10.1088/1475-7516/2010/10/017. arXiv: 1005.3551 [hep-th].

Camanho, Xian O. et al. (2016). "Causality Constraints on Corrections to the Graviton Three-Point Coupling". In: *JHEP* 02, p. 020. DOI: 10.1007/JHEP02(2016)020. arXiv: 1407.5597 [hep-th].

Carmi, Dean and Simon Caron-Huot (2020). "A Conformal Dispersion Relation: Correlations from Absorption". In: *JHEP* 09, p. 009. DOI: 10.1007/JHEP09(2020)009. arXiv: 1910.12123 [hep-th].

Carmi, Dean, Joao Penedones, et al. (2021). "Applications of dispersive sum rules: ϵ-expansion and holography". In: *SciPost Phys.* 10.6, p. 145. DOI: 10.21468/SciPostPhys.10.6.145. arXiv: 2009.13506 [hep-th].

Caron-Huot, S. (n.d.). "unpublished notes". In: ().

Caron-Huot, Simon (2017). "Analyticity in Spin in Conformal Theories". In: *JHEP* 09, p. 078. DOI: 10.1007/JHEP09(2017)078. arXiv: 1703.00278 [hep-th].

Caron-Huot, Simon (2023). "Holographic cameras: an eye for the bulk". In: *JHEP* 03, p. 047. DOI: 10.1007/JHEP03(2023)047. arXiv: 2211.11791 [hep-th].

Caron-Huot, Simon, Murat Koloğlu, et al. (Apr. 2023). "Detectors in weakly-coupled field theories". In: *Journal of High Energy Physics* 2023.4. ISSN: 1029-8479. DOI: 10.1007/jhep04(2023)014. URL: http://dx.doi.org/10.1007/JHEP04(2023)014.

Caron-Huot, Simon, Yue-Zhou Li, et al. (2023a). "Causality constraints on corrections to Einstein gravity". In: *JHEP* 05, p. 122. DOI: 10.1007/JHEP05(2023)122. arXiv: 2201.06602 [hep-th].

– (2023b). "Graviton partial waves and causality in higher dimensions". In: *Phys. Rev. D* 108.2, p. 026007. DOI: 10.1103/PhysRevD.108.026007. arXiv: 2205.01495 [hep-th].

Caron-Huot, Simon, Dalimil Mazac, et al. (2021a). "AdS bulk locality from sharp CFT bounds". In: *JHEP* 11, p. 164. DOI: 10.1007/JHEP11(2021)164. arXiv: 2106.10274 [hep-th].

– (2021b). "Dispersive CFT Sum Rules". In: *JHEP* 05, p. 243. DOI: 10.1007/JHEP05(2021)243. arXiv: 2008.04931 [hep-th].

– (2021c). "Sharp boundaries for the swampland". In: *JHEP* 07, p. 110. DOI: 10.1007/JHEP07(2021)110. arXiv: 2102.08951 [hep-th].

Caron-Huot, Simon and Vincent Van Duong (2021). "Extremal Effective Field Theories". In: *JHEP* 05, p. 280. DOI: 10.1007/JHEP05(2021)280. arXiv: 2011.02957 [hep-th].

Chakraborty, Priyesh and John Stout (Oct. 2023). "Light Scalars at the Cosmological Collider". In: arXiv: 2310.01494 [hep-th].

Chakraborty, Soumangsu et al. (2020). "Classification of all 3 particle S-matrices quadratic in photons or gravitons". In: *JHEP* 04, p. 110. DOI: 10.1007/JHEP04(2020)110. arXiv: 2001.07117 [hep-th].

Chandrasekaran, Venkatesa et al. (2023). "An algebra of observables for de Sitter space". In: *JHEP* 02, p. 082. DOI: 10.1007/JHEP02(2023)082. arXiv: 2206.10780 [hep-th].

Chang, Cyuan-Han, Murat Kologlu, et al. (2022). "Transverse spin in the light-ray OPE". In: *JHEP* 05, p. 059. DOI: 10.1007/JHEP05(2022)059. arXiv: 2010.04726 [hep-th].

Chang, Cyuan-Han, Yakov Landau, and David Simmons-Duffin (2025). "Spinning dispersive CFT sum rules and bulk scattering". In: *JHEP* 04, p. 016. DOI: 10.1007/JHEP04(2025)016. arXiv: 2311.04271 [hep-th].

Chen, Hongbin, A. Liam Fitzpatrick, and Denis Karateev (2022). "Nonperturbative bounds on scattering of massive scalar particles in $d \geq 2$". In: *JHEP* 12, p. 092. DOI: 10.1007/JHEP12(2022)092. arXiv: 2207.12448 [hep-th].

Chiang, Li-Yuan et al. (Apr. 2022). "De-projecting the EFThedron". In: arXiv: 2204.07140 [hep-th].

Chowdhury, Subham Dutta, Abhijit Gadde, et al. (2020). "Classifying and constraining local four photon and four graviton S-matrices". In: *JHEP* 02, p. 114. DOI: 10.1007/JHEP02(2020)114. arXiv: 1910.14392 [hep-th].

Chowdhury, Subham Dutta, Kausik Ghosh, et al. (2022). "Crossing Symmetric Spinning S-matrix Bootstrap: EFT bounds". In: *SciPost Phys.* 13.3, p. 051. DOI: 10.21468/SciPostPhys.13.3.051. arXiv: 2112.11755 [hep-th].

Cohen, Timothy and Daniel Green (2020). "Soft de Sitter Effective Theory". In: *JHEP* 12, p. 041. DOI: 10.1007/JHEP12(2020)041. arXiv: 2007.03693 [hep-th].

Cordova, Clay, Juan Maldacena, and Gustavo J. Turiaci (2017). "Bounds on OPE Coefficients from Interference Effects in the Conformal Collider". In: *JHEP* 11, p. 032. DOI: 10.1007/JHEP11(2017)032. arXiv: 1710.03199 [hep-th].

Córdova, Clay and Shu-Heng Shao (2018). "Light-ray Operators and the BMS Algebra". In: *Phys. Rev.* D98.12, p. 125015. DOI: 10.1103/PhysRevD.98.125015. arXiv: 1810.05706 [hep-th].

Correia, Miguel, Amit Sever, and Alexander Zhiboedov (2020). "An Analytical Toolkit for the S-matrix Bootstrap". In: arXiv: 2006.08221 [hep-th].

– (2022). "Probing multi-particle unitarity with the Landau equations". In: *SciPost Phys.* 13, p. 062. DOI: 10.21468/SciPostPhys.13.3.062. arXiv: 2111.12100 [hep-th].

Costa, Miguel S., Tobias Hansen, and João Penedones (2017). "Bounds for OPE coefficients on the Regge trajectory". In: *JHEP* 10, p. 197. DOI: 10.1007/JHEP10(2017)197. arXiv: 1707.07689 [hep-th].

Costa, Miguel S., Joao Penedones, et al. (2011). "Spinning Conformal Correlators". In: *JHEP* 11, p. 071. DOI: 10.1007/JHEP11(2011)071. arXiv: 1107.3554 [hep-th].

Cutkosky, R. E. (1960). "Singularities and discontinuities of Feynman amplitudes". In: *J. Math. Phys.* 1, pp. 429–433. DOI: 10.1063/1.1703676.

Di Francesco, Philippe, Pierre Mathieu, and David Senechal (1997). *Conformal Field Theory*. Springer.

Dirac, Paul A. M. (1936). "Wave equations in conformal space". In: *Annals Math.* 37, pp. 429–442. DOI: 10.2307/1968455.

Dolan, F.A. and H. Osborn (2002). "Superconformal symmetry, correlation functions and the operator product expansion". In: *Nucl.Phys.* B629, pp. 3–73. DOI: 10.1016/S0550-3213(02)00096-2. arXiv: hep-th/0112251 [hep-th].

Donath, Yaniv and Enrico Pajer (2024). "The in-out formalism for in-in correlators". In: *JHEP* 07, p. 064. DOI: 10.1007/JHEP07(2024)064. arXiv: 2402.05999 [hep-th].

Eden, R. J. et al. (1966). *The Analytic S-Matrix*. Cambridge University Press.

Einhorn, Martin B. and Finn Larsen (Jan. 2003). "Interacting quantum field theory in de Sitter vacua". In: *Physical Review D* 67.2. ISSN: 1089-4918. DOI: 10.1103/physrevd.67.024001. URL: http://dx.doi.org/10.1103/PhysRevD.67.024001.

Fitzpatrick, A. Liam and Jared Kaplan (2012). "Unitarity and the Holographic S-Matrix". In: *JHEP* 1210, p. 032. DOI: 10.1007/JHEP10(2012)032. arXiv: 1112.4845 [hep-th].

Fitzpatrick, A. Liam, Jared Kaplan, et al. (2013). "The Analytic Bootstrap and AdS Superhorizon Locality". In: *JHEP* 1312, p. 004. DOI: 10.1007/JHEP12(2013)004. arXiv: 1212.3616 [hep-th].

Ford, L. H. (1985). "Quantum Instability of De Sitter Space-time". In: *Phys. Rev. D* 31, p. 710. DOI: 10.1103/PhysRevD.31.710.

Ford, L. H. and Alexander Vilenkin (1986). "Global symmetry breaking in two-dimensional flat spacetime and in de Sitter spacetime". In: *Phys. Rev. D* 33, p. 2833. DOI: 10.1103/PhysRevD.33.2833.

Freytsis, Marat et al. (2023). "Multifield positivity bounds for inflation". In: *JHEP* 09, p. 041. DOI: 10.1007/JHEP09(2023)041. arXiv: 2210.10791 [hep-th].

Glimm, J. and Arthur M. Jaffe (1981). *Quantum Physics. a Functional Integral Point of View*. 417 p. New York, Usa: Springer.

Gonzo, Riccardo and Andrzej Pokraka (2021). "Light-ray operators, detectors and gravitational event shapes". In: *JHEP* 05, p. 015. DOI: 10.1007/JHEP05(2021)015. arXiv: 2012.01406 [hep-th].

Gopakumar, Rajesh, Aninda Sinha, and Ahmadullah Zahed (2021). "Crossing Symmetric Dispersion Relations for Mellin Amplitudes". In: *Phys. Rev. Lett.* 126.21, p. 211602. DOI: 10.1103/PhysRevLett.126.211602. arXiv: 2101.09017 [hep-th].

Green, Daniel (2023). "EFT for de Sitter Space". In: *Handbook of Quantum Gravity*. DOI: 10.1007/978-981-19-3079-9_6-1. arXiv: 2210.05820 [hep-th].

Grewal, Manvir and Y. T. Albert Law (2025). "Real-time observables in de Sitter thermodynamics". In: *JHEP* 10, p. 052. arXiv: 2403.06006 [hep-th].

Haag, R. (1992). *Local quantum physics: Fields, particles, algebras*.

Häring, Kelian and Alexander Zhiboedov (Feb. 2022). "Gravitational Regge bounds". In: arXiv: 2202.08280 [hep-th].

Hartman, Thomas, Sachin Jain, and Sandipan Kundu (2016). "Causality Constraints in Conformal Field Theory". In: *JHEP* 05, p. 099. DOI: 10.1007/JHEP05(2016)099. arXiv: 1509.00014 [hep-th].

Hartman, Thomas, Sandipan Kundu, and Amirhossein Tajdini (2017). "Averaged Null Energy Condition from Causality". In: *JHEP* 07, p. 066. DOI: 10.1007/JHEP07(2017)066. arXiv: 1610.05308 [hep-th].

Hartman, Thomas and Grégoire Mathys (2023). "Averaged null energy and the renormalization group". In: *JHEP* 12, p. 139. DOI: 10.1007/JHEP12(2023)139. arXiv: 2309.14409 [hep-th].

– (2024a). "Light-ray sum rules and the c-anomaly". In: *JHEP* 08, p. 008. DOI: 10.1007/JHEP08(2024)008. arXiv: 2405.10137 [hep-th].

– (2024b). "Null energy constraints on two-dimensional RG flows". In: *JHEP* 01, p. 102. DOI: 10.1007/JHEP01(2024)102. arXiv: 2310.15217 [hep-th].

Hayrapetyan, Aram et al. (2024). "Measurement of Energy Correlators inside Jets and Determination of the Strong Coupling αS(mZ)". In: *Phys. Rev. Lett.* 133.7, p. 071903. DOI: 10.1103/PhysRevLett.133.071903. arXiv: 2402.13864 [hep-ex].

Heemskerk, Idse et al. (2009). "Holography from Conformal Field Theory". In: *JHEP* 0910, p. 079. DOI: 10.1088/1126-6708/2009/10/079. arXiv: 0907.0151 [hep-th].

Henriksson, Johan et al. (2022). "Bounding violations of the weak gravity conjecture". In: *JHEP* 08, p. 184. DOI: 10.1007/JHEP08(2022)184. arXiv: 2203.08164 [hep-th].

Herrmann, Enrico, Murat Kologlu, and Ian Moult (2024). *Energy Correlators in Perturbative Quantum Gravity*. arXiv: 2412.05384 [hep-th]. URL: https://arxiv.org/abs/2412.05384.

Hofman, Diego M. and Juan Maldacena (2008). "Conformal collider physics: Energy and charge correlations". In: *JHEP* 05, p. 012. DOI: 10.1088/1126-6708/2008/05/012. arXiv: 0803.1467 [hep-th].

Hogervorst, Matthijs and Slava Rychkov (2013). "Radial Coordinates for Conformal Blocks". In: *Phys.Rev.* D87.10, p. 106004. DOI: 10.1103/PhysRevD.87.106004. arXiv: 1303.1111 [hep-th].

Hollands, Stefan and Robert M. Wald (2001). "Local Wick polynomials and time ordered products of quantum fields in curved spacetime". In: *Commun. Math. Phys.* 223, pp. 289–326.

– (2002). "Existence of local covariant time ordered products of quantum fields in curved spacetime". In: *Commun. Math. Phys.* 231, pp. 309–345.

– (2015). "Quantum fields in curved spacetime". In: *Phys. Rept.* 574, pp. 1–35. DOI: 10.1016/j.physrep.2015.02.001. arXiv: 1401.2026 [gr-qc].

Hu, Bei-Lok (Dec. 2018). “Infrared Behavior of Quantum Fields in Inflationary Cosmology – Issues and Approaches: an overview”. In: arXiv: 1812.11851 [gr-qc].

Karateev, Denis, Petr Kravchuk, and David Simmons-Duffin (2018). “Weight Shifting Operators and Conformal Blocks”. In: *JHEP* 02. [,91(2017)], p. 081. DOI: 10.1007/JHEP02(2018)081. arXiv: 1706.07813 [hep-th].

– (2019). “Harmonic Analysis and Mean Field Theory”. In: *JHEP* 10, p. 217. DOI: 10.1007/JHEP10(2019)217. arXiv: 1809.05111 [hep-th].

Knop, Waltraut and Dalimil Mazac (2022). “Dispersive sum rules in AdS_2”. In: *JHEP* 10, p. 038. DOI: 10.1007/JHEP10(2022)038. arXiv: 2203.11170 [hep-th].

Kologlu, Murat et al. (2020). “Shocks, Superconvergence, and a Stringy Equivalence Principle”. In: *JHEP* 11, p. 096. DOI: 10.1007/JHEP11(2020)096. arXiv: 1904.05905 [hep-th].

– (2021). “The light-ray OPE and conformal colliders”. In: *JHEP* 01, p. 128. DOI: 10.1007/JHEP01(2021)128. arXiv: 1905.01311 [hep-th].

Komargodski, Zohar and Alexander Zhiboedov (2013). “Convexity and Liberation at Large Spin”. In: *JHEP* 1311, p. 140. DOI: 10.1007/JHEP11(2013)140. arXiv: 1212.4103 [hep-th].

Korchemsky, Gregory P. and George F. Sterman (1999). “Power corrections to event shapes and factorization”. In: *Nucl. Phys. B* 555, pp. 335–351. DOI: 10.1016/S0550-3213(99)00308-9. arXiv: hep-ph/9902341.

Korchemsky, Gregory P. and Alexander Zhiboedov (Sept. 2021). “On the light-ray algebra in conformal field theories”. In: arXiv: 2109.13269 [hep-th].

Kos, Filip, David Poland, and David Simmons-Duffin (2014). “Bootstrapping Mixed Correlators in the 3D Ising Model”. In: *JHEP* 11, p. 109. DOI: 10.1007/JHEP11(2014)109. arXiv: 1406.4858 [hep-th].

Kos, Filip, David Poland, David Simmons-Duffin, and Alessandro Vichi (2016). “Precision islands in the Ising and $O(N)$ models”. In: *JHEP* 08, p. 036. DOI: 10.1007/JHEP08(2016)036. arXiv: 1603.04436 [hep-th].

Kravchuk, Petr (2018). “Casimir recursion relations for general conformal blocks”. In: *JHEP* 02. [,164(2017)], p. 011. DOI: 10.1007/JHEP02(2018)011. arXiv: 1709.05347 [hep-th].

Kravchuk, Petr, Jiaxin Qiao, and Slava Rychkov (2020). “Distributions in CFT. Part I. Cross-ratio space”. In: *JHEP* 05, p. 137. DOI: 10.1007/JHEP05(2020)137. arXiv: 2001.08778 [hep-th].

Kravchuk, Petr and David Simmons-Duffin (2018a). “Counting Conformal Correlators”. In: *JHEP* 02, p. 096. DOI: 10.1007/JHEP02(2018)096. arXiv: 1612.08987 [hep-th].

Kravchuk, Petr and David Simmons-Duffin (2018b). “Light-ray operators in conformal field theory”. In: *JHEP* 11. [,236(2018)], p. 102. DOI: 10.1007/JHEP11(2018)102. arXiv: 1805.00098 [hep-th].

Kristiano, Jason et al. (Nov. 2025). “Imprints of flat space analyticity in de Sitter S-matrix”. In: arXiv: 2511.22623 [hep-th].

Kulaxizi, Manuela, Andrei Parnachev, and Alexander Zhiboedov (2018). “Bulk Phase Shift, CFT Regge Limit and Einstein Gravity”. In: *JHEP* 06, p. 121. DOI: 10.1007/JHEP06(2018)121. arXiv: 1705.02934 [hep-th].

Law, Y. T. Albert (Jan. 2025). *De Sitter Horizon Edge Partition Functions*. arXiv: 2501.17912 [hep-th].

Lehmann, H., K. Symanzik, and W. Zimmermann (1955). “Zur Formulierung quantisierter Feldtheorien”. In: *Nuovo Cim.* 1, pp. 205–225.

Li, Yue-Zhou (2021). “Notes on flat-space limit of AdS/CFT”. In: *JHEP* 09, p. 027. DOI: 10.1007/JHEP09(2021)027. arXiv: 2106.04606 [hep-th].

– (Oct. 2023). “Effective field theory bootstrap, large-N χPT and holographic QCD”. In: arXiv: 2310.09698 [hep-th].

Liu, Junyu et al. (2019). “d-dimensional SYK, AdS Loops, and $6j$ Symbols”. In: *JHEP* 03, p. 052. DOI: 10.1007/JHEP03(2019)052. arXiv: 1808.00612 [hep-th].

Loparco, Mattia et al. (2023). “The Källén-Lehmann representation in de Sitter spacetime”. In: *JHEP* 12, p. 159. DOI: 10.1007/JHEP12(2023)159. arXiv: 2306.00090 [hep-th].

Luscher, M. and G. Mack (1975). “Global Conformal Invariance in Quantum Field Theory”. In: *Commun. Math. Phys.* 41, pp. 203–234. DOI: 10.1007/BF01608988.

Maldacena, Juan Martin (1998). “The Large N limit of superconformal field theories and supergravity”. In: *Adv. Theor. Math. Phys.* 2, pp. 231–252. DOI: 10.4310/ATMP.1998.v2.n2.a1. arXiv: hep-th/9711200.

Marolf, Donald and Ian A. Morrison (2010). “The IR stability of de Sitter: Loop corrections to scalar propagators”. In: *Phys. Rev. D* 82, p. 105032. DOI: 10.1103/PhysRevD.82.105032. arXiv: 1006.0035 [gr-qc].

Martin, Andre (1965). “Extension of the axiomatic analyticity domain of scattering amplitudes by unitarity. 1.” In: *Nuovo Cim.* A42, pp. 930–953. DOI: 10.1007/BF02720568.

Mazac, Dalimil (2016). “Analytic Bounds and Emergence of AdS_2 Physics from the Conformal Bootstrap”. In: arXiv: 1611.10060 [hep-th].

Mazac, Dalimil and Miguel F. Paulos (2019). “The analytic functional bootstrap. Part I: 1D CFTs and 2D S-matrices”. In: *JHEP* 02, p. 162. DOI: 10.1007/JHEP02(2019)162. arXiv: 1803.10233 [hep-th].

Mazáč, Dalimil, Leonardo Rastelli, and Xinan Zhou (2021). “A basis of analytic functionals for CFTs in general dimension”. In: *JHEP* 08, p. 140. DOI: 10.1007/JHEP08(2021)140. arXiv: 1910.12855 [hep-th].

McPeak, Brian, Marco Venuti, and Alessandro Vichi (Oct. 2023). “Adding subtractions: comparing the impact of different Regge behaviors”. In: arXiv: 2310.06888 [hep-th].

Meltzer, David (2021). “Dispersion Formulas in QFTs, CFTs, and Holography”. In: *JHEP* 05, p. 098. DOI: 10.1007/JHEP05(2021)098. arXiv: 2103.15839 [hep-th].

Meltzer, David and Eric Perlmutter (2018). “Beyond $a = c$: gravitational couplings to matter and the stress tensor OPE”. In: *JHEP* 07, p. 157. DOI: 10.1007/JHEP07(2018)157. arXiv: 1712.04861 [hep-th].

Meltzer, David, Eric Perlmutter, and Allic Sivaramakrishnan (2020). “Unitarity Methods in AdS/CFT”. In: *JHEP* 03, p. 061. DOI: 10.1007/JHEP03(2020)061. arXiv: 1912.09521 [hep-th].

Meltzer, David and Allic Sivaramakrishnan (2020). “CFT unitarity and the AdS Cutkosky rules”. In: *JHEP* 11, p. 073. DOI: 10.1007/JHEP11(2020)073. arXiv: 2008.11730 [hep-th].

Melville, Scott and Guilherme L. Pimentel (2024a). “A de Sitter S-matrix from amputated cosmological correlators”. In: *JHEP* 08, p. 211. DOI: 10.1007/JHEP08(2024)211. arXiv: 2404.05712 [hep-th].

– (2024b). “de Sitter S matrix for the masses”. In: *Phys. Rev. D* 110.10, p. 103530. DOI: 10.1103/PhysRevD.110.103530. arXiv: 2309.07092 [hep-th].

Moult, Ian and Hua Xing Zhu (June 2025). “Energy Correlators: A Journey From Theory to Experiment”. In: arXiv: 2506.09119 [hep-ph].

Mukhametzhanov, Baur and Alexander Zhiboedov (2019). “Analytic Euclidean Bootstrap”. In: *JHEP* 10, p. 270. DOI: 10.1007/JHEP10(2019)270. arXiv: 1808.03212 [hep-th].

Murakami, Jun and Masakazu Yano (2005). “On the volume of a hyperbolic and spherical tetrahedron”. In: *Communications in analysis and geometry* 13.2, pp. 379–400.

Osborn, H. and A.C. Petkou (1994). “Implications of conformal invariance in field theories for general dimensions”. In: *Annals Phys.* 231, pp. 311–362. DOI: 10.1006/aphy.1994.1045. arXiv: hep-th/9307010 [hep-th].

Osterwalder, Konrad and Robert Schrader (1973). “AXIOMS FOR EUCLIDEAN GREEN’S FUNCTIONS”. In: *Commun. Math. Phys.* 31, pp. 83–112. DOI: 10.1007/BF01645738.

– (1975). “Axioms for Euclidean Green’s Functions. 2.” In: *Commun. Math. Phys.* 42, p. 281. DOI: 10.1007/BF01608978.

Pappadopulo, Duccio et al. (2012). “OPE Convergence in Conformal Field Theory”. In: *Phys.Rev.* D86, p. 105043. DOI: 10.1103/PhysRevD.86.105043. arXiv: 1208.6449 [hep-th].

Parker, Leonard and David Toms (2009). *Quantum Field Theory in Curved Spacetime: Quantized Fields and Gravity*. Cambridge University Press.

Penedones, Joao, Joao A. Silva, and Alexander Zhiboedov (2020). “Nonperturbative Mellin Amplitudes: Existence, Properties, Applications”. In: *JHEP* 08, p. 031. DOI: 10.1007/JHEP08(2020)031. arXiv: 1912.11100 [hep-th].

Penedones, Joao, Kamran Salehi Vaziri, and Zimo Sun (2023). *Hilbert space of Quantum Field Theory in de Sitter spacetime*. arXiv: 2301.04146 [hep-th]. URL: https://arxiv.org/abs/2301.04146.

Penedones, João, Emilio Trevisani, and Masahito Yamazaki (2016). “Recursion Relations for Conformal Blocks”. In: *JHEP* 09, p. 070. DOI: 10.1007/JHEP09(2016)070. arXiv: 1509.00428 [hep-th].

Perlmutter, S. et al. (1998). “Discovery of a supernova explosion at half the age of the Universe and its cosmological implications”. In: *Nature* 391, pp. 51–54. DOI: 10.1038/34124. arXiv: astro-ph/9712212.

Peskin, Michael E. and Daniel V. Schroeder (1995). *An Introduction to Quantum Field Theory*. Addison-Wesley.

Pethybridge, Ben and Vladimir Schaub (2022). “Tensors and spinors in de Sitter space”. In: *JHEP* 06, p. 123. DOI: 10.1007/JHEP06(2022)123. arXiv: 2111.14899 [hep-th].

Pham, T. N. and Tran N. Truong (1985). “Evaluation of the Derivative Quartic Terms of the Meson Chiral Lagrangian From Forward Dispersion Relation”. In: *Phys. Rev. D* 31, p. 3027. DOI: 10.1103/PhysRevD.31.3027.

Poland, David, Slava Rychkov, and Alessandro Vichi (2019). “The Conformal Bootstrap: Theory, Numerical Techniques, and Applications”. In: *Rev. Mod. Phys.* 91.1. [Rev. Mod. Phys.91,015002(2019)], p. 15002. DOI: 10.1103/RevModPhys.91.015002. arXiv: 1805.04405 [hep-th].

Polyakov, A. M. (1974). “Nonhamiltonian approach to conformal quantum field theory”. In: *Zh. Eksp. Teor. Fiz.* 66. [Sov. Phys. JETP39,9(1974)], pp. 23–42.

– (Sept. 2012). “Infrared instability of the de Sitter space”. In: arXiv: 1209.4135 [hep-th].

Premkumar, Akhil (2024). “Regulating loops in de Sitter spacetime”. In: *Phys. Rev. D* 109.4, p. 045003. DOI: 10.1103/PhysRevD.109.045003. arXiv: 2110.12504 [hep-th].

Radzikowski, Marek J. (1996). “Micro-local approach to the Hadamard condition in quantum field theory on curved space-time”. In: *Commun. Math. Phys.* 179, pp. 529–553.

Rajaraman, Arvind (2010). “On the proper treatment of massless fields in Euclidean de Sitter space”. In: *Phys. Rev. D* 82, p. 123522. DOI: 10.1103/PhysRevD.82.123522. arXiv: 1008.1271 [hep-th].

Ratra, Bharat (1985). “Restoration of spontaneously broken continuous symmetries in de Sitter spacetime”. In: *Phys. Rev. D* 31, p. 1931. DOI: 10.1103/PhysRevD.31.1931.

Rattazzi, Riccardo et al. (2008). “Bounding scalar operator dimensions in 4D CFT”. In: *JHEP* 12, p. 031. DOI: 10.1088/1126-6708/2008/12/031. arXiv: 0807.0004 [hep-th].

Riess, Adam G. et al. (1998). “Observational evidence from supernovae for an accelerating universe and a cosmological constant”. In: *Astron. J.* 116, pp. 1009–1038. DOI: 10.1086/300499. arXiv: astro-ph/9805201.

Seery, David (2010). “Infrared effects in inflationary correlation functions”. In: *Class. Quant. Grav.* 27, p. 124005. DOI: 10.1088/0264-9381/27/12/124005. arXiv: 1005.1649 [astro-ph.CO].

El-Showk, Sheer and Miguel F. Paulos (2013). “Bootstrapping Conformal Field Theories with the Extremal Functional Method”. In: *Phys. Rev. Lett.* 111.24, p. 241601. DOI: 10.1103/PhysRevLett.111.241601. arXiv: 1211.2810 [hep-th].

El-Showk, Sheer, Miguel F. Paulos, et al. (2014). “Solving the 3d Ising Model with the Conformal Bootstrap II. c-Minimization and Precise Critical Exponents”. In: *J. Stat. Phys.* 157, p. 869. DOI: 10.1007/s10955-014-1042-7. arXiv: 1403.4545 [hep-th].

Simmons-Duffin, David (2014). “Projectors, Shadows, and Conformal Blocks”. In: *JHEP* 04, p. 146. DOI: 10.1007/JHEP04(2014)146. arXiv: 1204.3894 [hep-th].

– (2015). “A Semidefinite Program Solver for the Conformal Bootstrap”. In: *JHEP* 06, p. 174. DOI: 10.1007/JHEP06(2015)174. arXiv: 1502.02033 [hep-th].

– (2017). “The Conformal Bootstrap”. In: *Proceedings, Theoretical Advanced Study Institute in Elementary Particle Physics: New Frontiers in Fields and Strings (TASI 2015): Boulder, CO, USA, June 1-26, 2015*, pp. 1–74. DOI: 10.1142/9789813149441_0001. arXiv: 1602.07982 [hep-th]. URL: http://inspirehep.net/record/1424282/files/arXiv:1602.07982.pdf.

– (2023). *TASI 2023 Lectures: CFT and Observables on the Null Plane*. https://gitlab.com/davidsd/cft-null-plane-notes-tasi-2023.

Simmons-Duffin, David, Douglas Stanford, and Edward Witten (2018). “A spacetime derivation of the Lorentzian OPE inversion formula”. In: *JHEP* 07, p. 085. DOI: 10.1007/JHEP07(2018)085. arXiv: 1711.03816 [hep-th].

Sinha, Aninda and Ahmadullah Zahed (2021). "Crossing Symmetric Dispersion Relations in Quantum Field Theories". In: *Phys. Rev. Lett.* 126.18, p. 181601. DOI: 10.1103/PhysRevLett.126.181601. arXiv: 2012.04877 [hep-th].

Streater, R.F. and A.S. Wightman (2016). *PCT, Spin and Statistics, and All That*. Princeton Landmarks in Mathematics and Physics. Princeton University Press. ISBN: 9781400884230. URL: https://books.google.com/books?id=FyCTDAAAQBAJ.

Strominger, Andrew (2001). "The dS / CFT correspondence". In: *JHEP* 10, p. 034. DOI: 10.1088/1126-6708/2001/10/034. arXiv: hep-th/0106113.

Sun, Zimo (Aug. 2024). "A note on the representations of SO(1,d + 1)". In: *Reviews in Mathematical Physics* 37.01. ISSN: 1793-6659. DOI: 10.1142/s0129055x24300073. URL: http://dx.doi.org/10.1142/S0129055X24300073.

Susskind, Leonard (2021). "De Sitter Holography: Fluctuations, Anomalous Symmetry, and Wormholes". In: *Universe* 7.12, p. 464. DOI: 10.3390/universe7120464. arXiv: 2106.03964 [hep-th].

Sveshnikov, N. A. and F. V. Tkachov (1996). "Jets and quantum field theory". In: *Phys. Lett. B* 382. Ed. by B. B. Levchenko and V. I. Savrin, pp. 403–408. DOI: 10.1016/0370-2693(96)00558-8. arXiv: hep-ph/9512370.

Tipler, Frank J. (May 1978). "Energy conditions and spacetime singularities". In: *Phys. Rev. D* 17 (10), pp. 2521–2528. DOI: 10.1103/PhysRevD.17.2521. URL: https://link.aps.org/doi/10.1103/PhysRevD.17.2521.

Tolley, Andrew J., Zi-Yue Wang, and Shuang-Yong Zhou (2021). "New positivity bounds from full crossing symmetry". In: *JHEP* 05, p. 255. DOI: 10.1007/JHEP05(2021)255. arXiv: 2011.02400 [hep-th].

Wald, Robert M. (1994). *Quantum Field Theory in Curved Spacetime and Black Hole Thermodynamics*. University of Chicago Press.

Weinberg, Steven (1995). *The Quantum Theory of Fields. Vol. 1: Foundations*. Cambridge University Press.

Witten, Edward (1998). "Anti-de Sitter space and holography". In: *Adv. Theor. Math. Phys.* 2, pp. 253–291. DOI: 10.4310/ATMP.1998.v2.n2.a2. arXiv: hep-th/9802150.

– (2011). "Analytic Continuation Of Chern-Simons Theory". In: *AMS/IP Stud. Adv. Math.* 50. Ed. by Joergen E. Andersen et al., pp. 347–446. arXiv: 1001.2933 [hep-th].